creative commons

COMMONS DEED

저작자표시-비영리-변경금지 2.0 대한민국

이용자는 아래의 조건을 따르는 경우에 한하여 자유롭게

- 이 저작물을 복제, 배포, 전송, 전시, 공연 및 방송할 수 있습니다.

다음과 같은 조건을 따라야 합니다:

저작자표시. 귀하는 원저작자를 표시하여야 합니다.

비영리. 귀하는 이 저작물을 영리 목적으로 이용할 수 없습니다.

변경금지. 귀하는 이 저작물을 개작, 변형 또는 가공할 수 없습니다.

- 귀하는, 이 저작물의 재이용이나 배포의 경우, 이 저작물에 적용된 이용허락조건을 명확하게 나타내어야 합니다.
- 저작권자로부터 별도의 허가를 받으면 이러한 조건들은 적용되지 않습니다.

저작권법에 따른 이용자의 권리는 위의 내용에 의하여 영향을 받지 않습니다.

이것은 이용허락규약(Legal Code)을 이해하기 쉽게 요약한 것입니다.

Disclaimer

dCollection

공학박사학위논문

디젤엔진에서 연소 특성이 연소 소음에 미치는 영향

Effects of Combustion Characteristics on Combustion Noise in Diesel Engines

2016 년 2 월

서울대학교 대학원

기계항공공학부

이 승 현

디젤 엔진에서 연소 특성이 연소 소음에 미치는 영향

Effects of Combustion Characteristics on Combustion Noise in Diesel Engines

지도교수 민 경 덕

이 논문을 공학박사 학위논문으로 제출함
2015 년 10 월

서울대학교 대학원
기계항공공학부
이 승 현

이승현의 공학박사 학위논문을 인준함
2015 년 12

위 원 장_______________(인)

부위원장_______________(인)

위 원_______________(인)

위 원_______________(인)

위 원_______________(인)

Acknowledgements

A lot of help and advices from many people greatly facilitated the work of my Ph. D. thesis. I would like to express my special thanks to those people.

First and foremost, I would like to express my honor and gratitude to my advisor, Professor Kyoungdoug Min. During the course of my Ph. D., my knowledge and personality grew with his invaluable advices. He gave the inspirations of this study and his guidance and encouragement were the sources of power that overcame many difficulties during the project.

I would like to specially thank the project members who offered a great assistance and valuable discussions. Dr. Hoimyung Choi and Dr. Seungeun Yu also gave me the basic knowledge and inspirations as a senior. Jeongwoo Lee and Seungha Lee gave many insights. Youngju Lee, Sungmoon Lee, Yoonwoo Lee, Youngbok Lee and Sanghyun Chu assisted lots of research. Gyujin Kim and Hyungmook Kang, who joined the lab with me, gave beautiful memories of our friendships. Additionally, I am grateful to MinJae Kim, Namho Kim, Joohan Kim, Jaeman Park, Hwanyung Oh, Insuk Ko, Yuil Lee, Guesang Lee and JaeHyuk Cha, who are my colleagues and friends, for the unforgettable and joyful lab life and our deep friendships. My thanks go to all my graduate schoolmates.

It was my great honor to have the opportunity to participate the project with Hyundai motor company and I would like to thank In Soo Jung, Jaemin Jin and Dongchul Lee for the financial support and meaningful comments from plentiful experiences of the engine development.

Finally, I would like to present my deepest respect and gratitude to my parents, Jaekyung Lee and Munhee Chae, for their great sacrifice, thoughtful consideration, unimaginable patience, and endless love. Lastly, my thanks and appreciation go to Haeyoung Lee. Her love, understanding and companionship are elements that have sustained me throughout my graduate career.

Abstract

Effects of Combustion Characteristics on Combustion Noise in Diesel Engines

Seunghyun Lee
Department of Mechanical and Aerospace Engineering
The Graduate School
Seoul National University

The demand of diesel engines for passenger cars has increased due to their higher thermal efficiency, however, diesel engines have weaknesses; namely, the engine noise and the vibration. Especially, the combustion noise is significantly louder than that of gasoline engines due to their different combustion modes. In diesel engines, some fuel, which are already mixed with air, are rapidly burned after the ignition delay in the premixed combustion phase and the components of the engine block experience a rapid pressure rise, which is known as the main source of combustion noise. In this study, the relation between combustion characteristics and in-cylinder pressure excitation was investigated. In addition, the combustion characteristics of lower level excitation were studied. Finally, the closed control system using combustion noise index was developed to reduce the combustion noise.

In this study, a 1.6 liter diesel engine was used. The in-cylinder pressure, exhaust emissions and smoke were measured. Rapid prototype controller was used for the real time control system. Furthermore, a vehicle, which was equipped with the same engine, was used for bench test as well as the vehicle test.

The main source of combustion noise is from the in-cylinder pressure variation. The pressure is also affected by the change in heat release rate. Thus, in this study, the relation between the shape of heat release rate and the pressure excitation characteristics were studied. Through an engine experiment, it is hard to change the shape of heat release rate as we wish. Thus, the heat release rate was simulated by Wiebe functions. The 3 Wiebe functions are generally used to describe the diesel combustion. The pressure curve was reproduced by using the simulated heat release rate. Frequency analysis, FFT and 1/3 octave band analysis, were conducted to evaluate the excitation of the pressure curve. When more fuel was burned rapidly, the excitation level increased. When the combustion duration increased or the fuel quantity decreased, the combustion noise decreased. However, the start of combustion did not affect the combustion noise much. Pilot injection, which was used to reduce the combustion noise, decreased the combustion excitation of main combustion injection. However, the combustion of pilot injection considerably affected the total excitation.

The shape of heat release rate for reduction of combustion noise was investigated. When the combustion duration became long and the fuel was burned moderately, the combustion noise decreased. In addition, the split injection of the main injection effectively reduced the excitation. When 30% fuel was burned early, the rest of fuel continuously burned and the combustion noise was dramatically reduced with the same IMEP.

The injection strategies for the engine noise reduction was examined via engine bench tests. When injection parameters, SOI, swirl, injection pressure and EGR rate, were changed, the heat release shape and excitation characteristics were studied. The combustion noise could not be reduced from changing them without an emission deterioration. To prevent a formation of more emission and to reduce the combustion noise, early pilot injection strategy was applied. When the pilot injection quantity increased, the main injection fuel was burned smoothly. However, an increase of pilot injection quantity was anticipated to produce more smoke. To solve this dilemma, the early injection concept was applied to pilot injection because the combustion noise can be reduced without an emission increase through an early pilot injection.

Finally, a closed loop control system using CNI was developed for the reduction of combustion noise. The controller, which can measure the in-cylinder pressure and calculate CNI in real time, were developed using NI-PXI and LabVIEW. The combustion controller, which can modify the injection strategies, was developed using ES1000 and ASCET. SOI, injection pressure and pilot quantity were used as control parameters. The system applied to a vehicle. The current CNI level could be controlled to follow the target value in a transient operation. At that time, 1.2~2 kHz frequency of the cabin noise in the vehicle was reduced down to 4 dBA.

Keywords: Diesel engine, Combustion noise, Heat release rate, Closed loop control, Combustion noise reduction, Injection strategy.

Student Number: 2013-30207

Contents

Acknowledgements .... **i**

Abstract .... **ii**

List of Figures .... **ix**

List of Tables .... **xv**

Acronym .... **xvii**

Chapter 1. Introduction 1

1.1 Background and Motivation **1**

1.1.1 Motivation 1
1.1.2 Engine noise classification 2
1.1.3 Relation between engine noise and combustion 5
1.1.4 Reduction of combustion noise 8
1.1.5 Noise evaluation method 9
1.1.5.1 Engine noise evaluation method 9
1.1.5.2 Combustion noise index (CNI) 9
1.1.6 Closed loop control １２

1.2 Objectives **１３**

Chapter 2. Experimental Apparatus １４

2.1 Overall configuration **１４**

2.1.1 Engine test bench cell １４
2.1.2 Measurement of exhaust gas emissions １４

2.2 Multi-cylinder Diesel engine...17

2.3 Combustion control system 19
2.3.1 NI-PXI 19
2.3.2 ES-1000 20
2.3.3 Pressure sensor...20

Chapter 3. Relation between diesel combustion and combustion noise... 25

3.1 Simulation of heat release rate using Wiebe functions..................................25
3.1.1 Validation for the simulation of the heat release rate...................................28
3.1.2 Pressure reconstruction using Wiebe functions 32

3.2 Effect of heat release rate shape on combustion noise : Analysis of excitation of in-cylinder pressure changing Wiebe functions coefficients...........................33
3.2.1 Comparing motoring pressure and combustion pressure..............................34
3.2.2 Effects of Single Wiebe function shape on combustion noise 36
3.2.2.1 Effects of coefficient ‘a’...36
3.2.2.2 Effects of coefficient ‘m’ 36
3.2.2.3 Effects of combustion duration 37
3.2.2.4 Effects of start of combustion 37
3.2.2.5 Effects of total released heat 38
3.2.3 Effects of mixing controlled phase 38
3.2.4 Effects of pilot injection 39
3.2.4.1 Effects of pilot injection quantity..39

3.2.4.2 Effects of SOC of pilot injection....39
3.2.4.3 Effects of combustion duration of pilot injection....40

3.3 Optimization of heat release rate shape to reduce combustion noise 49
3.3.1 Optimization of heat release rate shape to minimize CNI using Wiebe functions 49
3.3.2 Optimized shapes of heat release rate for minimum CNI....50

Chapter 4. Injection strategies to reduce combustion noise... 57

4.1 Variation of heat release rate shape according to change of injection strategies via experiment 57
4.1.1 Main injection timing 57
4.1.2 Injection pressure....58
4.1.3 Swirl rate....58
4.1.4 EGR rate 58

4.2 Early pilot injection strategy to reduce combustion noise....67
4.2.1 Limitation of conventional diesel combustion....67
4.2.2 PCCI combustion of diesel 67
4.2.3 Early pilot injection combustion....68

Chapter 5. Closed loop control to reduce combustion noise .. 74

5.1 Characteristics of diesel engine noise according to EGR rate change during transient operation 74
5.1.1 EGR rate measurement....74
5.1.2 Combustion noise according to the EGR rate variation....76
5.1.3 CNI variation during transient operations....80

5.1.3.1 Transient operation 1. Speed and load change 80
5.1.3.2 Transient operation 2. Constant speed and load change.........................81

5.2 Concept of control 91

5.3 Control parameters 93
5.3.1 Start of injection 93
5.3.2 Other parameters: Pilot injection quantity, pilot injection timing, injection pressure and EGR rate 99
5.3.3 Interaction among injection parameters...103

5.4 Real time combustion control system to combustion noise.........................110
5.4.1 Overview of real time combustion control system 110
5.4.2 Calculation of CNI...110
5.4.3 Control of injection strategies..111

5.5 Results of the closed loop control 116
5.5.1 Vehicle test...116
5.5.2 Operating conditions and Results 116

Chapter 6. Conclusion.. 122

Bibliography.. 125

국 문 초 록 131

List of Figures

Figure 1.1 Classification of engine noise 4

Figure 1.2 In-cylinder pressure and heat release rate of diesel engine and gasoline engine (Diesel engine: Bore:77.2mm, Stroke:84.5mm, comp. ratio: 17.3, Gasoline engine: Bore & Stroke: 86mm, comp. ratio 10.5) 7

Figure 1.3 Correlation between measured noise and CNI changing injection strategies [39] １１

Figure 2.1 Schematic diagram of engine test and measurement equipment.............15

Figure 2.2 1.6 L Diesel engine 18

Figure 2.3 In-cylinder pressure sensor and glow plug adopter.................................24

Figure 3.1 Process of heat release simulation and pressure reconstruction...............26

Figure 3.2 Heat release rate simulation using three of Wiebe functions 30

Figure 3.3 FFT results of motoring and firing (speed: 1500 rpm, fuel mass: 13.5mg) 35

Figure 3.4 Effects of ‘m’ on combustion noise index...41

Figure 3.5 Effects of SOC on combustion noise index 42

Figure 3.6 Effects of combustion duration on combustion noise index 43

Figure 3.7 Effects of released heat on combustion noise index 44

Figure 3.8 Effect of ratio of premixed and diffusive combustion 45

Figure 3.9 Effects of pilot injection quantity...46

Figure 3.10 Effects of SOC of pilot injection..47

Figure 3.11 Effects of combustion duration of pilot injection..................................48

Figure 3.12 Optimal shape of heat release and pressure curve, 1/3 octave band (1).51

Figure 3.13 Optimal shape of heat release and pressure curve, 1/3 octave band (2).52

Figure 3.14 Optimal shape of heat release and pressure curve, 1/3 octave band (3).53

Figure 4.1 Heat release rate & in-cylinder pressure according to SOI change..........59

Figure 4.2 CNI, PM, NO and BEMP variation according to SOI change (Engine speed: 1500 rpm / fuel mass: 15 mg)...60

Figure 4.3 Heat release rate & in-cylinder pressure according to injection pressure change (Engine speed: 1500 rpm / fuel mass: 15 mg)............................61

Figure 4.4 CNI, PM, NO and BEMP variation according to injection pressure change (Engine speed: 1500 rpm / fuel mass: 15 mg)............................62

Figure 4.5 Heat release rate & in-cylinder pressure according to swirl valve open rate change (Engine speed: 1500 rpm / fuel mass: 15 mg)......................63

Figure 4.6 CNI, PM, NO and BEMP variation according to swirl open rate change (Engine speed: 1500 rpm / fuel mass: 15 mg)...64

Figure 4.7 Heat release rate & in-cylinder pressure according to EGR rate change (Engine speed: 1500 rpm / fuel mass: 15 mg) 65

Figure 4.8 CNI, PM, NO and BEMP variation according to EGR rate change (Engine speed: 1500 rpm / fuel mass: 15 mg) 66

Figure 4.9 Heat release, pressure and 1/3 octave band results of conventional diesel combustion including pilot injections (Engine speed: 1500 rpm / fuel mass: 15 mg) 70

Figure 4.10 Heat release, pressure and 1/3 octave band results of PCCI combustion including pilot injections 71

Figure 4.11 Heat release, pressure and 1/3 octave band results of early pilot injection 72

Figure 5.1 Thermocouples to measure the temperature of the air, the EGR gas and the intake manifold 78

Figure 5.2 In-cylinder pressure and RoHR variation according to EGR rate change79

Figure 5.3 Results of speed and load transient operation, ramp time: 2 s (a) Engine speed, (b) CNI, (c) EGR rate 83

Figure 5.4 Results of speed and load transient operation, ramp time: 5 s (a) Engine speed, (b) CNI, (c) EGR rate 84

Figure 5.5 Results of speed and load transient operation, ramp time: 10 s (a) Engine speed, (b) CNI, (c) EGR rate 85

Figure 5.6 Comparison of pressure and RoHR between transient operation and steady state 86

Figure 5.7 Results of load transient operation, ramp time: 1s (a) Engine speed, (b) CNI, (c) EGR rate....87

Figure 5.8 Results of load transient operation, ramp time: 2s (a) Engine speed, (b) CNI, (c) EGR rate....88

Figure 5.9 Results of load transient operation, ramp time: 5s (a) Engine speed, (b) CNI, (c) EGR rate....89

Figure 5.10 Comparison of pressure and RoHR between transient operation and steady state 90

Figure 5.11 Concept of combustion control using CNI for combustion noise reduction....92

Figure 5.12 CNI variation according to SOI change....94

Figure 5.13 Sensitivity analysis of CNI for SOI change @ 1500 rpm....95

Figure 5.14 Sensitivity analysis of CNI for SOI change @ 2000 rpm....96

Figure 5.15 Heat release rate and in-cylinder pressure according to SOI change @ 1500 rpm 97

Figure 5.16 Heat release rate and in-cylinder pressure according to SOI change @ 1750 rpm 98

Figure 5.17 Sensitivity analysis of CNI for pilot fuel quantity and injection pressure change...101

Figure 5.18 Sensitivity analysis of CNI for pilot timing and EGR rate change......102

Figure 5.19 CNI change when SOI is advanced by 3 CAD...................................105

Figure 5.20 CNI change when Pilot quantity increase by 0.2 mg...........................105

Figure 5.21 CNI change when injection pressure is reduced by 60 bar.................106

Figure 5.22 Arithmetically estimated CNI variation when SOI, pilot quantity and injection pressure are simultaneously changed....................................107

Figure 5.23 Experimental results CNI variation when SOI, pilot quantity and injection pressure are simultaneously changed....................................107

Figure 5.24 Control range using SOI..108

Figure 5.25 Control range using pilot quantity..108

Figure 5.26 Control range using injection pressure..109

Figure 5.27 CNI variation when the control ranges are limited for each parameters 109

Figure 5.28 Schematic diagram of closed loop control system using CNI to reduce combustion noise...113

Figure 5.29 CNI calculation using NI-PXI & LabVIEW.......................................114

Figure 5.30 Combustion control algorithm using ES1000 & ASCET....................115

Figure 5.31 test vehicle, 1.6 liter diesel enigne 118

Figure 5.32 closed loop control system set up in test vehicle 119

Figure 5.33 Transient operation of test for CNI 120

Figure 5.34 Target CNI and current CNI when the control was deactivated........... 120

Figure 5.35 Target CNI and current CNI when the control was activated 121

Figure 5.36 Controlled value of parameters during transient operation.................. 121

List of Tables

Table 2.1 Specifications of dynamometer 16

Table 2.2 Specifications of smoke meter..16

Table 2.3 Measurement principle of emission analyzer (MEXA-7100DEGR).........16

Table 2.4 Specifications of diesel engine 18

Table 2.5 Specifications of NI PXI...22

Table 2.6 Specifications of ES1000..23

Table 2.7 Specifications of in-cylinder pressure sensor 24

Table 3.1 Experiment condition for Validation for the simulation of the heat release rate 30

Table 3.2 Results of validation for the simulation of the heat release rate................31

Table 3.3 Variables for reconstruction of in-cylinder pressure..................................32

Table 3.4 Boundary conditions and optimal values of variables (1) 54

Table 3.5 Boundary conditions and optimal values of variables (2) 55

Table 3.6 Boundary conditions and optimal values of variables (3) 56

Table 4.1 Emissions, IMEP and CNI..73

Table 5.1 Maximum of pressure, pressure rise, RoHR and CNI according to EGR variation......82

Table 5.2 Specifications of test vehicle......118

Acronym

A/F	Air to Fuel ratio
ASCET	Advanced Simulation/Software and Control Engineering Tool
ATDC	After Top Dead Center
BDC	Bottom Dead Center
BMEP	Brake Mean Effective Pressure
BTDC	Before Top Dead Center
CA	Crank Angle
CA50	Crank Angle of 50 % mass fraction fuel burnt
CAFE	Corporate Average Fuel Economy
CAI	Controlled Auto Ignition
CAN	Controller Area Network
CI	Compression Ignition
CPS	Crank Position Sensor
CNI	Combustion Noise Index
DI	Direct Injection
DPF	Diesel Particulate Filter
ECU	Engine Control Unit
EGR	Exhaust Gas Recirculation
EMS	Engine Management System
FFT	Fast Fourier Transform
FS	Full Scale
FSN	Filter Smoke Number
HC	HydroCarbon
HRR	Hear Release Rate

HSDI	High Speed Direct Injection
HT	Heat Transfer
IMEP	Indicated Mean Effective Pressure
IVC	Intake Valve Close
IVO	Intake Valve Open
LTC	Low Temperature Combustion
MFB10	Mass Fraction Burned 10 %
MFB50	Mass Fraction Burned 50 %
MFB90	Mass Fraction Burned 90 %
MIT	Main Injection Timing
NDIR	Non-Dispersive InfraRed Sensor
NOx	Nitrogen Oxide
PCCI	Premixed Charge Compression Ignition
PID	Proportional, Integral and Derivative
PM	Particulate Matter
RPM	Revolution Per Minute
SCR	Selective Catalytic Reduction
SI	Spark Ignition
SOC	Start of Combustion
TDC	Top Dead Center
TDI	Turbocharged Direct Injection
THC	Total Hydrocarbon
UEGO	Universal Exhaust Gas Oxygen
VGT	Variable Geometry Turbine

Chapter 1. Introduction

1.1 Background and Motivation

1.1.1 Motivation

It is important to improve the fuel efficiency of manufactured vehicles because of the strict CO2 emission regulations. Diesel engines have been rapidly substituted for gasoline engines in light duty vehicles due to the potential for lower BSFC. However, diesel engines emit more NOx and PM emissions. Moreover, their noise and vibration are severe. Most countries have emission standard law, and numerous engineers have made an effort to meet them. Many equipment such as, EGR system, DPF, LNT and SCR have been developed and adopted in diesel engines to reduce emissions.[1]

The regulations for noise are usually not as stringent and only the exterior noise is restrained. The interior noise is rarely regulated. However, the interior noise directly affects consumer preference as well as the performance power and the fuel efficiency. When drivers and passengers ride in the vehicle to travel, they are kept in a confined space. Thus, a majority of consumers looks for comfort and reasonably quiet engine noise and vibration. They have requested quiet diesel engines and many efforts have been made to meet such demands.

1.1.2 Engine noise classification

Engine noise is classified into mechanical noise, aerodynamic noise and combustion noise shown in figure 1.1. [2] Mechanical noise which is produced by vibration or impact of motion engine components, includes valve train noise, timing system noise. These sounds are produced by the inertia force of engine components and becomes louder with an increasing speed. It is usually the main noise source during high-speed operations. Aerodynamic noise is mainly emitted by the pressure pulse, flow friction and turbulence of air and exhaust gas during the intake and exhaust processes. The aerodynamic noise could affect pass-by noise as well as the interior noise, however there is a trade-off between a reduction of the noise and an improvement of volumetric efficiency. The combustion noise is generated by the combustion process in cylinders. The combustion noise can be broken down into direct and indirect combustion noise. [3]

The direct combustion noise can be defined as the structure-borne noise originated by the gas pressure change in the combustion chambers. The direct combustion noise is radiated throughout the piston, the connecting rods, the crank shaft and the engine block. The rapid pressure change in the cylinder impacts the cylinder walls and makes a dynamic load on the engine parts. Moreover, a local pressure rise in the combustion chamber produces an impulsive pressure wave. The pressure wave then creates a high frequency oscillation through many reflections in the cylinder. [4]

The indirect combustion noise is not excited by the gas pressure but influenced by the combustion characteristics. The indirect combustion includes piston noise, crank shaft noise and the main bearing noise. The piston noise is the most dominant.

The piston impacts the cylinder wall through the secondary motion. This occurs especially when the direction of the piston movement is downward around TDC. The contacted wall side then changes to the opposite side, the piston strikes the cylinder wall and a harsh noise is generated. The secondary motion of the piston impacts the wall 2 ~ 10 times in each cycle and the noise level increases with the in-cylinder pressure increase. [3-9]

The combustion noise occurs at mid and high frequencies, which are both sensitive regions for human ears. The noise adversely affects the sound quality of a diesel engine. The combustion noise needs to be reduced through a combustion optimization.

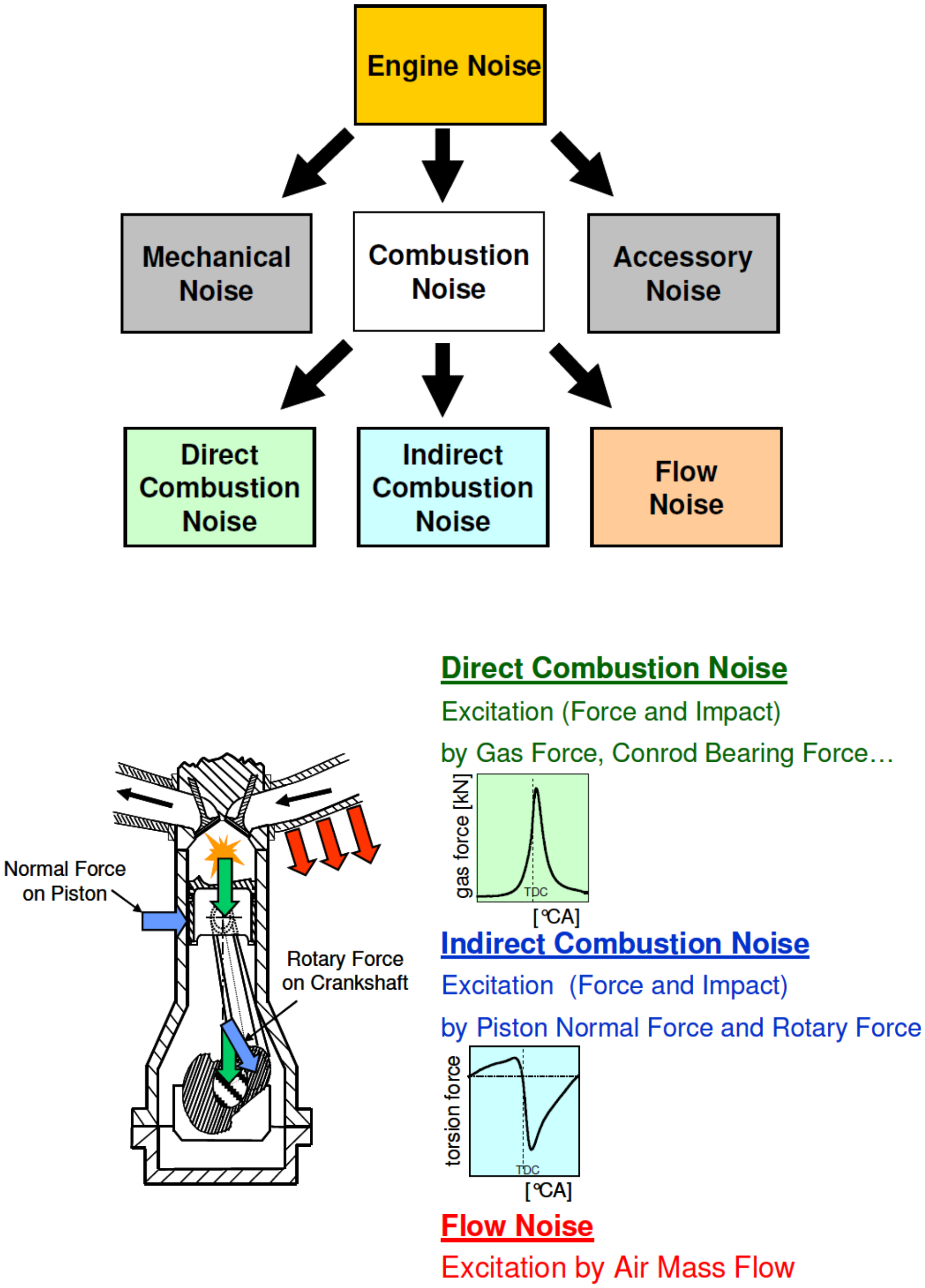
Engine Noise
Mechanical Noise
Combustion Noise
Accessory Noise
Direct Combustion Noise
Indirect Combustion Noise
Flow Noise
Normal Force on Piston
Rotary Force on Crankshaft
Direct Combustion Noise
Excitation (Force and Impact)
by Gas Force, Conrod Bearing Force…
gas force [kN]
TDC
[°CA]
Indirect Combustion Noise
Excitation (Force and Impact)
by Piston Normal Force and Rotary Force
torsion force
TDC
[°CA]
Flow Noise
Excitation by Air Mass Flow

Figure 1.1 Classification of engine noise [3]

1.1.3 Relation between engine noise and combustion

The combustion noise of diesel engine is usually louder than that of a gasoline engine due to a higher maximum in-cylinder pressure and the rapid pressure rise. Diesel engine has a higher compression ratio in order to improve thermal efficiency and combustion stability for auto-ignition. The rapid pressure rise originates from the rapid combustion in the early process of diesel combustion, which is the premixed combustion phase. Figure 1.2 shows the in-cylinder pressures and heat release rate of a diesel engine and a gasoline engine.

Diesel combustion consists of ignition delay, premixed combustion, mixing control combustion and late combustion. The injected fuel at high in-cylinder temperature and pressure undergoes both a chemical ignition delay and a physical ignition delay to be atomized, vaporized, and mixed with air. After the delay, auto-ignition is commenced, and some of fuel mixed air is simultaneously combusted; the combustion chamber suffers from a rapid rise in pressure. The dynamic load excites the cylinder wall and the piston; therefore, the vibration is transferred via the connecting rod, the crank shaft and the engine block. If more fuel is combusted in the premixed combustion phase, the combustion chamber will experience a higher dynamic load caused by a rapid pressure rise. As a result, more combustion noise will be generated. The ignition delay is a main parameter to affect the combustion noise emission, because the longer ignition delay supplies the more time to be prepared to be combusted.

Ignition delay is affected by the temperature, pressure and oxygen concentration in a cylinder. Thus, the compression ratio, injection timing and engine load which affect in-cylinder air temperature and pressure, are directly correlated. The higher compression ratio increases temperature and pressure. Injection timing can change the in-cylinder pressure temperature and pressure when fuel injection starts; a too early or a too late injection can increase the ignition delay. The higher engine load leads to a temperature increase of the cylinder wall, the piston and the EGR gas, which can make the in-cylinder temperature and pressure higher. In addition, the delay is affected by the oxygen concentration. The high level EGR rate to reduce NOx emission increases the ignition delay by reducing the concentration. The combustion noise is mainly generated at low- and mid-engine speeds and loads that are related to long ignition delays due to deceased oxygen concentration with higher EGR rate level. [10-17]

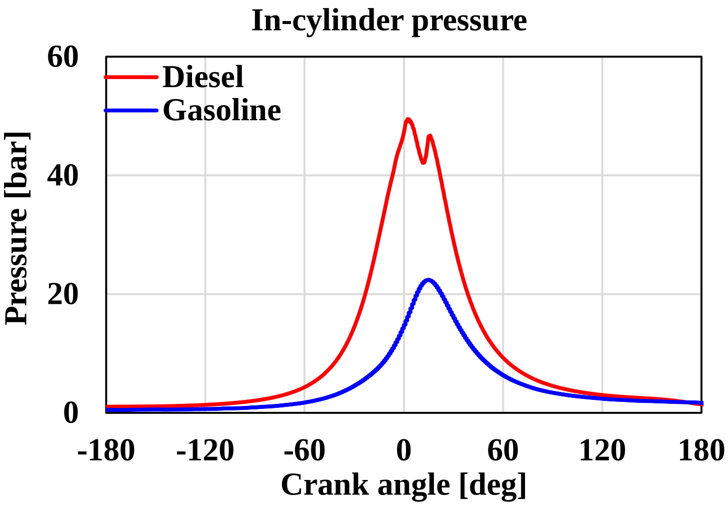

(a) In-cylinder pressure of gasoline engine and diesel engine

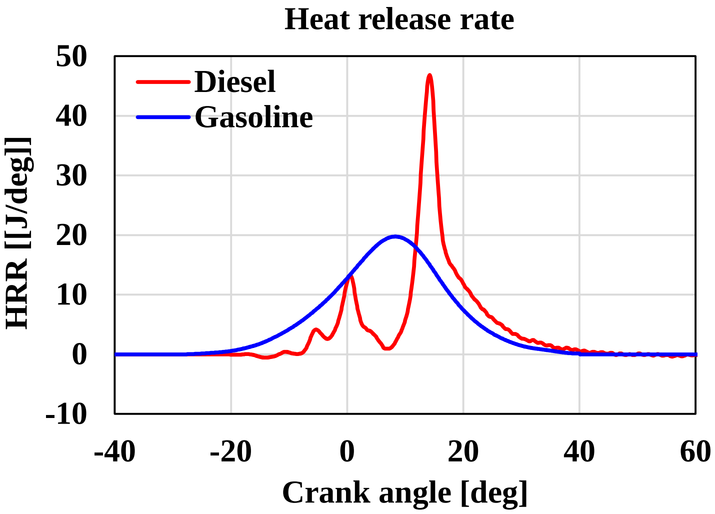

(b) Heat release rate of gasoline engine and diesel engine

Figure 1.2 In-cylinder pressure and heat release rate of diesel engine and gasoline engine (Diesel engine: Bore:77.2mm, Stroke:84.5mm, comp. ratio: 17.3, Gasoline engine: Bore & Stroke: 86mm, comp. ratio 10.5)

1.1.4 Reduction of combustion noise

The rapid pressure rise in cylinder is a source of combustion noise and it is caused by the rapid combustion. Thus, it is important to make the combustion speed slow in order to reduce combustion noise. As referred above, a rapid combustion in the premixed combustion phase in diesel engine combustion process, thus more fuel is burned, more rapid combustion is occurred.

Pilot injection is an effective way to reduce combustion noise because the combustion of pilot injection causes increasing temperature and pressure in the combustion chamber and shortens the ignition delay of the main injection when it starts. As a result, the amount of fuel injected during the ignition delay is greatly reduced and a smoother increase of in-cylinder pressure is obtained. The common rail system enables the control injection strategy such as injection number, pressure and timing. As a result, pilot injection could be applied to reduce the combustion noise. [18-23]

The other way to reduce the fuel quantity combusted in the premixed phase is to reduce the injection quantity of fuel. The rate shaping is an injection system which can control the injection rate. In the early process of injection, the rate is controlled to be reduced, after SOC the injection rate increase to inject target fuel quantity. As a result, the heat release rate could be controlled not to be harsh. Digital rate shaping is able to control the burning rate. Using the special injectors which have a very short dwell time, many injections are occurred instead of a conventional main injection. As a result, the fuel quantity, which is burned rapidly, reduces and the heat release rate can be kept a moderate level. [24-28]

1.1.5 Noise evaluation method

1.1.5.1 Engine noise evaluation method

The engine noise measurements require an expensive facility for testing, such as an anechoic room and microphones. Moreover, the separation of the combustion noise is difficult work. To overcome the shortage, the method using the in-cylinder pressure has been introduced. The pressure curve, the exciting source, is transferred through the engine parts and emitted from the block surface. In this process, the original excitation is attenuated according to the transfer characteristics of the parts. Both the pressure curve and the transfer characteristics can be presented as a function of frequency. If the attenuation characteristics are known and the in-cylinder pressure is measured, the noise can be estimated. Another method to evaluate noise via the in-cylinder pressure signal is using the regression equation of the variables that are the dominant parameters for combustion noise intensity such as the maximum pressure, the maximum pressure rise. These are effective evaluation techniques for research and development on improving combustion noise because engine noise can accurately and simply be estimated by measuring the in-cylinder pressure. [29-37]

1.1.5.2 Combustion noise index (CNI)

The engine noise has to be measured in a free field above a reflecting plane to obtain reliable results. However, the facility is expensive and needs a large space. Moreover, the many dynamometers which were previously used in facilities were not the correct type for transient testing. Thus, evaluation methodologies using in-cylinder pressure sensors instead of microphones have been developed. [38] In this study, the CNI was used for the combustion noise evaluation, which was introduced by Jung et al. The in-cylinder signal, functions of time, was converted to functions of frequency by the FFT. Then, the CNI was calculated through the summation of the 1~3.15 kHz range of the one third octave band level. The frequency range has a strong correlation with the combustion noise. Each octave band values are summed using a logarithm (equation 8). Actually, the CNI could not accurately evaluate the noise like as measuring with microphones. However, the CNI is able to represent the combustion noise level because the tendencies of the relation between the CNI and the combustion noise level are consistent. As shown in figure 1.3, the CNI has a good correlation with the measured combustion noise for broad sound level. Moreover, the correlation was kept even throughout the injection parameter change. Therefore, a relative comparison is possible, though an absolute comparison is difficult to achieve using the CNI. [39]

$$CNI(dB) = 10\log(10^{1kHz\,level/10} + 10^{1.25kHz\,level/10} + \cdots + 10^{3.15kHz\,level/10}) \qquad (1.1)$$

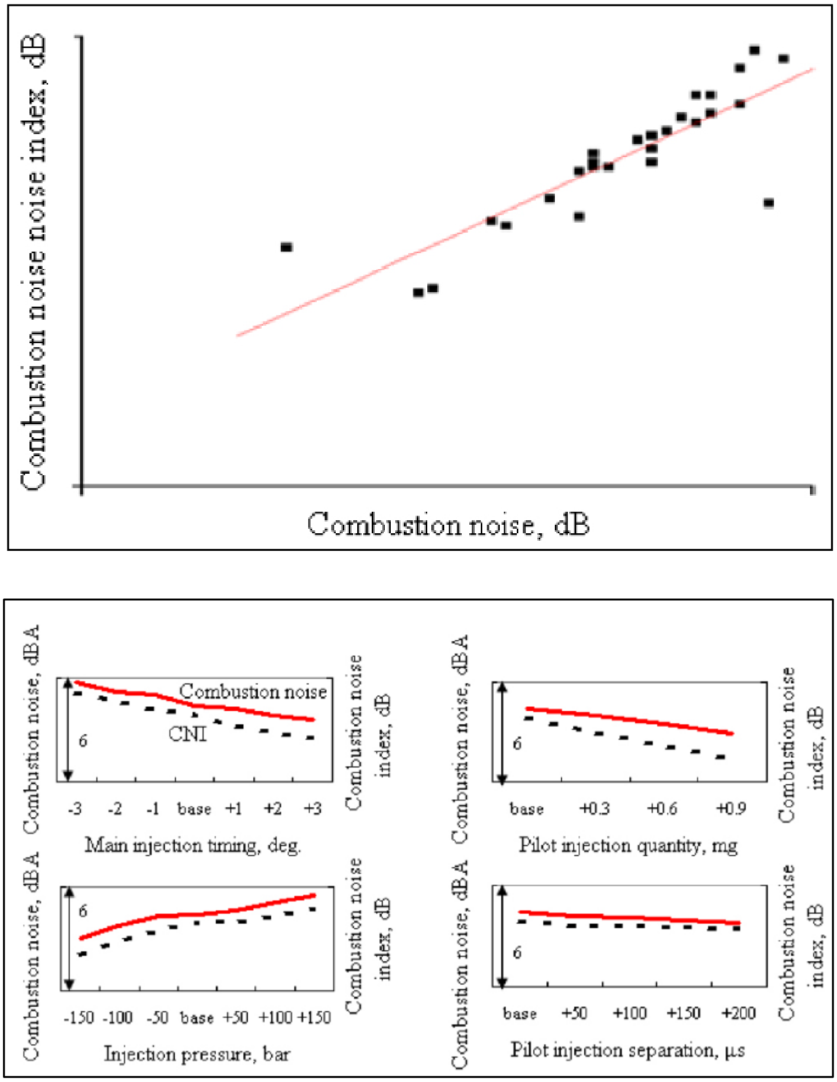

Figure 1.3 Correlation between measured noise and CNI changing injection strategies [39]

1.1.6 Closed loop control

The control of modern Diesel engines involves a large number of parameters, such as the start of injection, the EGR rate, the injection pressure, and the fuel quantity, etc. These parameters must be controlled for the engine to be operated in an optimal state. Some of these parameters are controlled in open-loop control, and others are controlled in closed-loop control mode. Open-loop control provides a fast response and a relatively easy control. However, it cannot handle changes in state caused by variating conditions such as aging of the injectors and fuel quality. On the other hand, closed-loop control monitors the present state so that any changes in conditions can be considered in the control mechanism. For Diesel engines, many studies have utilized closed-loop control with the closed loop collecting combustion state information as feedback. Combustion state information can be obtained directly from the in-cylinder pressure or indirectly from the combustion noise and vibration. For an indirect method, an accelerometer is used to measure vibration from the engine head or the surface of blocks and information can be obtained from these signals. This method is economically affordable due to the fact that combustion information of multi cylinders can be extracted by one accelerometer but obtainable information is limited and signals can be distorted by any noise source. Using the in-cylinder pressure is the most reliable method as well as a direct method. The rate of heat release (RoHR) can be calculated from the pressure data, and then a combustion parameter of interest, such as the 50 % mass fraction burned (MFB50), start of combustion (SOC) or the location of peak pressure (LPP), can be calculated from the RoHR. The control parameters are adjusted to set a target value for the combustion parameters. [40-42]

1.2 Objectives

The purpose of the present study is to look for a methodology to reduce combustion noise in diesel engines. In this study, the relation between diesel engine combustion and combustion noise was examined. Especially, the effects of the shape of heat release rate on the excitations, which were caused by in-cylinder pressure change, were investigated. In addition, the closed loop control system for the noise reduction was developed.

The detailed objectives of this study are :

1. Investigating effect of heat release rate shape on excitation which is generated by in-cylinder pressure change
2. Looking for the optimal shape to decrease the excitation
3. Evaluating effects of changes of injection strategies on heat release shape and the excitation
4. Looking for the injection strategies to reduce combustion noise
5. Examining CNI characteristics change during transient operations
6. A development of closed loop control system using combustion noise index for reduction of the noise

Chapter 2. Experimental Apparatus

2.1 Overall configuration

In this chapter, the experimental apparatus and test engine are introduced. The figure 2.1 shows the schematic diagram of them.

2.1.1 Engine test bench cell

The engine test was conducted in a test bench cell equipped with dynamometer, coolant controller, air conditioner, fuel controller and fuel meter. The engine was coupled with a 340 kW AC dynamometer to control revolution speed and torque for steady operations and transient operations. The specifications of the dynamometer is shown in Table 2.1. In the facility, the air temperature was controlled at 25℃. The coolant temperature of the engine was controlled at 90℃ during the experiment. The diesel fuel temperature was also controlled at 40 °C.

2.1.2 Measurement of exhaust gas emissions

The composition of exhaust gas were measured during the test. Concentration of O2, CO2, NOx, THC and CO were measured by the exhaust gas analyzer (HORIBA, MEXA-7100DEGR). PM was measured by a smoke meter. Tables 2.2 and 2.3 show the specifications of smoke meter and the exhaust gas analyzer (HORIBA, MEXA-7100DEGR). All species measured by the gas analyzer were measured in volume fraction (vol % / ppm) in the wet condition and the PM was measured in FSN (Filtered Smoke Number).

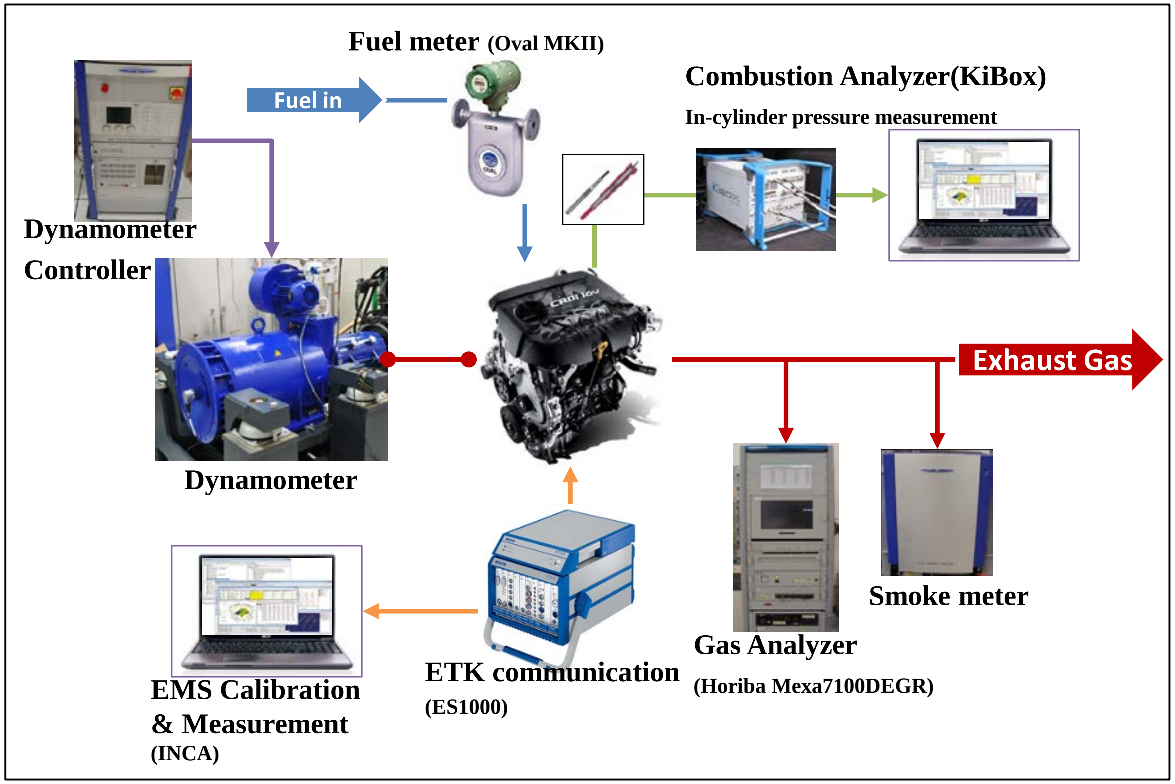
Fuel meter (Oval MKII)
Fuel in
Combustion Analyzer(KiBox)
In-cylinder pressure measurement
Dynamometer Controller
Dynamometer
Exhaust Gas
Smoke meter
Gas Analyzer
(Horiba Mexa7100DEGR)
ETK communication
(ES1000)
EMS Calibration & Measurement
(INCA)

Figure 2.1 Schematic diagram of engine test and measurement equipment

Table 2.1 Specifications of dynamometer

Item	Specification
Manufacturer	AVL
Model	PUMA 1.3 Test Automation system
Capacity	340 kW
Type	AC
Cooling	Air cooling

Table 2.2 Specifications of smoke meter

Item	Specification
Manufacturer	AVL
Model	AVL 415S
Measurement range	0 ~ 10 FSN / 0 ~ 32,000 mg/m³
Resolution	0.001 FSN / 0.01 mg/m³
Repeatability (as standard deviation)	$\sigma \leq \pm$(0.005 FSN + 3 % of measured value)
Reproducibility (as standard deviation)	$\sigma \leq \pm$(0.005 FSN + 6 % of measured value)

Table 2.3 Measurement principle of emission analyzer (MEXA-7100DEGR)

Emissions	Measurement principle
NOx	Chemiluminecent Detector
THC	Flame Ionization Detector
O_2, CO_2, CO	Non Dispersive Infrared Rays

2.2 Multi-cylinder Diesel engine

For this research, an in-line 4 cylinder 1.6 L Diesel engine was used. Figure 2.2 shows the target engine in this study. This engine has fuel injection equipment including solenoide type injector, common rail and high pressure pump, which enable injection pressure up to 1600 bar. A VGT(variable geometry turbocharger), a oxidation catalyst and DPF(Diesel Particle Filter) also were equipped. Detailed specifications of the engine is shown in Table 2.4.

Figure 2.2 1.6 L Diesel engine

Table 2.4 Specifications of diesel engine

Criteria	Specification
Layout	In-line 4 cylinder
Displacement volume	1582 cc
Max power	94 kW @ 4000 rpm
Max torque	26.5 kg.m @ 1900~2750 rpm
Bore	77.2 mm
Stroke	84.5 mm
Connecting rod	140 mm
Compression ratio	17.3
Fuel injector type	Solenoid type
ECU version	EDC 17

2.3 Combustion control system

Combustion control system consisted of a combustion analyzer and a combustion controller. The combustion analyzer calculated combustion noise index by using in-cylinder pressure signal and crank position signal. To calculate the combustion noise index in real-time for each cycle, a NI-PXI, which can measure analog signals with fast sampling rate and handle huge data processing, was used. The software was developed in LabVIEW. The combustion controller was developed using ES1000, which is a rapid prototype controller, because it can easily read and write values of the control parameters of ECU memory by ETK communication. The software was developed in ASCET. The calculated combustion noise index in NI-PXI was transferred to combustion controller using CAN bus communication.

2.3.1 NI-PXI

PXI is a rugged PC-based platform for measurement and automation systems. PXI combines PCI electrical-bus features with the modular, Eurocard packaging of CompactPCI and then adds specialized synchronization buses and key software features. The system which was used in this study included real time controller (NI PXI-8119), FPGA board (NI PXI-7842) and CNI bus communication board (NI PXI-8461). The pressure signal and CPS signal were measured using analog input channels of the FPGA board. The measured signals was passed on real-time controller through FIFO. The CNI was calculated in the real time controller and the result was sent by the CAN bus board to combustion controller, ES-1000. Figure 2.3 shows the NI-PXI. The detailed specifications are shown in table2.5

2.3.2 ES-1000

The combustion controller was developed using an ES1000. The ES1000 was a platform which consists of various function boards. In this research, a simulation board, CAN bus communication board, analog input board and ETK communication board were used. The simulation board is a rapid prototype controller which has real-time OS. It operates the combustion control algorithm which was developed in ASCET. The CAN bus communication board was used for data transfer from NI-PXI. ETK communication board was used to read and write values of ECU engine operating parameters. The combustion control algorithm was coded by using ASCET. ASCET is a model-based development of application software for embedded systems. It was designed to develop software for the automotive industry. The application software can be coded using block diagrams, state machine and C code and automatic code generation for rapid prototype is accessible.

2.3.3 Pressure sensor

The in-cylinder pressure measurement is an important part because combustion noise index was calculated by using the measurement. Therefore, the quality of the combustion control was determined by a great extent of the quality of the measured in-cylinder pressure signal. The pressure was measured by using a pressure sensor, Kistler type-6056. The sensor was installed using a glow plug adopter, which has a shape of a glowplug, and it was mounted in the 1st cylinder instead of the glowplug.

The charge signal from the sensor was converted to analog voltage signal through a charge amplifier. The converted signal was measured by the FPGA board of NI-PXI.

Table 2.5 Specifications of NI PXI

Criteria	Specification
PXI Controller Board (NI PXI-8119)	2.3 GHz quad-core Intel Core i7-3610QE processor 4GB, 1600 MHz DDR3 RAM
FPGA board (NI PXI-7842R)	8 analog inputs, independent sampling rates up to 200 kHz, 16-bit resolution, ±10 V 8 analog outputs, independent update rates up to 1 MHz, 16-bit resolution, ±10 V 96 digital lines configurable as inputs, outputs, counters, or custom logic at rates up to 40 MHz Virtex-5 LX50 FPGA programmable FPGA Module 3 DMA channels for high-speed data streaming
CAN board (NI PXI-8461/2)	2 CH, 1 MBit/s

Table 2.6 Specifications of ES1000

Criteria		Specification
Simulation Board	CPU	1 GHz
	RAM	256 MB SDRAM
A/D board		16 CH, 100 kHz/CH
D/A board		8 CH
Digital and PWM I/O board	Channel	16 CH input, 16 CH output 2 external trigger
	Frequency	1 Hz to 60 kHz
CAN Communication		4 CAN signal
ETK Communication		1 CH, 100 MBit/s

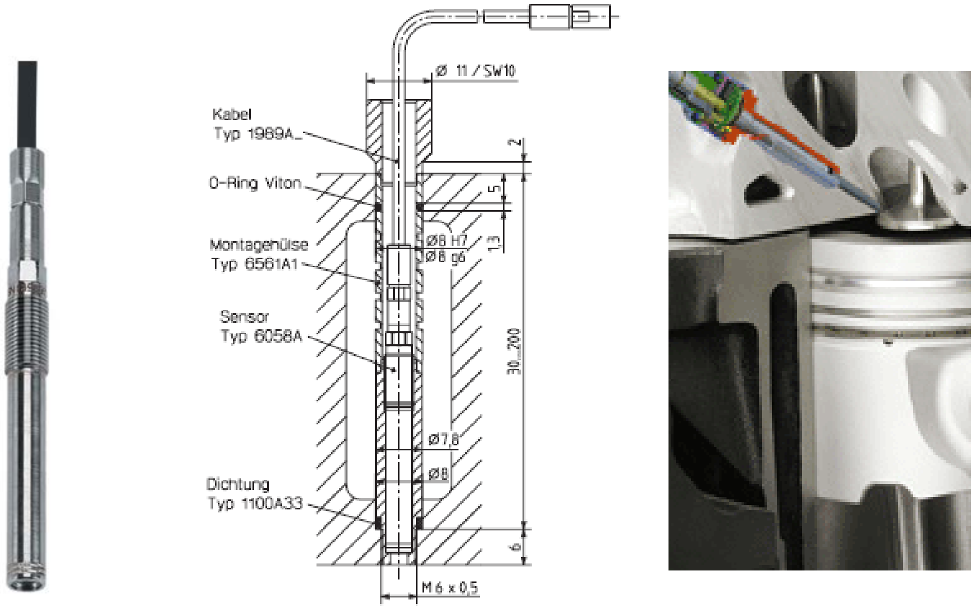
Ø 11 / SW10
Kabel
Typ 1989A
O-Ring Viton
Montagehülse
Typ 6561A1
Sensor
Typ 6058A
Dichtung
Typ 1100A33
Ø8 H7
Ø8 g6
Ø7,8
Ø8
2
5
13
30...200
6
M 6 x 0,5

Figure 2.3 In-cylinder pressure sensor and glow plug adopter

Table 2.7 Specifications of in-cylinder pressure sensor

Criteria	Specification
Measuring range	0~250 bar
Sensitivity	20 pC/bar
Operating temperature range	-20~350 ºC
Sensitivity shift	≤ ± 0.5%
Short term drift	≤ ± 0.5% bar
Weight with cable	30 g

Chapter 3. Relation between diesel combustion and combustion noise

3.1 Simulation of heat release rate using Wiebe functions

The in-cylinder pressure variation, which is the main source of combustion noise, was produced by the heat released from burning fuel. Thus, the shape of heat release rate directly affects combustion noise. However, it is very difficult to evaluate effect of shapes on combustion noise by experimentally changing them. Most of combustion control parameters, such as the pilot injection, boost pressure, SOC and compression ratio, are strongly dependent and affect the shape of heat release rate. Thus, the heat release rate was simulated using Wiebe function to unconstrainedly change the shape. In this chapter, the effects of shape of heat release rate on combustion noise index were examined and the better shapes of heat release rate to reduce the combustion noise were found by using the Wiebe function. The figure 3.1 shows the process of heat release rate simulation and pressure Diesel combustion and Wiebe function.

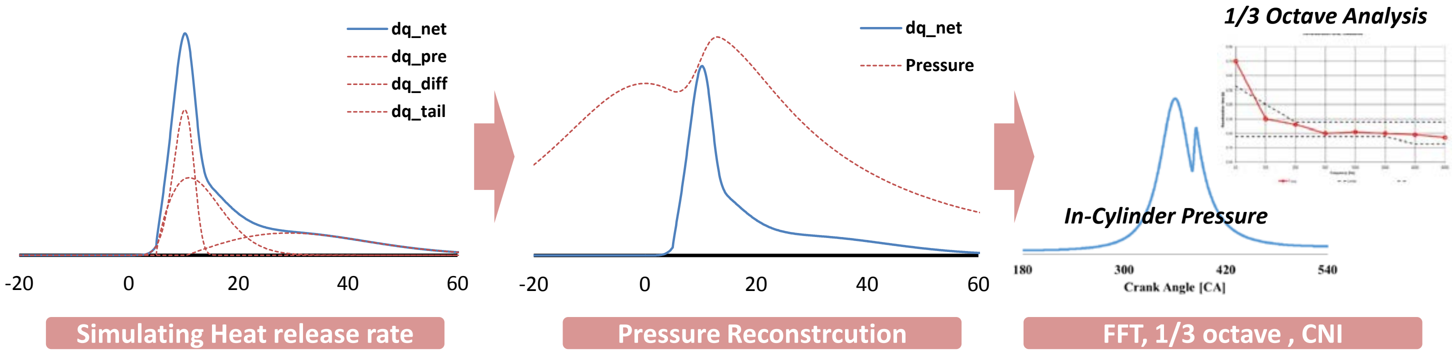

Figure 3.1 Process of heat release simulation and pressure reconstruction

The Wiebe function has been used to predict the pressure curve and temperatures in many other researches. The equation (3.1) shows the Wiebe function. The coefficient 'a' and 'm' are related to combustion characteristics and '$\theta_{duration}$' means the combustion duration. Since the function converges to 1, the total heat can be multiplied. The equation (3.2) shows heat release per crank angle degree when the total heat is Q_{total}.

$$\mathrm{X} = 1 - \exp\left[-a \cdot \frac{\theta-\theta_{soc}}{\theta_{duration}}^{m+1}\right] \tag{3.1}$$

$$\frac{dQ}{d\theta} = a \cdot (m+1) \cdot \left(\frac{Q_{total}}{\theta_{duration}}\right) \cdot \left(\frac{(\theta-\theta_{soc})}{\theta_{duration}}\right)^{m} \cdot \left(exp\left[-a \cdot \left(\frac{(\theta-\theta_{i})}{\theta_{duration}}\right)^{m+1}\right]\right) \tag{3.2}$$

The diesel engine combustion can be divided into 3 phases, which are premixed combustion, mixing controlled combustion and late combustion. Each phase has different characteristics, start timing of combustion, burning rate and combustion duration. The rapid combustions were shown during the short period in premixed combustion phase. On the other hand, diffusive combustion has a relatively long combustion duration because it needs extra time to be mixed with air. Therefore, simulating diesel combustion using single Wiebe function was hard to be coincided with the experimental results. Thus, Ghojel at el. used double Wiebe function to describe the premixed combustion and diffusive combustion independently [43]. However, since the late combustion has a much longer combustion period than the mixing controlled combustion, they have to be considered separately to improve the accuracy of the simulation. Hence, three of Wiebe function were used to simulate diesel combustion in this study. They can be summed linearly, thus the equation is shown as equations (3.3) and (3.4). [44-46]

$$\mathrm{X} = \sum_i 1 - \exp\left[-a_i \cdot \frac{\theta-\theta_{i,soc}}{\theta_{i,duration}}^{m_i+1}\right] \tag{3.3}$$

$$\frac{dQ}{d\theta} = \sum_i a_i \cdot (m_i + 1) \cdot \left(\frac{Q_{i,total}}{\theta_{i,duration}}\right) \cdot \left(\frac{(\theta-\theta_{i,soc})}{\theta_{i,duration}}\right)^{m_i} \cdot \left(exp\left[-a\left(\frac{(\theta-\theta_i)}{\theta_{i,duration}}\right)^{m_i+1}\right]\right) \tag{3.4}$$

3.1.1 Validation for the simulation of the heat release rate

The simulated heat release rate curves were compared with the experiment results. The experimental cases are shown Table 3.1. The engine speed was 1500 rpm and fuel quantity was 15 mg. To find a variation of heat release rate when the injection strategies are changed. The parameters, SOI, injection pressure, swirl intensity and EGR rate, which are used to affect combustion characteristics, were changed. The heat release rates were calculated by equation (3.5). Note that heat transfer was not considered.

$$\frac{dQ}{d\theta} = \left(\frac{\gamma}{\gamma-1}\right) p \frac{dV}{d\theta} + \frac{1}{\gamma-1} V \frac{dP}{d\theta} \tag{3.5}$$

The Wiebe functions were fitted to experimental heat release rates. The fitting was executed for only the main combustion, thought the double pilot injection were included in the experimental results. Figure 3.1 shows the results of fitting. The Wiebe functions were able to describe real heat release rate. Table 3.1 shows coefficients values. One wiebe function has five coefficients, thus triple Wiebe function has 15 coefficients. To minimize the difference of the simulated heat release rate and the real heat release rate, 'fmincon' function of Matlab was used. Table 3.2 shows the results of validation. '$m_{premixed}$' was varied from 2.44 to 5, 'm_{mixing}' from 0.4 to 0.8 and m_{late} 'was not significantly varied; however, the variation was just about 1. '$\theta_{premixed,duration}$' was varied from 11.9 to 14.5, '$\theta_{premixed,duration}$' from 25.8 to 29.2 and '$\theta_{late,duration}$' from 62.2 to 70. 91.

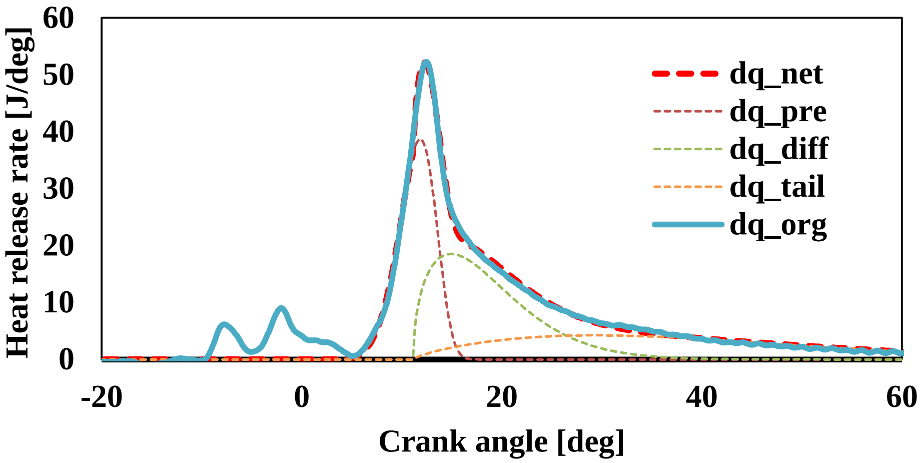

Figure 3.2 Heat release rate simulation using three of Wiebe functions

Table 3.1 Experiment condition for Validation for the simulation of the heat release rate

Injection Parameter	Variation
Main Fuel Quantity	±1.5 mg
Main Injection Timing	±3 *CAD*
Injection pressure	±100 *bar*
Swirl valve	+ 20%p / + 40%p
Pilot Quantity	±0.3 mg
Pilot Injection Timing	+2 / +4
EGR rate	± 5%p

Table 3.2 Results of validation for the simulation of the heat release rate

		Coefficients of Wiebe function					
		A	m	SOC	Duration	Q	Q ratio
Premixed	Low	6.7	2.1	1.7	11.2	437	0.3
	Upper	7.1	5	7.1	14.6	533	0.4
Diffusion	Low	7	0.4	5.5	23.1	437	0.3
	Upper	7	0.8	15	29.4	533	0.4
Tail	Low	7	0.7	5.5	61.7	437	0.4
	Upper	7	1.2	15	69.2	533	0.2

3.1.2 Pressure reconstruction using Wiebe functions

Pressure curve was reconstructed by changing the shape of heat release rate to evaluate the excitation intensity caused by the combustion in a cylinder. To reconstruct the pressure curve using heat release rate, an inverse operation of equation 3.5 was used. The used values of parameters are shown in table 3.3. The engine geometries are the same from the engine used and γ was 1.3. The heat loss occurred by heat transfer was not considered. After attaining the pressure curve, the heat release rate was calculated again to compare the original heat release rate. The two curves of heat release rate were almost identical.

Table 3.3 Variables for reconstruction of in-cylinder pressure

Variables	Value
Bore	77.2 mm
Stroke	84.5 mm
Connecting rod length	140 mm
Compression ratio	17.3
Specific heat	1.3

3.2 Effect of heat release rate shape on combustion noise : Analysis of excitation of in-cylinder pressure changing Wiebe functions coefficients

Fast Fourier Transform (FFT) was used to analyze the excitation by in-cylinder pressure. For the FFT analysis, the time base pressure data, which are measured with the same time interval were needed. However, the reconstructed pressure curves were angle based data with the same crank angle interval. In real engines, the angular velocity is not constant but it oscillates according to the strokes. In this study, the oscillation was not considered and the angular velocity was assumed as a constant. Thus, the time based pressure data were calculated from an interpolation of angle base data. The results of FFT were varied accordingly to the sample number. Thus, when the engine speed is changed, the sample number of one cycle should also be changed. Considering that, FFT was calculated with 50 % overlap for 10 cycles. The sample number was 4096 and hanning windows was applied to get rid of the unexpected noise. The one third-octave band was also used to analysis of frequency of in-cylinder pressure excitation. Moreover, to evaluate the combustion noise, the CNI was calculated.

3.2.1 Comparing motoring pressure and combustion pressure

The combustion noise was mainly generated by in-cylinder pressure change. There are two main cause for the pressure changes. The first one is the compression and expansion process of a piston. The other one is a combustion process. Thus the effects of them on excitation were analyzed separately. Figure 3.2 shows the combustion pressure, motoring pressure and the difference of them. The difference was calculated by subtracting the motoring pressure from the combustion pressure. Figure 3.3 shows the results of FFT of them. The FFT results of the motoring pressure converges to zero above 400 Hz. Moreover, above 400 Hz, the FFT results of combustion pressure and the pressure difference are almost the same. Therefore, the compression and expansion processes affect only below 400 Hz, and the combustion process only affects frequency above 400 Hz because the signals were superimposed. Therefore, it can be concluded that the frequency signals of above 400 Hz were generated by the combustion phenomenon.

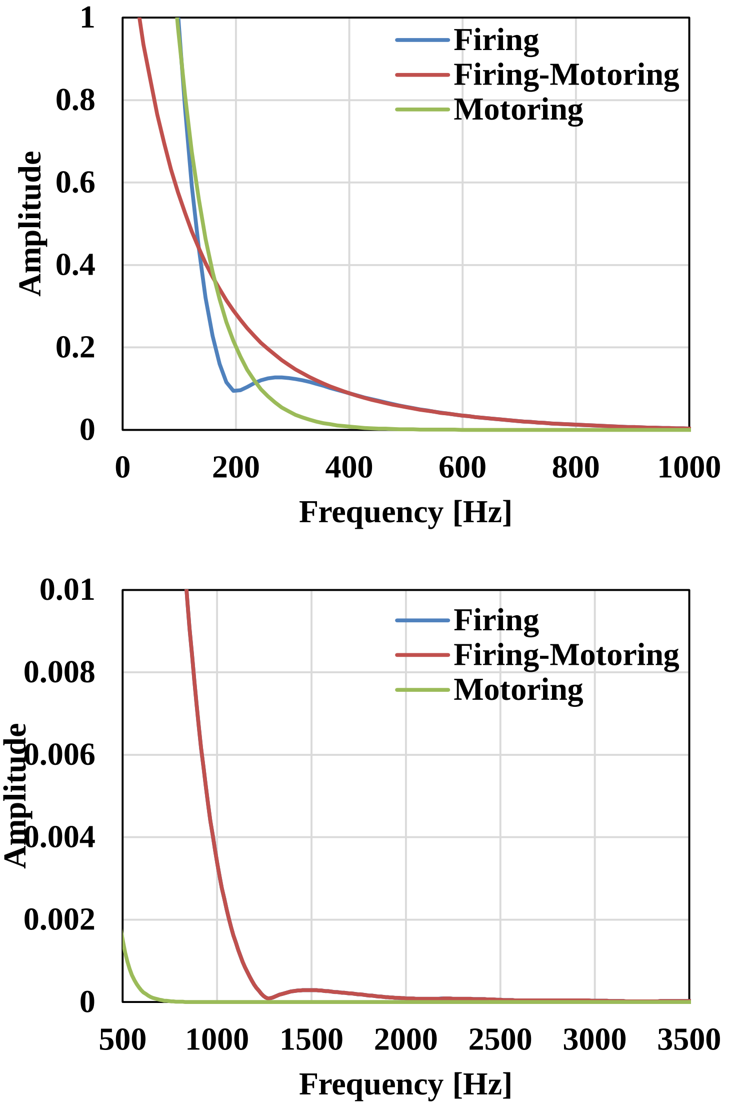

Figure 3.3 FFT results of motoring and firing (speed: 1500 rpm, fuel mass: 13.5mg)

3.2.2 Effects of Single Wiebe function shape on combustion noise

One Wiebe function has 5 coefficients and each coefficient determines the shape of a function. In this chapter, effects of a Wiebe function shape on combustion noise by changing the coefficients are invested. The coefficient ‘a’ and ‘m’ affect the burning rate. When the ‘a’ is increased, the combustion is proceeded rapidly. When the ‘m’ is decreased, more fuel is burned early with the same combustion duration. ‘$\theta_{duration}$’ means combustion duration and θ_{soc} means the crank angle of the combustion initiation. Since the function converges to 1, the total heat release can be multiplied to apply the total heat release quantity.

3.2.2.1 Effects of coefficient ‘a’

When ‘a’ is increased, more fuel is burned in the early stage of combustion duration. Thus, the heat release rate also increases and a rapid pressure rise occurs.

3.2.2.2 Effects of coefficient ‘m’

As ‘m’ is increased, more fuel is combusted in the late stage of combustion duration and as ‘m’ is decreased, more fuel is burned prematurely (figure 3.4). When ‘m’ decreased, the heat release rate became sharp and higher. It caused a rapid pressure rise. The in-cylinder pressure also became higher because the combustion phase was advanced. However, when ‘m’ was increased, more burned fuel was combusted in an early period and it caused a higher heat release rate and a rapid pressure rise. However, because the combustion phase was retarded, the in-cylinder pressure did not increase much. Since, the pressure rise made the CNI increase, when ‘m’ was 2; the CNI was at a minimum value. When ‘m’ was 3; the CNI slightly increased. On the other hand, frequency above 1.6 kHz decreased. Thus, it is concluded that when ‘m’ has a value between 2 and 3 the excitation of in-cylinder pressure is the weakest.

3.2.2.3 Effects of combustion duration

The effects of combustion duration were investigated here. Figure 3.6 shows the variation of pressure, heat release rate and excitations. To minimize effects of other parameters, the combustion phases of them were fixed. When the combustion duration became short, the heat release rate became higher because the total released heat are the same. It makes a rapid pressure rise. The 1/3 octave band results show that levels are increased in all frequency band. It means that the combustion duration have to be long to reduce the combustion noise. However, because it has a trade off with IMEP, it has to be optimized for real engineering.

3.2.2.4 Effects of start of combustion

The effects of SOC were investigated and the results are shown in figure 3.5. When the same heat is released, if the volume of the combustion chamber was changed, then the in-cylinder pressure also changes. Thus, when the SOC was changed, the corresponding volume also changed. The SOC was changed with the same shape of heat release rate showin in Figure 3.5. The pressure level increased when the SOC was advanced and the IMEP was increased as well. It was clearer with the apparent heat release rate. When the SOC was advanced, the apparent heat release rate shapes were not changed much, only the scales were changed. Additionally, the important thing was that the number of in-cylinder pressure peak could not affect excitation. Though, when SOC was 3° ATDC, in-cylinder pressure had 2 peaks and when SOC was 3° BTDC, in-cylinder pressure had one peak, however, they had similar apparent heat release rate shapes. The FFT, 1/3 octave band and CNI were not varied much when the SOC were changed. However, because IMEP was significantly changed, when the optimal shape of heat release rate is determined, the SOC was able to be separately optimized to improve IMEP, though when the SOC was changed, the heat release rate shape was also changed in real engine experiment.

3.2.2.5 Effects of total released heat

When the total heat quantities were changed with other fixed parameters, results are shown in Figure 3.7. They look similar to the variations of combustion duration. It was because that increased heat cause increase the maximum value of heat release rate, thus, it caused a rapid pressure rise. FFT and 1/3 octave band showed an increase in all frequency regions.

3.2.3 Effects of mixing controlled phase

After fuel injection, some of the injected fuel were mixed with air during an ignition delay, and they were burned rapidly in the premixed combustion phase. With the more burned fuel in the premixed combustion, the heat release rate became much sharper in the early stage of the total combustion duration shown in Figure 3.8. It led to an increase in pressure peak. In addition, as the burned fuel in the premixed combustion phase increased, 1 kHz frequency level was increased. However, frequency over 1.6 kHz decreased. It is because the pressure peak is affected under 1 kHz frequency and the ‘m’ of diffusive combustion phase is much less than the premixed combustion. Thus, as the duration of the premixed combustion became short and the shape became sharp, effects of the premixed combustion became dominant.

3.2.4 Effects of pilot injection

Most of the modern diesel engines equipped with the common rail system use multiple injections. The pilot injections which were injected before the main injection were effective for reducing combustion noise because those make ignition delay of main injection and lower heat release rate are produced. However, combustion noise which was produced by just the combustion of pilot injection had not been investigated. In this study, effects of the quantity and SOC of pilot injection are examined.

3.2.4.1 Effects of pilot injection quantity

The heat released by pilot injection combustion were varied from 25 J to 45 J. The results are shown in figure 3.9. When the injection quantity increase, the frequency over 1.6 kHz are increase, but 1 kHz was decrease as shown in figure 3.9. The results of CNI were not much changed. However, because high frequency increase, the sound quality could be changed.

3.2.4.2 Effects of SOC of pilot injection

The SOC of pilot injection were changed from 5° BTDC CAD to -15° BTDC CAD. As previously referred, when the only one Wiebe function was investigated, the SOC does not affect CNI and other frequency characteristics. However, one more

Wiebe, diffusive combustion, was added, the SOC affected the excitation of pressure. The SOC of pilot is very similar to that. When the SOC were 7.5° BTDC CAD and 15° BTDC CAD, the only 1.2 kHz frequency decrease as shown in figure 3.10

3.2.4.3 Effects of combustion duration of pilot injection

The durations of combustion were changed from 5 CAD to 13 CAD. The effects of duration variation were similar to effects of change of fuel quantities. As shown figure 3.11, the pilot duration does not much affect in-cylinder pressure. In the apparent heat release rate, the pressure rise is smoother in very early of combustion, when the pilot combustion duration was longer. It significantly affected frequency over 1.2 kHz. Thus, combustion characteristics of pilot injection was important to reduce excitation over 1.2 kHz.

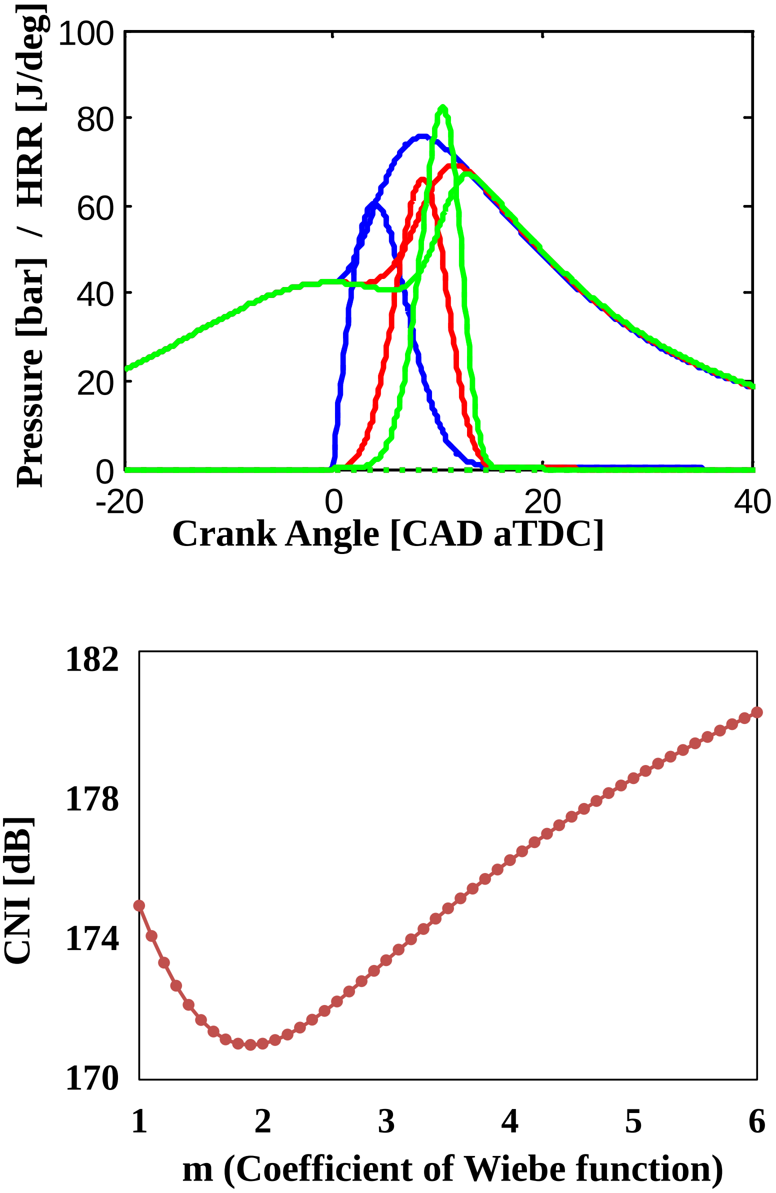

Figure 3.4 Effects of ‘m’ on combustion noise index

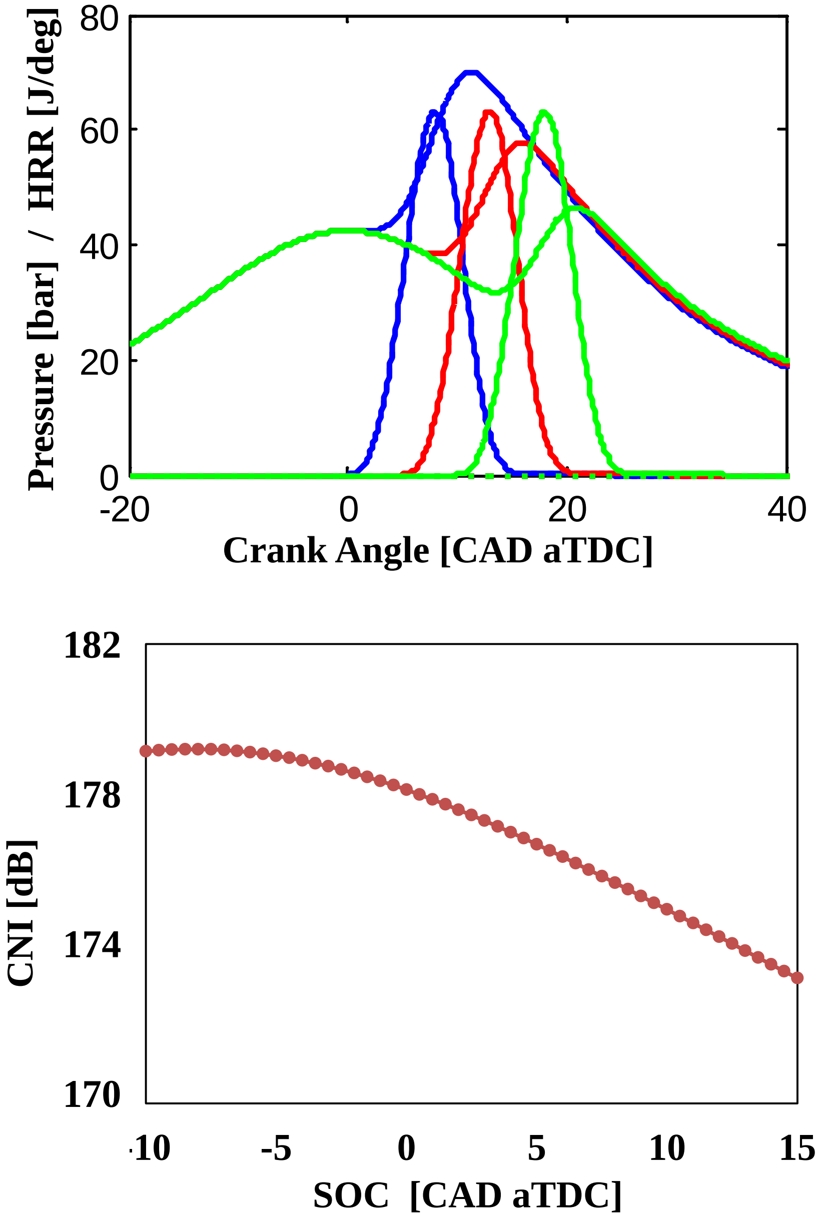

Figure 3.5 Effects of SOC on combustion noise index

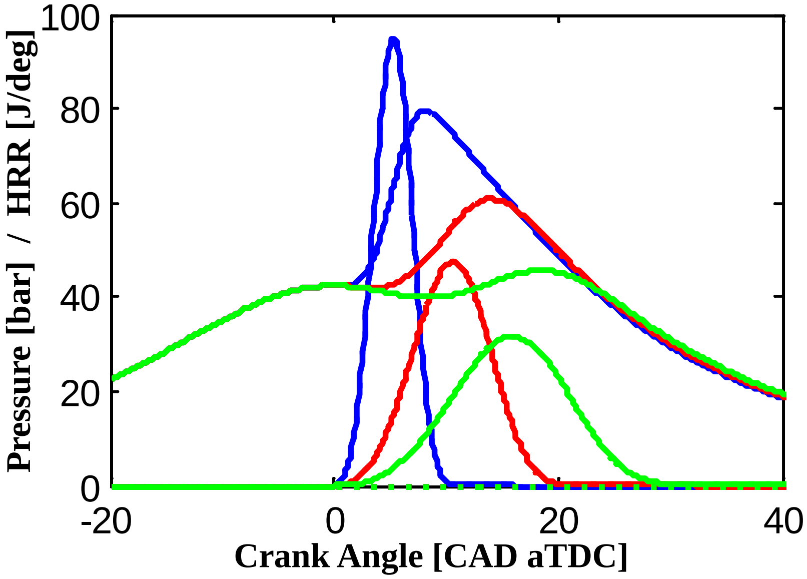

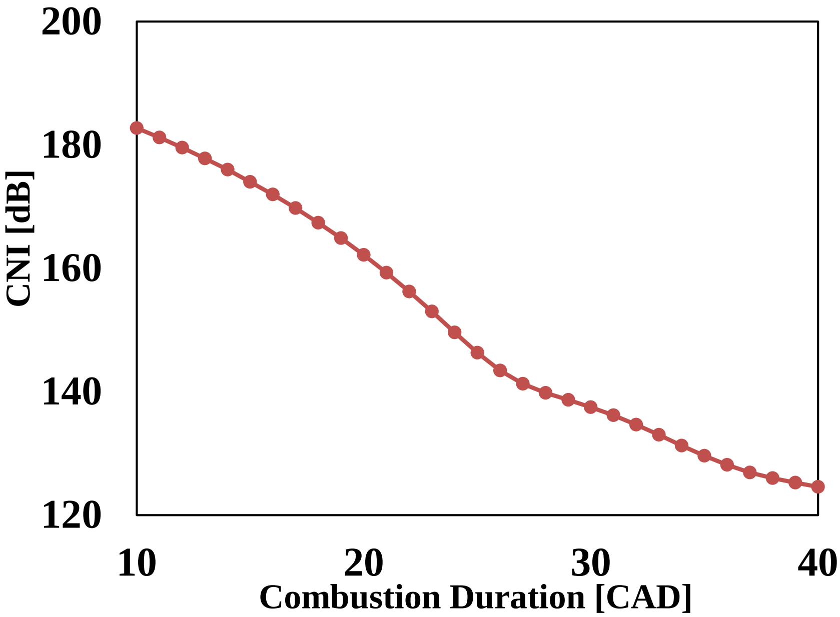

Figure 3.6 Effects of combustion duration on combustion noise index

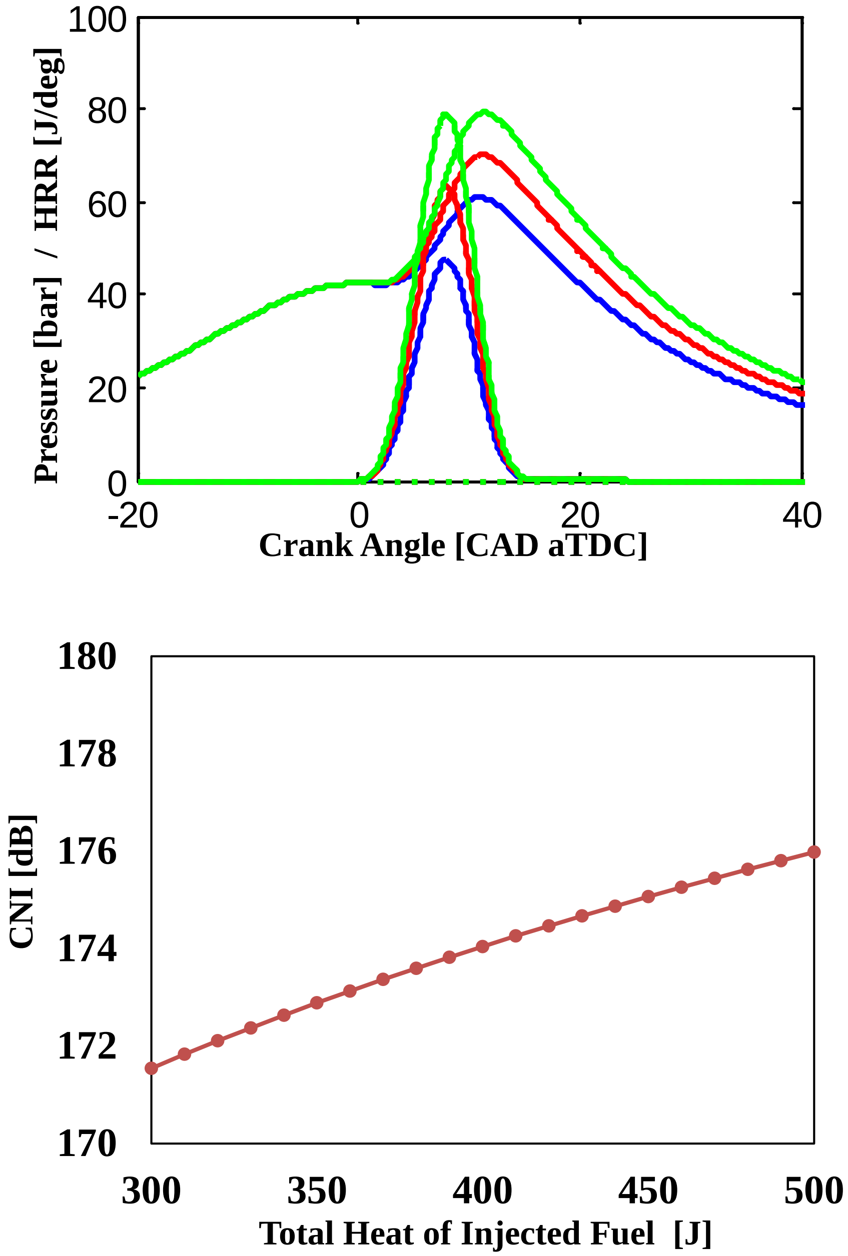

Figure 3.7 Effects of released heat on combustion noise index

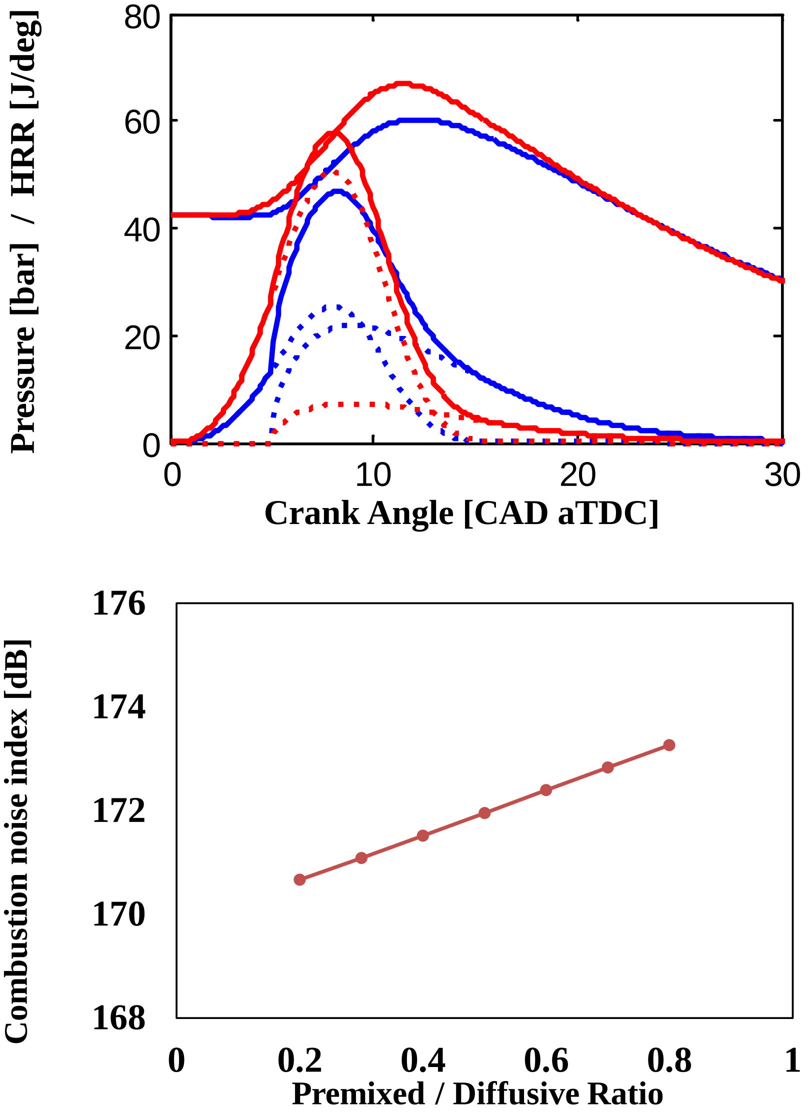

Figure 3.8 Effect of ratio of premixed and diffusive combustion

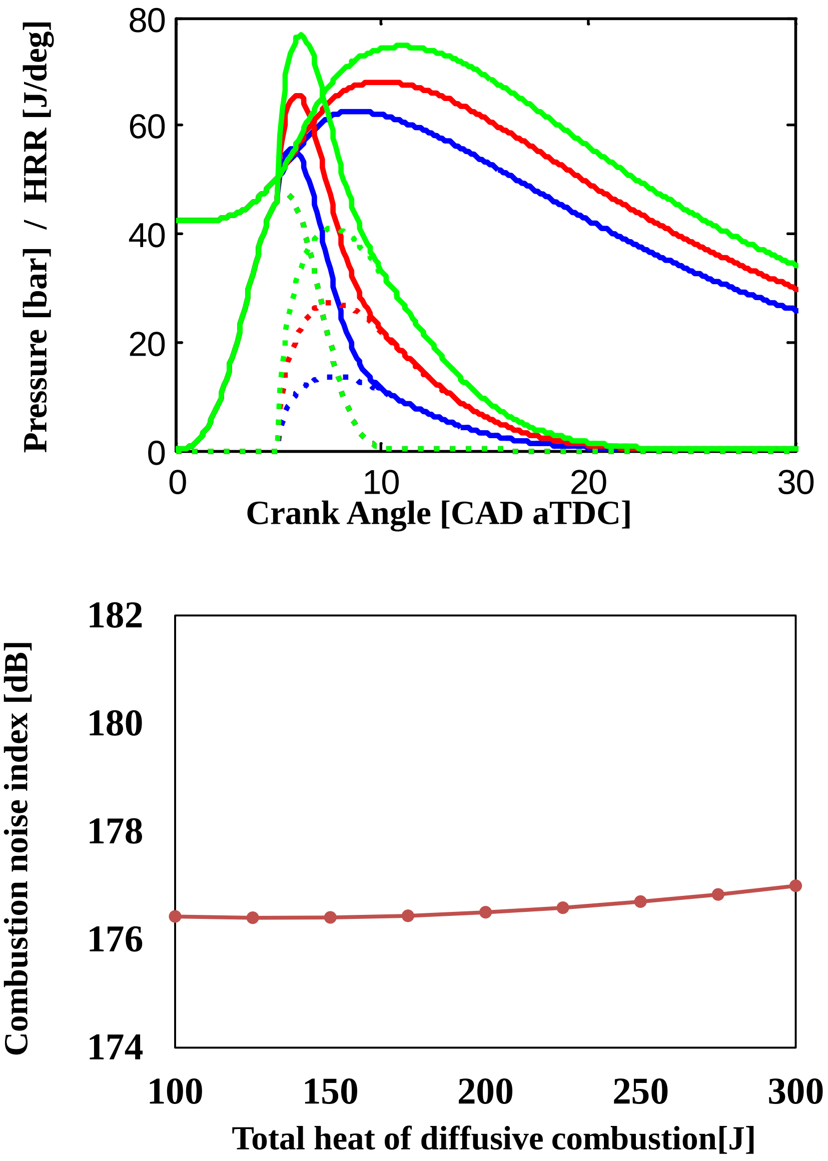

Figure 3.9 Effects of pilot injection quantity

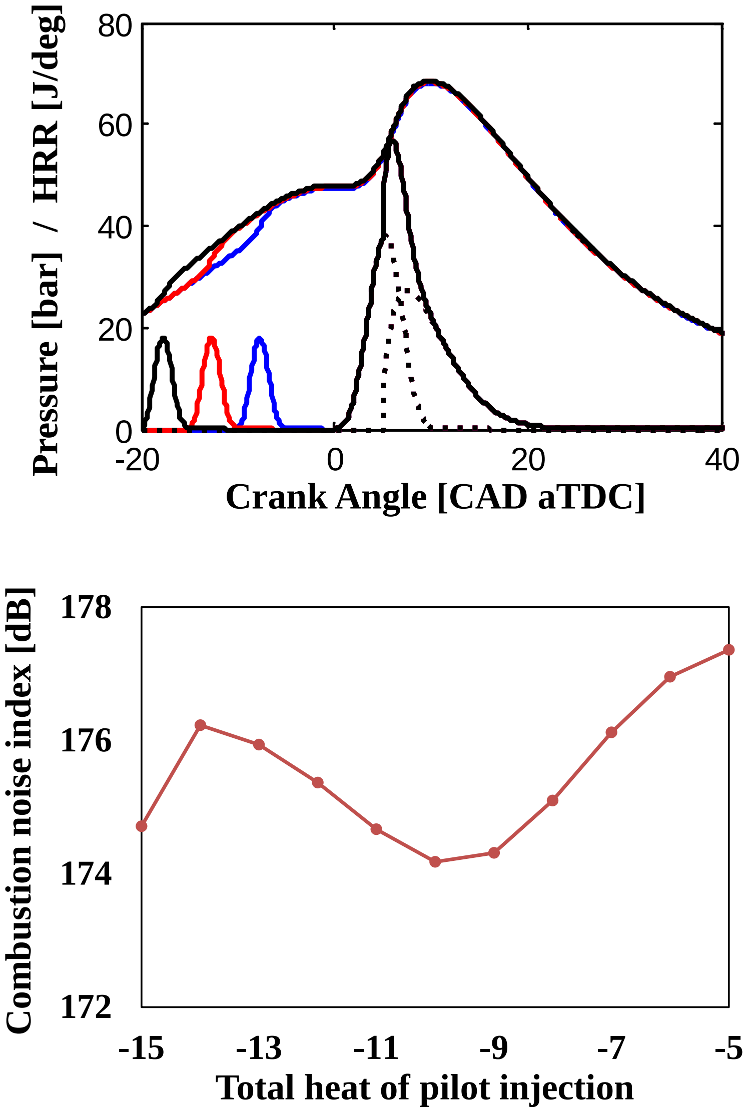

Figure 3.10 Effects of SOC of pilot injection

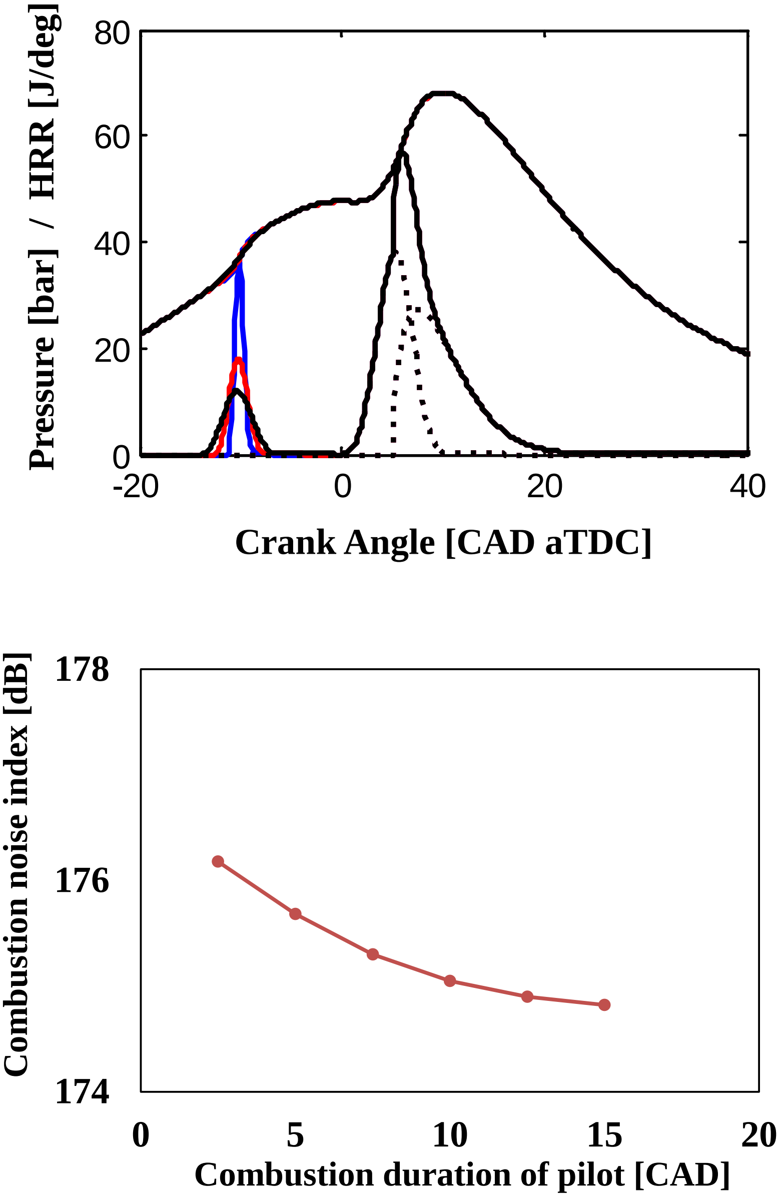

Figure 3.11 Effects of combustion duration of pilot injection

3.3 Optimization of heat release rate shape to reduce combustion noise

3.3.1 Optimization of heat release rate shape to minimize CNI using Wiebe functions

In the previous chapter, the effects of heat release rate shape changing the coefficients of Wiebe functions were described. In this chapter, the optimal shapes to minimize the CNI are investigated. The diesel combustion was simulated using three of Wiebe functions. The one Wiebe function had five coefficients. Thus, fifteen coefficients had to be optimized. The coefficients are constrained by boundary conditions, because unconstrained variables could cause unrealistic shapes. The boundary conditions were determined through experimental results. ′m_premixed’ was varied from 2.44 to 5, ‘m_mixing’ from 0.4 to 0.8 and m_late’was not significantly varied; however, the variation was just about 1. ‘θ_(premixed,duration)’ was varied from 11.9 to 14.5, ‘θ_(premixed,duration)’ from 25.8 to 29.2 and ‘θ_(late,duration)’ from 62.2 to 70. 91. The boundary is shown in Tables 3.4~3.6. In addition, the system, which have 15 coefficients, has many local optimum points. The starting point can affect the optimum values. Thus, optimum points were determined from the seven of the starting points, then, the final optimum value, which has a minimum CNI level, was determined. The optimization was using ‘fmincon’ which is a optimization function of matlab. The optimization is conducted when engine speed is 1500 rpm and total released heat is 480 J.

3.3.2 Optimized shapes of heat release rate for minimum CNI

The boundary conditions were set as shown in table 3.4. Figure 3.12 shows the heat release rate, pressure curve and results of 1/3 octave band analysis. The determined values of variables were close to the boundary conditions. That means that optimum shape for the reduction of combustion noise was determined when the burning rate was slow and the duration is long and the SOC was retarded. These were already known as ways to reduce combustion noise.

To find new shape, constraint of the SOC was remove. The boundary conditions are shown in table 3.5. The other results are shown in figure 3.13. The start of combustion of figure 3.13 was 20° BTDC CAD. The combustion duration of diffusive combustion was not on the boundary. The duration became short than first optimization, however, the CNI decreased by 8 dB. The premixed phase and diffusive phase were much close and they made a smooth curve. It was observed that one Wiebe function has a long combustion duration.

However, it is impossible that the start of combustion is 20° BTDC CAD in conventional diesel combustion. To find more realistic heat release shape, the SOC was fixed by TDC and the premixed fuel ratio was constrained by 20%. The boundary conditions are shown as table 3.6, and the results are shown in figure 3.14. The CNI was 144 dB which decreased by 19 dB. It was a significant change. It is important for the reduction of combustion noise that the heat release rate being a smooth continuous curve.

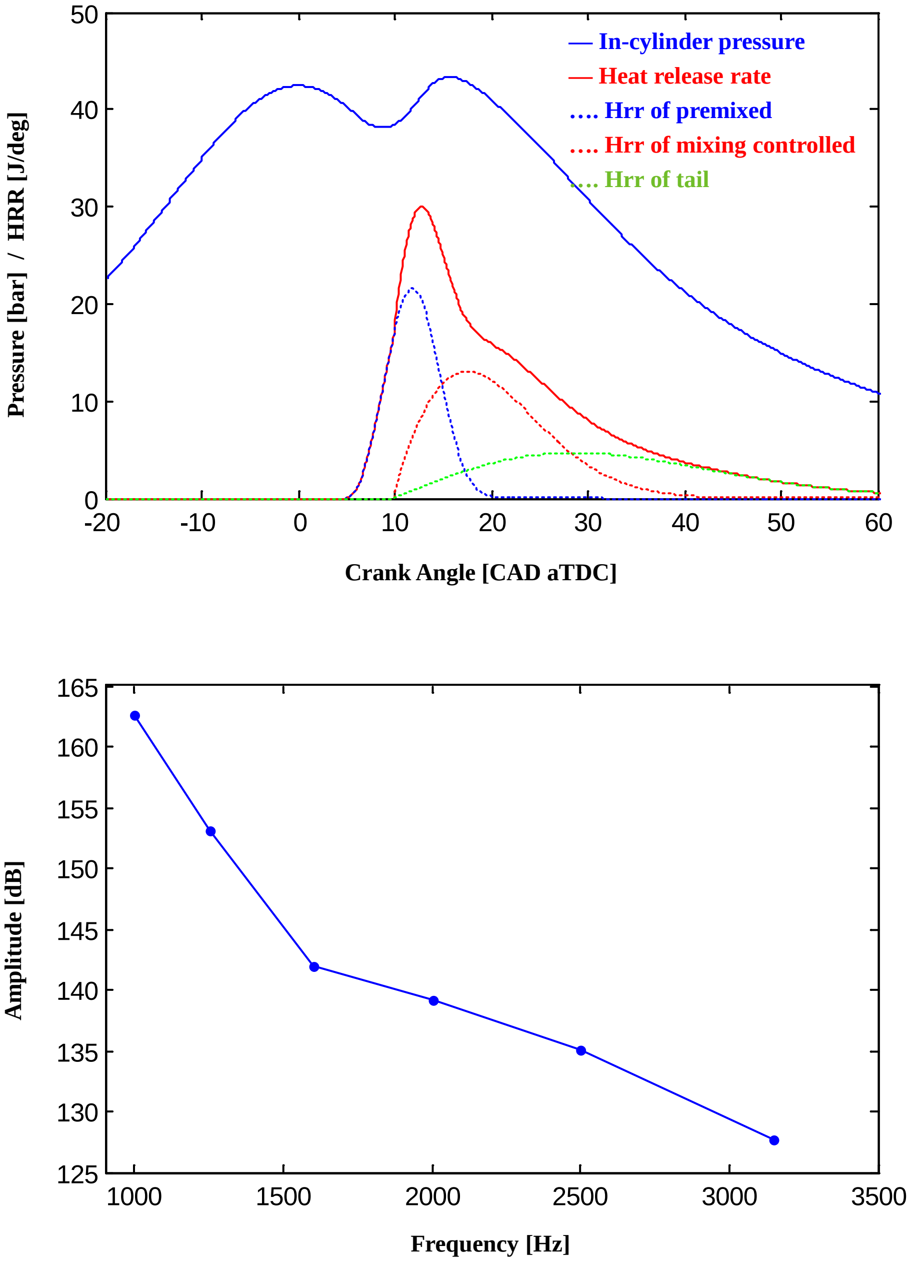

Figure 3.12 Optimal shape of heat release and pressure curve, 1/3 octave band (1)

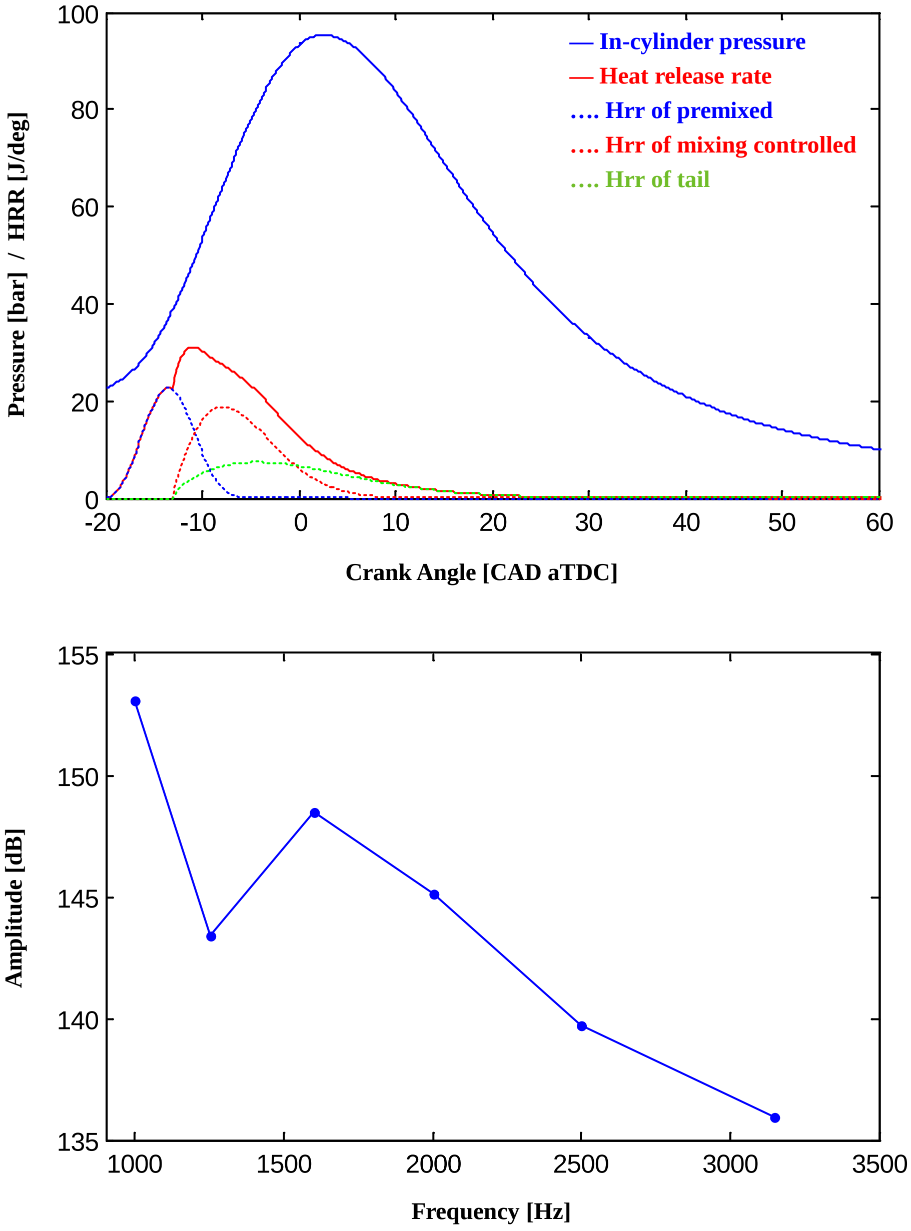

Figure 3.13 Optimal shape of heat release and pressure curve, 1/3 octave band (2)

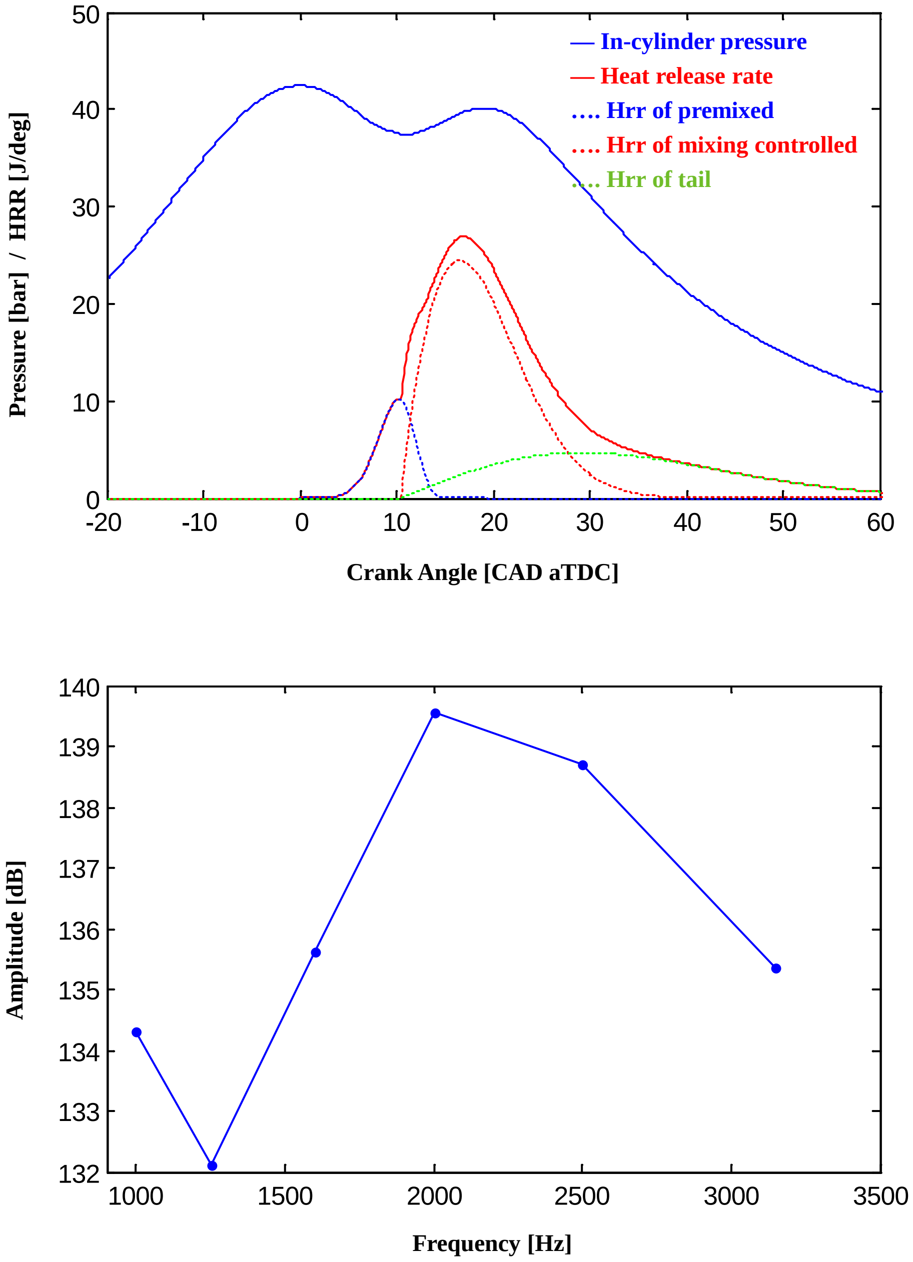

Figure 3.14 Optimal shape of heat release and pressure curve, 1/3 octave band (3)

Table 3.4 Boundary conditions and optimal values of variables (1)

		Coefficients of Wiebe function						CNI
		a	m	SOC	Duration	Q	Q ratio	
Premixed	Low	7	2	-5	5	480	0.1	163.11
	Upper	7	5	5	15	480	0.4	
	Optimum	7	2	5	15	480	0.3	
Diffusion	Low	7	0.4	-5	20	480	0.1	
	Upper	7	0.8	20	60	480	0.4	
	Optimum	7	0.8	10	35	480	0.4	
Tail	Low	7	0.4	-5	40	480	-	
	Upper	7	1	20	70	480	-	
	Optimum	7	1	10	70	480	-	

Table 3.5 Boundary conditions and optimal values of variables (2)

		Coefficients of Wiebe function						CNI
		a	m	SOC	Duration	Q	Q ratio	
Premixed	Low	7	2	-20	5	480	0.1	155.35
	Upper	7	5	5	15	480	0.4	
	Optimum	7	2	-20	14.3	480	0.3	
Diffusion	Low	7	0.4	-20	20	480	0.1	
	Upper	7	0.8	20	60	480	0.4	
	Optimum	7	0.8	-13	24.27	480	0.4	
Tail	Low	7	0.4	-5	40	480	-	
	Upper	7	1	20	70	480	-	
	Optimum	7	0.7	-13	48.5	480	-	

Table 3.6 Boundary conditions and optimal values of variables (3)

		Coefficients of Wiebe function						CNI
		a	m	SOC	Duration	Q	Q ratio	
Premixed	Low	7	3.5	0	5	480	0.1	144.5
	Upper	7	5	0	15	480	0.2	
	Optimum	7	5	0	14.6	480	0.1	
Diffusion	Low	7	0.4	0	20	480	0.1	
	Upper	7	0.8	15	60	480	0.8	
	Optimum	7	0.8	10	27.9	480	0.6	
Tail	Low	7	0.4	-20	40	480	-	
	Upper	7	1	20	70	480	-	
	Optimum	7	1	10.6	70	480	-	

Chapter 4. Injection strategies to reduce combustion noise

4.1 Variation of heat release rate shape according to change of injection strategies via experiment

The CNI variation was investigated when the injection strategies were changed. Injection parameters, which can affect the shape of heat release rate, were SOI, injection pressure, Swirl ratio and EGR rate. Three level of each parameter was compared. The engine speed was 1500 rpm and fuel injection quantity was 13.5mg. In addition, to consider emissions, NO and PM were measured together. The CNI was calculated by using in-cylinder pressure.

4.1.1 Main injection timing

The main injection timings were changed from 3° BTDC CAD to -3° BTDC CAD. When the injection was advanced, the peak of heat release rate decreased. The CNI also decreased. It was because the atmosphere temperature increased when the SOI was advanced. Thus, the ignition delay became short and the fuel quantity of the premixed combustion decreased. At that time, the NO emission increased because the flame temperature increased. The PM emission was also increased because the time to be mixed with air was not sufficient. Figures 4.1 and 4.2 show the in-cylinder pressure, heat release rate and the emissions when the SOI was changed.

4.1.2 Injection pressure

The injection pressures were increased and decreased by 100 bar (figure 4.3). The peak of heat release rate were high when the pressure increased. It was because the mixing of air and fuel was enhanced and more burned fuel in premixed combustion phase. The CNI were also increased. When the injection pressure was low, the PM more produced because the mixing was not enough. The NO decreased because when the pressure decreased, the combustion phase was retarded (figure 4.4).

4.1.3 Swirl rate

The swirl ratio was not measured. The relative intensities of swirl were guessed by the swirl valve openness. The swirl valve were 5%, 20% and 55 %. When the swirl valve is closed, swirl ratio increases. More burned fuel in premixed combustion phase with high swirl ratio because the higher swirl ratio enhances the mixing of air and fuel. The NO increase and PM decrease shown in figures 4.5 and 4.6.

4.1.4 EGR rate

The EGR rate was changed by 5% . When the EGR rate was increased, the peak of heat release rate also became high. It is because the higher EGR rate makes the ignition delay longer. The NO was very sensitive to the EGR rate. When the EGR rate increased 5%, the NOx decreased by 50 %. When the EGR rate increased, the increase in ignition delay allowed time for the fuel and air to mix, thus more fuel was burned in the premixed combustion phase. Therefore, a higher level of EGR rate made the peak of the heat release rate even higher (figure 4.7 and 4.8).

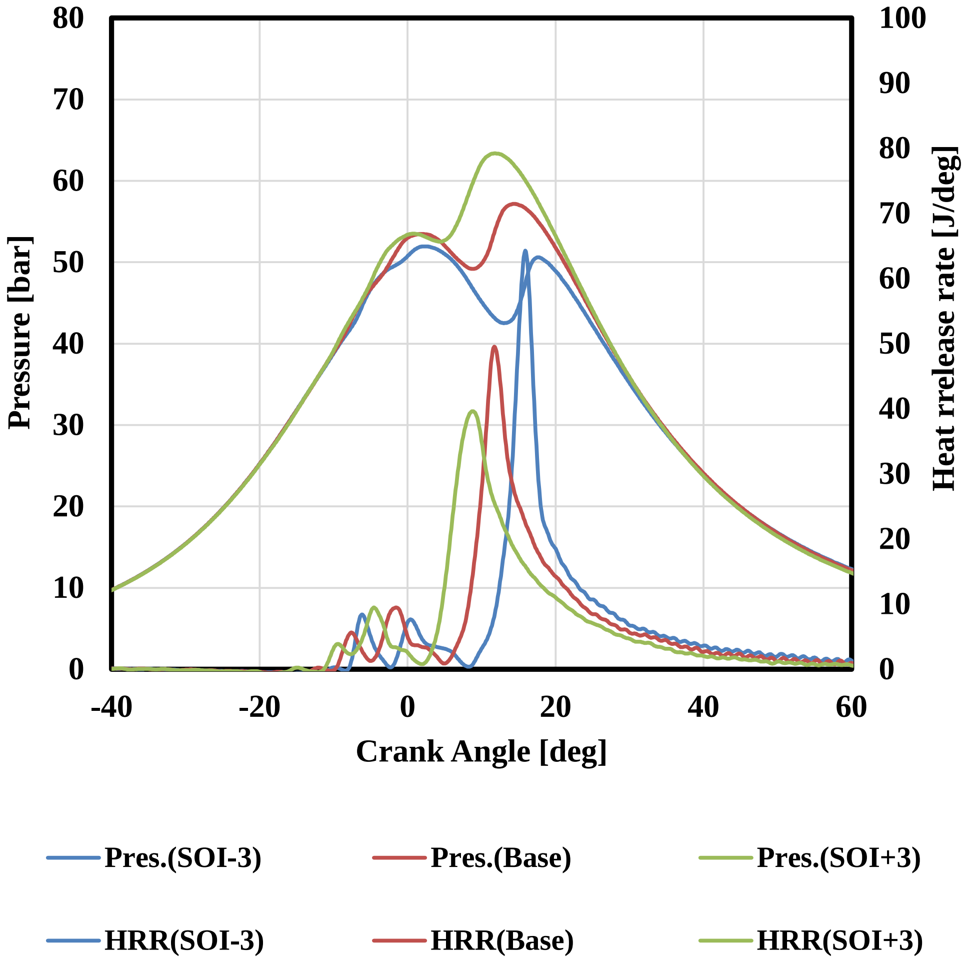

Figure 4.1 Heat release rate & in-cylinder pressure according to SOI change

(Engine speed: 1500 rpm / fuel mass: 15 mg)

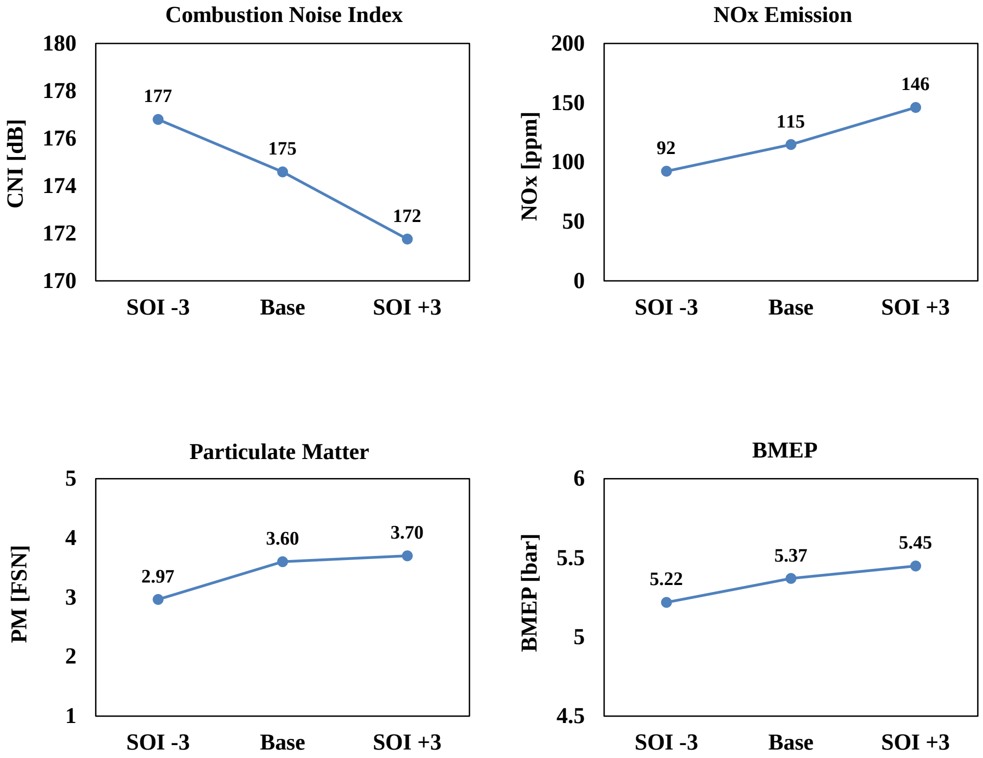

Figure 4.2 CNI, PM, NO and BEMP variation according to SOI change

(Engine speed: 1500 rpm / fuel mass: 15 mg)

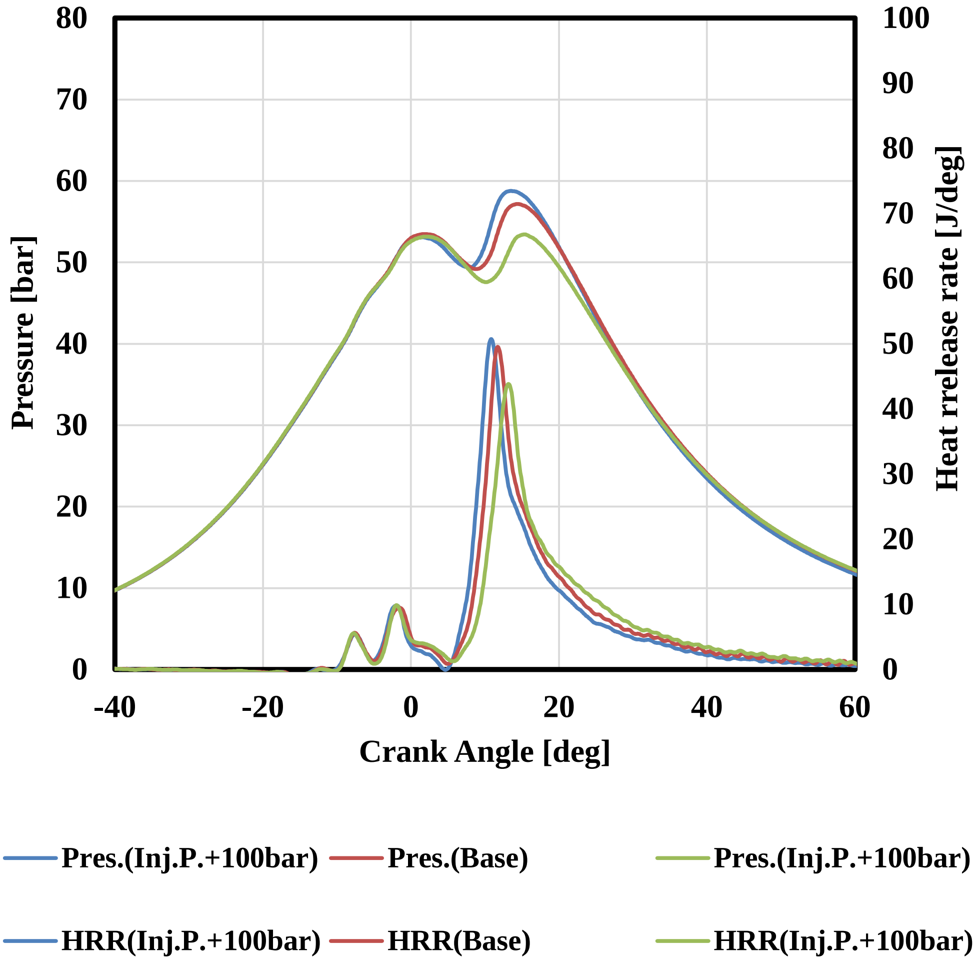

Figure 4.3 Heat release rate & in-cylinder pressure according to injection pressure change (Engine speed: 1500 rpm / fuel mass: 15 mg)

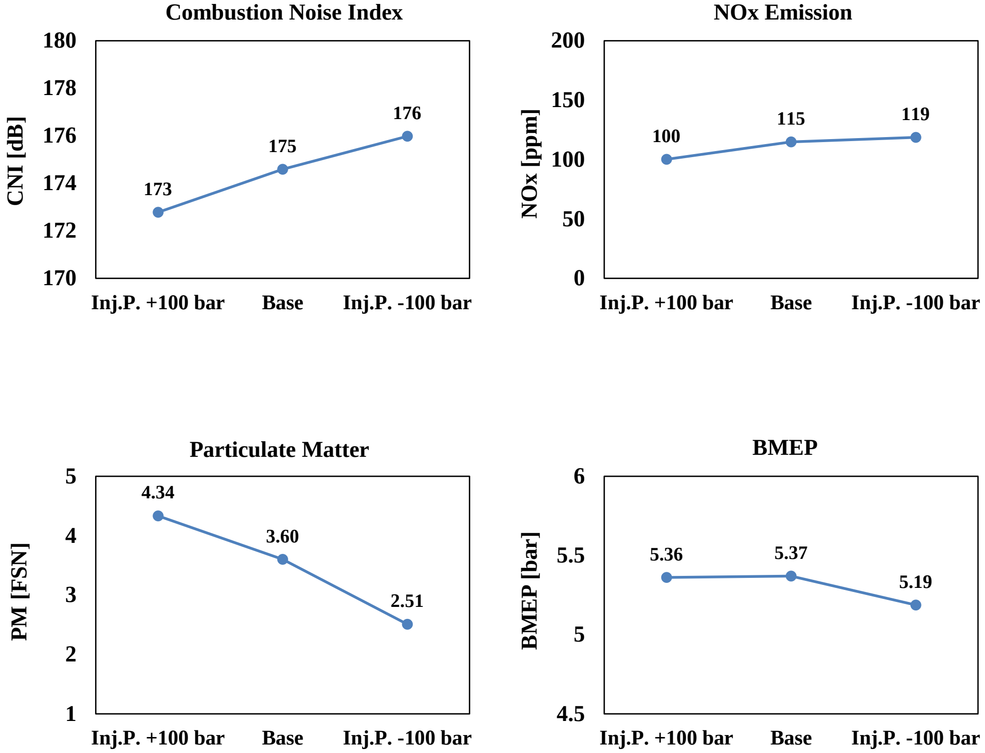

Figure 4.4 CNI, PM, NO and BEMP variation according to injection pressure change (Engine speed: 1500 rpm / fuel mass: 15 mg)

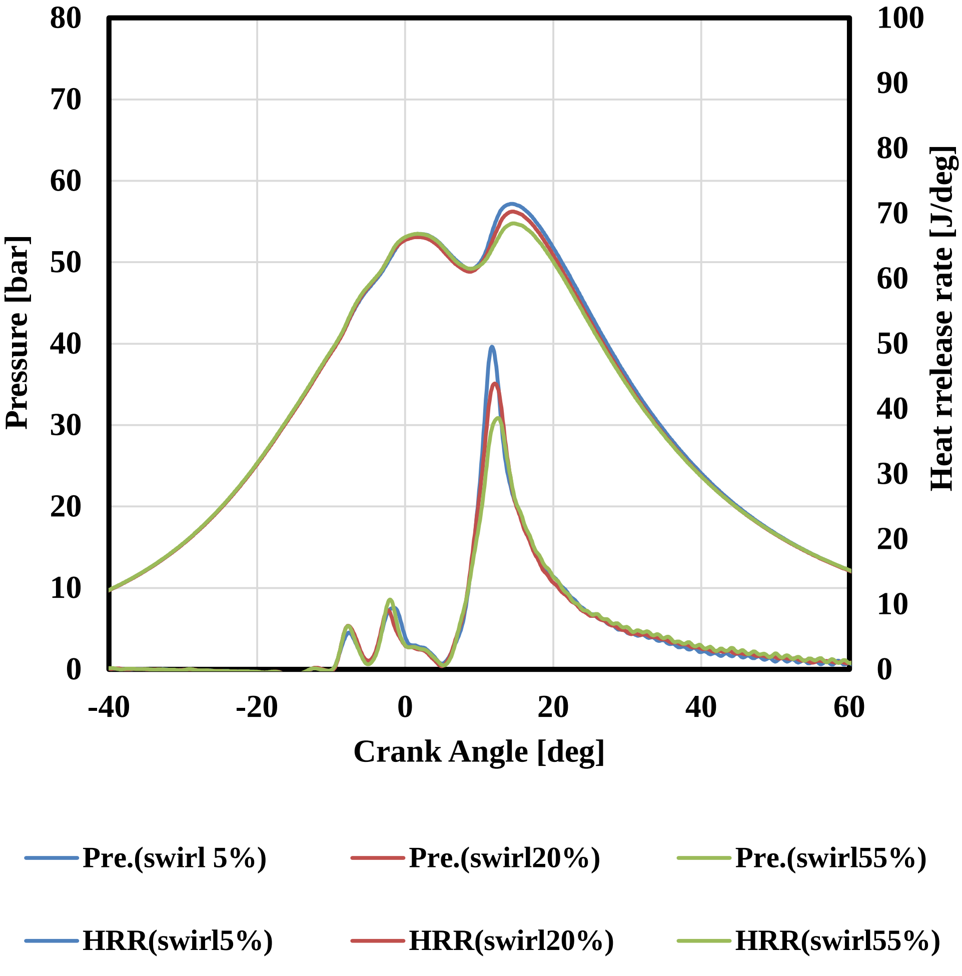

Figure 4.5 Heat release rate & in-cylinder pressure according to swirl valve open rate change (Engine speed: 1500 rpm / fuel mass: 15 mg)

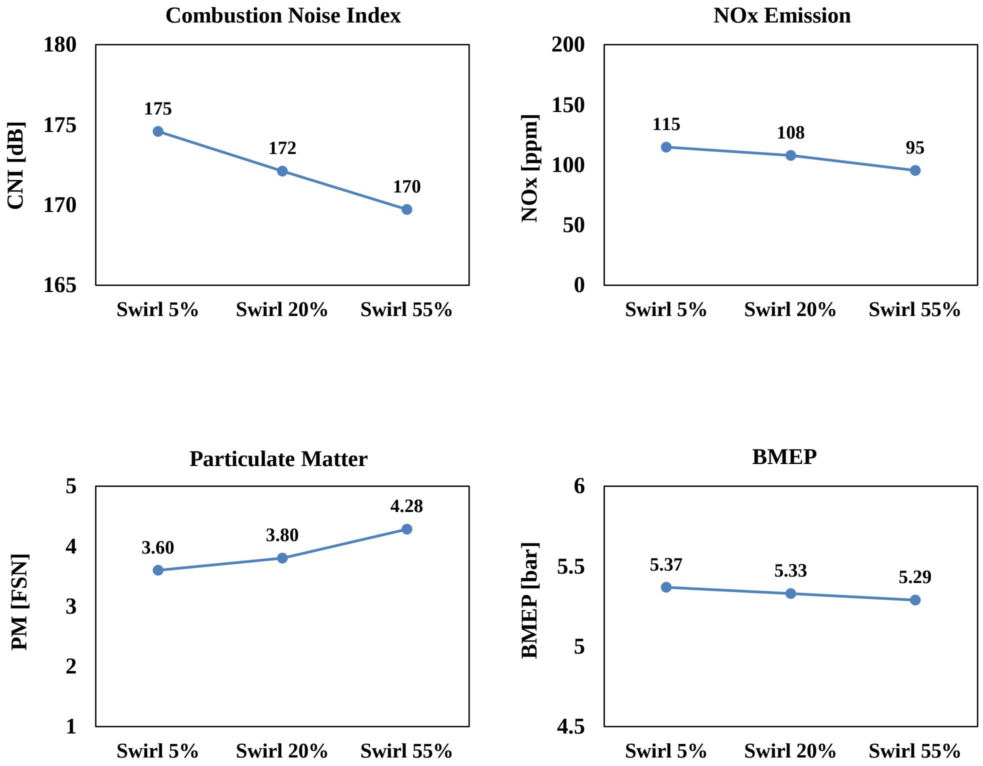

Figure 4.6 CNI, PM, NO and BEMP variation according to swirl open rate change

(Engine speed: 1500 rpm / fuel mass: 15 mg)

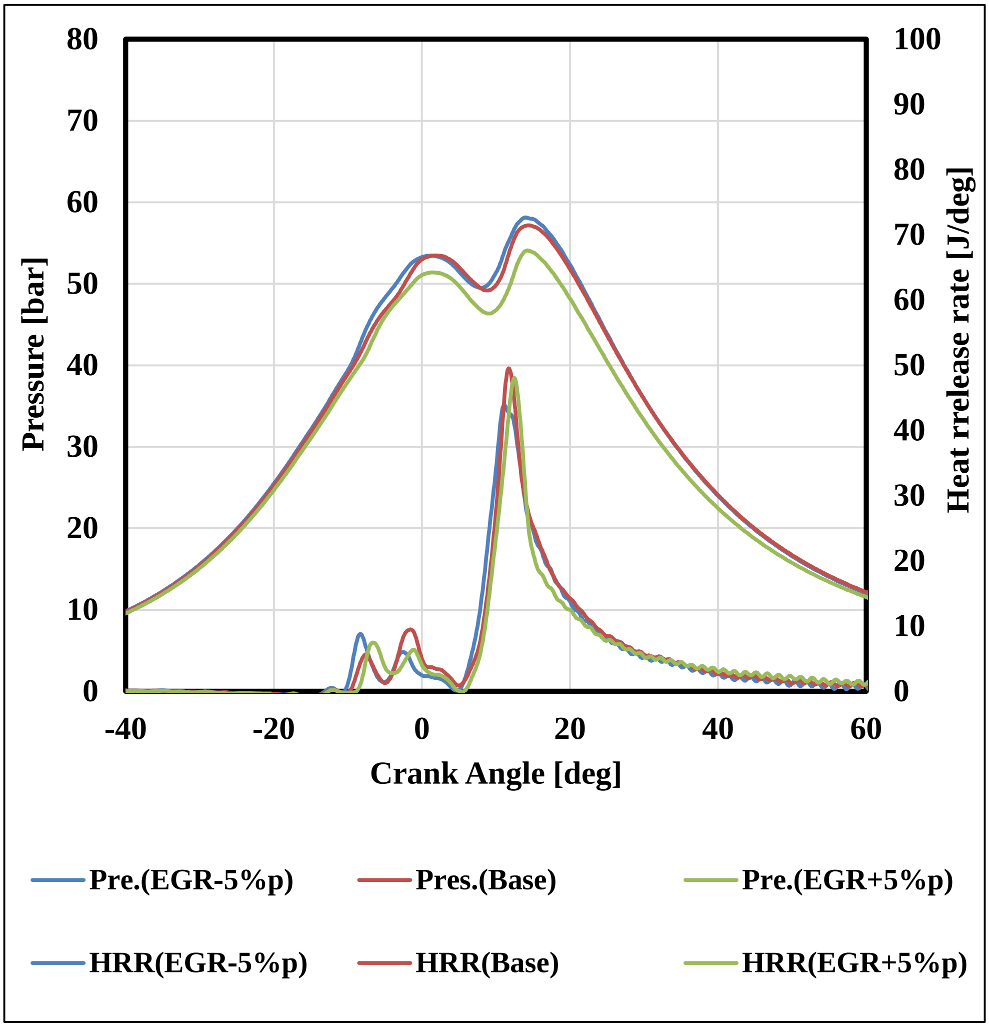

Figure 4.7 Heat release rate & in-cylinder pressure according to EGR rate change

(Engine speed: 1500 rpm / fuel mass: 15 mg)

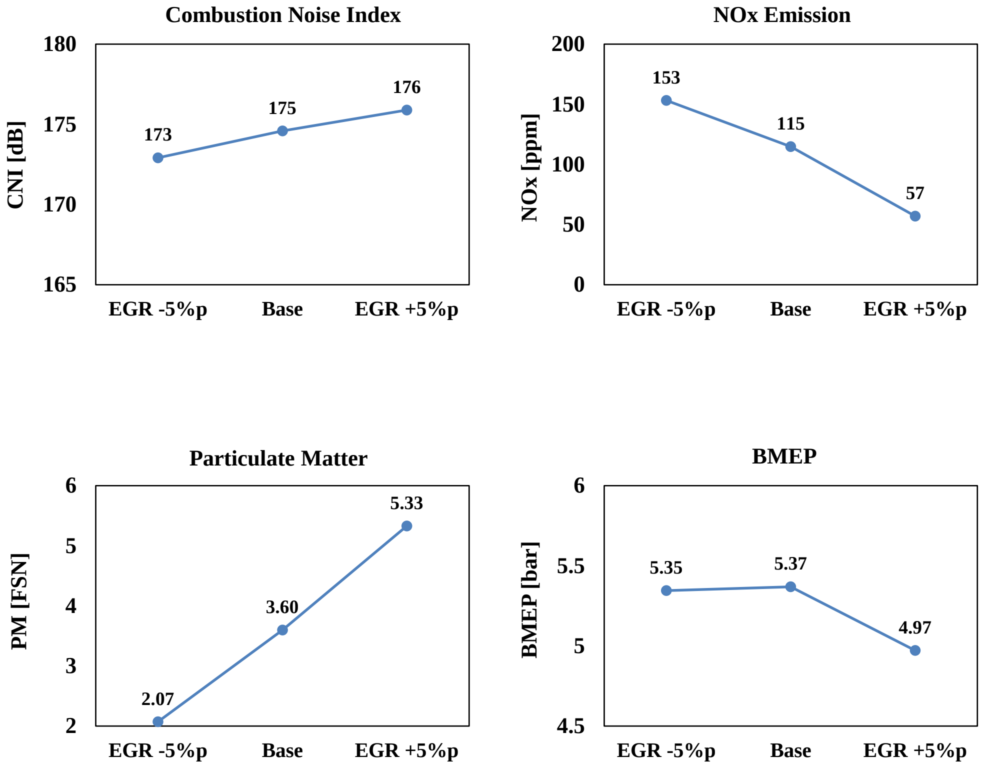

Figure 4.8 CNI, PM, NO and BEMP variation according to EGR rate change

(Engine speed: 1500 rpm / fuel mass: 15 mg)

4.2 Early pilot injection strategy to reduce combustion noise

4.2.1 Limitation of conventional diesel combustion

The conventional fuel injection strategies include pilot injection which is the injection of a little fuel before the main injection. The pilot injection increases the in-cylinder gas temperature and pressure when fuel was mainly injected. Thus, the ignition delay was decreased and the fuel of the main injection was burned smoothly. Moreover, some of the total fuel were already burned, the fuel of the main injection reduced for same IMEP. The pilot injection was very effective to reduce combustion noise. However, more fuel quantity of pilot injection was achievable to increase the soot formation and the combustion noise caused by the pilot burning itself.

4.2.2 PCCI combustion of diesel

The low temperature combustion has been studied as a way to reduce NOx and soot formation simultaneously. The PCCI is an injection strategy for them. In the PCCI, the fuel was injected before TDC (usually before 30° BTDC CAD), then, was mixed with air for much longer time before the ignition. The well-mixed fuel and air make premixed mixture; most of fuel was burned as a premixed combustion after the long ignition delay. Since, the flame temperature are low, less NOx was produced. Moreover, the amount soot was reduced because the fuel and air were mixed well without the fuel rich region, which can enhance the PM formation. However, the PCCI combustion had a short burning duration, and caused the rapid pressure rise which made a louder combustion noise. Moreover, The HC emission increased and the control of ignition timing was difficult. Thus, PCCI was not used in the manufactured vehicles. [47-49]

4.2.3 Early pilot injection combustion

The pilot injection starts at 10~20° BTDC CAD in traditional diesel engine injection. However, in early pilot injection, the fuel is injected before 30° BTDC CAD, thus the injected fuel has enough time to be mixed with air with longer ignition delay. While, the start of main injection is similar to that of the traditional injection. The fuel of pilot injection is combusted by PCCI and fuel of the main injection is burned by the diffusive combustion. In conventional injection strategies, the jet fuel of the main injection is formed around the burned pilot injection, because the pilot and the main injection are close, and local rich region appears. That is the reason why excessive pilot quantity increases the soot formation. The early pilot injection forms a well-mixed air-fuel mixture because it has a long ignition delay. It helps the main injection to be mixed with air, as a result, soot formation is reduced. Therefore, using the early pilot injection and smooth combustion are possible due to the short ignition delay of the main injection and the increased pilot injection quantity. [50-54]

The early pilot injection was tested at 1500 rpm and 13.5 mg of fuel. Figures 4.9 and 4.10 show heat release rates and octave analysis results of a conventional case and a PCCI case. When the early pilot injection was applied, the heat release of both the main injection and the pilot injection was smoother than that of the conventional case and the PCCI case. It leads to reduce the combustion excitation. The CNI deceased from 175 dB to 170 dB. All of frequency was reduced. At that time, the NOx, PM and indicated thermal efficiency (ITE) were equivalent to that of the conventional data.

When the pilot combustion and the main combustion were close, the CNI level was at the lowest as shown in chapter 3.3. However, the strategy was not possible via the traditional injection strategies because the closed split injection caused a lot of smoke. While, it could be possible using the early pilot injection. The heat release rate and frequency analysis results are shown in figure 4.11. Table 4.3 shows the emissions and ITE. The frequency under 1.5 kHz was dramatically reduced and PM was reduced too.

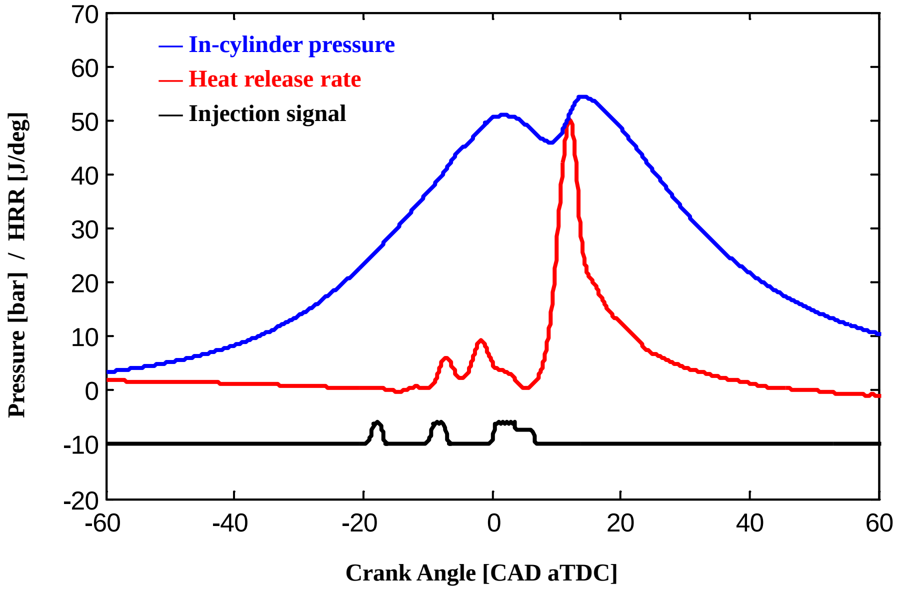

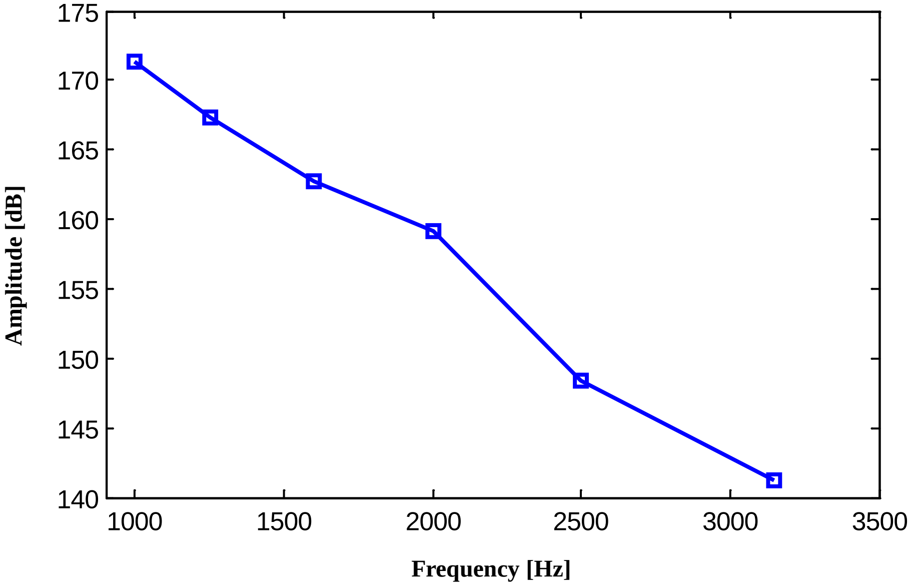

Figure 4.9 Heat release, pressure and 1/3 octave band results of conventional diesel combustion including pilot injections (Engine speed: 1500 rpm / fuel mass: 15 mg)

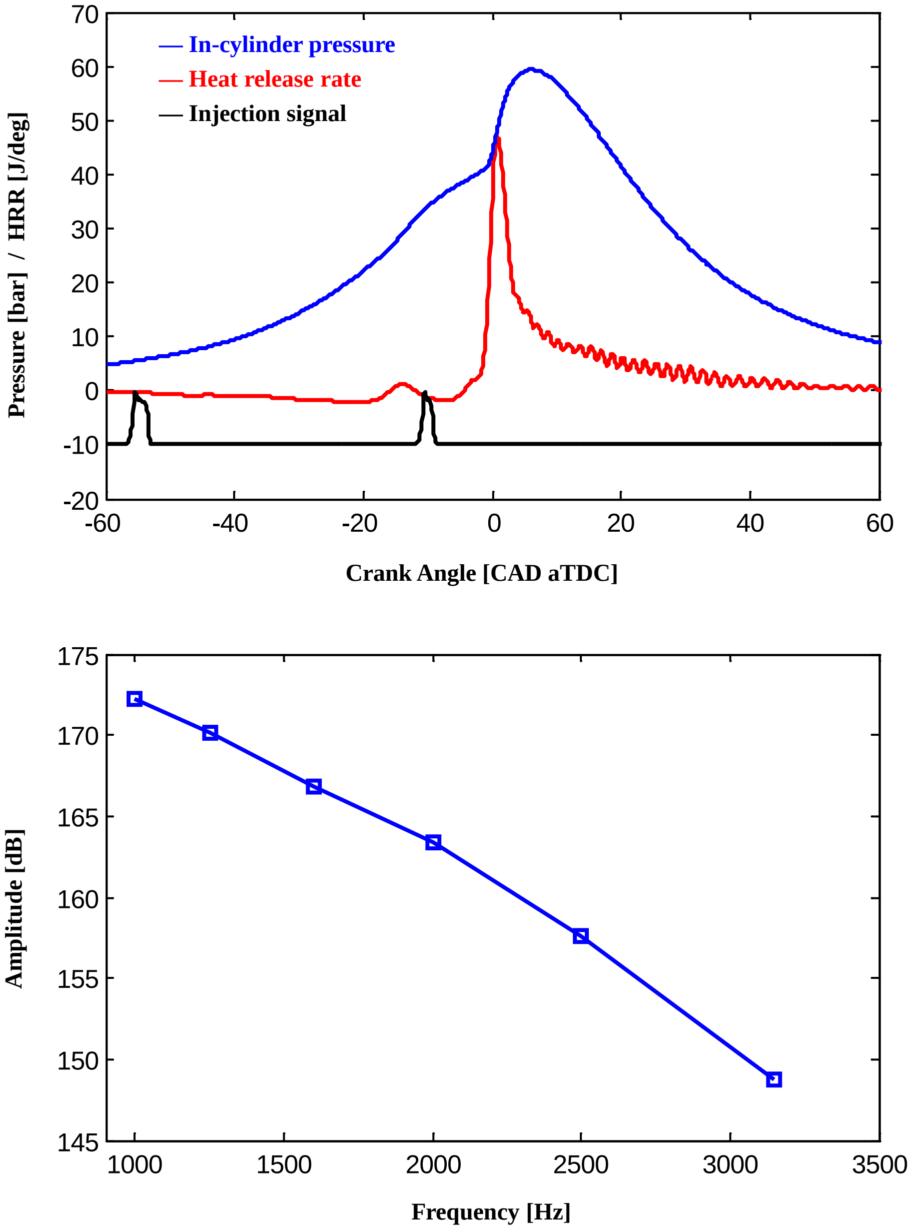

Figure 4.10 Heat release, pressure and 1/3 octave band results of PCCI combustion including pilot injections

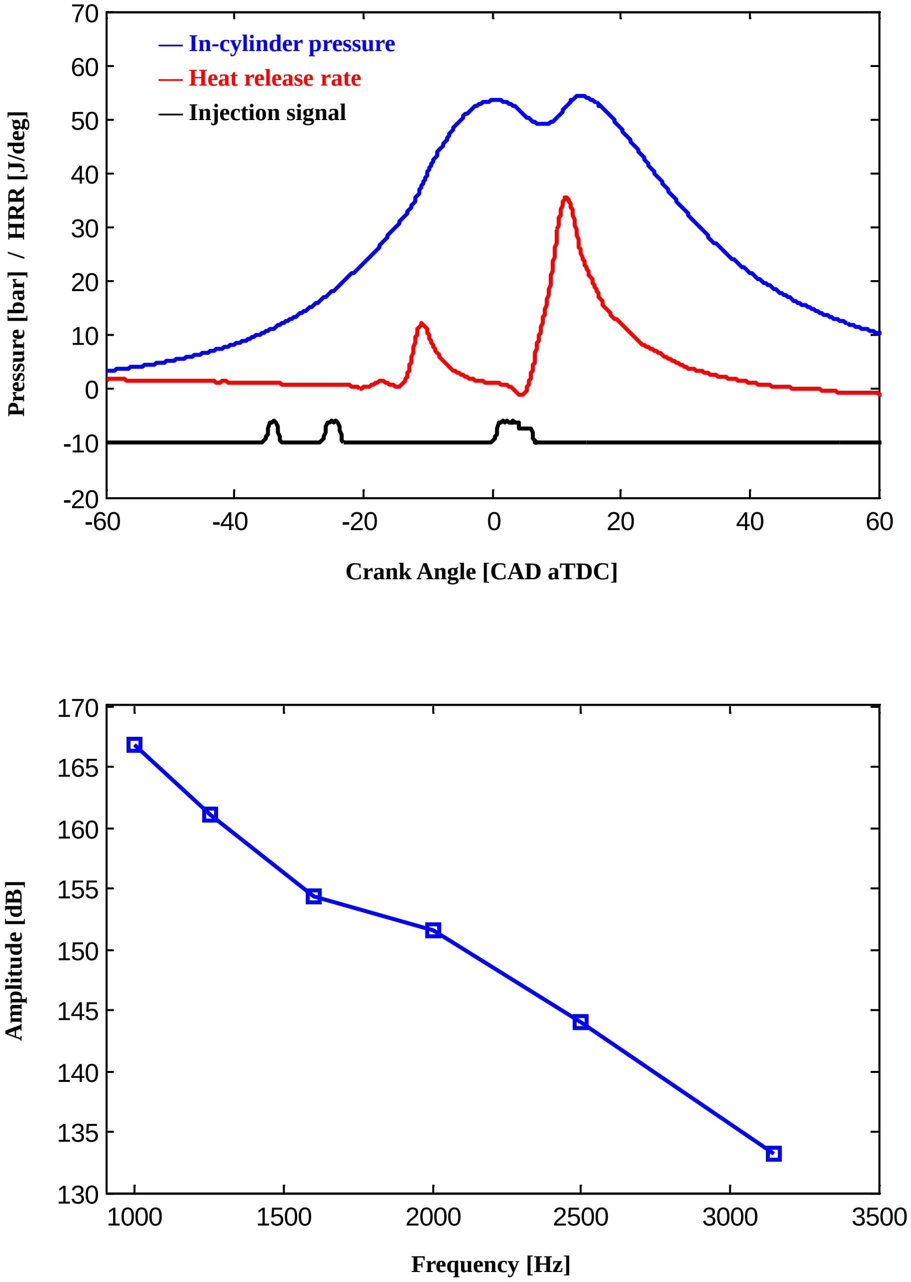

Figure 4.11 Heat release, pressure and 1/3 octave band results of early pilot injection

Table 4.1 Emissions, IMEP and CNI

Case description	NOx [ppm]	PM [FSN]	IMEP [bar]	CNI [dB]
Conventional Diesel	109.4	4.351	6.8	172.6
PCCI including pilot injections	68	0.183	4.9	175.4
Early pilot injection	101.4	4.19	6.78	168.7

Chapter 5. Closed loop control to reduce combustion noise

5.1 Characteristics of diesel engine noise according to EGR rate change during transient operation

In this study, the characteristics of diesel engine noise according to the EGR rate change during transient operation were investigated. A 1.6 liter diesel engine was used. The engine revolution speed and load were changed with a varied ramp time. In addition, this study examined transient operations with a constant engine speed and increased engine load. The EGR rate was measured by using fast response thermocouples during the transient operations. The combustion noise was evaluated via CNI calculation

5.1.1 EGR rate measurement

The EGR rate is usually calculated by measuring the concentration of carbon dioxide in intake and exhaust manifolds. The concentration of carbon dioxide is conventionally determined by the NDIR method, which usually is greater than the 1 second response time; this response time is too slow to measure the EGR rate during a transient engine operation

The methodology of evaluating the EGR rate using the temperature of intake manifold, the cooled air and the EGR gas was explained in the previous research [55]. The EGR rate can be calculated using equation (5.1) with the assumptions that the specific heat capacity of the air and the EGR are assumed to be equal and heat transfer is neglected.

$$EGR\,rate = \frac{m_{EGR}}{m_{EGR} + m_{air}} = \frac{T_{mixture} - T_{air}}{T_{EGR} - T_{air}} \tag{5.1}$$

The cooled EGR gas and air are mixed in the intake manifold; however, the mixture is not uniform because of the considerable temperature differences. Because the gases are temporarily stratified, heat transfer occurs between the EGR gas, the cooled air and the intake manifold. The EGR gas loses heat to the intake manifold while the air gains the heat. The heat transfer model was adopted to consider this phenomenon. [56]

If effects of heat transfer is taken into account,

$$\dot{H}_{mix} = \dot{H}_{air} + \dot{H}_{EGR} + \dot{Q}_{in} + \dot{Q}_{out} \tag{5.2}$$

$$c_p \dot{m}_{mix}(T_{mix,HT} - T_0) = c_p \dot{m}_{air}(T_{air} - T_0) + c_p \dot{m}_{EGR}(T_{EGR} - T_0) + hA_{air}(T_{wall} + T_{air}) - hA_{EGR}(T_{EGR} - T_{wall}) \tag{5.3}$$

$$T_{mix,HT} = (1 - EGRrate) \times T_{air} + EGRrate \times T_{EGR} + hA_{air}(T_{wall} - T_{air}) - hA_{EGR}(T_{EGR} - T_{wall}) \tag{5.4}$$

$$T_{mix,HT} = T_{mix,noHT} + \Delta T \tag{5.5}$$

$$\Delta T = \frac{h}{c_p \dot{m}_{mix}}[A_{air}(T_{wall} - T_{air}) - A_{EGR}(T_{EGR} - T_{wall})] \tag{5.6}$$

$$EGR\,rate = \frac{m_{EGR}}{m_{EGR} + m_{air}} = \frac{(T_{mixture} + \Delta T) - T_{air}}{T_{EGR} - T_{air}} \tag{5.7}$$

where H_{air}, H_{EGR} and H_{mix} are the enthalpies of the air, the EGR gas and the mixed gas, respectively. $c_{p,air}$, $c_{p,EGR}$ and $c_{p,mix}$ are the specific heat capacity at constant pressure of the air, the EGR gas and the mixed gas, respectively. Q_{in} is the heat that the air gains, and Q_{out} is the heat loss by the EGR gas. T_{air}, T_{EGR} and T_{mix} are measured values. The heat transfer coefficient of h is determined from the intake manifold, assumed to be a pipe. Nu and Re are obtained by considering the pressure, rpm and geometry of the intake manifold. ΔT is the temperature variation due to the heat transfer to the inner surface of the intake manifold. The EGR rate considering the heat transfer is represented as equation (5.7). The radiative heat transfer to the surrounding area is ignored.

The temperature of the air, the EGR gas and the intake manifold were measured using fast respond thermocouples which were made by 100 μm diameter R-type wires and exposed type. The response time is less than 0.05 seconds. The gastemperature was measured by NI- with a 100 Hz sampling rate. Figure 5.1 shows the positions of the thermocouples to measure the temperature of cooled air, the cooled EGR gas and the intake manifold. The EGR distribution to each cylinder is different because the mixture of EGR gas and air is not homogenous. To evaluate the EGR rate of the #1 cylinder, the temperature of the mixture was measured close to the cylinder. (figure 5.1). The EGR rate measured using thermocouples was verified with an exhaust gas analyzer (Horiba MEXA 7100 DEGR) at steady states.

5.1.2 Combustion noise according to the EGR rate variation

The combustion noise change according to the EGR rate variation was examined by using the CNI. The operating condition was 1750 rpm and the fuel injection quantities are 17.5 mg. The only EGR valve openness was changed and their EGR rates were 30%, 25% and 18%. Figure 5.2 shows the results and table 1 represents the maximum pressure, pressure rise, RoHR and CNI, respectively. The CNI was at the highest when the EGR rate was at 30%; the value reduced as the EGR rate decreased. The EGR rate affected the ignition delay. The ignition delay became longer when the oxygen concentration was lower. The high level EGR rate limited the concentration due to the dilution effect. The longer ignition delay caused the more fuel to be combusted in the premixed combustion phase, thus the RoHR peak and pressure rise become greater, which have a considerable effect on combustion noise.

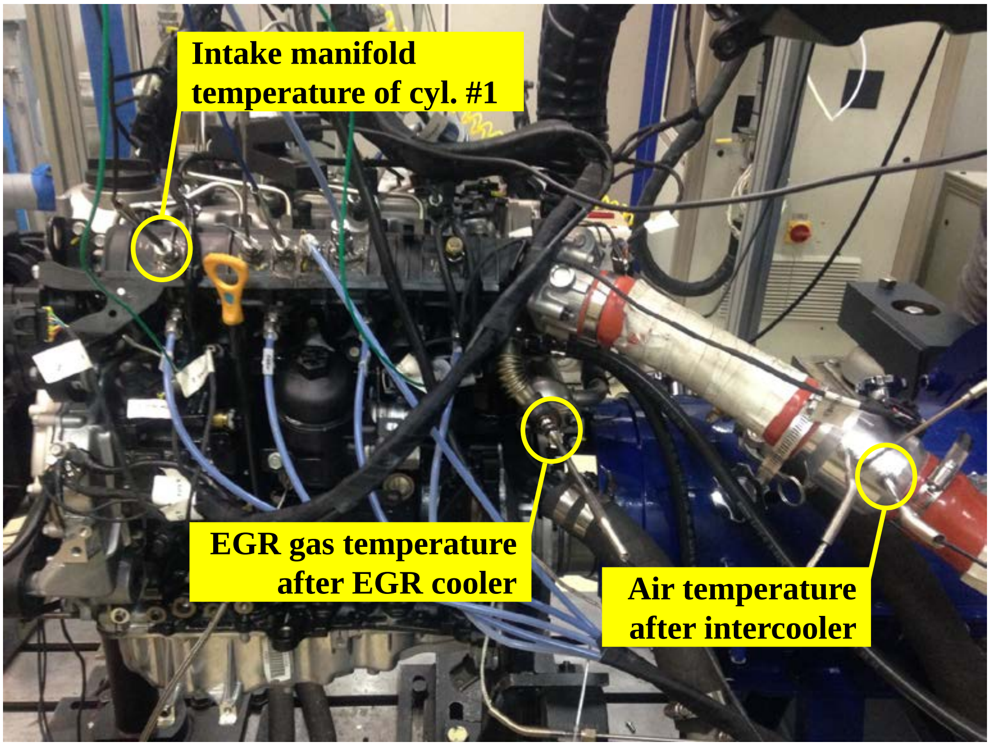
Intake manifold temperature of cyl. #1
EGR gas temperature after EGR cooler
Air temperature after intercooler

Figure 5.1 Thermocouples to measure the temperature of the air, the EGR gas and the intake manifold

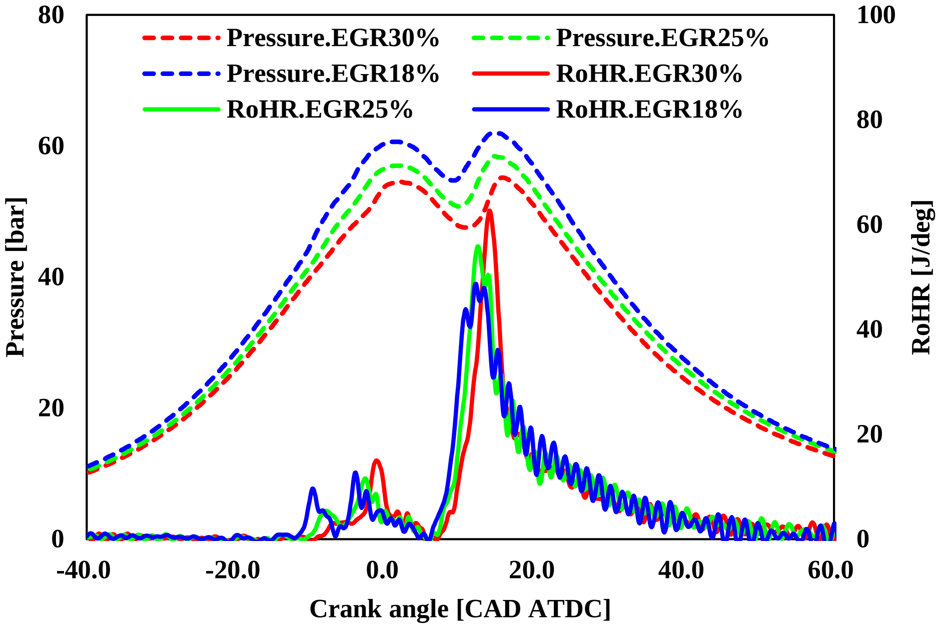

Figure 5.2 In-cylinder pressure and RoHR variation according to EGR rate change

5.1.3 CNI variation during transient operations

5.1.3.1 Transient operation 1. Speed and load change

The CNI was examined when the engine operating condition were changed to 1750 rpm and BMEP 8 bar from 1250 rpm and BMEP 2 bar while varying the ramp time to 2, 5, and 10 seconds. These operating conditions usually occur when a vehicle starts in the first or the second gear. The gear ratio is high and the engine speed rapidly increases. Figures 5.3~ 5.5 show the results. Moreover, to compare to the steady state, the constant engine speed and load states were examined per 100 rpm increase. The blue lines in the figures indicate transient operation results, and the red dots indicate the steady operation results. When the ramp time was shorter, the difference between the transient and the steady results of the CNI were greater; particularly when the engine speed was 1650 RPM and ramp time was 2 seconds, the CNI difference was at the greatest at 4 dB. The EGR rate was measured using the thermocouples. The EGR trends were very similar to that of the CNI. The difference of transient and steady state operations was larger, when the ramp time was shorter.

Figure 5.6 shows the in-cylinder pressure and the RoHR curves of a cycle during the transient operation with 2 seconds ramp time. The blue line shows transient operation and red line shows steady operation. Both were operated at the same engine speed and load, fuel injection quantity, 1650 rpm and 16.13 mg per cycle. The RoHR peak of transient operation was greater than at steady operation. This occured because of the EGR rate difference effect on ignition delay. The steady operation, which has lower EGR rate level, has a shorter ignition delay. As a result, less fuel is combusted in the premixed combustion phase, and the pressure curve is milder. The surplus EGR rate in the transient operation cause the rapid combustion, which lead to the CNI increase.

5.1.3.2 Transient operation 2. Constant speed and load change

The load was increased to 18 mg per cycle from 8 mg with a constant engine speed of1750 rpm. This condition usually occurs when a vehicle is accelerating in a high gear at high speed. Because the effective inertia of the vehicle in a high gear is much greater than a lower gear, the engine speed does not vary rapidly. The ramp times were varied to 1, 2, and 5 seconds. Steady operations were examined when the injected fuel quantities were 10 mg, 12 mg, 14 mg and 16 mg per cycle. Figures 5.7~5.9 show the results.

The CNI was calculated to evaluate the combustion noise. The difference in CNI between transient and steady state operation was the largest at 2 dB when the injection fuel was 16 mg. The EGR rate was measured by the thermocouples; when the fuel quantity changes during transient operation, the EGR rate was higher. When the fuel quantity was 16 mg, the largest EGR rate difference occurs. The higher EGR rate lengthened the ignition delay and raises the peak of the RoHR. Figure 10 shows the in-cylinder pressure and the RoHR curves of a cycle during the transient operation with 1 seconds ramp time. The surplus EGR which caused the sharp combustion lead to higher CNI level. This phenomenon is similar to the ones found in the transient operation.

Table 5.1 Maximum of pressure, pressure rise, RoHR and CNI according to EGR variation

EGR rate	Max. Pressure [bar]	Max. Pressure rise [bar/deg]	Max. RoHR [J/deg]	CNI [dB]
30%	55.2	3.11	62.7	178.2
25%	58.4	2.83	55.9	177.5
18%	61.9	2.50	48.7	176.1

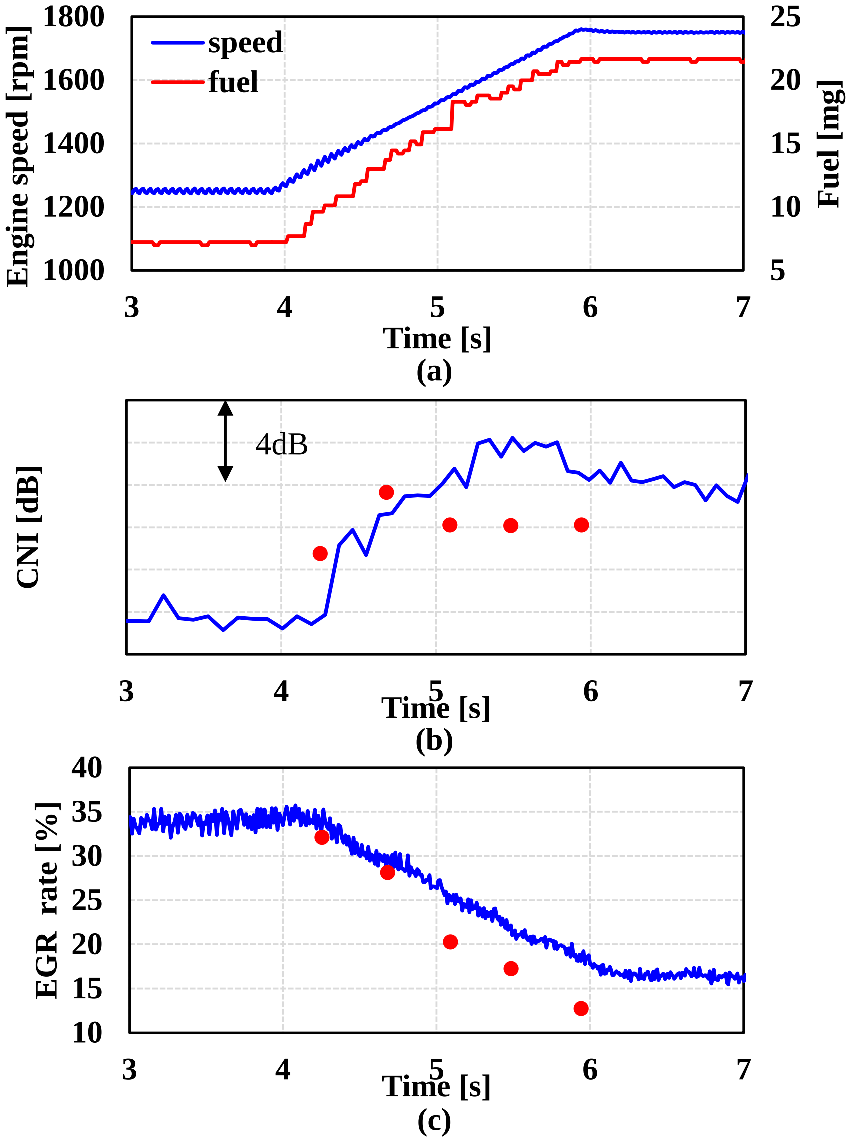

Figure 5.3 Results of speed and load transient operation, ramp time: 2 s (a) Engine speed, (b) CNI, (c) EGR rate

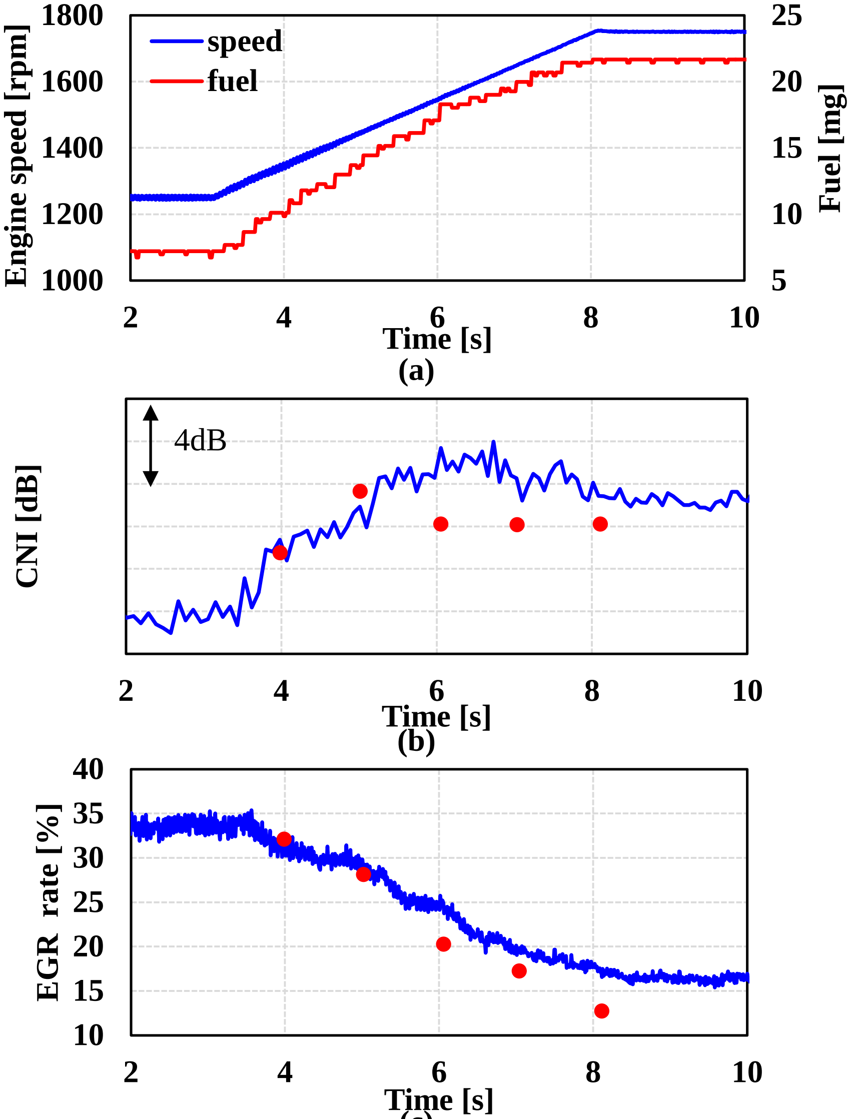

(a)

(b)

(c)

Figure 5.4 Results of speed and load transient operation, ramp time: 5 s

(a) Engine speed, (b) CNI, (c) EGR rate

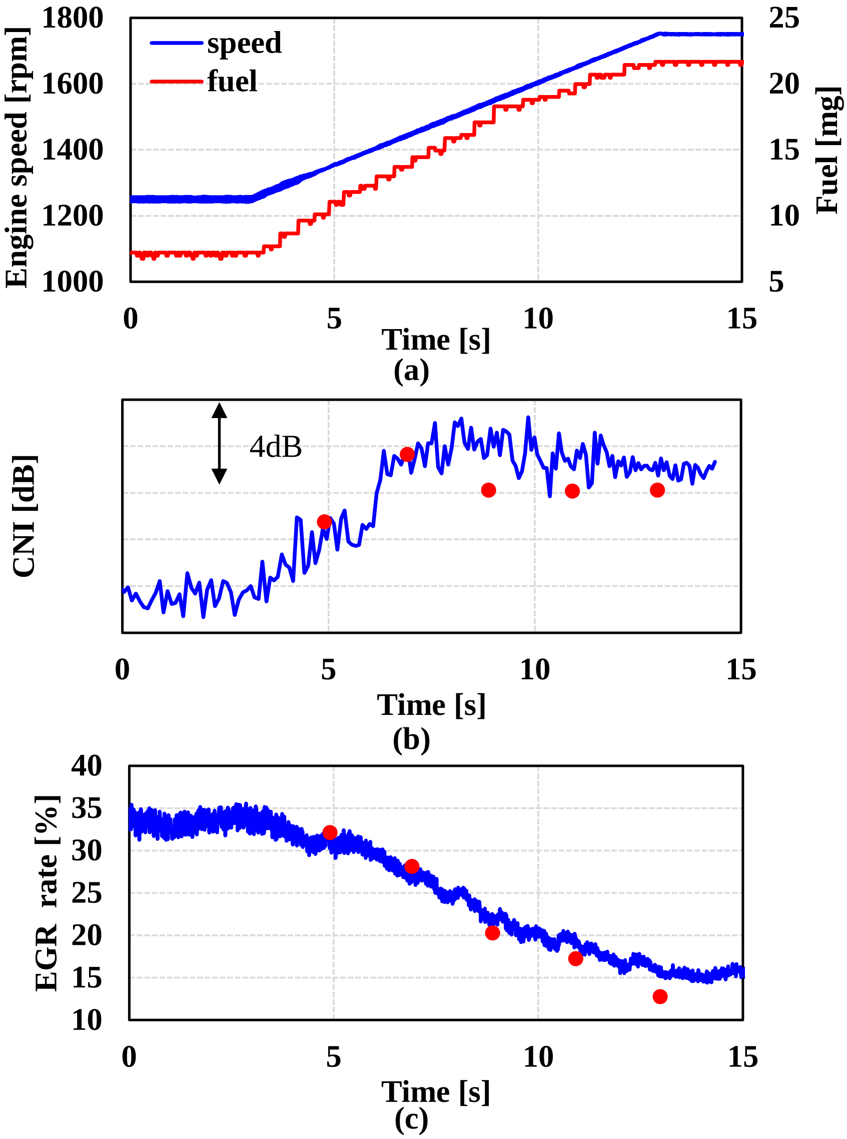

Figure 5.5 Results of speed and load transient operation, ramp time: 10 s

(a) Engine speed, (b) CNI, (c) EGR rate

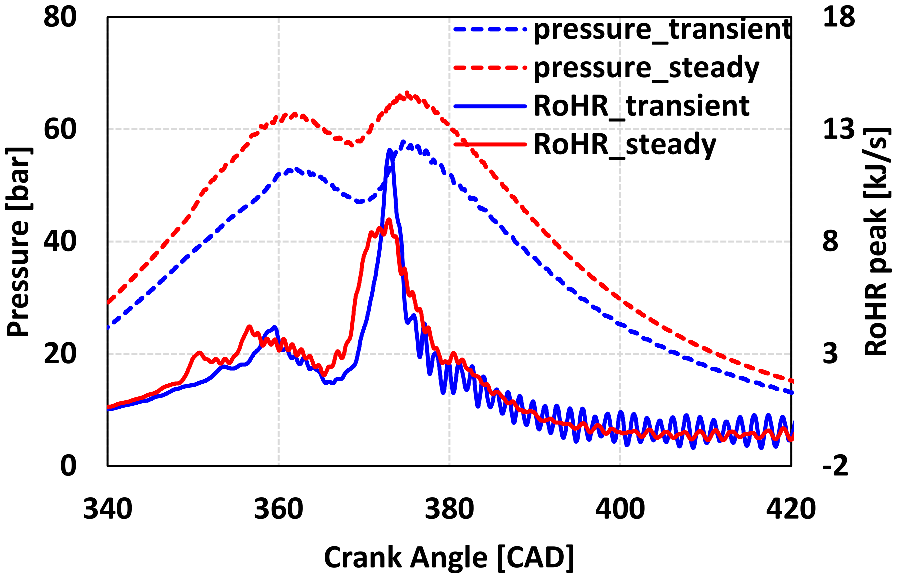

Figure 5.6 Comparison of pressure and RoHR between transient operation and steady state

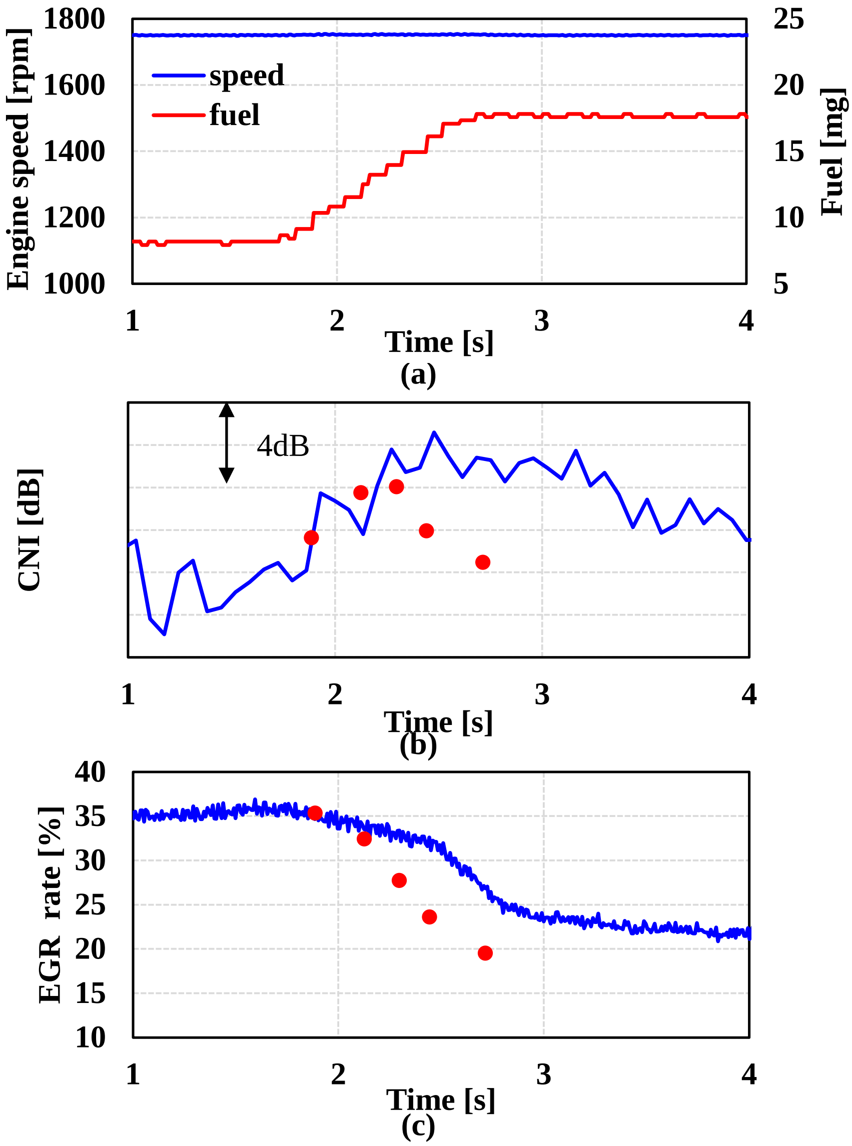

Figure 5.7 Results of load transient operation, ramp time: 1s (a) Engine speed, (b) CNI, (c) EGR rate

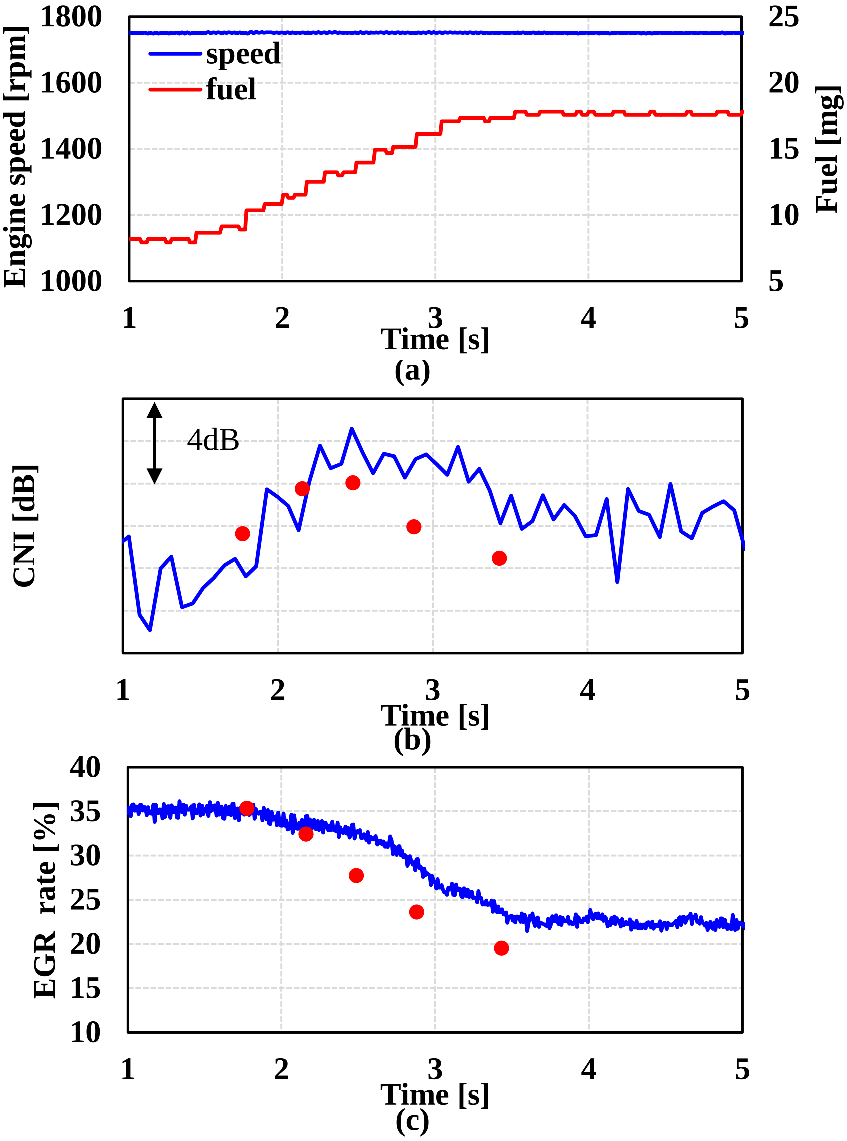

Figure 5.8 Results of load transient operation, ramp time: 2s (a) Engine speed, (b) CNI, (c) EGR rate

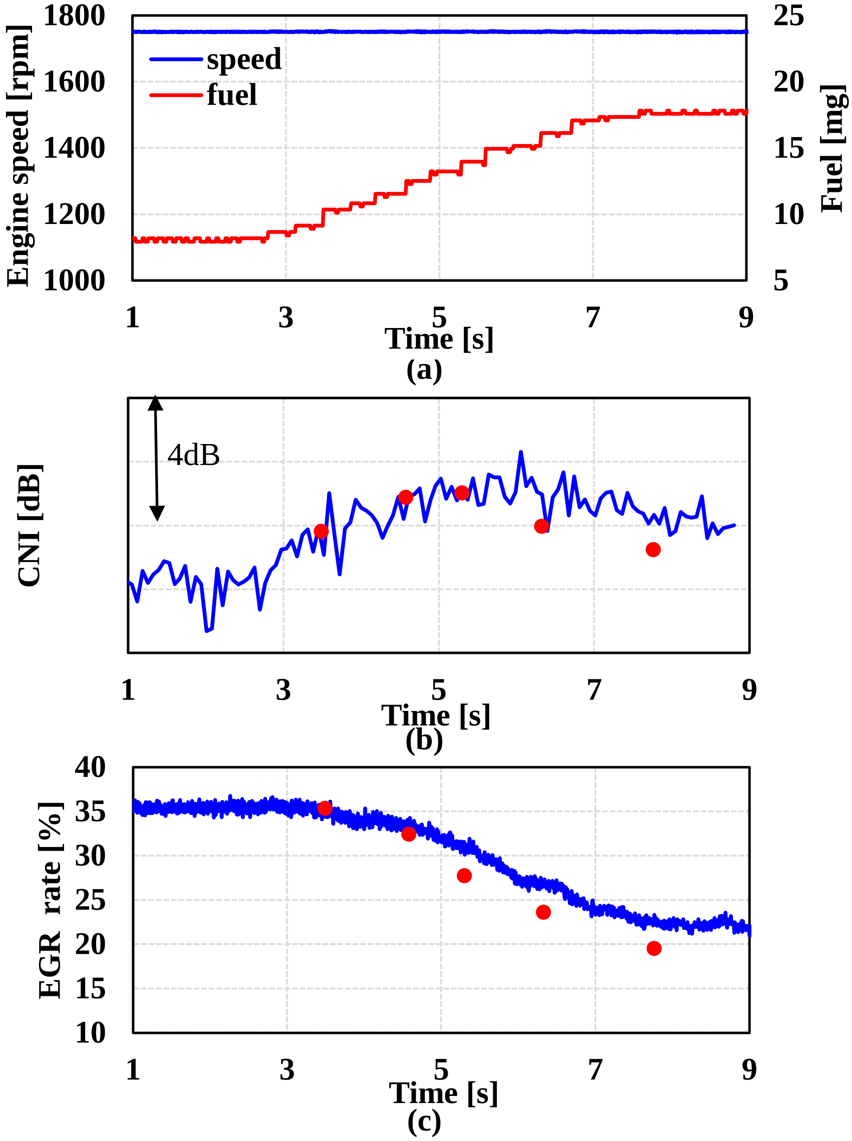

Figure 5.9 Results of load transient operation, ramp time: 5s (a) Engine speed, (b) CNI, (c) EGR rate

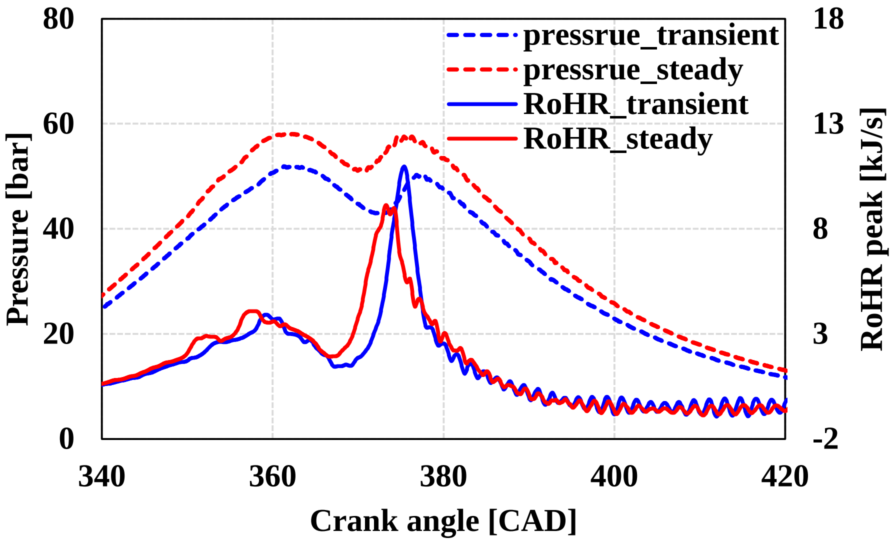

Figure 5.10 Comparison of pressure and RoHR between transient operation and steady state

5.2 Concept of control

Engine noise and emissions are sensitive to environmental condition changes because these changes affect the combustion of diesel. For example, noise can be worsened by reducing the amount of pilot injection due to the injector aging and EGR rate mismatching caused by fouling occurring in the EGR system, turbo charger lag and intake temperature variation. Moreover, the combustion noise could be changed during a transient operation as referred in 5.1. [57-59]

Closed-loop control is one way to solve these problems. The control system uses combustion information, such as the MFB50 and IMEP, which is calculated from the in-cylinder pressure, measured by a pressure sensor integrated with the glow plug. The injection strategy is determined according to the feed-back. Many researchers have developed these technologies aim to reduce emissions. However, if combustion noise is used as feedback in this sense, when applying this closed-loop control principle, the sound quality deterioration could be prevented. Therefore, this study, closed loop combustion control system using CNI for reduction of combustion noise have been developed. [60]

Figure 5.11 shows the concept of combustion control using CNI for combustion noise reduction. The control system consisted of CNI calculation and combustion control. In-cylinder pressure was measured and CNI was calculated in CNI calculator. The results of CNI calculation is passed on combustion controller which can control of EMS variables. The combustion controller was operated to create an algorithm and modify injection strategies to change the combustion characteristics and combustion noise, or combustion noise index. This process was repeated until the target was achieved

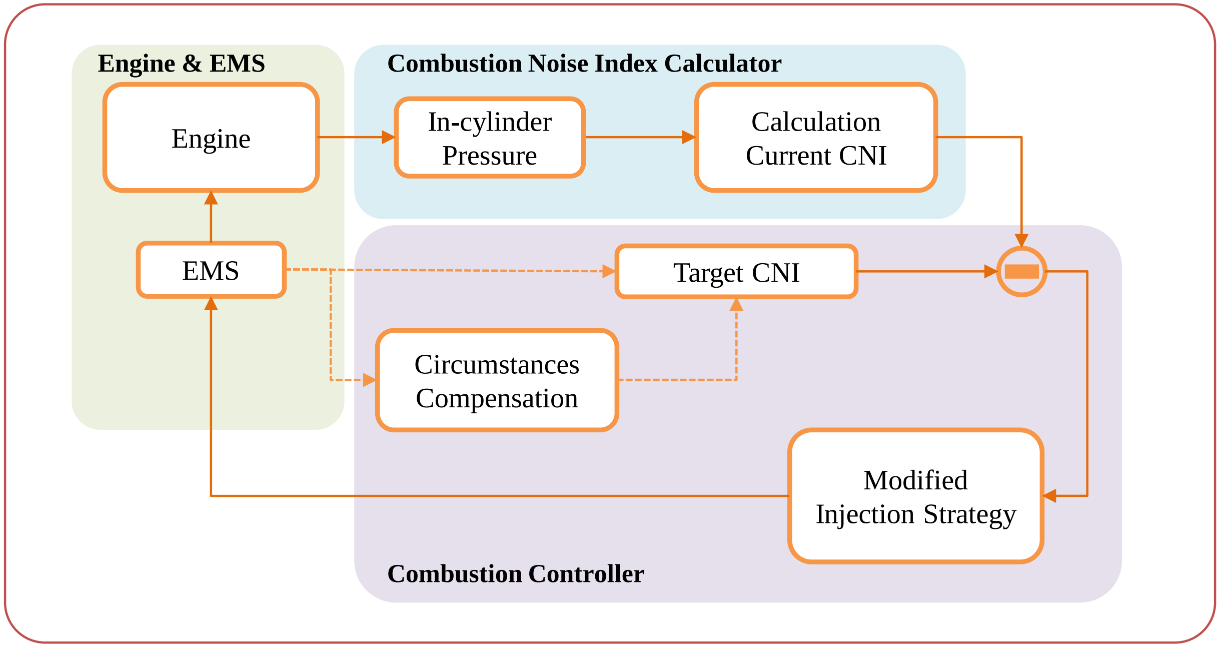
Engine & EMS
Combustion Noise Index Calculator
Engine
In-cylinder Pressure
Calculation Current CNI
EMS
Target CNI
Circumstances Compensation
Modified Injection Strategy
Combustion Controller

Figure 5.11 Concept of combustion control using CNI for combustion noise reduction

5.3 Control parameters

To determine the control parameter for CNI control, the sensitivities of the parameters, which are SOI, pilot quantity, injection pressure and EGR, for CNI were investigated.

5.3.1 Start of injection

The SOI of the main injection were varied from -2° BTDC CAD to 3° BTDC CAD. The engine speed was changed from 1250 rpm to 2500 rpm and fuel quantity was varied from 12.5 mg to 25 mg. Figure 5.12 shows CNI when the SOI were changed. The CNI levels were high where engine speed was 1750 rpm and fuel quantity was about 15 mg, though the SOI were changed.

The sensitivity of SOI for CNI was examined. Figures 5.13 and 5.14 show CNI level and SOI, respectively when the engine speed were 1500 rpm and 2000 rpm. The fuel quantity was varied between 12.5 and 25 mg. The CNI decreased by advancing SOI when the fuel quantity was 12.5~20 mg. However, when the fuel quantity was over 20 mg, the correlation between of CNI and SOI is week. That means the CNI could not be controlled by changing the SOI at the operation points. Figures 5.15 and 5.16 show the heat release rate when the SOI varied. At 15mg of fuel, when the SOI was advanced, the peak of heat release rate lowered. However, at 22.5 mg of fuel, when the SOI was advanced, the peak did not decrease. That was the reason why the CNI could not be controlled by the SOI when the fuel quantity was over 20 mg.

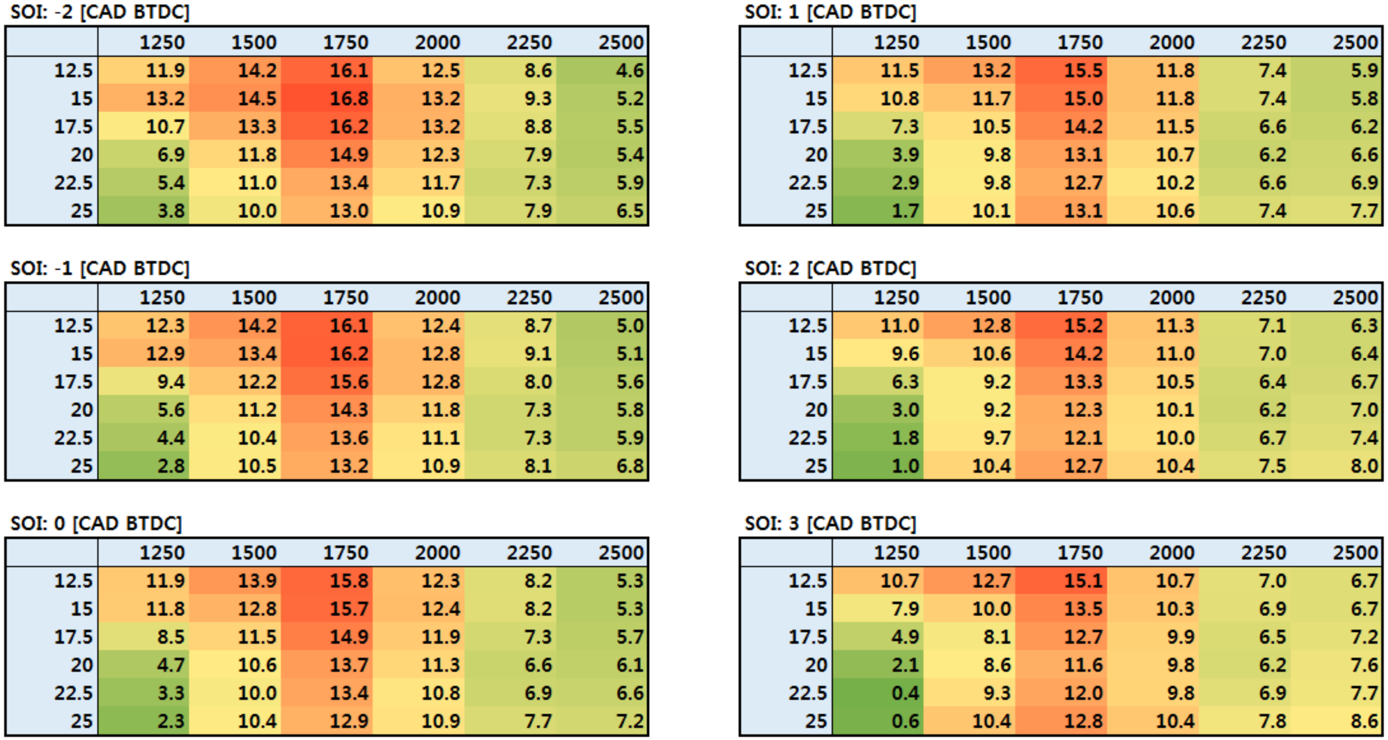

SOI: -2 [CAD BTDC]

	1250	1500	1750	2000	2250	2500
12.5	11.9	14.2	16.1	12.5	8.6	4.6
15	13.2	14.5	16.8	13.2	9.3	5.2
17.5	10.7	13.3	16.2	13.2	8.8	5.5
20	6.9	11.8	14.9	12.3	7.9	5.4
22.5	5.4	11.0	13.4	11.7	7.3	5.9
25	3.8	10.0	13.0	10.9	7.9	6.5

SOI: -1 [CAD BTDC]

	1250	1500	1750	2000	2250	2500
12.5	12.3	14.2	16.1	12.4	8.7	5.0
15	12.9	13.4	16.2	12.8	9.1	5.1
17.5	9.4	12.2	15.6	12.8	8.0	5.6
20	5.6	11.2	14.3	11.8	7.3	5.8
22.5	4.4	10.4	13.6	11.1	7.3	5.9
25	2.8	10.5	13.2	10.9	8.1	6.8

SOI: 0 [CAD BTDC]

	1250	1500	1750	2000	2250	2500
12.5	11.9	13.9	15.8	12.3	8.2	5.3
15	11.8	12.8	15.7	12.4	8.2	5.3
17.5	8.5	11.5	14.9	11.9	7.3	5.7
20	4.7	10.6	13.7	11.3	6.6	6.1
22.5	3.3	10.0	13.4	10.8	6.9	6.6
25	2.3	10.4	12.9	10.9	7.7	7.2

SOI: 1 [CAD BTDC]

	1250	1500	1750	2000	2250	2500
12.5	11.5	13.2	15.5	11.8	7.4	5.9
15	10.8	11.7	15.0	11.8	7.4	5.8
17.5	7.3	10.5	14.2	11.5	6.6	6.2
20	3.9	9.8	13.1	10.7	6.2	6.6
22.5	2.9	9.8	12.7	10.2	6.6	6.9
25	1.7	10.1	13.1	10.6	7.4	7.7

SOI: 2 [CAD BTDC]

	1250	1500	1750	2000	2250	2500
12.5	11.0	12.8	15.2	11.3	7.1	6.3
15	9.6	10.6	14.2	11.0	7.0	6.4
17.5	6.3	9.2	13.3	10.5	6.4	6.7
20	3.0	9.2	12.3	10.1	6.2	7.0
22.5	1.8	9.7	12.1	10.0	6.7	7.4
25	1.0	10.4	12.7	10.4	7.5	8.0

SOI: 3 [CAD BTDC]

	1250	1500	1750	2000	2250	2500
12.5	10.7	12.7	15.1	10.7	7.0	6.7
15	7.9	10.0	13.5	10.3	6.9	6.7
17.5	4.9	8.1	12.7	9.9	6.5	7.2
20	2.1	8.6	11.6	9.8	6.2	7.6
22.5	0.4	9.3	12.0	9.8	6.9	7.7
25	0.6	10.4	12.8	10.4	7.8	8.6

Figure 5.12 CNI variation according to SOI change

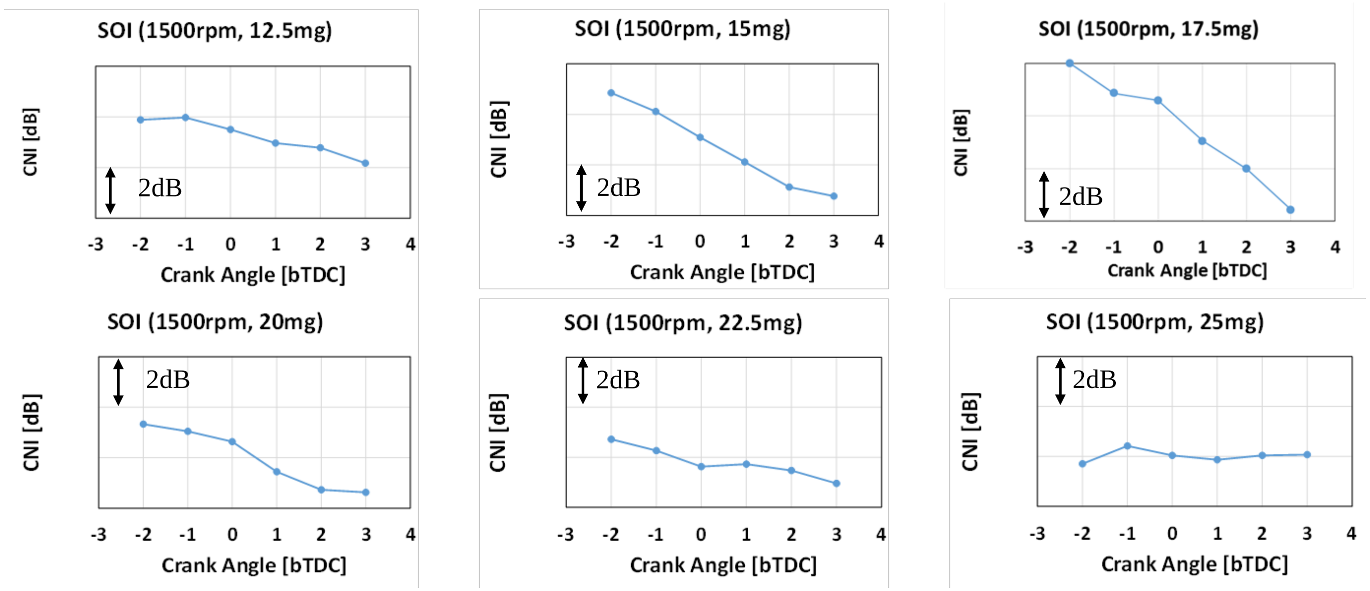

SOI (1500rpm, 12.5mg)

SOI (1500rpm, 15mg)

SOI (1500rpm, 17.5mg)

SOI (1500rpm, 20mg)

SOI (1500rpm, 22.5mg)

SOI (1500rpm, 25mg)

Figure 5.13 Sensitivity analysis of CNI for SOI change @ 1500 rpm

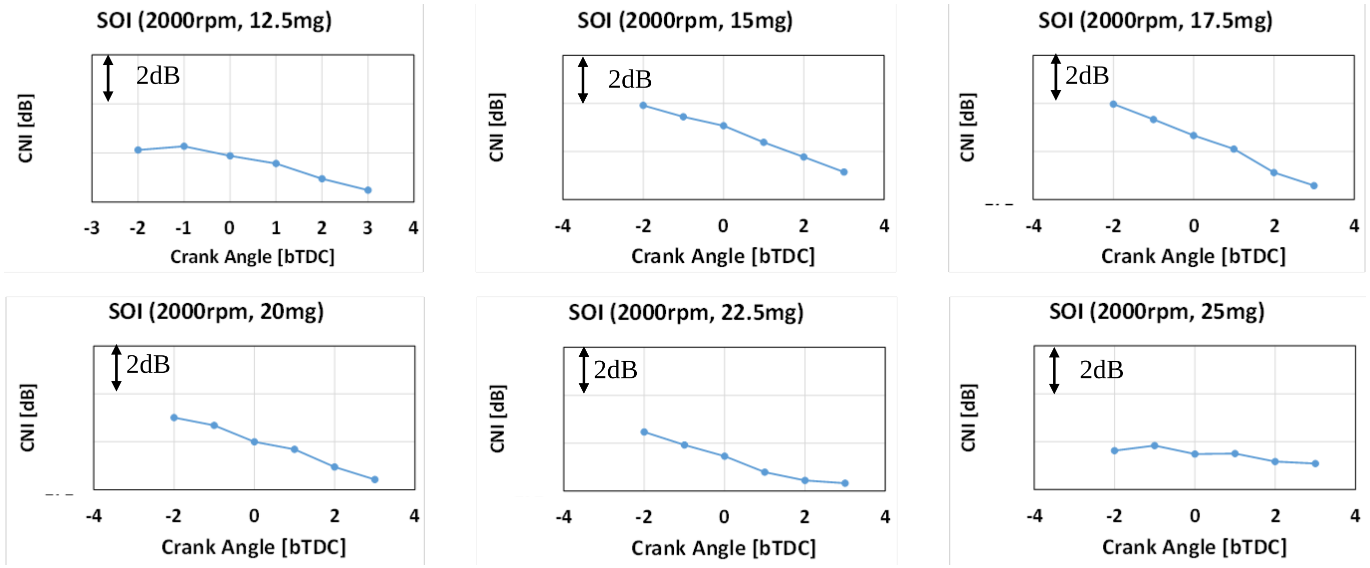

Figure 5.14 Sensitivity analysis of CNI for SOI change @ 2000 rpm

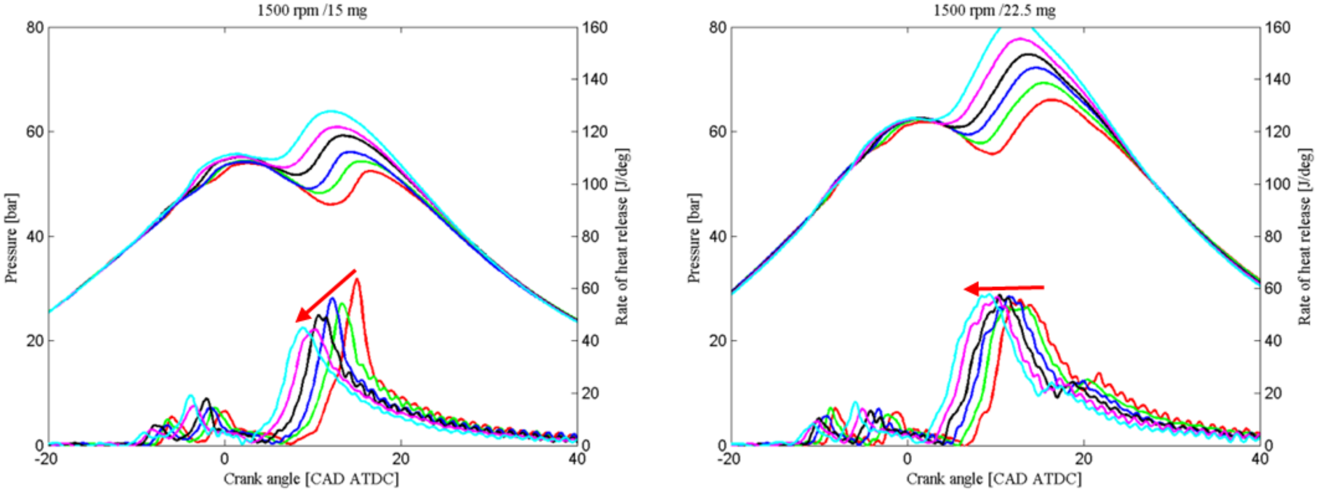

Figure 5.15 Heat release rate and in-cylinder pressure according to SOI change @ 1500 rpm

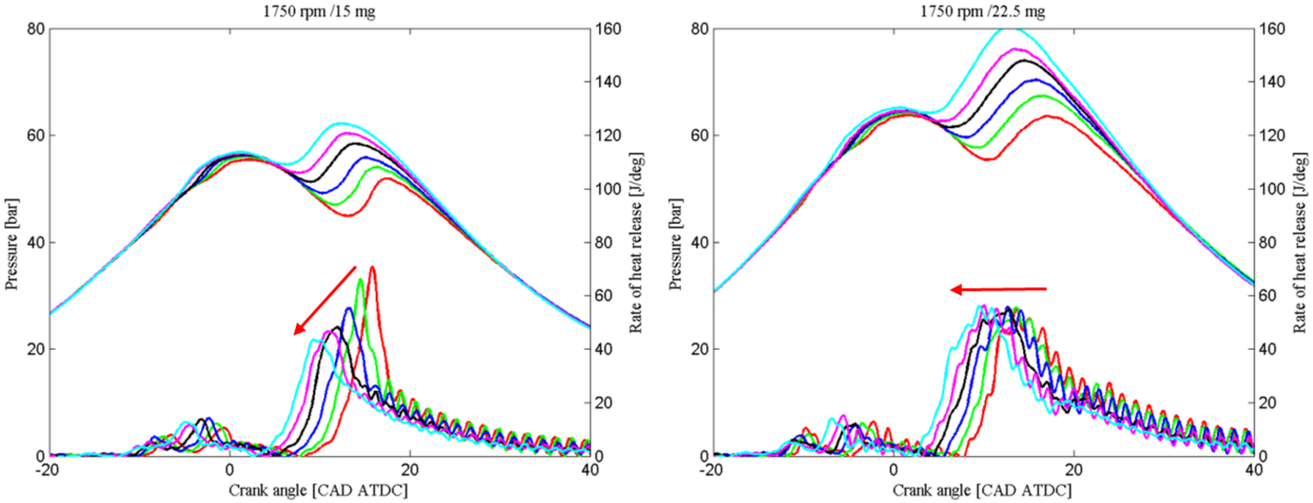

Figure 5.16 Heat release rate and in-cylinder pressure according to SOI change @ 1750 rpm

5.3.2 Other parameters: Pilot injection quantity, pilot injection timing, injection pressure and EGR rate

The sensitivity of other parameters, which are pilot injection quantity, pilot injection timing, injection pressure and EGR rate, are shown in figures 5.17 and 5.18. The pilot injection was increased by 0.3 mg and decreased by 0.3 mg. When the fuel quantity of pilot injection increased, the CNI decreased. However, the sensitivity was very low at 20mg of fuel quantity.

Injection pressure was increased and decreased by 50 bar. When injection pressure was reduced, the CNI decreased. Moreover, when the fuel quantity was even over 20 mg, the linearity was remained. It means that the injection pressure could be a parameter, which can control the CNI level for aboard operating region. Figure 5.19 shows the heat release rate. The peak of heat release rate decreased with a lower injection pressure.

The pilot injection timing was also investigated because it affects the in-cylinder gas temperature and pressure when the main fuel was injected. When the timing was changed, the CNI was varied. According to the operating point, the tendency was changed, thus, the pilot timing was not proper to be used as parameters to control the CNI level.

The EGR rate was also investigated. The EGR rate changed due to oxygen concentration in cylinder and ignition delay. When the EGR rate was high, a rapid combustion occurred because more fuel was burned in the premixed combustion phase. When the EGR rate was low, the CNI also decreased. The tendency and sensitivity were acceptable to be used as parameters to control the CNI. However, air supply system has a delay, thus it is hard to control the CNI by changing the EGR rate. In addition, NOx emission was very sensitive to the EGR rate, thus if the EGR rate was decreased to control CNI, NOx emission could have increased.

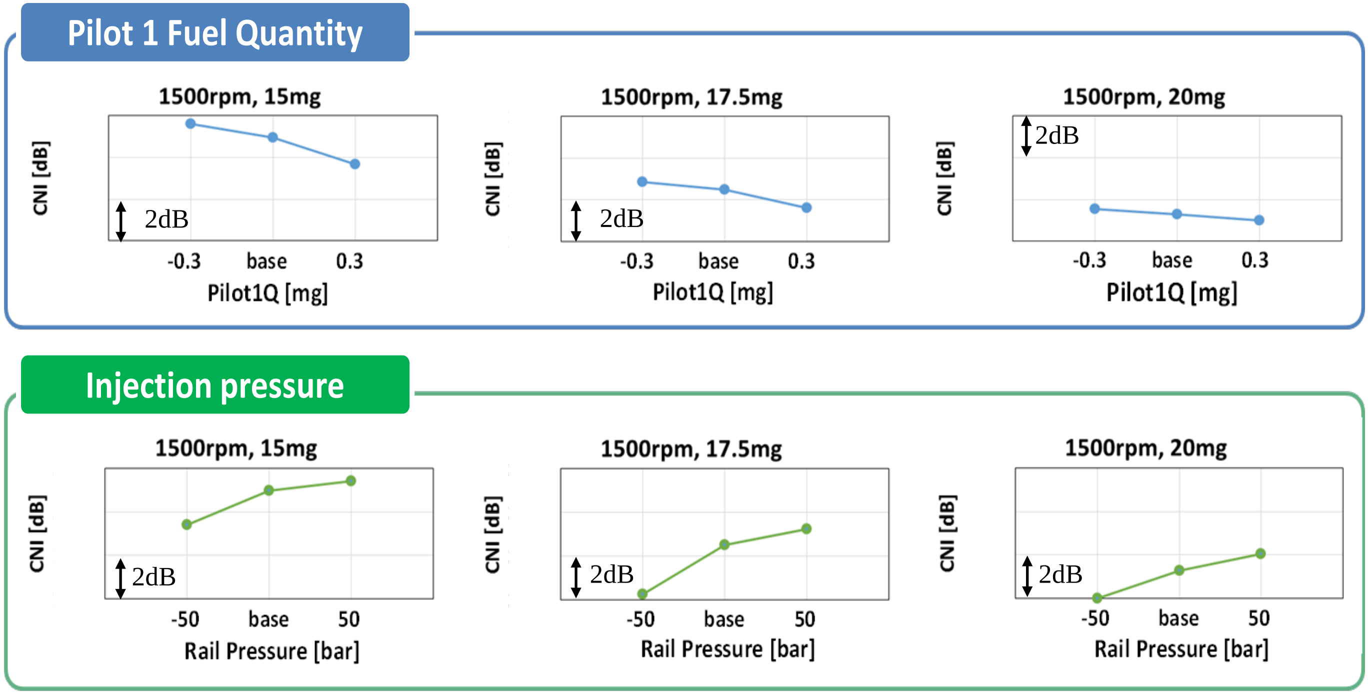

Figure 5.17 Sensitivity analysis of CNI for pilot fuel quantity and injection pressure change

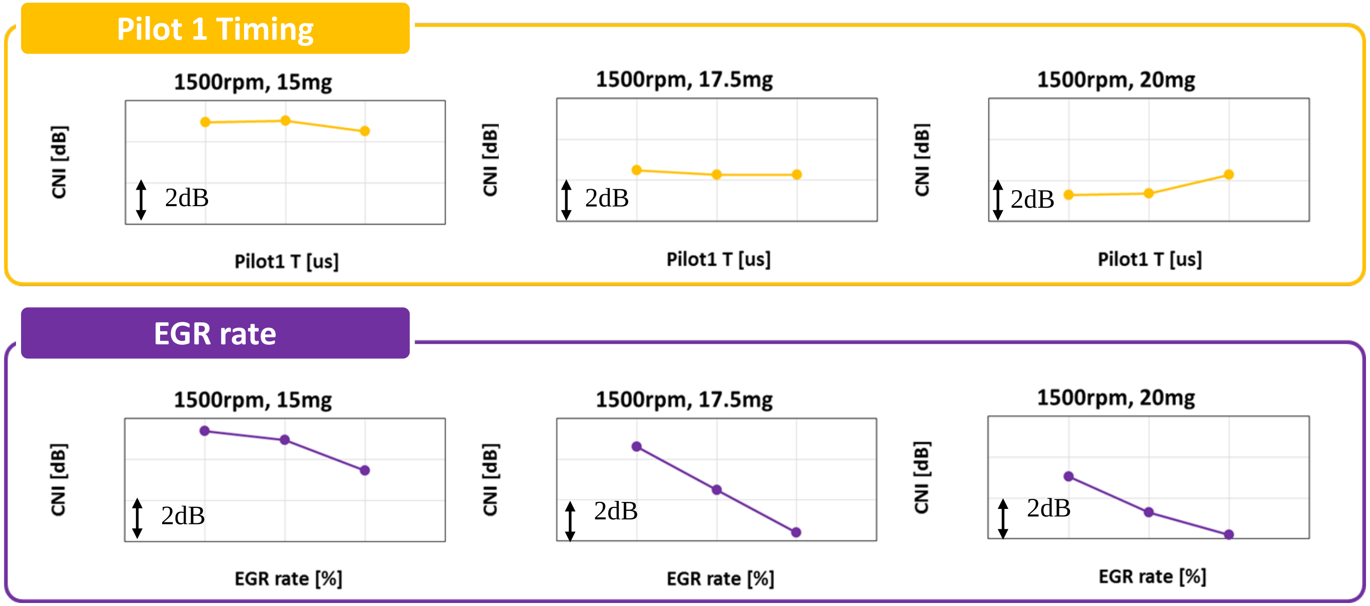

Figure 5.18 Sensitivity analysis of CNI for pilot timing and EGR rate change

5.3.3 Interaction among injection parameters

As previously referred, the main injection timing, pilot quantity and rail pressure were proper to be used as parameters to control CNI level. However, some of them had different tendency according to operating conditions. Thus, if they were simultaneously used to control the CNI level, they would make synergy or potential conflicts with other parameters. To use them together, the interaction among of them were investigated.

At first, the SOI, Pilot quantity and injection pressure were separately changed. The engine speed was changed from 1250 rpm to 2750 rpm and total fuel quantity was changed from 10 mg ~ 40 mg. That was possible to cover the general operating condition. Figure 5.19 shows a different CNI level when the SOI was 3CAD advanced and when the SOI was at the base condition. Blue means decreasing of the CNI and RED means increasing of the CNI. In other words, the blue region means that the SOI can be used as control parameter. The SOI advance was mainly effective in the region of 1250~2000 rpm and 10~20 mg fuel quantity.

The injection pressure was reduced by 60 bar. Figure 5.21 shows the difference of CNI level between reduced injection pressure and the base injection pressure. The control of injection pressure was effective in all operating points. Especially, when the engine speed is under 1500 rpm, changing the rail pressure was effective to reduce the CNI level.

The pilot injection quantity was increased by 0.3 mg. The decreased pilot injection quantity was effective under 25 mg of fuel and all engine speed. However, that was less effective than the SOI and the injection pressure as shown in figure 5.20

To investigate the interaction among the advanced SOI, reduction of injection pressure and increase of pilot injection, they were applied simultaneously. If there were no cross effects among them, effects of each parameters would be linearly summed when they are used together. Figures 5.22 and 5.23 show estimated values when the effects of them were arithmetically summed and results when in-cylinder pressure were measured by experiment, in which the all of parameter were changed. The gap between estimated value and experimental results are not considerable. Thus, they can be simultaneously used to control the CNI level, because they did not have negative cross effects. Moreover, if the operating region, in which each of the parameters is used, is limited, the available operating region is extended. The application operating regions are shown in figures 5.24-26 and the results of CNI are shown in figure 5.27.

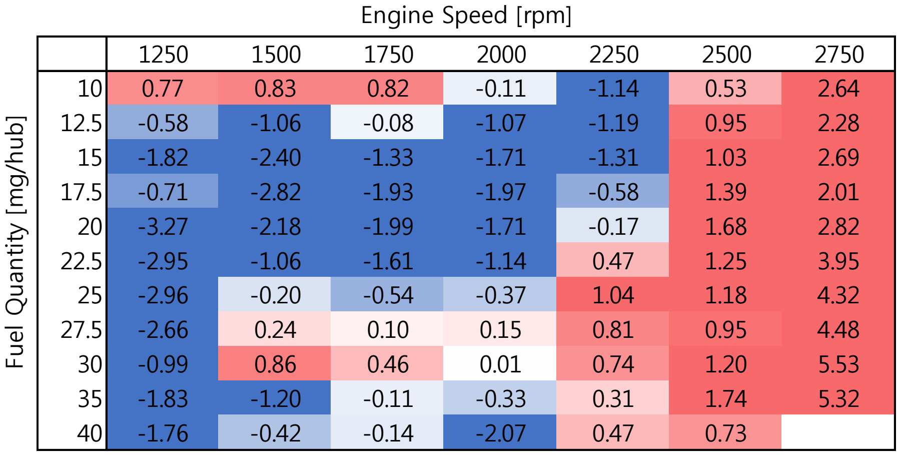

	Engine Speed [rpm]						
Fuel Quantity [mg/hub]	1250	1500	1750	2000	2250	2500	2750
10	0.77	0.83	0.82	-0.11	-1.14	0.53	2.64
12.5	-0.58	-1.06	-0.08	-1.07	-1.19	0.95	2.28
15	-1.82	-2.40	-1.33	-1.71	-1.31	1.03	2.69
17.5	-0.71	-2.82	-1.93	-1.97	-0.58	1.39	2.01
20	-3.27	-2.18	-1.99	-1.71	-0.17	1.68	2.82
22.5	-2.95	-1.06	-1.61	-1.14	0.47	1.25	3.95
25	-2.96	-0.20	-0.54	-0.37	1.04	1.18	4.32
27.5	-2.66	0.24	0.10	0.15	0.81	0.95	4.48
30	-0.99	0.86	0.46	0.01	0.74	1.20	5.53
35	-1.83	-1.20	-0.11	-0.33	0.31	1.74	5.32
40	-1.76	-0.42	-0.14	-2.07	0.47	0.73	

Figure 5.19 CNI change when SOI is advanced by 3 CAD

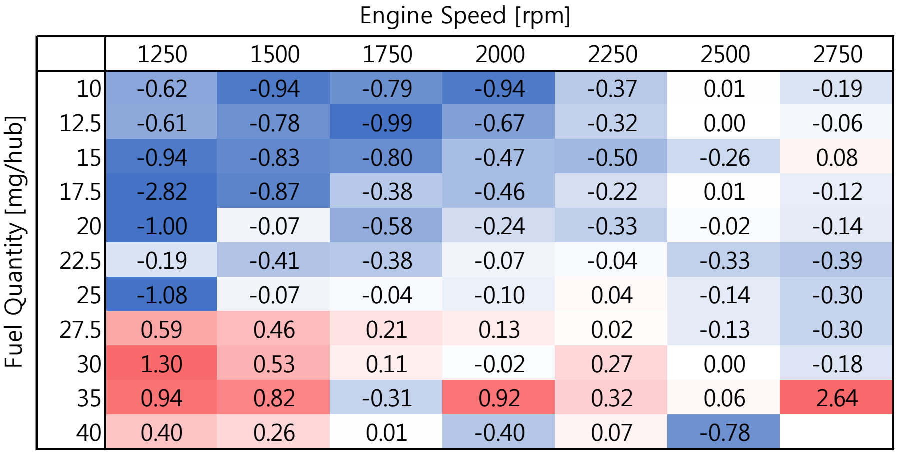

	Engine Speed [rpm]						
Fuel Quantity [mg/hub]	1250	1500	1750	2000	2250	2500	2750
10	-0.62	-0.94	-0.79	-0.94	-0.37	0.01	-0.19
12.5	-0.61	-0.78	-0.99	-0.67	-0.32	0.00	-0.06
15	-0.94	-0.83	-0.80	-0.47	-0.50	-0.26	0.08
17.5	-2.82	-0.87	-0.38	-0.46	-0.22	0.01	-0.12
20	-1.00	-0.07	-0.58	-0.24	-0.33	-0.02	-0.14
22.5	-0.19	-0.41	-0.38	-0.07	-0.04	-0.33	-0.39
25	-1.08	-0.07	-0.04	-0.10	0.04	-0.14	-0.30
27.5	0.59	0.46	0.21	0.13	0.02	-0.13	-0.30
30	1.30	0.53	0.11	-0.02	0.27	0.00	-0.18
35	0.94	0.82	-0.31	0.92	0.32	0.06	2.64
40	0.40	0.26	0.01	-0.40	0.07	-0.78	

Figure 5.20 CNI change when Pilot quantity increase by 0.2 mg

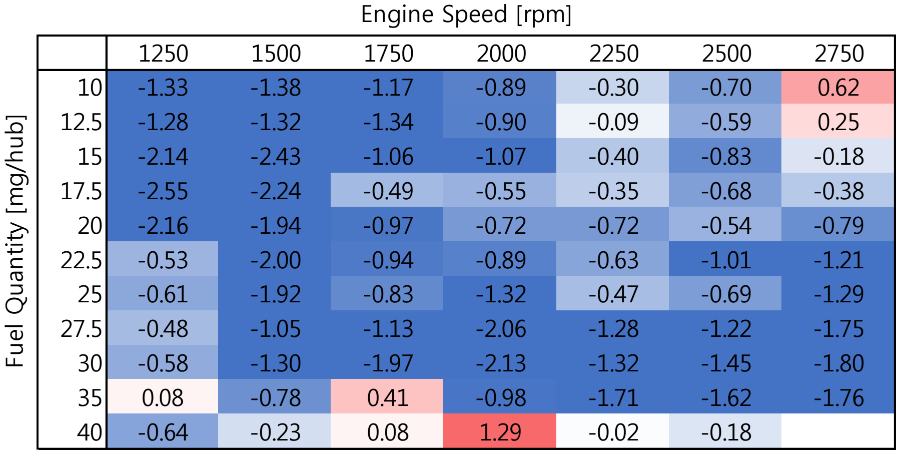

Fuel Quantity [mg/hub]	Engine Speed [rpm] 1250	1500	1750	2000	2250	2500	2750
10	-1.33	-1.38	-1.17	-0.89	-0.30	-0.70	0.62
12.5	-1.28	-1.32	-1.34	-0.90	-0.09	-0.59	0.25
15	-2.14	-2.43	-1.06	-1.07	-0.40	-0.83	-0.18
17.5	-2.55	-2.24	-0.49	-0.55	-0.35	-0.68	-0.38
20	-2.16	-1.94	-0.97	-0.72	-0.72	-0.54	-0.79
22.5	-0.53	-2.00	-0.94	-0.89	-0.63	-1.01	-1.21
25	-0.61	-1.92	-0.83	-1.32	-0.47	-0.69	-1.29
27.5	-0.48	-1.05	-1.13	-2.06	-1.28	-1.22	-1.75
30	-0.58	-1.30	-1.97	-2.13	-1.32	-1.45	-1.80
35	0.08	-0.78	0.41	-0.98	-1.71	-1.62	-1.76
40	-0.64	-0.23	0.08	1.29	-0.02	-0.18	

Figure 5.21 CNI change when injection pressure is reduced by 60 bar

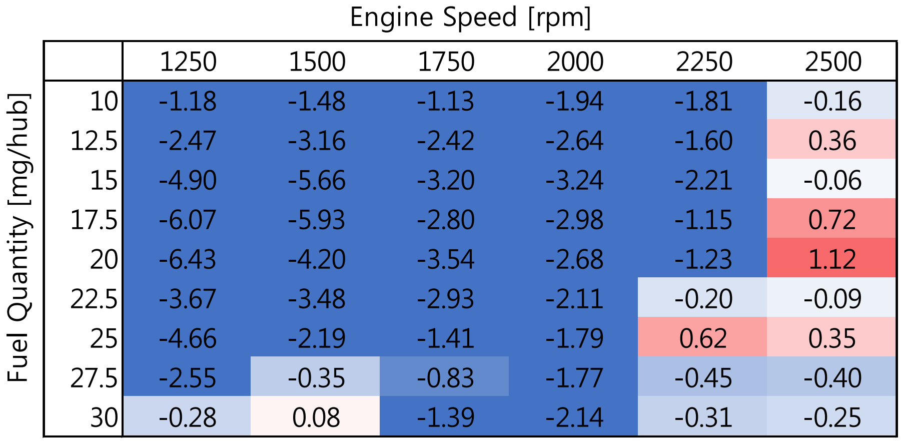

Engine Speed [rpm]

Fuel Quantity [mg/hub]	1250	1500	1750	2000	2250	2500
10	-1.18	-1.48	-1.13	-1.94	-1.81	-0.16
12.5	-2.47	-3.16	-2.42	-2.64	-1.60	0.36
15	-4.90	-5.66	-3.20	-3.24	-2.21	-0.06
17.5	-6.07	-5.93	-2.80	-2.98	-1.15	0.72
20	-6.43	-4.20	-3.54	-2.68	-1.23	1.12
22.5	-3.67	-3.48	-2.93	-2.11	-0.20	-0.09
25	-4.66	-2.19	-1.41	-1.79	0.62	0.35
27.5	-2.55	-0.35	-0.83	-1.77	-0.45	-0.40
30	-0.28	0.08	-1.39	-2.14	-0.31	-0.25

Figure 5.22 Arithmetically estimated CNI variation when SOI, pilot quantity and injection pressure are simultaneously changed

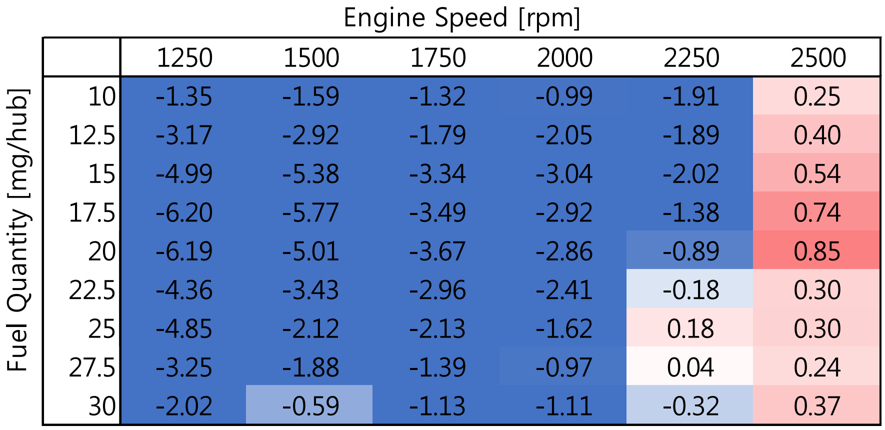

Engine Speed [rpm]

Fuel Quantity [mg/hub]	1250	1500	1750	2000	2250	2500
10	-1.35	-1.59	-1.32	-0.99	-1.91	0.25
12.5	-3.17	-2.92	-1.79	-2.05	-1.89	0.40
15	-4.99	-5.38	-3.34	-3.04	-2.02	0.54
17.5	-6.20	-5.77	-3.49	-2.92	-1.38	0.74
20	-6.19	-5.01	-3.67	-2.86	-0.89	0.85
22.5	-4.36	-3.43	-2.96	-2.41	-0.18	0.30
25	-4.85	-2.12	-2.13	-1.62	0.18	0.30
27.5	-3.25	-1.88	-1.39	-0.97	0.04	0.24
30	-2.02	-0.59	-1.13	-1.11	-0.32	0.37

Figure 5.23 Experimental results CNI variation when SOI, pilot quantity and injection pressure are simultaneously changed

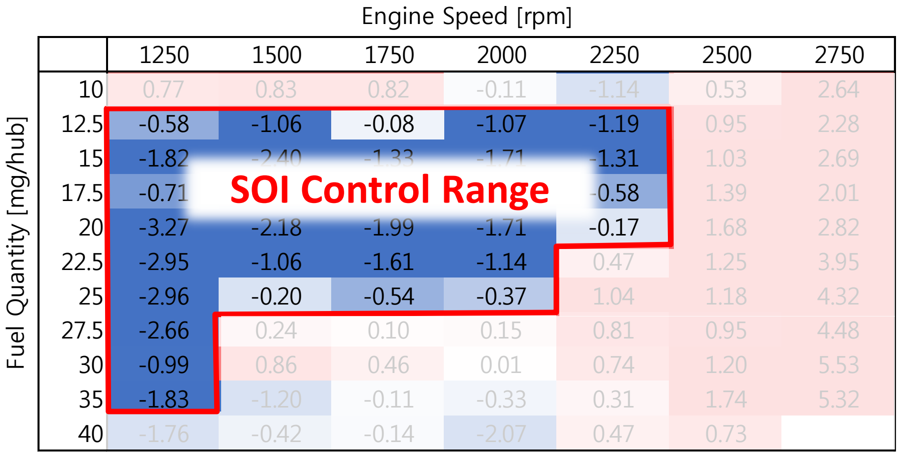
SOI Control Range

Engine Speed [rpm]

Fuel Quantity [mg/hub]	1250	1500	1750	2000	2250	2500	2750
10	0.77	0.83	0.82	-0.11	-1.14	0.53	2.64
12.5	-0.58	-1.06	-0.08	-1.07	-1.19	0.95	2.28
15	-1.82	-2.40	-1.33	-1.71	-1.31	1.03	2.69
17.5	-0.71	[illegible]	[illegible]	[illegible]	-0.58	1.39	2.01
20	-3.27	-2.18	-1.99	-1.71	-0.17	1.68	2.82
22.5	-2.95	-1.06	-1.61	-1.14	0.47	1.25	3.95
25	-2.96	-0.20	-0.54	-0.37	1.04	1.18	4.32
27.5	-2.66	0.24	0.10	0.15	0.81	0.95	4.48
30	-0.99	0.86	0.46	0.01	0.74	1.20	5.53
35	-1.83	-1.20	-0.11	-0.33	0.31	1.74	5.32
40	-1.76	-0.42	-0.14	-2.07	0.47	0.73	

Figure 5.24 Control range using SOI

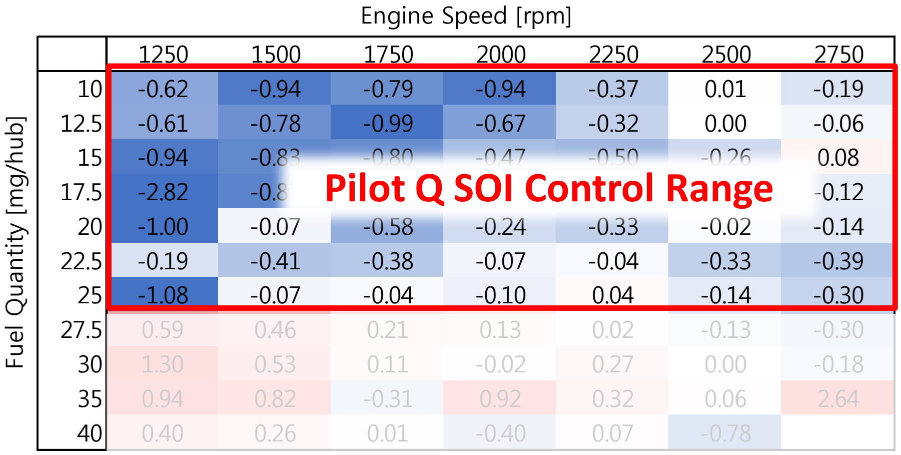
Pilot Q SOI Control Range

Engine Speed [rpm]

Fuel Quantity [mg/hub]	1250	1500	1750	2000	2250	2500	2750
10	-0.62	-0.94	-0.79	-0.94	-0.37	0.01	-0.19
12.5	-0.61	-0.78	-0.99	-0.67	-0.32	0.00	-0.06
15	-0.94	-0.83	-0.80	-0.47	-0.50	-0.26	0.08
17.5	-2.82	-0.8	[illegible]	[illegible]	[illegible]	[illegible]	-0.12
20	-1.00	-0.07	-0.58	-0.24	-0.33	-0.02	-0.14
22.5	-0.19	-0.41	-0.38	-0.07	-0.04	-0.33	-0.39
25	-1.08	-0.07	-0.04	-0.10	0.04	-0.14	-0.30
27.5	0.59	0.46	0.21	0.13	0.02	-0.13	-0.30
30	1.30	0.53	0.11	-0.02	0.27	0.00	-0.18
35	0.94	0.82	-0.31	0.92	0.32	0.06	2.64
40	0.40	0.26	0.01	-0.40	0.07	-0.78	

Figure 5.25 Control range using pilot quantity

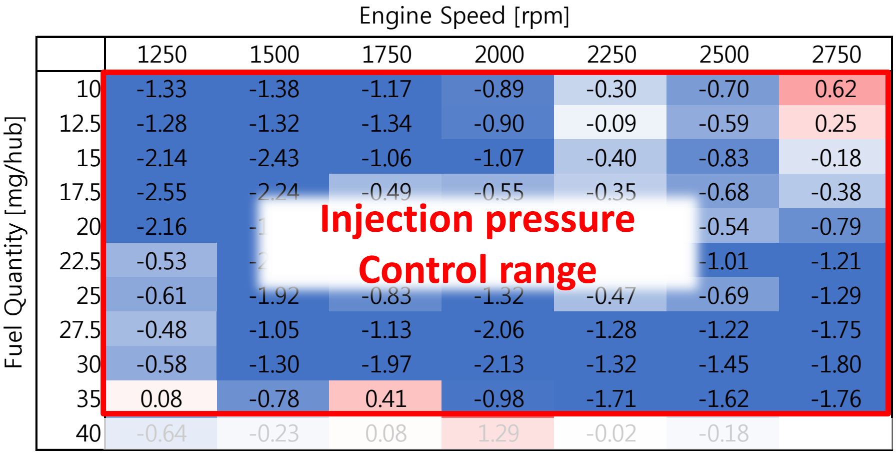
Injection pressure
Control range

Engine Speed [rpm]

Fuel Quantity [mg/hub]	1250	1500	1750	2000	2250	2500	2750
10	-1.33	-1.38	-1.17	-0.89	-0.30	-0.70	0.62
12.5	-1.28	-1.32	-1.34	-0.90	-0.09	-0.59	0.25
15	-2.14	-2.43	-1.06	-1.07	-0.40	-0.83	-0.18
17.5	-2.55	-2.24	-0.49	-0.55	-0.35	-0.68	-0.38
20	-2.16	[illegible]	[illegible]	[illegible]	[illegible]	-0.54	-0.79
22.5	-0.53	[illegible]	[illegible]	[illegible]	[illegible]	-1.01	-1.21
25	-0.61	-1.92	-0.83	-1.32	-0.47	-0.69	-1.29
27.5	-0.48	-1.05	-1.13	-2.06	-1.28	-1.22	-1.75
30	-0.58	-1.30	-1.97	-2.13	-1.32	-1.45	-1.80
35	0.08	-0.78	0.41	-0.98	-1.71	-1.62	-1.76
40	-0.64	-0.23	0.08	1.29	-0.02	-0.18	

Figure 5.26 Control range using injection pressure

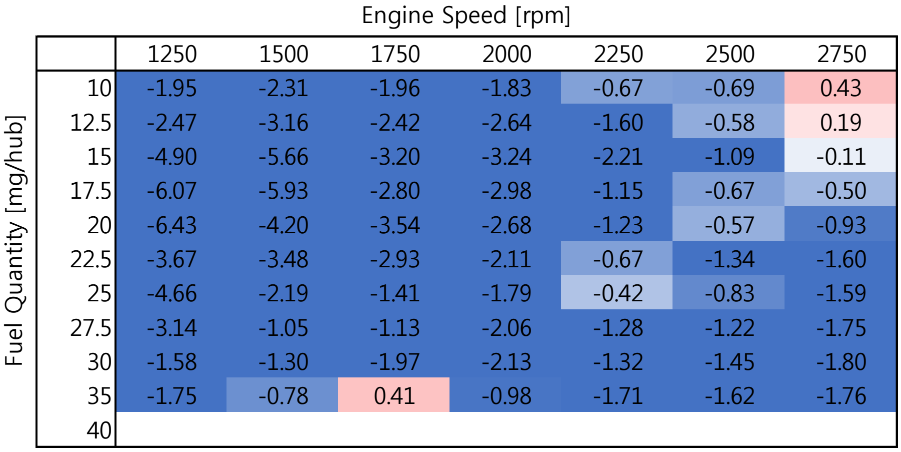

Engine Speed [rpm]

Fuel Quantity [mg/hub]	1250	1500	1750	2000	2250	2500	2750
10	-1.95	-2.31	-1.96	-1.83	-0.67	-0.69	0.43
12.5	-2.47	-3.16	-2.42	-2.64	-1.60	-0.58	0.19
15	-4.90	-5.66	-3.20	-3.24	-2.21	-1.09	-0.11
17.5	-6.07	-5.93	-2.80	-2.98	-1.15	-0.67	-0.50
20	-6.43	-4.20	-3.54	-2.68	-1.23	-0.57	-0.93
22.5	-3.67	-3.48	-2.93	-2.11	-0.67	-1.34	-1.60
25	-4.66	-2.19	-1.41	-1.79	-0.42	-0.83	-1.59
27.5	-3.14	-1.05	-1.13	-2.06	-1.28	-1.22	-1.75
30	-1.58	-1.30	-1.97	-2.13	-1.32	-1.45	-1.80
35	-1.75	-0.78	0.41	-0.98	-1.71	-1.62	-1.76
40							

Figure 5.27 CNI variation when the control ranges are limited for each parameters

5.4 Real time combustion control system to combustion noise

5.4.1 Overview of real time combustion control system

The system has 3 parts which are measurements of in-cylinder pressure, calculation of CNI and control of injection strategies. Figure 5.32 shows schematic diagram of the control system. The pressure was measured by using a charge type pressure sensor and charge amplifier. The CNI was calculation using the NI-PXI. The software was coded by LabVIEW. The injection strategy were modified in the ES1000. The control software was coded by ASCET. The NI-PXI and ES1000 communicated each other using CAN bus.

5.4.2 Calculation of CNI

The CNI was calculated using NI-PXI as shown in figure 5.33. The process of CNI calculation included FFT, thus the pressure samples had to be measured with same time interval. To obtain the time based samples, a Field-Programmable Gate Array (FPGA) board was used. The FPGA board is an integrated circuit designed to be configured by a customer or a designer after manufacturing. The in-cylinder pressure signal was acquired with Crank Position Sensor (CPS) signal which was also used in EMS (engine management system). Using the CPS signal, the crank angle information of the pressure signal was measured. The CNI calculation has to be finished within one cycle for cycle by cycle control. The whole pressure signal of one cycle was not used, but only pressure signal from -180 CAD to 180 CAD, in which the combustion process occurred, was used for CNI calculation. The acquired pressure data were transferred to real time controller via FIFO in the NI-PXI. In the real time controller, FFT of pressure signal was first calculated. Then, octave analysis of the FFT results were executed, and finally CNI was calculated. The CNI value transfer to ES1000 via CAN bus communication. All of the process were completed within one cycle. The process of calculation was described in figure 5.33.

5.4.3 Control of injection strategies

When the CNI calculation was completed, the results were transferred to combustion controller. The combustion controller compared target CNI level and current CNI level and modifies the injection strategies when the current CNI level higher than target level. Figure5.34 shows the schematic diagram of combustion controller.

The combustion controller consisted of 5 parts. The first part was data input and output. In the part, the EMS data, such as, engine speed, fuel quantity, rail pressure, pilot quantity, SOI, etc. were measured. In addition, the current CNI level, which was calculated in the NI-PXI, was read and current engine operation condition was sent to the NI-PXI via CAN bus communication.

In the control mode part, it was determined whether the control system was activated or deactivated according to the engine operation condition. When the engine speed was too high or when the fuel quantity was too much, the CNI could not be controlled. Thus, the controllable operating condition had to be discriminated. It was able to distinguish the transient of activation and deactivation. That was helpful to reduce the shock of change of operating mode.

Next, the current CNI level, which was obtained via CAN bus, was compared to target CNI level. The target level was determined from lookup table using engine speed and fuel quantity. The table was able to be changed according to operating condition because the original injection strategies of EMS were changed when the operating condition varied. The difference of current value and target was sent to PID controller.

In the PID controller part, the injection parameters, which was SOI, rail pressure and pilot quantity, was controlled to follow the target CNI level for current value. The PID controllers was independent because they have different sensitivity and limitation. The gains of each PID controller were tuned according operating conditions. The limitation of them were set to improve robustness.

The last part was communication with EMS. The ES1000 and EMS communicate via ETK protocol. The original value of variables of EMS were replaced modified values in combustion controller. To apply next cycle, at least the bypass had to be completed before 90° BTDC CAD.

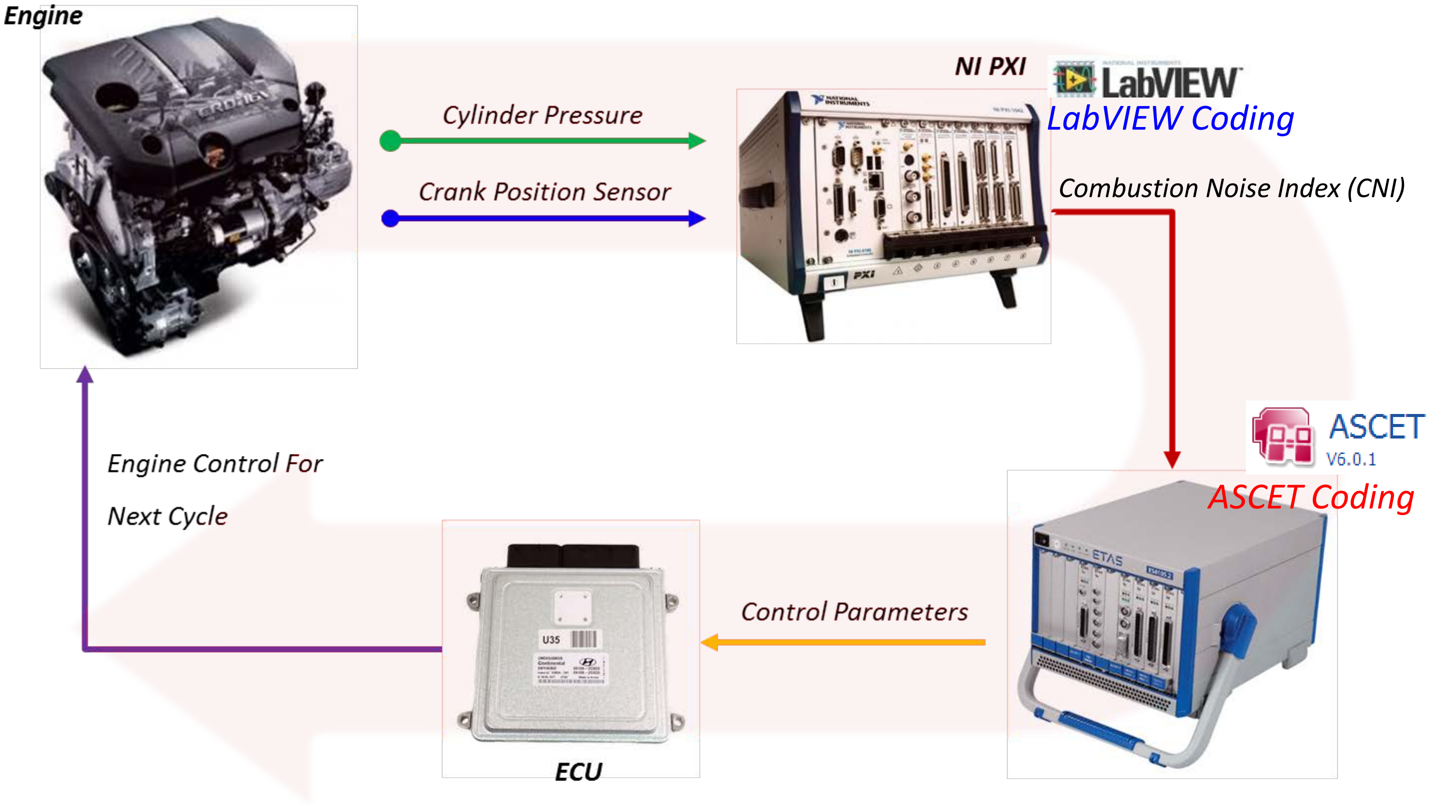
Engine
Cylinder Pressure
Crank Position Sensor
NI PXI
LabVIEW
LabVIEW Coding
Combustion Noise Index (CNI)
ASCET
V6.0.1
ASCET Coding
Engine Control For
Next Cycle
Control Parameters
ECU

Figure 5.28 Schematic diagram of closed loop control system using CNI to reduce combustion noise

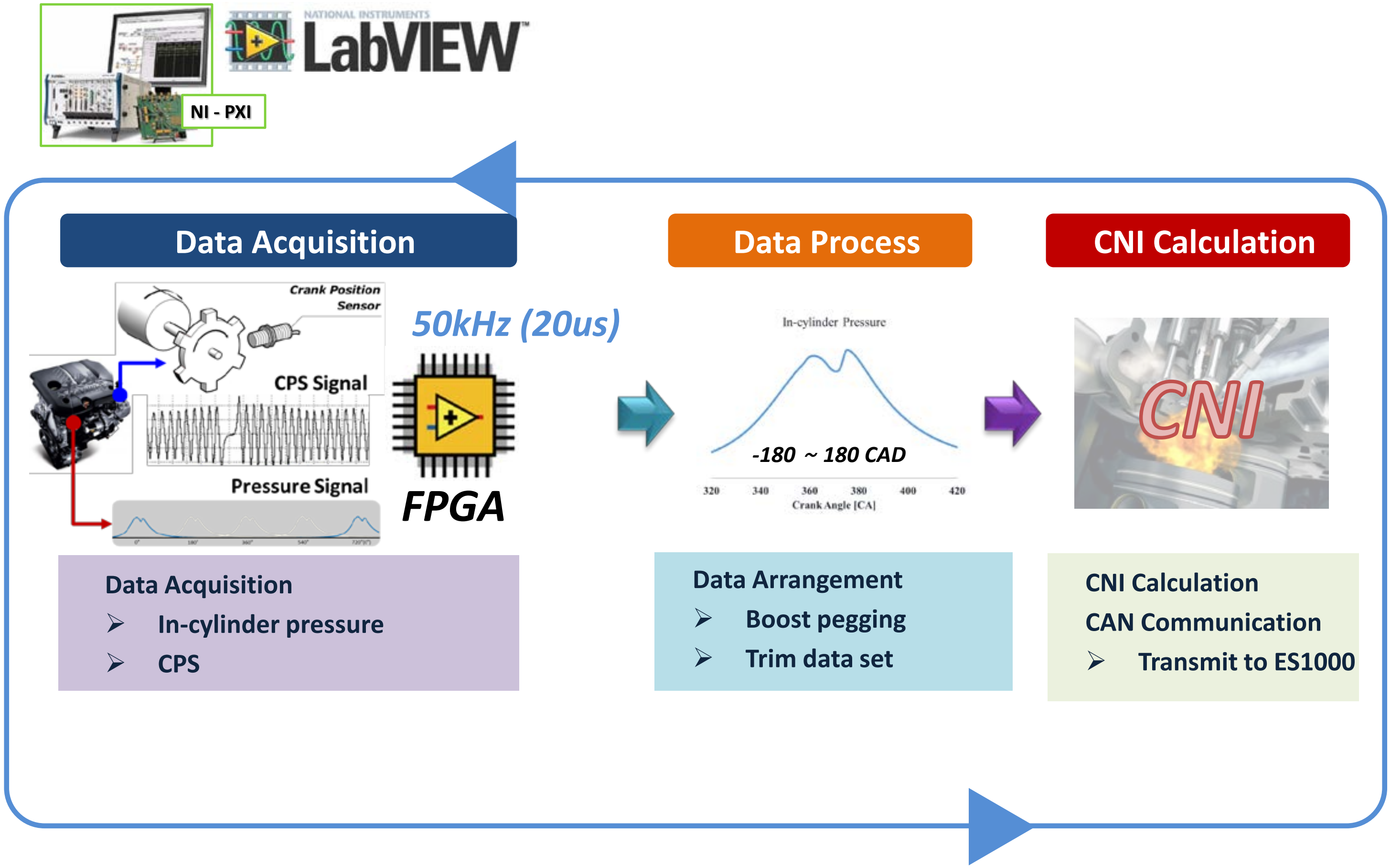
NI - PXI
NATIONAL INSTRUMENTS
LabVIEW
Data Acquisition
Data Process
CNI Calculation
Crank Position Sensor
CPS Signal
Pressure Signal
50kHz (20us)
FPGA
In-cylinder Pressure
-180 ~ 180 CAD
320
340
360
380
400
420
Crank Angle [CA]
CNI
Data Acquisition
➢ In-cylinder pressure
➢ CPS
Data Arrangement
➢ Boost pegging
➢ Trim data set
CNI Calculation
CAN Communication
➢ Transmit to ES1000

Figure 5.29 CNI calculation using NI-PXI & LabVIEW

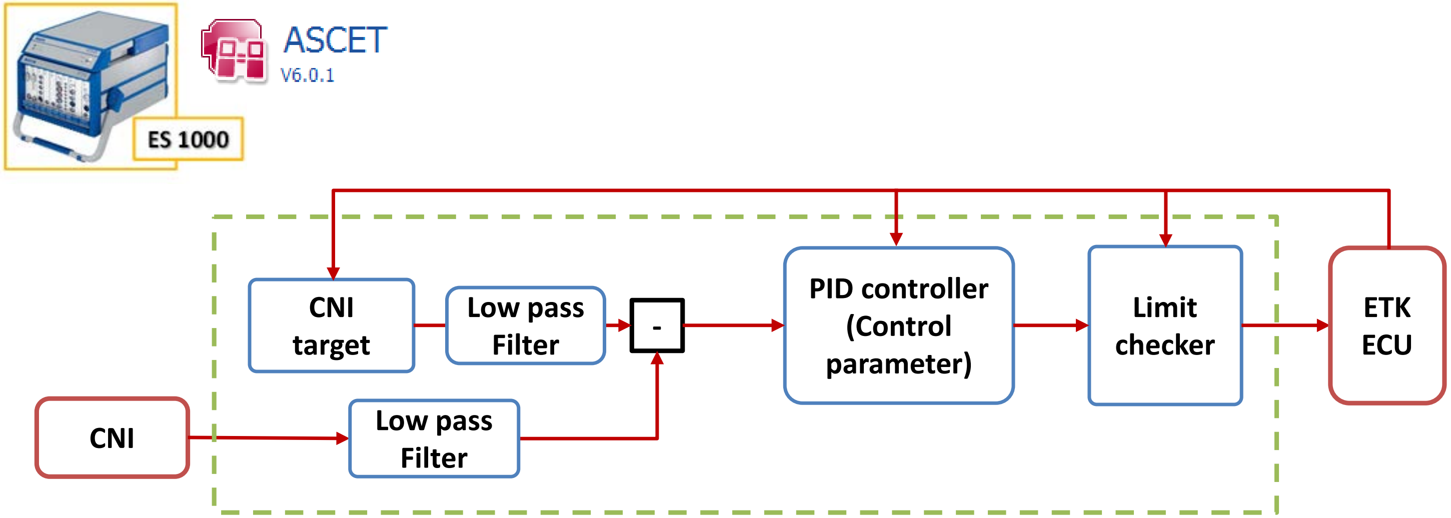
ES 1000
ASCET
V6.0.1
CNI target
Low pass Filter
-
PID controller (Control parameter)
Limit checker
ETK ECU
CNI
Low pass Filter

Figure 5.30 Combustion control algorithm using ES1000 & ASCET

5.5 Results of the closed loop control

5.5.1 Vehicle test

The closed loop control system to reduce combustion noise was applied to a vehicle. Figure 5.36 shows the test vehicle and table 5.2 displays specification of the vehicle. The vehicle is five door small family case and the engine is the same type of one used in test bench. Figure5.36 shows the vehicle in which the control system is equipped. The pressure sensor was installed in the first cylinder. The Kibox, NI-PXI and ES1000 were set up. To power supply, 220V invertor and extra battery were carried too.

The noise was measured in the cabin of the vehicle. A binaurales headset type microphone are used and the noise was measured by SQuadriga II (head acoustics). The driver wore headset type microphone to measure the sound for driver hearing.

5.5.2 Operating conditions and Results

Figure 5.37 shows the operating condition. The vehicle was accelerated to 60 kph with light tip-in. the engine speed was varied from 800 rpm to 2000 rpm and fuel injection quantity was changed from 5 to 23 mg/cycle·cylinder.

Figure5.38 shows the current CNI level and target value when the control system was deactivated. There was a significant gap between the current level and the target, which was up to 6dB. Figure5.39 shows results when the control system was activated. The current CNI level could follow the target value during the transient operation.

Figure 5.40 shows behaviors of injection parameters. SOI, injection pressure and pilot quantity were adjusted to follow the target. At that time, the cabin noise was reduced. Especially, the noise of 1.2 kHz ~2 kHz diminished up to 4 dB(A)

Figure 5.31 test vehicle, 1.6 liter diesel enigne

Table 5.2 Specifications of test vehicle

Criteria	Specification
Vehicle model	K3(YD)
Transmission	6-speed automatic
Driven type	Front-wheel drive
Maximum power	128 hp
Maximum torque	28.5 kg·m
Weight	1,340 kg

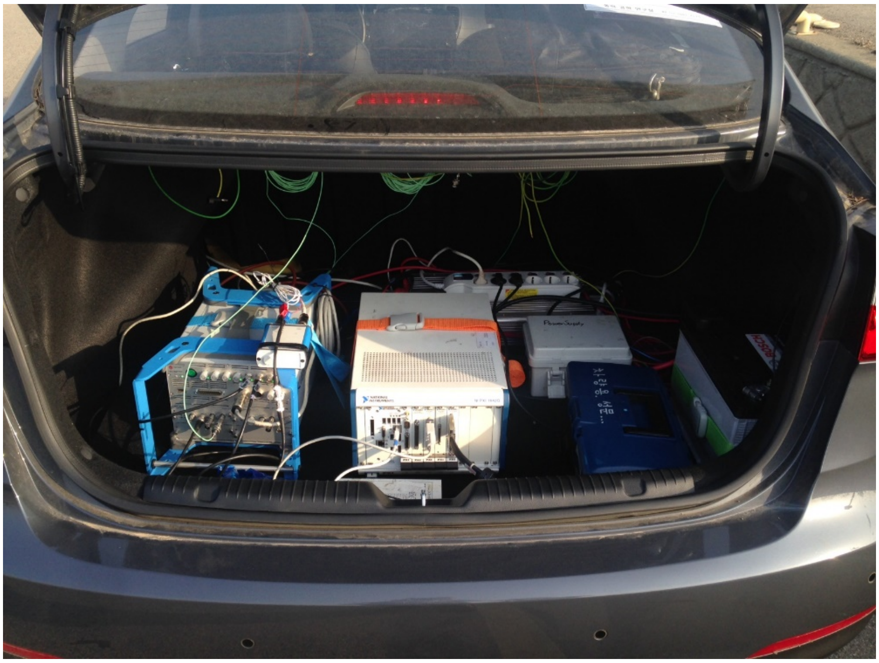

Figure 5.32 closed loop control system set up in test vehicle

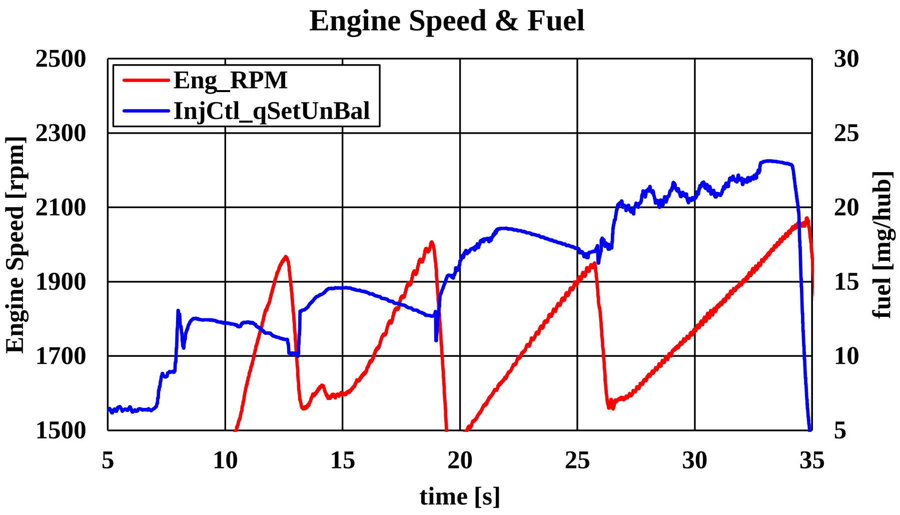

Figure 5.33 Transient operation of test for CNI

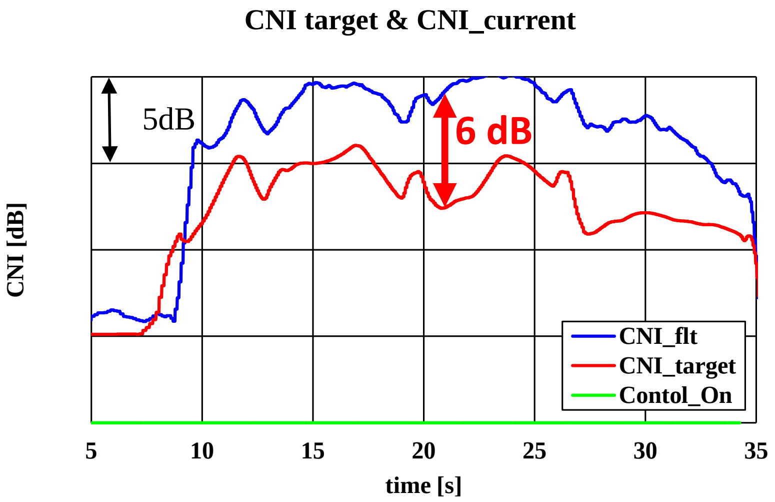

Figure 5.34 Target CNI and current CNI when the control was deactivated

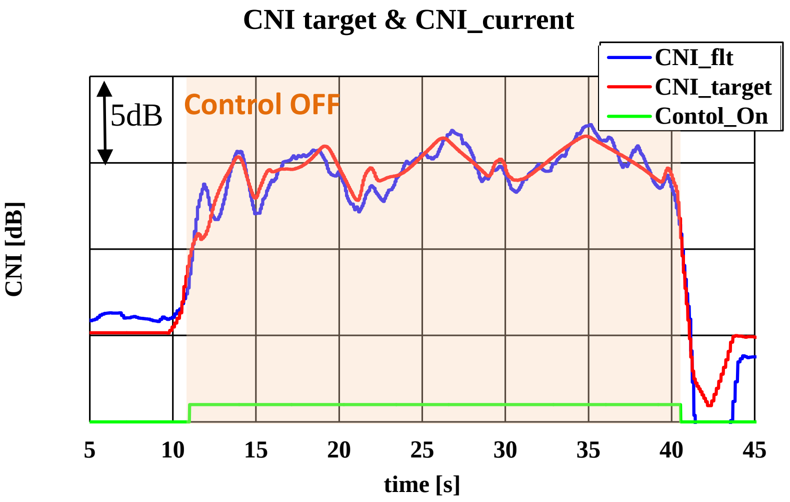

Figure 5.35 Target CNI and current CNI when the control was activated

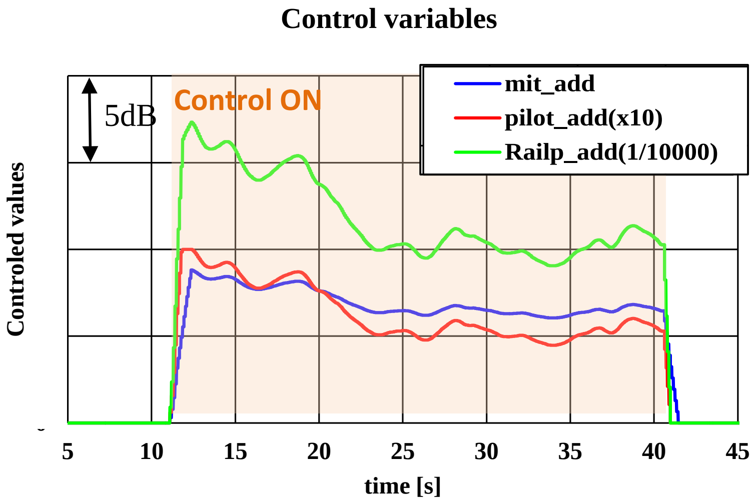

Figure 5.36 Controlled value of parameters during transient operation

Chapter 6. Conclusion

The objective of this study was to look for the methodologies to reduce combustion noise in diesel engines. The relations between diesel engine combustion and combustion noise were examined and the closed loop control system for the noise reduction was developed.

In this study, a 1.6 liter diesel engine was used. The in-cylinder pressure, emissions and PM were measured by using a gas analyzer and a smoke meter. Rapid prototype controllers were used for the real time control system and NI-PXI was used to calculate the current CNI in real time. In addition, a vehicle, which was equipped with the same type engine under the same bench test, was used to evaluate the effects of closed loop control on reduction combustion noise.

First, in this study, the relations between the shape of heat release rate and pressure excitation characteristics were studied. The heat release rate was simulated by Wiebe functions to freely transform the shape. The 3 Wiebe funcions were used to describe the diesel combustion. Each of the function meant the premixed combustion, the mixing controlled combustion and the late combustion. Using the simulated heat release rate, the pressure curve was reproduced and the frequency analysis was conducted. When fuel was rapidly burned, the excitation level increased. When the coefficient ‘m’, which is related with the burning speed, was in between 2 and 3 the combustion excitation was at the lowest. When the combustion duration increased or the fuel quantity decreased, combustion noise decreased. However, the start of combustion did not significantly affect the combustion noise. Pilot injection, which was used to reduce combustion noise, decreased the combustion excitation of combustion from the main injection. However, the combustion of pilot injection considerably affected the total excitation.

The shape of heat release rate for reduction of combustion noise was investigated. When the combustion duration became long and the fuel burned moderately, the combustion noise decreased. In addition, a split injection of the main injection was effective to reduce the excitation. When 30% fuel was burned early, the rest of fuel continuously burned and the combustion noise was dramatically reduced with the same IMEP.

The injection strategies for the reduction of engine noise was examined via the engine bench tests. When injection parameters, SOI, swirl, injection pressure and EGR rate, were changed, the heat release shape and excitation characteristics were studied. The combustion noise could be reduced; however, more smoke was produced except for the EGR control from changing them. The EGR rate significantly affected the NOx emission. To prevent a formation of more emissions and to reduce the combustion noise, early pilot injection strategy was applied. When the pilot injection quantity increased, the main injection quantities decreased for the same IMEP. However, an increase of pilot injection quantity may produce more smoke. To solve the dilemma, the early injection concept was applied to the pilot injection. Since, the early pilot was injected before 30 CAD° BTDC, the fuel of the main injection was deliberately mixed with air; albeit, the pilot injection quantity increased. Through, the early pilot injection, the combustion noise could be reduced without an increase of emission.

Finally, closed loop control system using the CNI was developed to reduce combustion noise. The controller, which can measure the in-cylinder pressure and calculate CNI in real time, were developed using NI-PXI and LabVIEW. The combustion controller, which can modify the injection strategies by communication with EMS, was developed using ES1000 and ASCET. SOI, injection pressure and pilot quantities were used as control parameters. Since, they did not have negative cross effects, the controller changed them simultaneously to follow the target value for the current combustion noise index level. The system was applied to a vehicle. The current CNI level could be controlled to follow the target value in transient operations. During the transient operations, the cabin noise in the vehicle was measured with microphones. AS a result, 1.2~2 kHz frequency of the noise was reduced down to 4 dBA.

Bibliography

[1] T. V. Johnson, "Review of Vehicular Emissions Trends," *SAE International Journal of Engines,* vol. 8, 2015.

[2] G. Sheng, *Vehicle noise, vibration, and sound qualtity*: SAE International, 2012.

[3] Tousignant T., Wellmann T., Govindswamy K., Heuer S., and Workings M., "Application of Combustion Sound Level (CSL) Analysis for Powertrain," *SAE Technical Paper,* 2009.

[4] K. G. Johnson, K. Mollenhauer, and H. Tschöke, *Handbook of diesel engines*: Springer Science & Business Media, 2010.

[5] M. E. Badaoui, J. Danière, F. Guillet, and C. Servière, "Separation of combustion noise and piston-slap in diesel engine—Part I: Separation of combustion noise and piston-slap in diesel engine by cyclic Wiener filtering," *Mechanical Systems and Signal Processing,* vol. 19, pp. 1209-1217, 2005.

[6] C. Servière, J. L. Lacoume, and M. El Badaoui, "Separation of combustion noise and piston-slap in diesel engine—Part II: Separation of combustion noise and piston-slap using blind source separation methods," *Mechanical Systems and Signal Processing,* vol. 19, pp. 1218-1229, 2005.

[7] K. Torii, "Method Using Multiple Regression Analysis to Separate Engine Radiation Noise into the Contributions of Combustion Noise and Mechanical Noise in the Time Domain," *SAE International Journal of Engines,* vol. 7, pp. 1502-1513, 2014.

[8] S. Raveendra, S. Sureshkumar, M.-T. Cheng, L. Na, and T. Abe, "Noise Source Identification in an Automotive Powerplant," *SAE Technical Paper,* 2003.

[9] X. Liu and R. B. Randall, "Blind source separation of internal combustion engine piston slap from other measured vibration signals," *Mechanical Systems and Signal Processing,* vol. 19, pp. 1196-1208, 2005.

[10] J. B. Heywood, *Internal combustion engine fundamentals* vol. 930: Mcgraw-hill New York, 1988.

[11] D. N. Assanis, Z. S. Filipi, S. B. Fiveland, and M. Syrimis, "A Predictive Ignition Delay Correlation Under Steady-State and Transient Operation of a Direct Injection Diesel Engine," *Journal of Engineering for Gas Turbines and Power,* vol. 125, p. 450, 2003.

[12] N. Ladommatos, S. M. Abdelhalim, H. Zhao, and Z. Hu, "Effects of EGR on heat release in diesel combustion," *SAE Technical Paper*1998.

[13] M. Badami, F. Millo, and D. D'amato, "Experimental investigation on soot and NOx formation in a DI common rail diesel engine with pilot injection," *SAE Technical Paper*2001.

[14] A. Maiboom, X. Tauzia, and J.-F. Hétet, "Experimental study of various effects of exhaust gas recirculation (EGR) on combustion and emissions of an automotive direct injection diesel engine," *Energy,* vol. 33, pp. 22-34, 2008.

[15] A. Maiboom, X. Tauzia, J.-F. Hétet, M. Cormerais, M. Tounsi, T. Jaine*, et al.*, "Various effects of EGR on combustion and emissions on an automotive DI Diesel engine: numerical and experimental study," *SAE Technical Paper*2007.

[16] W. Ping, S. Xi-geng, X. Dong-xin, Z. Hai-tao, M. Xiao-wen, and G. Yu-lin, "Effect of Combustion Process on DI Diesel Engine Combustion Noise," *SAE Technical Paper*, 2007.

[17] M. Pontoppidan, A. Demaio, G. Bella, and R. Rotondi, "Parametric Study of Physical Requirements for Optimization of the EGR-rate and the Spray Formation for Minimum Emissions Production over a Broad Range of Load/Speed Conditions," *SAE Technical Paper*2006.

[18] L. Zhang, "A study of pilot injection in a DI diesel engine," *SAE Technical Paper*, 1999.

[19] A. Trueba, B. Barbeau, O. Pajot, and K. Mokaddem, "Pilot injection timing effect on the main injection development and combustion in a DI diesel engine," *SAE Technical Paper*2002.

[20] P. Carlucci, A. Ficarella, and D. Laforgia, "Effects of pilot injection parameters on combustion for common rail diesel engines," *SAE Technical Paper*, 2003.

[21] R. Mobasheri and Z. Peng, "Investigation of pilot and multiple injection parameters on mixture formation and combustion characteristics in a heavy duty DI-Diesel engine," *SAE Technical Paper*, 2012.

[22] T. Fuyuto, M. Taki, R. Ueda, Y. Hattori, H. Kuzuyama, and T. Umehara, "Noise and Emissions Reduction by Second Injection in Diesel PCCI Combustion with Split Injection," *SAE International Journal of Engines,* vol. 7, pp. 1900-1910, 2014.

[23] P. Dimitriou, W. Wang, J. Peng, L. Cheng, M. Wellers, and B. Gao, "Analysis of Diesel Engine In-Cylinder Air-Fuel Mixing with Homogeneity Factor: Combined Effects of Pilot Injection Strategies and Air Motion," *SAE International Journal of Engines,* vol. 7, pp. 2045-2060, 2014.

[24] S. Kohketsu, K. Tanabe, and K. Mori, "Flexibly controlled injection rate shape with next generation common rail system for heavy duty DI diesel engines," *SAE Technical Paper*, 2000.

[25] F. Atzler, O. Kastner, R. Rotondi, and A. Weigand, "Multiple injection and rate shaping Part 1: Emissions reduction in passenger car Diesel engines Computational investigation ", S. T. Paper, Ed., ed, 2009.

[26] F. Atzler, O. Kastner, R. Rotondi, and A. Weigand, "Multiple injection and rate shaping Part 2: Emissions reduction in passenger car Diesel engines Computational investigation," *SAE Technical Paper*2009.

[27] J. Hinkelbein, C. Sandikcioglu, S. Pischinger, M. Lamping, and T. Körfer, "Control of the diesel combustion process via advanced closed loop combustion control and a flexible injection rate shaping tool," *SAE International Journal of Fuels and Lubricants,* vol. 2, pp. 362-375, 2009.

[28] C. Jörg, T. Schnorbus, S. Jarvis, B. Neaves, K. Bandila, and D. Neumann, "Feedforward Control Approach for Digital Combustion Rate Shaping Realizing Predefined Combustion Processes," *SAE International Journal of Engines,* vol. 8, 2015.

[29] A. A. Saad and N. El-Sebai, "Combustion noise prediction inside diesel engine," *SAE Technical Paper*, 1999.

[30] T. Papenfus, D. Genuit, K. Kang, I. Jung, and J. Jin, "Method of NVH quality rating of diesel combustion noise using typical driving modes," *SAE paper,* pp. 01-2078, 2009.

[31] R. P. Bhagate, V. Nadanasabapathy, and K. Mohan, "Powertrain Noise & Sound Quality Refinement for New Generation Common Rail Engines," *SAE Technical Paper*, 2010.

[32] M. V. Rao, J. Frank, and P. Raghavendran, "Measurement Technique for Quantifying Structure Borne and Air Borne Noise Levels in Utility Vehicle," *SAE Technical Paper,* vol. 1, 2014.

[33] T. Tousignant and K. Govindswamy, "Virtual Powertrain Installation for Diesel Engine Sound Quality Development in a Light Duty Vehicle Application," *SAE Technical Paper,* vol. 1, 2014.

[34] M. D. Redel-Macías, C. Hervás-Martínez, S. Pinzi, P. A. Gutiérrez, A. J. Cubero-Atienza, and M. P. Dorado, "Noise prediction of a diesel engine fueled with olive pomace oil methyl ester blended with diesel fuel," *Fuel,* vol. 98, pp. 280-287, 2012.

[35] A. J. Torregrosa, A. Broatch, J. Martín, and L. Monelletta, "Combustion noise level assessment in direct injection Diesel engines by means of in-cylinder pressure components," *Measurement Science and Technology,* vol. 18, pp. 2131-2142, 2007.

[36] F. Payri, A. Broatch, B. Tormos, and V. Marant, "New methodology for in-cylinder pressure analysis in direct injection diesel engines—application to combustion noise," *Measurement Science and Technology,* vol. 16, pp. 540-547, 2005.

[37] F. Payri, A. Broatch, X. Margot, and L. Monelletta, "Sound quality assessment of Diesel combustion noise using in-cylinder pressure components," *Measurement Science and Technology,* vol. 20, p. 015107, 2009.

[38] Engine Sound Level Measurement Procedure (J1074), SAE International, 2000

[39] I. Jung, J. Jin, H. So, C. Nam, and K. Won, "An Advanced Method for Developing Combustion Noise through the Analysis of Diesel Combustion," *SAE International Journal of Engines,* vol. 6, pp. 1379-1385, 2013.

[40] T. Schnorbus, S. Pischinger, T. Körfer, M. Lamping, D. Tomazic, and M. Tatur, "Diesel combustion control with closed-loop control of the injection strategy," *SAE Technical Paper*, 2008.

[41] R. Finesso and E. Spessa, "A Feed-Forward Approach for the Real-Time Estimation and Control of MFB50 and SOI In Diesel Engines," *SAE International Journal of Engines,* vol. 7, pp. 528-549, 2014.

[42] Q. Zhu, S. Wang, R. Prucka, M. Prucka, and H. Dourra, "Model-Based Control-Oriented Combustion Phasing Feedback for Fast CA50 Estimation," *SAE International Journal of Engines,* vol. 8, 2015.

[43] J. Ghojel, D. Honnery, and K. Al-Khaleefi, "Performance, emissions and heat release characteristics of direct injection diesel engine operating on diesel oil emulsion", *J.Appl. Thermal Enging,* 2006, Vol. 26, 2132-2141.

[44] S. Loganathan, R. Murali Manohar, R. Thamaraikannan, R. Dhanasekaran, A. Rameshbabu, and V. Krishnamoorthy, "Direct Injection Diesel Engine Rate of Heat Release Prediction using Universal Load Correction Factor in Double Wiebe Function for Performance Simulation," *SAE Technical Paper,* vol. 1, 2012.

[45] C. Saad, F. maroteaux, J.-B. Millet, and F. Aubertin, "Combustion Modeling of a Direct Injection Diesel Engine Using Double Wiebe Functions: Application to HiL Real-Time Simulations," *SAE Technical Paper,* vol. 1, 2011.

[46] S. Kulah, T. Donkers, and F. Willems, "Virtual Cylinder Pressure Sensor for Transient Operation in Heavy-Duty Engines," *SAE International Journal of Engines,* vol. 8, 2015.

[47] J. s. Benajes, S. Molina, R. Novella, and R. r. Amorim, "Study on Low Temperature Combustion for Light-Duty Diesel Engines," *Energy & Fuels,* vol. 24, pp. 355-364, 2010.

[48] E. Doosje, F. Willems, R. Baert, and M. Van Dijk, "Experimental Study into a Hybrid PCCI/CI Concept for Next-Generation Heavy-Duty Diesel Engines," *SAE Technical Paper,* vol. 1, 2012.

[49] A. Wagemakers and C. Leermakers, "Review on the effects of dual-fuel operation, using diesel and gaseous fuels, on emissions and performance," *SAE Technical Paper*, 2012.

[50] D. Sahoo, P. C. Miles, J. Trost, and A. Leipertz, "The Impact of Fuel Mass, Injection Pressure, Ambient Temperature, and Swirl Ratio on the Mixture Preparation of a Pilot Injection," *SAE International Journal of Engines,* vol. 6, pp. 1716-1730, 2013.

[51] D. Laforgia, A. Ficarella, and P. Carlucci, "Effects on combustion and emissions of early and pilot fuel injections in diesel engines," *International Journal of Engine Research*, vol. 6, pp. 43-60, 2005.

[52] A. J. Torregrosa, A. Broatch, A. García, and L. F. Mónico, "Sensitivity of combustion noise and NOx and soot emissions to pilot injection in PCCI Diesel engines," *Applied Energy,* vol. 104, pp. 149-157, 2013.

[53] H. Ogawa, K. Tashiro, M. Numata, T. Obe, and G. Shibata, "Influence of Fuel Volatility on Evaporation Characteristics of Diesel Sprays in Various Low Temperature and Low Density Surrounding Conditions Like at Early Pilot or Late Post Injections," *SAE Technical Paper*, 2015.

[54] M. Huo, M. Wang, and C.-F. Lee, "Computational Study of the Equivalence Ratio Distribution from a Diesel Pilot Injection with Different Piston Geometry, Injection Timing and Velocity Initialization in a HSDI Engine," *SAE Technical Paper,* vol. 1, 2014.

[55] Y. Han, Z. Liu, J. Zhao, Y. Xu, J. Li and K. Li, “EGR Response in a Turbo-charged and After-cooled DI Diesel Engine and its Effects on Smoke Opacity”, *SAE Technical Paper*, 2008.

[56] S. Lee, J. Lee, S. Lee, D. Kim and Y. Lee, "Study on Reduction of Diesel Engine Out Emission through Closed Loop Control based on the In-Cylinder Pressure with EGR Model," *SAE Technical Paper*, 2013.

[57] S. Lee, S. Lee, K. Min, and I. Jung, "Characteristics of Diesel Engine Noise According to EGR Rate Change during Transient Operation," *SAE Technical Paper* 0148-7191, 2015.

[58] C. D. Rakopoulos, A. M. Dimaratos, E. G. Giakoumis, and D. C. Rakopoulos, "Study of turbocharged diesel engine operation, pollutant emissions and combustion noise radiation during starting with bio-diesel or n-butanol diesel fuel blends," *Applied Energy,* vol. 88, pp. 3905-3916, 2011.

[59] M. Dhaenens, G. Van Der Linden, J. Nehl, and R. Thiele, "Analysis of Transient Noise Behavior of a Truck Diesel Engine," *SAE Technical Paper*, 2001.

[60] S. Yu, H. Choi, S. Cho, K. Han, and K. Min, "Development of engine control using the in-cylinder pressure signal in a high speed direct injection diesel engine," *International Journal of Automotive Technology*, vol. 14, pp. 175-182, 2013.

국 문 초 록

디젤 엔진은 효율이 좋은 반면 소음이 많이 발생한다는 단점이 있다. 특히, 연소에 의하여 발생하는 소음인 연소음은 디젤 엔진의 주요 소음원이다. 실린더 내의 압력은 점화 지연 후 연료의 동시다발적인 연소로 인하여 급격히 상승하게 되는데 이것이 연소음의 주요 가진원으로 알려져 있다.

따라서 본 연구에서는 연소 특성과 연소음 간의 관계에 대한 연구를 열 발생률의 형상과 연소음 지수를 이용하여 수행하였다. 뿐만 아니라 연소로 인한 가진을 최소화 할 수 있는 방법에 대한 연구를 수행하였다. 끝으로, 연소음 지수를 피드백 컨트롤에 적용하여 연소 소음 수준을 제어할 수 있는 실시간 제어 시스템을 개발하였다.

본 연구에서는 1.6 리터 디젤 엔진을 사용하였다. 연소 압력센서 (Kistler)와 charge amplifier 를 이용하여 연소 압력을 측정하고, 이를 통하여 열발생률 및 연소음 지수를 구하였다. NOx(NO) 등 배기 가스는 Horiba Mexa-7100 을 이용하여 측정하였으며, smoke 의 경우 smoke meter (AVL)를 이용하여 측정하였다. 실시간 제어 시스템은 ES1000 과 NI-PXI 를 이용하여 개발하였다. 실험 차량은 대상시험에서 사용한 것과 같은 1.6 리터 디젤 엔진과 자동 변속기가 장착되어 있는 승용차량을 이용하였다.

디젤 엔진의 연소 특성은 실린더 압력 측정 후 열 발생률을 계산하여 분석할 수 있으나 실험적으로 열 발생률의 모양을 임의로 변경하는 것은 제약이 매우 크다고 할 수 있다. 그러한 이유로 Wiebe 함수를 이용하여 모사하였다. 디젤 연소를 정확하게 모사하기 위하여 3 개의 Wiebe 함수를 사용하였으며, 각각 premixed combustion, mixing controlled combustion 그리고 late combustion 을 대표한다. 열 발생률의

형상은 Wiebe 함수의 계수 변경을 통하여 여러 형태로 변형되었고, 만들어진 열 발생률을 이용하여 압력 곡선을 생성한 후 이를 FFT 및 1/3 옥타브 밴드 분석, 연소음 지수를 이용하여 가진 정도를 평가하였다. 연소 속도가 초반에 급격히 상승하거나 또는 후반부에 급격히 상승할 경우 모두 연소 가진이 크게 발생하였으며, Wiebe 함수의 계수 m 이 2 ~ 3 인 경우의 열 발생률 형상이 가장 적은 연소 가진을 보였다. 또한 연소 구간이 길게 일어날 수록 가진이 적게 나타났고, 연소되는 연료의 양이 많을수록 연소 가진이 크게 일어났다. 그러나 열 발생률 형태가 같을 경우에는 연소 시작 시점은 연소 가진에 큰 영향을 미치지 않았다. 한편 Mixing controlled 연소의 경우, 연소음 지수의 수준에는 큰 영향을 미치지 않았으나 주파수 분석 결과 1.6 kHz 이상의 영역에서 영향을 미치는 것으로 나타났다. 또한 premixed combustion phase 와 mixing controlled phase 간의 시간 간격 및 pilot 연소와 main 연소 간의 시간 간격 또한 연소 가진에 상당한 영향을 미치면서 최적점이 생겨났다. Pilot 연소는 main 연소 가진을 획기적으로 줄일 수 있기 때문에 소음 저감에 매우 큰 효과가 있다. 그러나 pilot 연소에 의해 발생하는 소음 또한 전체 수준을 증가 시키는 원인이 될 수 있기 때문에 pilot 의 연소 특성 개선 또한 연소음을 줄이기 위한 중요한 요인이라고 할 수 있다. 뿐만 아니라 Wiebe 함수를 이용하여 IMEP 수준을 유지하면서 연소 가진을 최소화 할 수 있는 열 발생률 모양을 최적화를 통하여 도출하였다.

다음으로 엔진 시험에서 연소 가진을 최소화 할 수 있는 분사 전략에 대한 연구를 수행하였다. 주분사 시기, 분사 압력, swirl 및 EGR 율에 대한 열 발생률 모양의 변화를 살펴 보았다. 열 발생률의 기울기가 완만할수록, 그리고 연소 시간이 길수록 소음이 적게 발생하는 것을 발견하였다. 그러나 ERG rate 를 제외한 모든 경우에 대해서는 연소 가진이 적게 발생할 경우, PM 이 증가하는 것을 확인할 수 있었다. EGR rate 의 경우 연소음 감소를 위하여 수준을 낮출 경우 NO 발생이 급격히

증가하였다. 따라서 기존의 방법으로는 배출가스 악화 없이 소음을 줄이는 것은 어렵기 때문에 이를 보안하고자 early pilot 분사 전략을 적용하였다. Pilot 의 연료량이 증가하게 될 경우, 열 발생률의 상승을 억제 할 수 있기 때문에 소음을 저감할 수 있지만 과도한 PM 이 발생할 수 있다. 이는 연속된 연료 jet 의 분사로 인하여 공기와의 혼합이 어렵기 때문이다. 이러한 단점을 해결하고자 PCCI 연소를 pilot 연소에 적용하였다. Pilot 을 20~40° BTDC 부근에서 분사하여 점화 지연을 증가시켜 PCCI 연소가 이루어 질 수 있도록 한 후 나머지 연료를 분사를 하였다. 이를 통하여 주분사의 연료와 공기와의 혼합이 개선되어 smoke 의 증가 없이 연소음을 감소 시킬 수 있었다.

마지막으로, 연소음 지수를 활용하는 연소 제어를 통하여 발생하는 연소음 수준을 제어하는 연구를 수행하였다. 이를 위하여 실시간으로 연소 압력을 측정하고, 연소음 지수를 산출할 수 있는 장치를 NI-PXI 를 이용하여 개발하였으며 이를 이용한 연소음 제어 알고리즘은 ES1000 을 이용하여 구성하였다. 주분사 시기, 분사 압력 및 pilot 분사량 조절은 모두 소음에 효과가 있었으며, 상호작용이 크지 않았다. 이 세 가지의 연소 제어 인자를 이용하여 엔진에서 실시간으로 발생하는 연소음 수준이 목표 값을 추종할 수 있도록 제어기를 구성하였다. 이를 위하여 차량 실험을 설계하여 그 효과를 확인하였다. 그 결과, 완가속 조건에서 차량의 실내 소음은 1.2 kHz~ 2 kHz 의 구간에서 최대 4dB 감소 하였다.

주요어 : 디젤 엔진 소음, 연소음, 연소제어, 연소 가진, 열발생률

학번 : 2013-30207

creative commons

C O M M O N S D E E D

저작자표시-비영리-변경금지 **2.0** 대한민국

이용자는 아래의 조건을 따르는 경우에 한하여 자유롭게

- 이 저작물을 복제, 배포, 전송, 전시, 공연 및 방송할 수 있습니다.

다음과 같은 조건을 따라야 합니다:

저작자표시. 귀하는 원저작자를 표시하여야 합니다.

비영리. 귀하는 이 저작물을 영리 목적으로 이용할 수 없습니다.

변경금지. 귀하는 이 저작물을 개작, 변형 또는 가공할 수 없습니다.

- 귀하는, 이 저작물의 재이용이나 배포의 경우, 이 저작물에 적용된 이용허락조건을 명확하게 나타내어야 합니다.
- 저작권자로부터 별도의 허가를 받으면 이러한 조건들은 적용되지 않습니다.

저작권법에 따른 이용자의 권리는 위의 내용에 의하여 영향을 받지 않습니다.

이것은 이용허락규약(Legal Code)을 이해하기 쉽게 요약한 것입니다.

Disclaimer

dCollection

공학박사학위논문

디젤엔진에서 연소 특성이 연소 소음에 미치는 영향

Effects of Combustion Characteristics on Combustion Noise in Diesel Engines

2016 년 2 월

서울대학교 대학원

기계항공공학부

이 승 현

디젤 엔진에서 연소 특성이 연소 소음에 미치는 영향

Effects of Combustion Characteristics on Combustion Noise in Diesel Engines

지도교수 민 경 덕

이 논문을 공학박사 학위논문으로 제출함
2015 년 10 월

서울대학교 대학원
기계항공공학부
이 승 현

이승현의 공학박사 학위논문을 인준함
2015 년 12

위 원 장______________(인)

부위원장______________(인)

위　　원______________(인)

위　　원______________(인)

위　　원______________(인)

Acknowledgements

A lot of help and advices from many people greatly facilitated the work of my Ph. D. thesis. I would like to express my special thanks to those people.

First and foremost, I would like to express my honor and gratitude to my advisor, Professor Kyoungdoug Min. During the course of my Ph. D., my knowledge and personality grew with his invaluable advices. He gave the inspirations of this study and his guidance and encouragement were the sources of power that overcame many difficulties during the project.

I would like to specially thank the project members who offered a great assistance and valuable discussions. Dr. Hoimyung Choi and Dr. Seungeun Yu also gave me the basic knowledge and inspirations as a senior. Jeongwoo Lee and Seungha Lee gave many insights. Youngju Lee, Sungmoon Lee, Yoonwoo Lee, Youngbok Lee and Sanghyun Chu assisted lots of research. Gyujin Kim and Hyungmook Kang, who joined the lab with me, gave beautiful memories of our friendships. Additionally, I am grateful to MinJae Kim, Namho Kim, Joohan Kim, Jaeman Park, Hwanyung Oh, Insuk Ko, Yuil Lee, Guesang Lee and JaeHyuk Cha, who are my colleagues and friends, for the unforgettable and joyful lab life and our deep friendships. My thanks go to all my graduate schoolmates.

It was my great honor to have the opportunity to participate the project with Hyundai motor company and I would like to thank In Soo Jung, Jaemin Jin and Dongchul Lee for the financial support and meaningful comments from plentiful experiences of the engine development.

Finally, I would like to present my deepest respect and gratitude to my parents, Jaekyung Lee and Munhee Chae, for their great sacrifice, thoughtful consideration, unimaginable patience, and endless love. Lastly, my thanks and appreciation go to Haeyoung Lee. Her love, understanding and companionship are elements that have sustained me throughout my graduate career.

Abstract

Effects of Combustion Characteristics on Combustion Noise in Diesel Engines

Seunghyun Lee
Department of Mechanical and Aerospace Engineering
The Graduate School
Seoul National University

The demand of diesel engines for passenger cars has increased due to their higher thermal efficiency, however, diesel engines have weaknesses; namely, the engine noise and the vibration. Especially, the combustion noise is significantly louder than that of gasoline engines due to their different combustion modes. In diesel engines, some fuel, which are already mixed with air, are rapidly burned after the ignition delay in the premixed combustion phase and the components of the engine block experience a rapid pressure rise, which is known as the main source of combustion noise. In this study, the relation between combustion characteristics and in-cylinder pressure excitation was investigated. In addition, the combustion characteristics of lower level excitation were studied. Finally, the closed control system using combustion noise index was developed to reduce the combustion noise.

In this study, a 1.6 liter diesel engine was used. The in-cylinder pressure, exhaust emissions and smoke were measured. Rapid prototype controller was used for the real time control system. Furthermore, a vehicle, which was equipped with the same engine, was used for bench test as well as the vehicle test.

The main source of combustion noise is from the in-cylinder pressure variation. The pressure is also affected by the change in heat release rate. Thus, in this study, the relation between the shape of heat release rate and the pressure excitation

characteristics were studied. Through an engine experiment, it is hard to change the shape of heat release rate as we wish. Thus, the heat release rate was simulated by Wiebe functions. The 3 Wiebe functions are generally used to describe the diesel combustion. The pressure curve was reproduced by using the simulated heat release rate. Frequency analysis, FFT and 1/3 octave band analysis, were conducted to evaluate the excitation of the pressure curve. When more fuel was burned rapidly, the excitation level increased. When the combustion duration increased or the fuel quantity decreased, the combustion noise decreased. However, the start of combustion did not affect the combustion noise much. Pilot injection, which was used to reduce the combustion noise, decreased the combustion excitation of main combustion injection. However, the combustion of pilot injection considerably affected the total excitation.

The shape of heat release rate for reduction of combustion noise was investigated. When the combustion duration became long and the fuel was burned moderately, the combustion noise decreased. In addition, the split injection of the main injection effectively reduced the excitation. When 30% fuel was burned early, the rest of fuel continuously burned and the combustion noise was dramatically reduced with the same IMEP.

The injection strategies for the engine noise reduction was examined via engine bench tests. When injection parameters, SOI, swirl, injection pressure and EGR rate, were changed, the heat release shape and excitation characteristics were studied. The combustion noise could not be reduced from changing them without an emission deterioration. To prevent a formation of more emission and to reduce the combustion noise, early pilot injection strategy was applied. When the pilot injection quantity increased, the main injection fuel was burned smoothly. However, an increase of pilot injection quantity was anticipated to produce more smoke. To solve this dilemma, the early injection concept was applied to pilot injection because the combustion noise can be reduced without an emission increase through an early pilot injection.

Finally, a closed loop control system using CNI was developed for the reduction of combustion noise. The controller, which can measure the in-cylinder pressure and

calculate CNI in real time, were developed using NI-PXI and LabVIEW. The combustion controller, which can modify the injection strategies, was developed using ES1000 and ASCET. SOI, injection pressure and pilot quantity were used as control parameters. The system applied to a vehicle. The current CNI level could be controlled to follow the target value in a transient operation. At that time, 1.2~2 kHz frequency of the cabin noise in the vehicle was reduced down to 4 dBA.

Keywords: Diesel engine, Combustion noise, Heat release rate, Closed loop control, Combustion noise reduction, Injection strategy.

Student Number: 2013-30207

Contents

Acknowledgements i

Abstract ii

List of Figures ix

List of Tables xv

Acronym xvii

Chapter 1. Introduction １

1.1 Background and Motivation 1

1.1.1 Motivation 1

1.1.2 Engine noise classification 2

1.1.3 Relation between engine noise and combustion 5

1.1.4 Reduction of combustion noise 8

1.1.5 Noise evaluation method 9

1.1.5.1 Engine noise evaluation method 9

1.1.5.2 Combustion noise index (CNI) 9

1.1.6 Closed loop control １２

1.2 Objectives １３

Chapter 2. Experimental Apparatus １４

2.1 Overall configuration １４

2.1.1 Engine test bench cell １４
2.1.2 Measurement of exhaust gas emissions １４

2.2 Multi-cylinder Diesel engine..**17**

2.3 Combustion control system **19**
2.3.1 NI-PXI 19
2.3.2 ES-1000 20
2.3.3 Pressure sensor...20

Chapter 3. Relation between diesel combustion and combustion noise... 25

3.1 Simulation of heat release rate using Wiebe functions..................................**25**
3.1.1 Validation for the simulation of the heat release rate...................................28
3.1.2 Pressure reconstruction using Wiebe functions 32

3.2 Effect of heat release rate shape on combustion noise : Analysis of excitation of in-cylinder pressure changing Wiebe functions coefficients...........................**33**
3.2.1 Comparing motoring pressure and combustion pressure..............................34
3.2.2 Effects of Single Wiebe function shape on combustion noise 36
3.2.2.1 Effects of coefficient ‘a’...36
3.2.2.2 Effects of coefficient ‘m’ 36
3.2.2.3 Effects of combustion duration 37
3.2.2.4 Effects of start of combustion 37
3.2.2.5 Effects of total released heat 38
3.2.3 Effects of mixing controlled phase 38
3.2.4 Effects of pilot injection 39
3.2.4.1 Effects of pilot injection quantity..39

3.2.4.2 Effects of SOC of pilot injection..39
3.2.4.3 Effects of combustion duration of pilot injection..................................40

3.3 Optimization of heat release rate shape to reduce combustion noise 49
3.3.1 Optimization of heat release rate shape to minimize CNI using Wiebe functions 49
3.3.2 Optimized shapes of heat release rate for minimum CNI............................50

Chapter 4. Injection strategies to reduce combustion noise... 57

4.1 Variation of heat release rate shape according to change of injection strategies via experiment 57
4.1.1 Main injection timing 57
4.1.2 Injection pressure...58
4.1.3 Swirl rate...58
4.1.4 EGR rate 58

4.2 Early pilot injection strategy to reduce combustion noise............................67
4.2.1 Limitation of conventional diesel combustion...67
4.2.2 PCCI combustion of diesel 67
4.2.3 Early pilot injection combustion..68

Chapter 5. Closed loop control to reduce combustion noise .. 74

5.1 Characteristics of diesel engine noise according to EGR rate change during transient operation 74
5.1.1 EGR rate measurement...74
5.1.2 Combustion noise according to the EGR rate variation...............................76
5.1.3 CNI variation during transient operations..80

5.1.3.1 Transient operation 1. Speed and load change 80
5.1.3.2 Transient operation 2. Constant speed and load change.........................81

5.2 Concept of control 91

5.3 Control parameters 93
5.3.1 Start of injection 93
5.3.2 Other parameters: Pilot injection quantity, pilot injection timing, injection pressure and EGR rate 99
5.3.3 Interaction among injection parameters...103

5.4 Real time combustion control system to combustion noise.........................110
5.4.1 Overview of real time combustion control system 110
5.4.2 Calculation of CNI...110
5.4.3 Control of injection strategies..111

5.5 Results of the closed loop control 116
5.5.1 Vehicle test..116
5.5.2 Operating conditions and Results 116

Chapter 6. Conclusion.. 122

Bibliography... 125

국문초록 131

List of Figures

Figure 1.1 Classification of engine noise 4

Figure 1.2 In-cylinder pressure and heat release rate of diesel engine and gasoline engine (Diesel engine: Bore:77.2mm, Stroke:84.5mm, comp. ratio: 17.3, Gasoline engine: Bore & Stroke: 86mm, comp. ratio 10.5) 7

Figure 1.3 Correlation between measured noise and CNI changing injection strategies [39] １１

Figure 2.1 Schematic diagram of engine test and measurement equipment.............15

Figure 2.2 1.6 L Diesel engine 18

Figure 2.3 In-cylinder pressure sensor and glow plug adopter..................................24

Figure 3.1 Process of heat release simulation and pressure reconstruction...............26

Figure 3.2 Heat release rate simulation using three of Wiebe functions 30

Figure 3.3 FFT results of motoring and firing (speed: 1500 rpm, fuel mass: 13.5mg) 35

Figure 3.4 Effects of ‘m’ on combustion noise index...41

Figure 3.5 Effects of SOC on combustion noise index 42

Figure 3.6 Effects of combustion duration on combustion noise index 43

Figure 3.7 Effects of released heat on combustion noise index 44

Figure 3.8 Effect of ratio of premixed and diffusive combustion 45

Figure 3.9 Effects of pilot injection quantity...46

Figure 3.10 Effects of SOC of pilot injection..47

Figure 3.11 Effects of combustion duration of pilot injection..................................48

Figure 3.12 Optimal shape of heat release and pressure curve, 1/3 octave band (1).51

Figure 3.13 Optimal shape of heat release and pressure curve, 1/3 octave band (2).52

Figure 3.14 Optimal shape of heat release and pressure curve, 1/3 octave band (3).53

Figure 4.1 Heat release rate & in-cylinder pressure according to SOI change..........59

Figure 4.2 CNI, PM, NO and BEMP variation according to SOI change (Engine speed: 1500 rpm / fuel mass: 15 mg)...60

Figure 4.3 Heat release rate & in-cylinder pressure according to injection pressure change (Engine speed: 1500 rpm / fuel mass: 15 mg).............................61

Figure 4.4 CNI, PM, NO and BEMP variation according to injection pressure change (Engine speed: 1500 rpm / fuel mass: 15 mg).............................62

Figure 4.5 Heat release rate & in-cylinder pressure according to swirl valve open rate change (Engine speed: 1500 rpm / fuel mass: 15 mg)......................63

Figure 4.6 CNI, PM, NO and BEMP variation according to swirl open rate change (Engine speed: 1500 rpm / fuel mass: 15 mg)...64

Figure 4.7 Heat release rate & in-cylinder pressure according to EGR rate change (Engine speed: 1500 rpm / fuel mass: 15 mg)..65

Figure 4.8 CNI, PM, NO and BEMP variation according to EGR rate change (Engine speed: 1500 rpm / fuel mass: 15 mg)..66

Figure 4.9 Heat release, pressure and 1/3 octave band results of conventional diesel combustion including pilot injections (Engine speed: 1500 rpm / fuel mass: 15 mg) 70

Figure 4.10 Heat release, pressure and 1/3 octave band results of PCCI combustion including pilot injections...71

Figure 4.11 Heat release, pressure and 1/3 octave band results of early pilot injection 72

Figure 5.1 Thermocouples to measure the temperature of the air, the EGR gas and the intake manifold...78

Figure 5.2 In-cylinder pressure and RoHR variation according to EGR rate change79

Figure 5.3 Results of speed and load transient operation, ramp time: 2 s (a) Engine speed, (b) CNI, (c) EGR rate 83

Figure 5.4 Results of speed and load transient operation, ramp time: 5 s (a) Engine speed, (b) CNI, (c) EGR rate 84

Figure 5.5 Results of speed and load transient operation, ramp time: 10 s (a) Engine speed, (b) CNI, (c) EGR rate 85

Figure 5.6 Comparison of pressure and RoHR between transient operation and steady state 86

Figure 5.7 Results of load transient operation, ramp time: 1s (a) Engine speed, (b) CNI, (c) EGR rate....87

Figure 5.8 Results of load transient operation, ramp time: 2s (a) Engine speed, (b) CNI, (c) EGR rate....88

Figure 5.9 Results of load transient operation, ramp time: 5s (a) Engine speed, (b) CNI, (c) EGR rate....89

Figure 5.10 Comparison of pressure and RoHR between transient operation and steady state 90

Figure 5.11 Concept of combustion control using CNI for combustion noise reduction....92

Figure 5.12 CNI variation according to SOI change....94

Figure 5.13 Sensitivity analysis of CNI for SOI change @ 1500 rpm....95

Figure 5.14 Sensitivity analysis of CNI for SOI change @ 2000 rpm....96

Figure 5.15 Heat release rate and in-cylinder pressure according to SOI change @ 1500 rpm 97

Figure 5.16 Heat release rate and in-cylinder pressure according to SOI change @ 1750 rpm 98

Figure 5.17 Sensitivity analysis of CNI for pilot fuel quantity and injection pressure change....101

Figure 5.18 Sensitivity analysis of CNI for pilot timing and EGR rate change......102

Figure 5.19 CNI change when SOI is advanced by 3 CAD....105

Figure 5.20 CNI change when Pilot quantity increase by 0.2 mg....105

Figure 5.21 CNI change when injection pressure is reduced by 60 bar....106

Figure 5.22 Arithmetically estimated CNI variation when SOI, pilot quantity and injection pressure are simultaneously changed....107

Figure 5.23 Experimental results CNI variation when SOI, pilot quantity and injection pressure are simultaneously changed....107

Figure 5.24 Control range using SOI....108

Figure 5.25 Control range using pilot quantity....108

Figure 5.26 Control range using injection pressure....109

Figure 5.27 CNI variation when the control ranges are limited for each parameters....109

Figure 5.28 Schematic diagram of closed loop control system using CNI to reduce combustion noise....113

Figure 5.29 CNI calculation using NI-PXI & LabVIEW....114

Figure 5.30 Combustion control algorithm using ES1000 & ASCET....115

Figure 5.31 test vehicle, 1.6 liter diesel enigne 118

Figure 5.32 closed loop control system set up in test vehicle 119

Figure 5.33 Transient operation of test for CNI 120

Figure 5.34 Target CNI and current CNI when the control was deactivated...........120

Figure 5.35 Target CNI and current CNI when the control was activated 121

Figure 5.36 Controlled value of parameters during transient operation..................121

List of Tables

Table 2.1 Specifications of dynamometer 16

Table 2.2 Specifications of smoke meter 16

Table 2.3 Measurement principle of emission analyzer (MEXA-7100DEGR) 16

Table 2.4 Specifications of diesel engine 18

Table 2.5 Specifications of NI PXI 22

Table 2.6 Specifications of ES1000 23

Table 2.7 Specifications of in-cylinder pressure sensor 24

Table 3.1 Experiment condition for Validation for the simulation of the heat release rate 30

Table 3.2 Results of validation for the simulation of the heat release rate 31

Table 3.3 Variables for reconstruction of in-cylinder pressure 32

Table 3.4 Boundary conditions and optimal values of variables (1) 54

Table 3.5 Boundary conditions and optimal values of variables (2) 55

Table 3.6 Boundary conditions and optimal values of variables (3) 56

Table 4.1 Emissions, IMEP and CNI 73

Table 5.1 Maximum of pressure, pressure rise, RoHR and CNI according to EGR variation..82

Table 5.2 Specifications of test vehicle 118

Acronym

A/F	Air to Fuel ratio
ASCET	Advanced Simulation/Software and Control Engineering Tool
ATDC	After Top Dead Center
BDC	Bottom Dead Center
BMEP	Brake Mean Effective Pressure
BTDC	Before Top Dead Center
CA	Crank Angle
CA50	Crank Angle of 50 % mass fraction fuel burnt
CAFE	Corporate Average Fuel Economy
CAI	Controlled Auto Ignition
CAN	Controller Area Network
CI	Compression Ignition
CPS	Crank Position Sensor
CNI	Combustion Noise Index
DI	Direct Injection
DPF	Diesel Particulate Filter
ECU	Engine Control Unit
EGR	Exhaust Gas Recirculation
EMS	Engine Management System
FFT	Fast Fourier Transform
FS	Full Scale
FSN	Filter Smoke Number
HC	HydroCarbon
HRR	Hear Release Rate

HSDI	High Speed Direct Injection
HT	Heat Transfer
IMEP	Indicated Mean Effective Pressure
IVC	Intake Valve Close
IVO	Intake Valve Open
LTC	Low Temperature Combustion
MFB10	Mass Fraction Burned 10 %
MFB50	Mass Fraction Burned 50 %
MFB90	Mass Fraction Burned 90 %
MIT	Main Injection Timing
NDIR	Non-Dispersive InfraRed Sensor
NOx	Nitrogen Oxide
PCCI	Premixed Charge Compression Ignition
PID	Proportional, Integral and Derivative
PM	Particulate Matter
RPM	Revolution Per Minute
SCR	Selective Catalytic Reduction
SI	Spark Ignition
SOC	Start of Combustion
TDC	Top Dead Center
TDI	Turbocharged Direct Injection
THC	Total Hydrocarbon
UEGO	Universal Exhaust Gas Oxygen
VGT	Variable Geometry Turbine

Chapter 1. Introduction

1.1 Background and Motivation

1.1.1 Motivation

It is important to improve the fuel efficiency of manufactured vehicles because of the strict CO2 emission regulations. Diesel engines have been rapidly substituted for gasoline engines in light duty vehicles due to the potential for lower BSFC. However, diesel engines emit more NOx and PM emissions. Moreover, their noise and vibration are severe. Most countries have emission standard law, and numerous engineers have made an effort to meet them. Many equipment such as, EGR system, DPF, LNT and SCR have been developed and adopted in diesel engines to reduce emissions.[1]

The regulations for noise are usually not as stringent and only the exterior noise is restrained. The interior noise is rarely regulated. However, the interior noise directly affects consumer preference as well as the performance power and the fuel efficiency. When drivers and passengers ride in the vehicle to travel, they are kept in a confined space. Thus, a majority of consumers looks for comfort and reasonably quiet engine noise and vibration. They have requested quiet diesel engines and many efforts have been made to meet such demands.

1.1.2 Engine noise classification

Engine noise is classified into mechanical noise, aerodynamic noise and combustion noise shown in figure 1.1. [2] Mechanical noise which is produced by vibration or impact of motion engine components, includes valve train noise, timing system noise. These sounds are produced by the inertia force of engine components and becomes louder with an increasing speed. It is usually the main noise source during high-speed operations. Aerodynamic noise is mainly emitted by the pressure pulse, flow friction and turbulence of air and exhaust gas during the intake and exhaust processes. The aerodynamic noise could affect pass-by noise as well as the interior noise, however there is a trade-off between a reduction of the noise and an improvement of volumetric efficiency. The combustion noise is generated by the combustion process in cylinders. The combustion noise can be broken down into direct and indirect combustion noise. [3]

The direct combustion noise can be defined as the structure-borne noise originated by the gas pressure change in the combustion chambers. The direct combustion noise is radiated throughout the piston, the connecting rods, the crank shaft and the engine block. The rapid pressure change in the cylinder impacts the cylinder walls and makes a dynamic load on the engine parts. Moreover, a local pressure rise in the combustion chamber produces an impulsive pressure wave. The pressure wave then creates a high frequency oscillation through many reflections in the cylinder. [4]

The indirect combustion noise is not excited by the gas pressure but influenced by the combustion characteristics. The indirect combustion includes piston noise, crank shaft noise and the main bearing noise. The piston noise is the most dominant.

The piston impacts the cylinder wall through the secondary motion. This occurs especially when the direction of the piston movement is downward around TDC. The contacted wall side then changes to the opposite side, the piston strikes the cylinder wall and a harsh noise is generated. The secondary motion of the piston impacts the wall 2 ~ 10 times in each cycle and the noise level increases with the in-cylinder pressure increase. [3-9]

The combustion noise occurs at mid and high frequencies, which are both sensitive regions for human ears. The noise adversely affects the sound quality of a diesel engine. The combustion noise needs to be reduced through a combustion optimization.

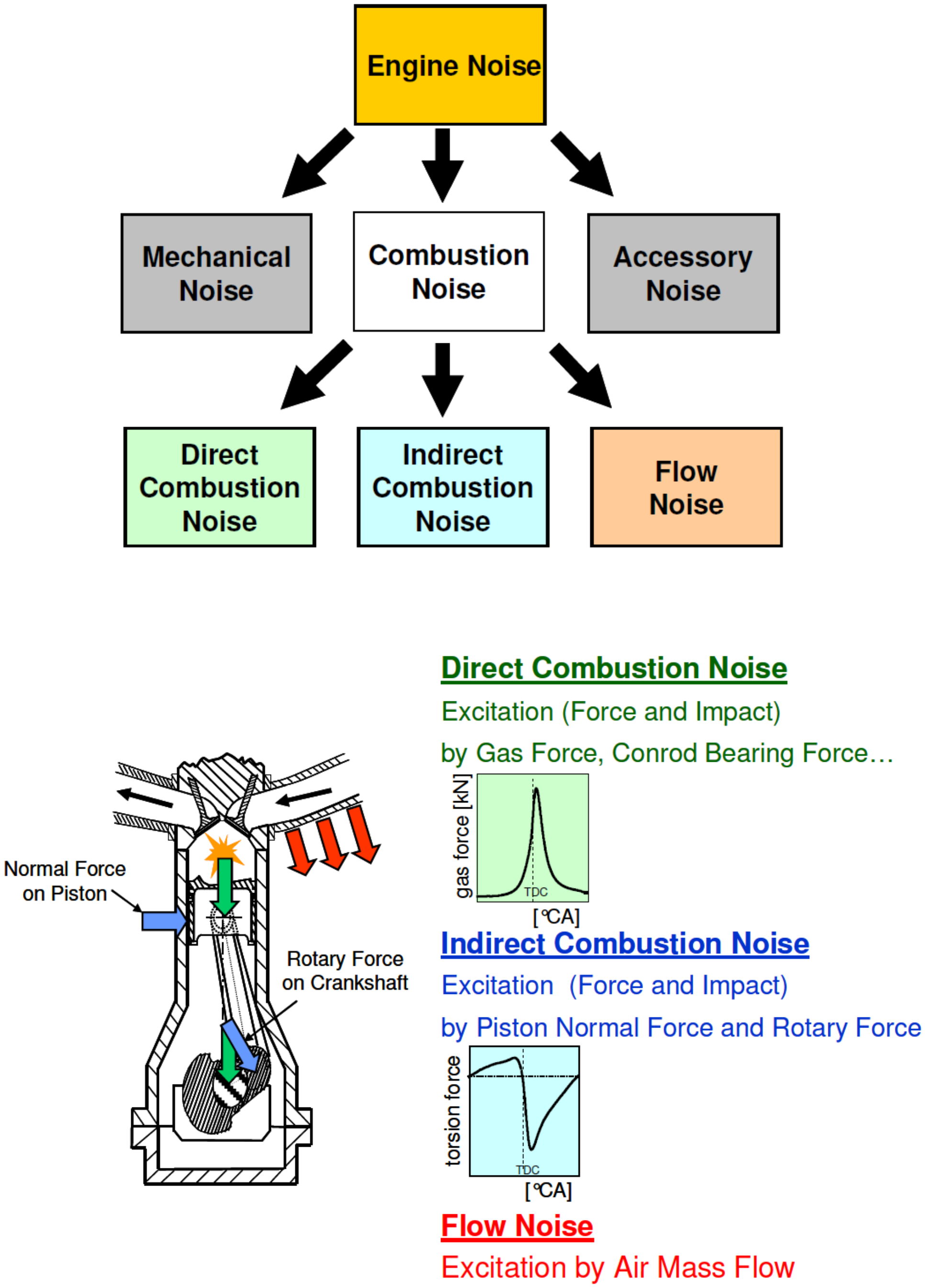
Engine Noise
Mechanical Noise
Combustion Noise
Accessory Noise
Direct Combustion Noise
Indirect Combustion Noise
Flow Noise
Normal Force on Piston
Rotary Force on Crankshaft
Direct Combustion Noise
Excitation (Force and Impact)
by Gas Force, Conrod Bearing Force…
gas force [kN]
TDC
[°CA]
Indirect Combustion Noise
Excitation (Force and Impact)
by Piston Normal Force and Rotary Force
torsion force
TDC
[°CA]
Flow Noise
Excitation by Air Mass Flow

Figure 1.1 Classification of engine noise [3]

1.1.3 Relation between engine noise and combustion

The combustion noise of diesel engine is usually louder than that of a gasoline engine due to a higher maximum in-cylinder pressure and the rapid pressure rise. Diesel engine has a higher compression ratio in order to improve thermal efficiency and combustion stability for auto-ignition. The rapid pressure rise originates from the rapid combustion in the early process of diesel combustion, which is the premixed combustion phase. Figure 1.2 shows the in-cylinder pressures and heat release rate of a diesel engine and a gasoline engine.

Diesel combustion consists of ignition delay, premixed combustion, mixing control combustion and late combustion. The injected fuel at high in-cylinder temperature and pressure undergoes both a chemical ignition delay and a physical ignition delay to be atomized, vaporized, and mixed with air. After the delay, auto-ignition is commenced, and some of fuel mixed air is simultaneously combusted; the combustion chamber suffers from a rapid rise in pressure. The dynamic load excites the cylinder wall and the piston; therefore, the vibration is transferred via the connecting rod, the crank shaft and the engine block. If more fuel is combusted in the premixed combustion phase, the combustion chamber will experience a higher dynamic load caused by a rapid pressure rise. As a result, more combustion noise will be generated. The ignition delay is a main parameter to affect the combustion noise emission, because the longer ignition delay supplies the more time to be prepared to be combusted.

Ignition delay is affected by the temperature, pressure and oxygen concentration in a cylinder. Thus, the compression ratio, injection timing and engine load which affect in-cylinder air temperature and pressure, are directly correlated. The higher compression ratio increases temperature and pressure. Injection timing can change the in-cylinder pressure temperature and pressure when fuel injection starts; a too early or a too late injection can increase the ignition delay. The higher engine load leads to a temperature increase of the cylinder wall, the piston and the EGR gas, which can make the in-cylinder temperature and pressure higher. In addition, the delay is affected by the oxygen concentration. The high level EGR rate to reduce NOx emission increases the ignition delay by reducing the concentration. The combustion noise is mainly generated at low- and mid-engine speeds and loads that are related to long ignition delays due to deceased oxygen concentration with higher EGR rate level. [10-17]

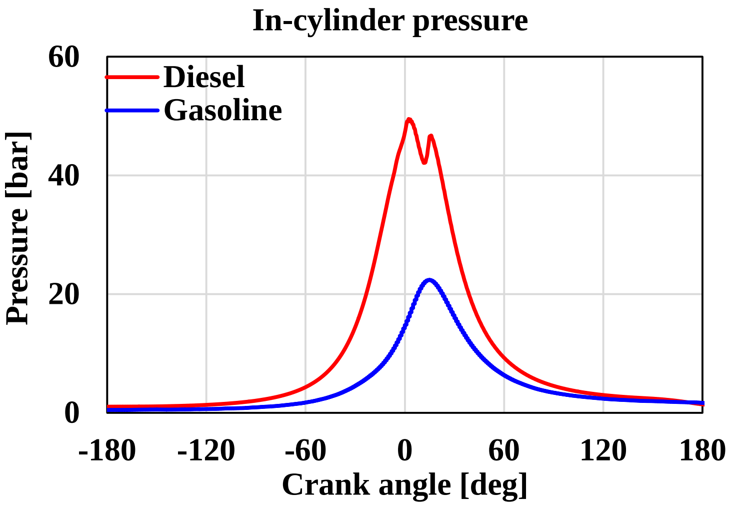

(a) In-cylinder pressure of gasoline engine and diesel engine

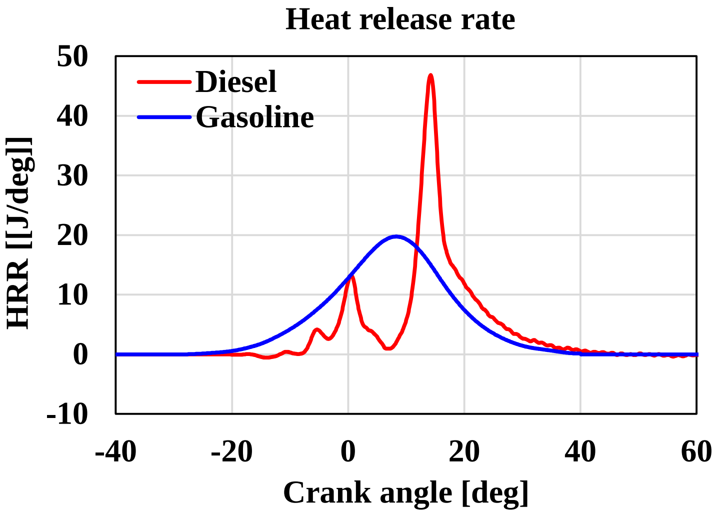

(b) Heat release rate of gasoline engine and diesel engine

Figure 1.2 In-cylinder pressure and heat release rate of diesel engine and gasoline engine (Diesel engine: Bore:77.2mm, Stroke:84.5mm, comp. ratio: 17.3, Gasoline engine: Bore & Stroke: 86mm, comp. ratio 10.5)

1.1.4 Reduction of combustion noise

The rapid pressure rise in cylinder is a source of combustion noise and it is caused by the rapid combustion. Thus, it is important to make the combustion speed slow in order to reduce combustion noise. As referred above, a rapid combustion in the premixed combustion phase in diesel engine combustion process, thus more fuel is burned, more rapid combustion is occurred.

Pilot injection is an effective way to reduce combustion noise because the combustion of pilot injection causes increasing temperature and pressure in the combustion chamber and shortens the ignition delay of the main injection when it starts. As a result, the amount of fuel injected during the ignition delay is greatly reduced and a smoother increase of in-cylinder pressure is obtained. The common rail system enables the control injection strategy such as injection number, pressure and timing. As a result, pilot injection could be applied to reduce the combustion noise. [18-23]

The other way to reduce the fuel quantity combusted in the premixed phase is to reduce the injection quantity of fuel. The rate shaping is an injection system which can control the injection rate. In the early process of injection, the rate is controlled to be reduced, after SOC the injection rate increase to inject target fuel quantity. As a result, the heat release rate could be controlled not to be harsh. Digital rate shaping is able to control the burning rate. Using the special injectors which have a very short dwell time, many injections are occurred instead of a conventional main injection. As a result, the fuel quantity, which is burned rapidly, reduces and the heat release rate can be kept a moderate level. [24-28]

1.1.5 Noise evaluation method

1.1.5.1 Engine noise evaluation method

The engine noise measurements require an expensive facility for testing, such as an anechoic room and microphones. Moreover, the separation of the combustion noise is difficult work. To overcome the shortage, the method using the in-cylinder pressure has been introduced. The pressure curve, the exciting source, is transferred through the engine parts and emitted from the block surface. In this process, the original excitation is attenuated according to the transfer characteristics of the parts. Both the pressure curve and the transfer characteristics can be presented as a function of frequency. If the attenuation characteristics are known and the in-cylinder pressure is measured, the noise can be estimated. Another method to evaluate noise via the in-cylinder pressure signal is using the regression equation of the variables that are the dominant parameters for combustion noise intensity such as the maximum pressure, the maximum pressure rise. These are effective evaluation techniques for research and development on improving combustion noise because engine noise can accurately and simply be estimated by measuring the in-cylinder pressure. [29-37]

1.1.5.2 Combustion noise index (CNI)

The engine noise has to be measured in a free field above a reflecting plane to obtain reliable results. However, the facility is expensive and needs a large space. Moreover, the many dynamometers which were previously used in facilities were not the correct type for transient testing. Thus, evaluation methodologies using in-cylinder pressure sensors instead of microphones have been developed. [38] In this study, the CNI was used for the combustion noise evaluation, which was introduced by Jung et al. The in-cylinder signal, functions of time, was converted to functions of frequency by the FFT. Then, the CNI was calculated through the summation of the 1~3.15 kHz range of the one third octave band level. The frequency range has a strong correlation with the combustion noise. Each octave band values are summed using a logarithm (equation 8). Actually, the CNI could not accurately evaluate the noise like as measuring with microphones. However, the CNI is able to represent the combustion noise level because the tendencies of the relation between the CNI and the combustion noise level are consistent. As shown in figure 1.3, the CNI has a good correlation with the measured combustion noise for broad sound level. Moreover, the correlation was kept even throughout the injection parameter change. Therefore, a relative comparison is possible, though an absolute comparison is difficult to achieve using the CNI. [39]

$$CNI(dB) = 10\log(10^{1kHz\,level/10} + 10^{1.25kHz\,level/10} + \cdots + 10^{3.15kHz\,level/10}) \qquad (1.1)$$

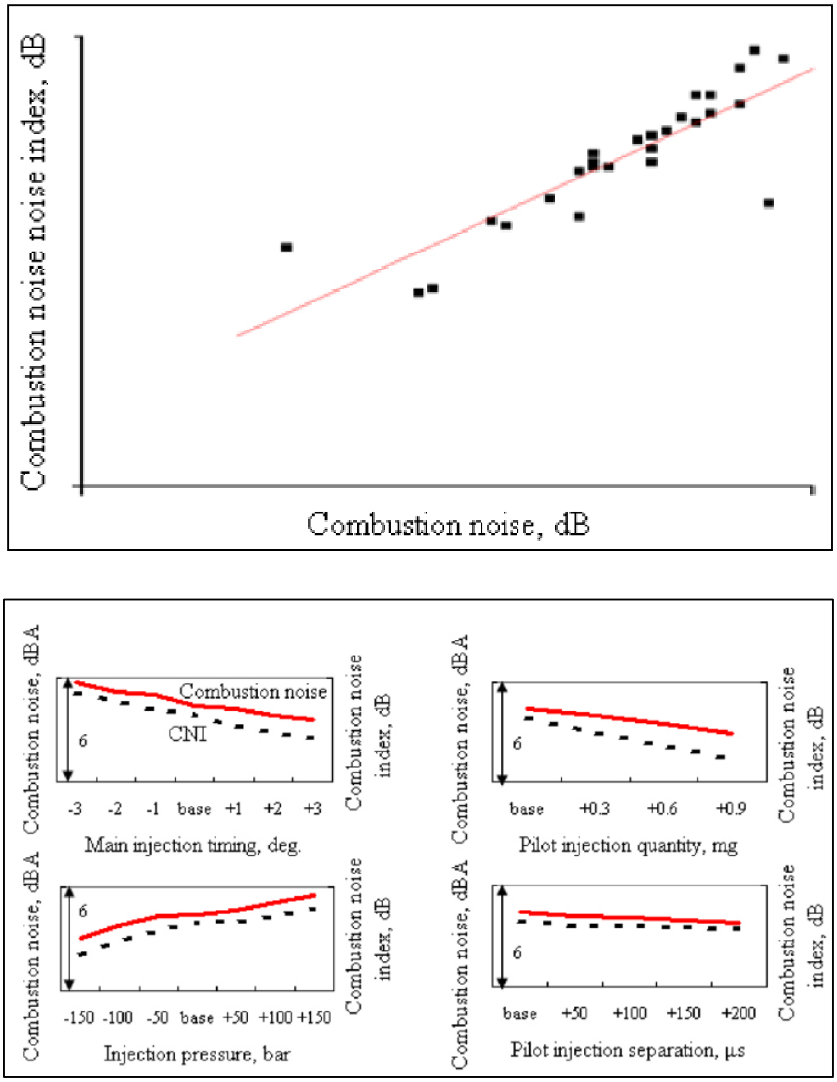

Figure 1.3 Correlation between measured noise and CNI changing injection strategies [39]

1.1.6 Closed loop control

The control of modern Diesel engines involves a large number of parameters, such as the start of injection, the EGR rate, the injection pressure, and the fuel quantity, etc. These parameters must be controlled for the engine to be operated in an optimal state. Some of these parameters are controlled in open-loop control, and others are controlled in closed-loop control mode. Open-loop control provides a fast response and a relatively easy control. However, it cannot handle changes in state caused by variating conditions such as aging of the injectors and fuel quality. On the other hand, closed-loop control monitors the present state so that any changes in conditions can be considered in the control mechanism. For Diesel engines, many studies have utilized closed-loop control with the closed loop collecting combustion state information as feedback. Combustion state information can be obtained directly from the in-cylinder pressure or indirectly from the combustion noise and vibration. For an indirect method, an accelerometer is used to measure vibration from the engine head or the surface of blocks and information can be obtained from these signals. This method is economically affordable due to the fact that combustion information of multi cylinders can be extracted by one accelerometer but obtainable information is limited and signals can be distorted by any noise source. Using the in-cylinder pressure is the most reliable method as well as a direct method. The rate of heat release (RoHR) can be calculated from the pressure data, and then a combustion parameter of interest, such as the 50 % mass fraction burned (MFB50), start of combustion (SOC) or the location of peak pressure (LPP), can be calculated from the RoHR. The control parameters are adjusted to set a target value for the combustion parameters. [40-42]

1.2 Objectives

The purpose of the present study is to look for a methodology to reduce combustion noise in diesel engines. In this study, the relation between diesel engine combustion and combustion noise was examined. Especially, the effects of the shape of heat release rate on the excitations, which were caused by in-cylinder pressure change, were investigated. In addition, the closed loop control system for the noise reduction was developed.

The detailed objectives of this study are :

1. Investigating effect of heat release rate shape on excitation which is generated by in-cylinder pressure change
2. Looking for the optimal shape to decrease the excitation
3. Evaluating effects of changes of injection strategies on heat release shape and the excitation
4. Looking for the injection strategies to reduce combustion noise
5. Examining CNI characteristics change during transient operations
6. A development of closed loop control system using combustion noise index for reduction of the noise

Chapter 2. Experimental Apparatus

2.1 Overall configuration

In this chapter, the experimental apparatus and test engine are introduced. The figure 2.1 shows the schematic diagram of them.

2.1.1 Engine test bench cell

The engine test was conducted in a test bench cell equipped with dynamometer, coolant controller, air conditioner, fuel controller and fuel meter. The engine was coupled with a 340 kW AC dynamometer to control revolution speed and torque for steady operations and transient operations. The specifications of the dynamometer is shown in Table 2.1. In the facility, the air temperature was controlled at 25℃. The coolant temperature of the engine was controlled at 90℃ during the experiment. The diesel fuel temperature was also controlled at 40 °C.

2.1.2 Measurement of exhaust gas emissions

The composition of exhaust gas were measured during the test. Concentration of O2, CO2, NOx, THC and CO were measured by the exhaust gas analyzer (HORIBA, MEXA-7100DEGR). PM was measured by a smoke meter. Tables 2.2 and 2.3 show the specifications of smoke meter and the exhaust gas analyzer (HORIBA, MEXA-7100DEGR). All species measured by the gas analyzer were measured in volume fraction (vol % / ppm) in the wet condition and the PM was measured in FSN (Filtered Smoke Number).

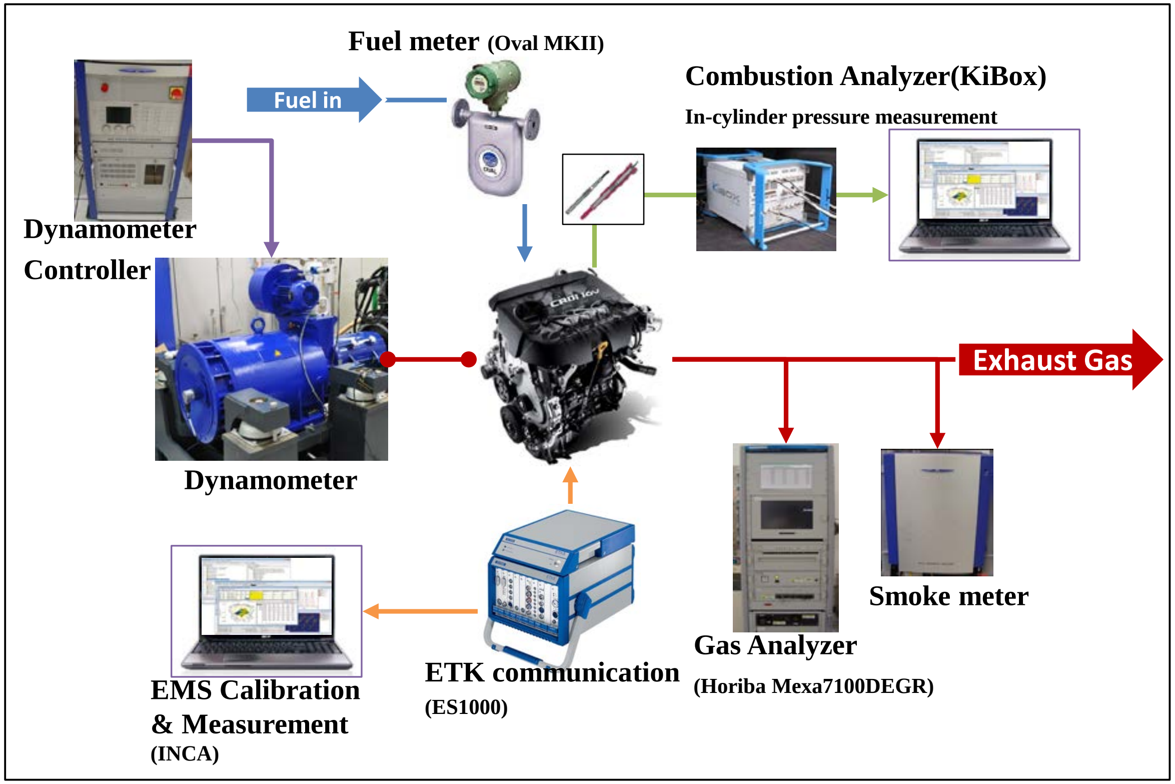
Fuel meter (Oval MKII)
Combustion Analyzer(KiBox)
In-cylinder pressure measurement
Fuel in
Dynamometer
Controller
Exhaust Gas
Dynamometer
Smoke meter
Gas Analyzer
(Horiba Mexa7100DEGR)
ETK communication
(ES1000)
EMS Calibration
& Measurement
(INCA)

Figure 2.1 Schematic diagram of engine test and measurement equipment

Table 2.1 Specifications of dynamometer

Item	Specification
Manufacturer	AVL
Model	PUMA 1.3 Test Automation system
Capacity	340 kW
Type	AC
Cooling	Air cooling

Table 2.2 Specifications of smoke meter

Item	Specification
Manufacturer	AVL
Model	AVL 415S
Measurement range	0 ~ 10 FSN / 0 ~ 32,000 mg/m³
Resolution	0.001 FSN / 0.01 mg/m³
Repeatability (as standard deviation)	$\sigma \leq \pm$(0.005 FSN + 3 % of measured value)
Reproducibility (as standard deviation)	$\sigma \leq \pm$(0.005 FSN + 6 % of measured value)

Table 2.3 Measurement principle of emission analyzer (MEXA-7100DEGR)

Emissions	Measurement principle
NOx	Chemiluminecent Detector
THC	Flame Ionization Detector
O_2, CO_2, CO	Non Dispersive Infrared Rays

2.2 Multi-cylinder Diesel engine

For this research, an in-line 4 cylinder 1.6 L Diesel engine was used. Figure 2.2 shows the target engine in this study. This engine has fuel injection equipment including solenoide type injector, common rail and high pressure pump, which enable injection pressure up to 1600 bar. A VGT(variable geometry turbocharger), a oxidation catalyst and DPF(Diesel Particle Filter) also were equipped. Detailed specifications of the engine is shown in Table 2.4.

Figure 2.2 1.6 L Diesel engine

Table 2.4 Specifications of diesel engine

Criteria	Specification
Layout	In-line 4 cylinder
Displacement volume	1582 cc
Max power	94 kW @ 4000 rpm
Max torque	26.5 kg.m @ 1900~2750 rpm
Bore	77.2 mm
Stroke	84.5 mm
Connecting rod	140 mm
Compression ratio	17.3
Fuel injector type	Solenoid type
ECU version	EDC 17

2.3 Combustion control system

Combustion control system consisted of a combustion analyzer and a combustion controller. The combustion analyzer calculated combustion noise index by using in-cylinder pressure signal and crank position signal. To calculate the combustion noise index in real-time for each cycle, a NI-PXI, which can measure analog signals with fast sampling rate and handle huge data processing, was used. The software was developed in LabVIEW. The combustion controller was developed using ES1000, which is a rapid prototype controller, because it can easily read and write values of the control parameters of ECU memory by ETK communication. The software was developed in ASCET. The calculated combustion noise index in NI-PXI was transferred to combustion controller using CAN bus communication.

2.3.1 NI-PXI

PXI is a rugged PC-based platform for measurement and automation systems. PXI combines PCI electrical-bus features with the modular, Eurocard packaging of CompactPCI and then adds specialized synchronization buses and key software features. The system which was used in this study included real time controller (NI PXI-8119), FPGA board (NI PXI-7842) and CNI bus communication board (NI PXI-8461). The pressure signal and CPS signal were measured using analog input channels of the FPGA board. The measured signals was passed on real-time controller through FIFO. The CNI was calculated in the real time controller and the result was sent by the CAN bus board to combustion controller, ES-1000. Figure 2.3 shows the NI-PXI. The detailed specifications are shown in table2.5

2.3.2 ES-1000

The combustion controller was developed using an ES1000. The ES1000 was a platform which consists of various function boards. In this research, a simulation board, CAN bus communication board, analog input board and ETK communication board were used. The simulation board is a rapid prototype controller which has real-time OS. It operates the combustion control algorithm which was developed in ASCET. The CAN bus communication board was used for data transfer from NI-PXI. ETK communication board was used to read and write values of ECU engine operating parameters. The combustion control algorithm was coded by using ASCET. ASCET is a model-based development of application software for embedded systems. It was designed to develop software for the automotive industry. The application software can be coded using block diagrams, state machine and C code and automatic code generation for rapid prototype is accessible.

2.3.3 Pressure sensor

The in-cylinder pressure measurement is an important part because combustion noise index was calculated by using the measurement. Therefore, the quality of the combustion control was determined by a great extent of the quality of the measured in-cylinder pressure signal. The pressure was measured by using a pressure sensor, Kistler type-6056. The sensor was installed using a glow plug adopter, which has a shape of a glowplug, and it was mounted in the 1st cylinder instead of the glowplug.

The charge signal from the sensor was converted to analog voltage signal through a charge amplifier. The converted signal was measured by the FPGA board of NI-PXI.

Table 2.5 Specifications of NI PXI

Criteria	Specification
PXI Controller Board (NI PXI-8119)	2.3 GHz quad-core Intel Core i7-3610QE processor 4GB, 1600 MHz DDR3 RAM
FPGA board (NI PXI-7842R)	8 analog inputs, independent sampling rates up to 200 kHz, 16-bit resolution, ±10 V 8 analog outputs, independent update rates up to 1 MHz, 16-bit resolution, ±10 V 96 digital lines configurable as inputs, outputs, counters, or custom logic at rates up to 40 MHz Virtex-5 LX50 FPGA programmable FPGA Module 3 DMA channels for high-speed data streaming
CAN board (NI PXI-8461/2)	2 CH, 1 MBit/s

Table 2.6 Specifications of ES1000

Criteria		Specification
Simulation Board	CPU	1 GHz
	RAM	256 MB SDRAM
A/D board		16 CH, 100 kHz/CH
D/A board		8 CH
Digital and PWM I/O board	Channel	16 CH input, 16 CH output 2 external trigger
	Frequency	1 Hz to 60 kHz
CAN Communication		4 CAN signal
ETK Communication		1 CH, 100 MBit/s

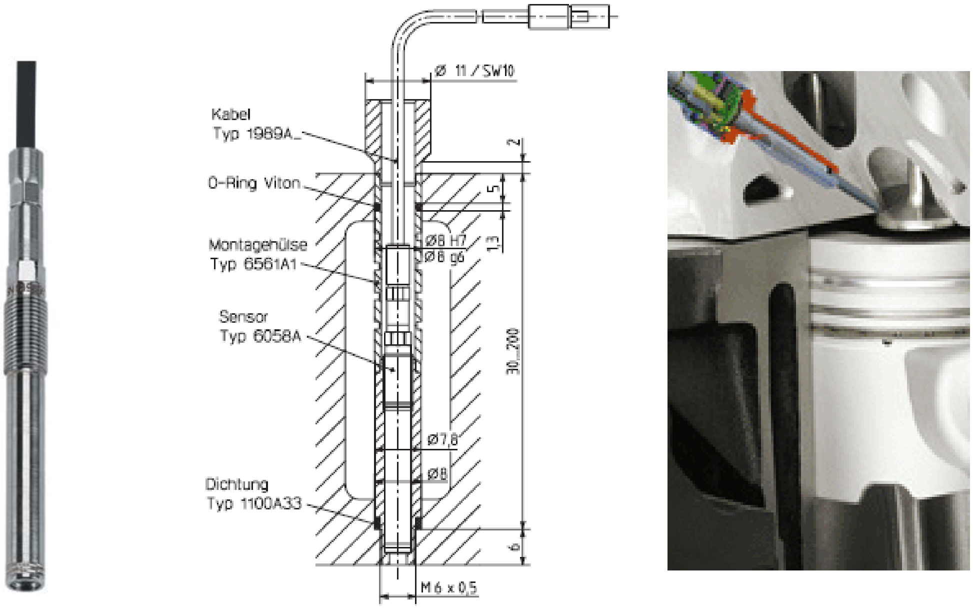
Ø 11 / SW10
Kabel
Typ 1989A_
O-Ring Viton
Montagehülse
Typ 6561A1
Sensor
Typ 6058A
Dichtung
Typ 1100A33
Ø8 H7
Ø8 g6
Ø7,8
Ø8
2
5
13
30...200
6
M 6 x 0,5

Figure 2.3 In-cylinder pressure sensor and glow plug adopter

Table 2.7 Specifications of in-cylinder pressure sensor

Criteria	Specification
Measuring range	0~250 bar
Sensitivity	20 pC/bar
Operating temperature range	-20~350 ºC
Sensitivity shift	≤ ± 0.5%
Short term drift	≤ ± 0.5% bar
Weight with cable	30 g

Chapter 3. Relation between diesel combustion and combustion noise

3.1 Simulation of heat release rate using Wiebe functions

The in-cylinder pressure variation, which is the main source of combustion noise, was produced by the heat released from burning fuel. Thus, the shape of heat release rate directly affects combustion noise. However, it is very difficult to evaluate effect of shapes on combustion noise by experimentally changing them. Most of combustion control parameters, such as the pilot injection, boost pressure, SOC and compression ratio, are strongly dependent and affect the shape of heat release rate. Thus, the heat release rate was simulated using Wiebe function to unconstrainedly change the shape. In this chapter, the effects of shape of heat release rate on combustion noise index were examined and the better shapes of heat release rate to reduce the combustion noise were found by using the Wiebe function. The figure 3.1 shows the process of heat release rate simulation and pressure Diesel combustion and Wiebe function.

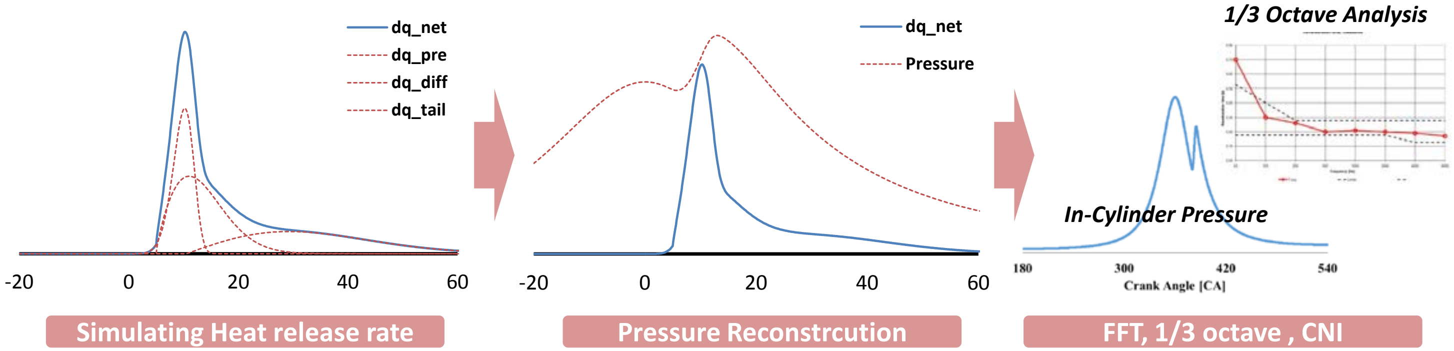

Figure 3.1 Process of heat release simulation and pressure reconstruction

The Wiebe function has been used to predict the pressure curve and temperatures in many other researches. The equation (3.1) shows the Wiebe function. The coefficient 'a' and 'm' are related to combustion characteristics and '$\theta_{duration}$' means the combustion duration. Since the function converges to 1, the total heat can be multiplied. The equation (3.2) shows heat release per crank angle degree when the total heat is Q_{total}.

$$\mathrm{X} = 1 - \exp\left[-a \cdot \frac{\theta-\theta_{soc}}{\theta_{duration}}^{m+1}\right] \tag{3.1}$$

$$\frac{dQ}{d\theta} = a \cdot (m+1) \cdot \left(\frac{Q_{total}}{\theta_{duration}}\right) \cdot \left(\frac{(\theta-\theta_{soc})}{\theta_{duration}}\right)^{m} \cdot \left(exp\left[-a \cdot \left(\frac{(\theta-\theta_{i})}{\theta_{duration}}\right)^{m+1}\right]\right) \tag{3.2}$$

The diesel engine combustion can be divided into 3 phases, which are premixed combustion, mixing controlled combustion and late combustion. Each phase has different characteristics, start timing of combustion, burning rate and combustion duration. The rapid combustions were shown during the short period in premixed combustion phase. On the other hand, diffusive combustion has a relatively long combustion duration because it needs extra time to be mixed with air. Therefore, simulating diesel combustion using single Wiebe function was hard to be coincided with the experimental results. Thus, Ghojel at el. used double Wiebe function to describe the premixed combustion and diffusive combustion independently [43]. However, since the late combustion has a much longer combustion period than the mixing controlled combustion, they have to be considered separately to improve the accuracy of the simulation. Hence, three of Wiebe function were used to simulate diesel combustion in this study. They can be summed linearly, thus the equation is shown as equations (3.3) and (3.4). [44-46]

$$\mathrm{X} = \sum_i 1 - \exp\left[-a_i \cdot \frac{\theta - \theta_{i,soc}}{\theta_{i,duration}}^{m_i+1}\right] \tag{3.3}$$

$$\frac{dQ}{d\theta} = \sum_i a_i \cdot (m_i + 1) \cdot \left(\frac{Q_{i,total}}{\theta_{i,duration}}\right) \cdot \left(\frac{(\theta - \theta_{i,soc})}{\theta_{i,duration}}\right)^{m_i} \cdot \left(exp\left[-a\left(\frac{(\theta - \theta_i)}{\theta_{i,duration}}\right)^{m_i+1}\right]\right) \tag{3.4}$$

3.1.1 Validation for the simulation of the heat release rate

The simulated heat release rate curves were compared with the experiment results. The experimental cases are shown Table 3.1. The engine speed was 1500 rpm and fuel quantity was 15 mg. To find a variation of heat release rate when the injection strategies are changed. The parameters, SOI, injection pressure, swirl intensity and EGR rate, which are used to affect combustion characteristics, were changed. The heat release rates were calculated by equation (3.5). Note that heat transfer was not considered.

$$\frac{dQ}{d\theta} = \left(\frac{\gamma}{\gamma-1}\right) p \frac{dV}{d\theta} + \frac{1}{\gamma-1} V \frac{dP}{d\theta} \tag{3.5}$$

The Wiebe functions were fitted to experimental heat release rates. The fitting was executed for only the main combustion, thought the double pilot injection were included in the experimental results. Figure 3.1 shows the results of fitting. The Wiebe functions were able to describe real heat release rate. Table 3.1 shows coefficients values. One wiebe function has five coefficients, thus triple Wiebe function has 15 coefficients. To minimize the difference of the simulated heat release rate and the real heat release rate, 'fmincon' function of Matlab was used. Table 3.2 shows the results of validation. '$m_{premixed}$' was varied from 2.44 to 5, 'm_{mixing}' from 0.4 to 0.8 and m_{late} 'was not significantly varied; however, the variation was just about 1. '$\theta_{premixed,duration}$' was varied from 11.9 to 14.5, '$\theta_{premixed,duration}$' from 25.8 to 29.2 and '$\theta_{late,duration}$' from 62.2 to 70. 91.

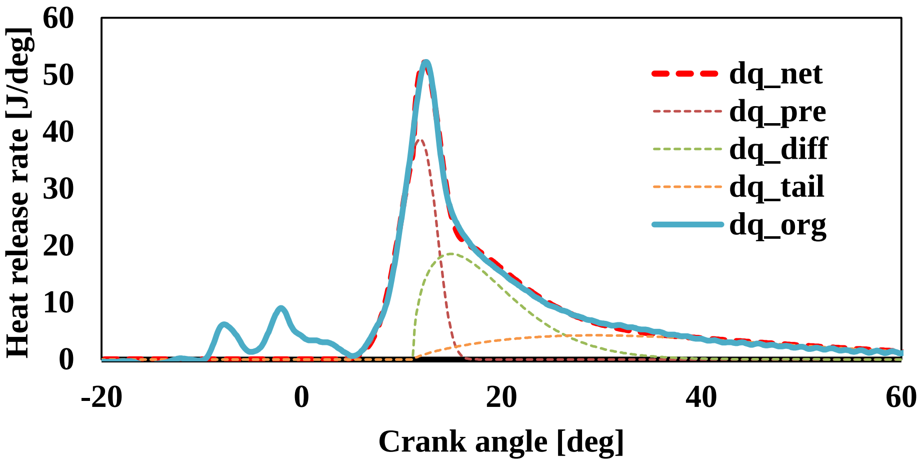

Figure 3.2 Heat release rate simulation using three of Wiebe functions

Table 3.1 Experiment condition for Validation for the simulation of the heat release rate

Injection Parameter	Variation
Main Fuel Quantity	±1.5 mg
Main Injection Timing	±3 *CAD*
Injection pressure	±100 *bar*
Swirl valve	+ 20%p / + 40%p
Pilot Quantity	±0.3 mg
Pilot Injection Timing	+2 / +4
EGR rate	± 5%p

Table 3.2 Results of validation for the simulation of the heat release rate

		Coefficients of Wiebe function					
		A	m	SOC	Duration	Q	Q ratio
Premixed	Low	6.7	2.1	1.7	11.2	437	0.3
	Upper	7.1	5	7.1	14.6	533	0.4
Diffusion	Low	7	0.4	5.5	23.1	437	0.3
	Upper	7	0.8	15	29.4	533	0.4
Tail	Low	7	0.7	5.5	61.7	437	0.4
	Upper	7	1.2	15	69.2	533	0.2

3.1.2 Pressure reconstruction using Wiebe functions

Pressure curve was reconstructed by changing the shape of heat release rate to evaluate the excitation intensity caused by the combustion in a cylinder. To reconstruct the pressure curve using heat release rate, an inverse operation of equation 3.5 was used. The used values of parameters are shown in table 3.3. The engine geometries are the same from the engine used and γ was 1.3. The heat loss occurred by heat transfer was not considered. After attaining the pressure curve, the heat release rate was calculated again to compare the original heat release rate. The two curves of heat release rate were almost identical.

Table 3.3 Variables for reconstruction of in-cylinder pressure

Variables	Value
Bore	77.2 mm
Stroke	84.5 mm
Connecting rod length	140 mm
Compression ratio	17.3
Specific heat	1.3

3.2 Effect of heat release rate shape on combustion noise : Analysis of excitation of in-cylinder pressure changing Wiebe functions coefficients

Fast Fourier Transform (FFT) was used to analyze the excitation by in-cylinder pressure. For the FFT analysis, the time base pressure data, which are measured with the same time interval were needed. However, the reconstructed pressure curves were angle based data with the same crank angle interval. In real engines, the angular velocity is not constant but it oscillates according to the strokes. In this study, the oscillation was not considered and the angular velocity was assumed as a constant. Thus, the time based pressure data were calculated from an interpolation of angle base data. The results of FFT were varied accordingly to the sample number. Thus, when the engine speed is changed, the sample number of one cycle should also be changed. Considering that, FFT was calculated with 50 % overlap for 10 cycles. The sample number was 4096 and hanning windows was applied to get rid of the unexpected noise. The one third-octave band was also used to analysis of frequency of in-cylinder pressure excitation. Moreover, to evaluate the combustion noise, the CNI was calculated.

3.2.1 Comparing motoring pressure and combustion pressure

The combustion noise was mainly generated by in-cylinder pressure change. There are two main cause for the pressure changes. The first one is the compression and expansion process of a piston. The other one is a combustion process. Thus the effects of them on excitation were analyzed separately. Figure 3.2 shows the combustion pressure, motoring pressure and the difference of them. The difference was calculated by subtracting the motoring pressure from the combustion pressure. Figure 3.3 shows the results of FFT of them. The FFT results of the motoring pressure converges to zero above 400 Hz. Moreover, above 400 Hz, the FFT results of combustion pressure and the pressure difference are almost the same. Therefore, the compression and expansion processes affect only below 400 Hz, and the combustion process only affects frequency above 400 Hz because the signals were superimposed. Therefore, it can be concluded that the frequency signals of above 400 Hz were generated by the combustion phenomenon.

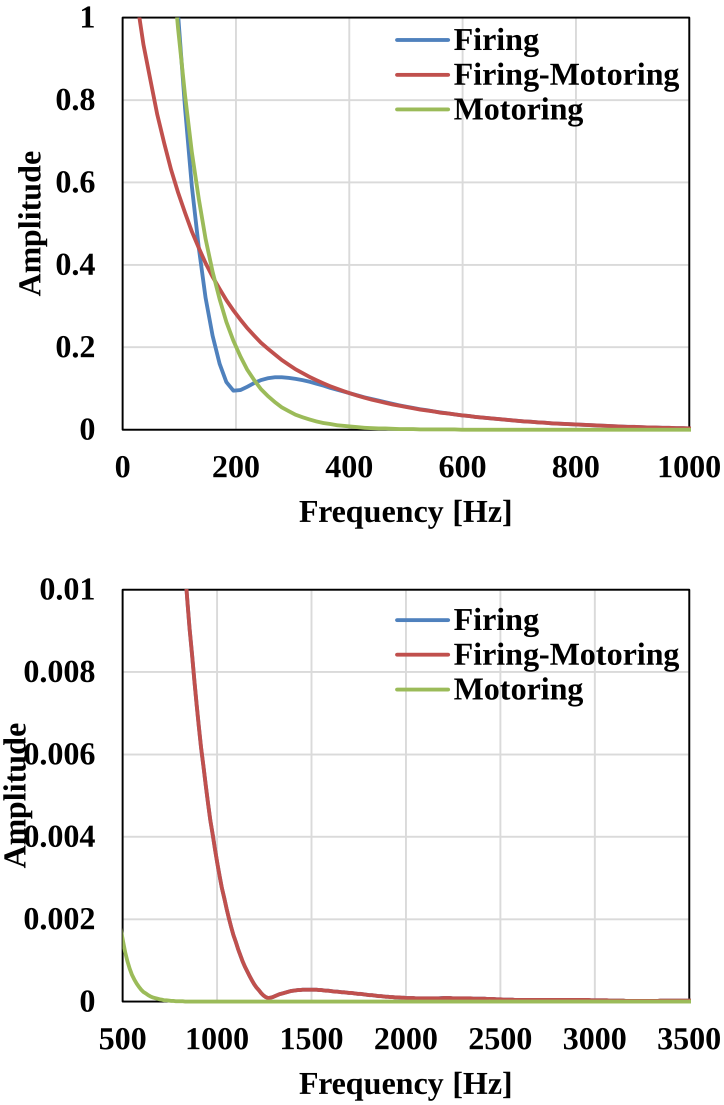

Figure 3.3 FFT results of motoring and firing (speed: 1500 rpm, fuel mass: 13.5mg)

3.2.2 Effects of Single Wiebe function shape on combustion noise

One Wiebe function has 5 coefficients and each coefficient determines the shape of a function. In this chapter, effects of a Wiebe function shape on combustion noise by changing the coefficients are invested. The coefficient ‘a’ and ‘m’ affect the burning rate. When the ‘a’ is increased, the combustion is proceeded rapidly. When the ‘m’ is decreased, more fuel is burned early with the same combustion duration. ‘$\theta_{duration}$’ means combustion duration and θ_{soc} means the crank angle of the combustion initiation. Since the function converges to 1, the total heat release can be multiplied to apply the total heat release quantity.

3.2.2.1 Effects of coefficient ‘a’

When ‘a’ is increased, more fuel is burned in the early stage of combustion duration. Thus, the heat release rate also increases and a rapid pressure rise occurs.

3.2.2.2 Effects of coefficient ‘m’

As ‘m’ is increased, more fuel is combusted in the late stage of combustion duration and as ‘m’ is decreased, more fuel is burned prematurely (figure 3.4). When ‘m’ decreased, the heat release rate became sharp and higher. It caused a rapid pressure rise. The in-cylinder pressure also became higher because the combustion phase was advanced. However, when ‘m’ was increased, more burned fuel was combusted in an early period and it caused a higher heat release rate and a rapid pressure rise. However, because the combustion phase was retarded, the in-cylinder pressure did not increase much. Since, the pressure rise made the CNI increase, when ‘m’ was 2; the CNI was at a minimum value. When ‘m’ was 3; the CNI slightly increased. On the other hand, frequency above 1.6 kHz decreased. Thus, it is concluded that when ‘m’ has a value between 2 and 3 the excitation of in-cylinder pressure is the weakest.

3.2.2.3 Effects of combustion duration

The effects of combustion duration were investigated here. Figure 3.6 shows the variation of pressure, heat release rate and excitations. To minimize effects of other parameters, the combustion phases of them were fixed. When the combustion duration became short, the heat release rate became higher because the total released heat are the same. It makes a rapid pressure rise. The 1/3 octave band results show that levels are increased in all frequency band. It means that the combustion duration have to be long to reduce the combustion noise. However, because it has a trade off with IMEP, it has to be optimized for real engineering.

3.2.2.4 Effects of start of combustion

The effects of SOC were investigated and the results are shown in figure 3.5. When the same heat is released, if the volume of the combustion chamber was changed, then the in-cylinder pressure also changes. Thus, when the SOC was changed, the corresponding volume also changed. The SOC was changed with the same shape of heat release rate showin in Figure 3.5. The pressure level increased when the SOC was advanced and the IMEP was increased as well. It was clearer with the apparent heat release rate. When the SOC was advanced, the apparent heat release rate shapes were not changed much, only the scales were changed. Additionally, the important thing was that the number of in-cylinder pressure peak could not affect excitation. Though, when SOC was 3° ATDC, in-cylinder pressure had 2 peaks and when SOC was 3° BTDC, in-cylinder pressure had one peak, however, they had similar apparent heat release rate shapes. The FFT, 1/3 octave band and CNI were not varied much when the SOC were changed. However, because IMEP was significantly changed, when the optimal shape of heat release rate is determined, the SOC was able to be separately optimized to improve IMEP, though when the SOC was changed, the heat release rate shape was also changed in real engine experiment.

3.2.2.5 Effects of total released heat

When the total heat quantities were changed with other fixed parameters, results are shown in Figure 3.7. They look similar to the variations of combustion duration. It was because that increased heat cause increase the maximum value of heat release rate, thus, it caused a rapid pressure rise. FFT and 1/3 octave band showed an increase in all frequency regions.

3.2.3 Effects of mixing controlled phase

After fuel injection, some of the injected fuel were mixed with air during an ignition delay, and they were burned rapidly in the premixed combustion phase. With the more burned fuel in the premixed combustion, the heat release rate became much sharper in the early stage of the total combustion duration shown in Figure 3.8. It led to an increase in pressure peak. In addition, as the burned fuel in the premixed combustion phase increased, 1 kHz frequency level was increased. However, frequency over 1.6 kHz decreased. It is because the pressure peak is affected under 1 kHz frequency and the ‘m’ of diffusive combustion phase is much less than the premixed combustion. Thus, as the duration of the premixed combustion became short and the shape became sharp, effects of the premixed combustion became dominant.

3.2.4 Effects of pilot injection

Most of the modern diesel engines equipped with the common rail system use multiple injections. The pilot injections which were injected before the main injection were effective for reducing combustion noise because those make ignition delay of main injection and lower heat release rate are produced. However, combustion noise which was produced by just the combustion of pilot injection had not been investigated. In this study, effects of the quantity and SOC of pilot injection are examined.

3.2.4.1 Effects of pilot injection quantity

The heat released by pilot injection combustion were varied from 25 J to 45 J. The results are shown in figure 3.9. When the injection quantity increase, the frequency over 1.6 kHz are increase, but 1 kHz was decrease as shown in figure 3.9. The results of CNI were not much changed. However, because high frequency increase, the sound quality could be changed.

3.2.4.2 Effects of SOC of pilot injection

The SOC of pilot injection were changed from 5° BTDC CAD to -15° BTDC CAD. As previously referred, when the only one Wiebe function was investigated, the SOC does not affect CNI and other frequency characteristics. However, one more

Wiebe, diffusive combustion, was added, the SOC affected the excitation of pressure. The SOC of pilot is very similar to that. When the SOC were 7.5° BTDC CAD and 15° BTDC CAD, the only 1.2 kHz frequency decrease as shown in figure 3.10

3.2.4.3 Effects of combustion duration of pilot injection

The durations of combustion were changed from 5 CAD to 13 CAD. The effects of duration variation were similar to effects of change of fuel quantities. As shown figure 3.11, the pilot duration does not much affect in-cylinder pressure. In the apparent heat release rate, the pressure rise is smoother in very early of combustion, when the pilot combustion duration was longer. It significantly affected frequency over 1.2 kHz. Thus, combustion characteristics of pilot injection was important to reduce excitation over 1.2 kHz.

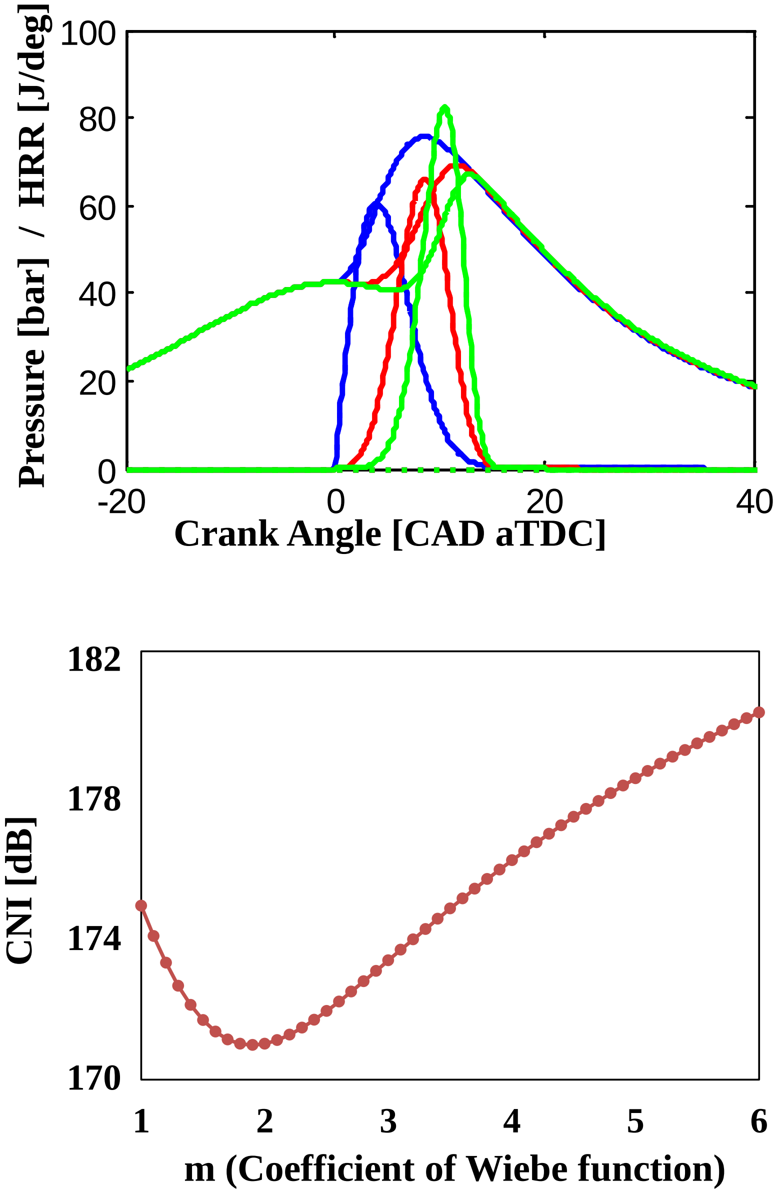

Figure 3.4 Effects of ‘m’ on combustion noise index

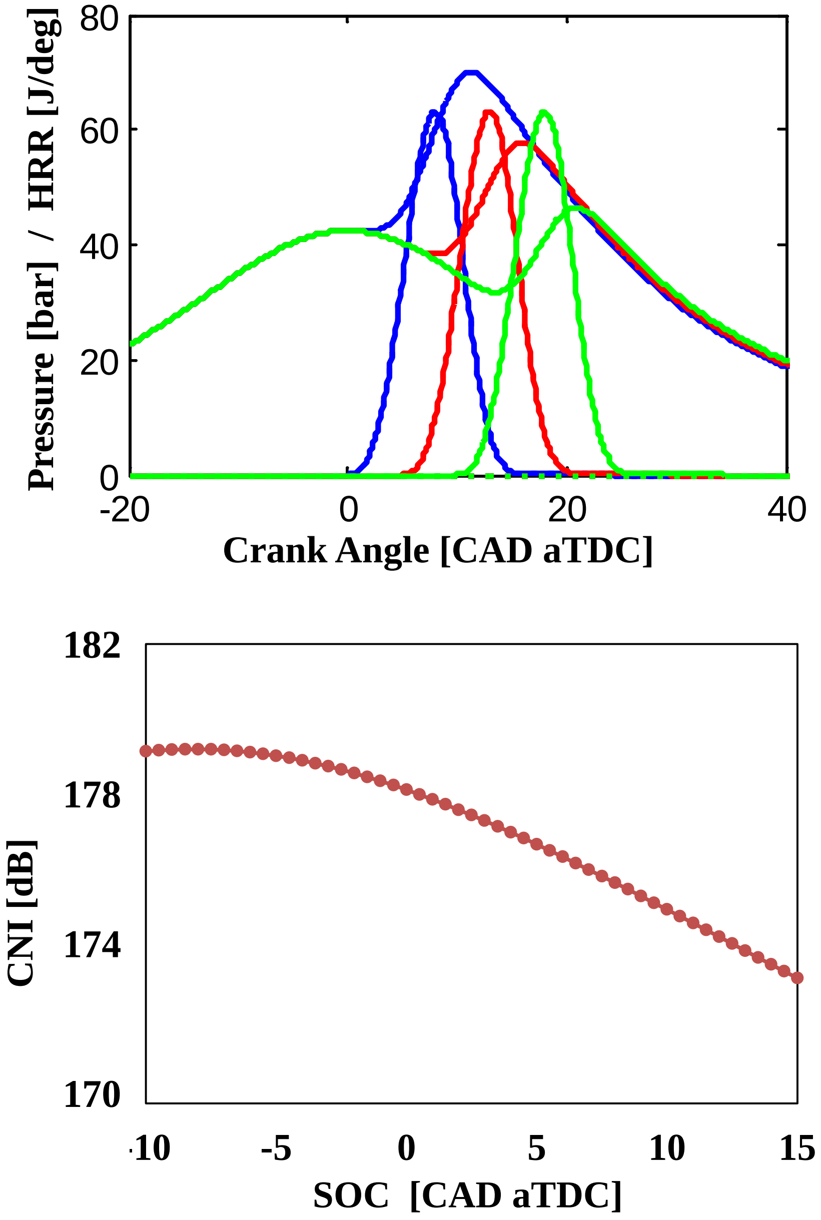

Figure 3.5 Effects of SOC on combustion noise index

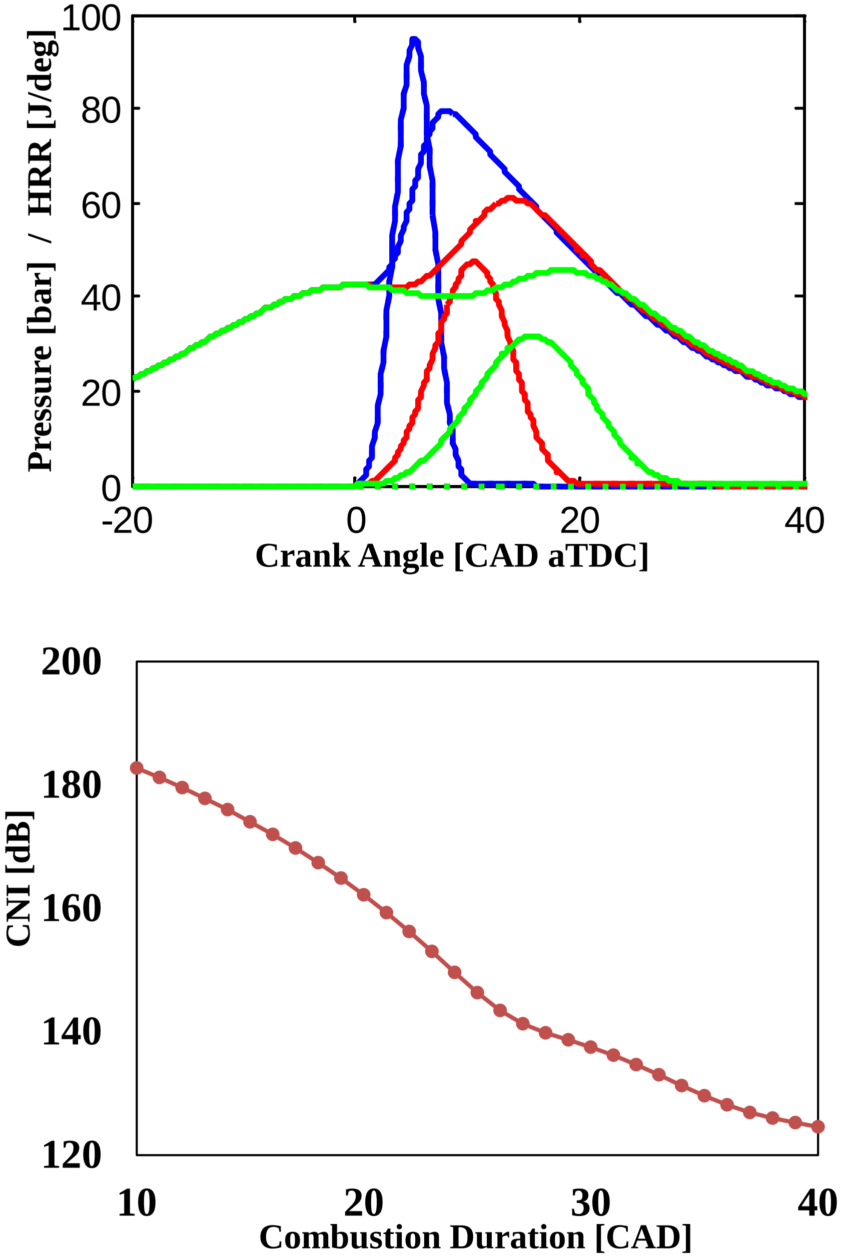

Figure 3.6 Effects of combustion duration on combustion noise index

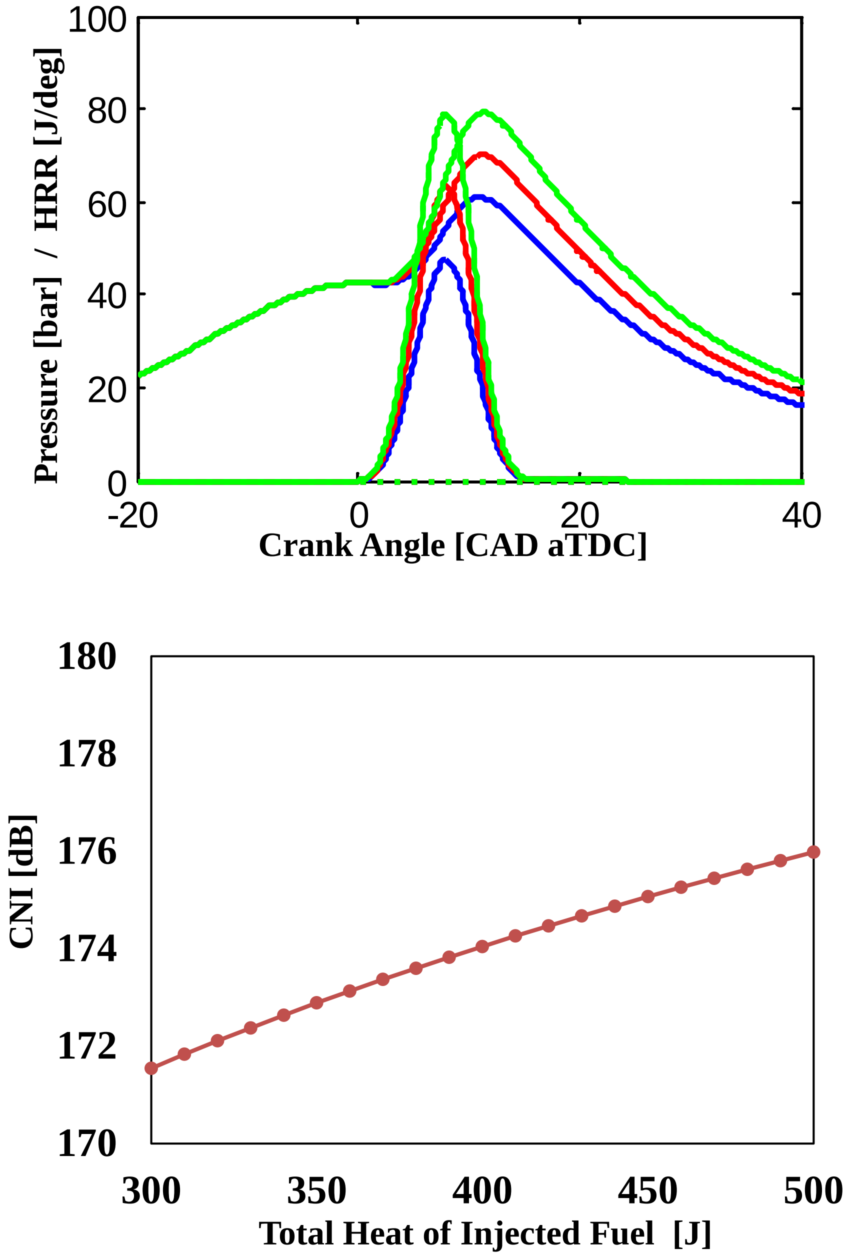

Figure 3.7 Effects of released heat on combustion noise index

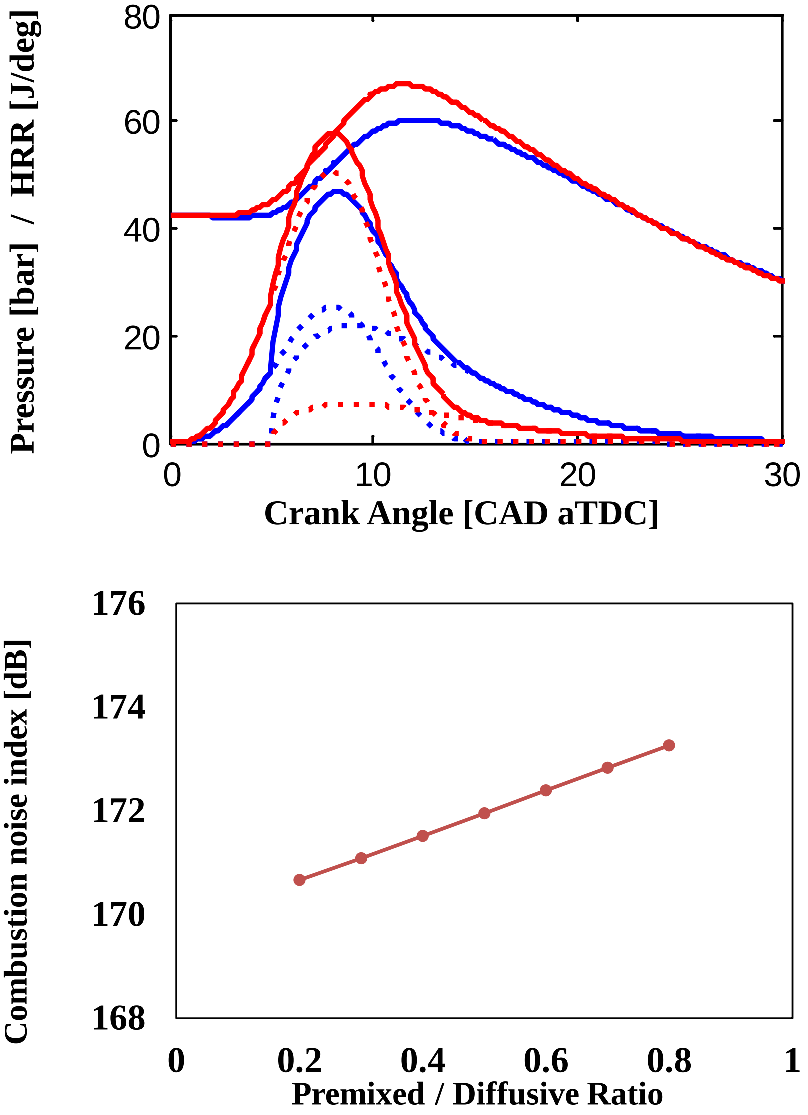

Figure 3.8 Effect of ratio of premixed and diffusive combustion

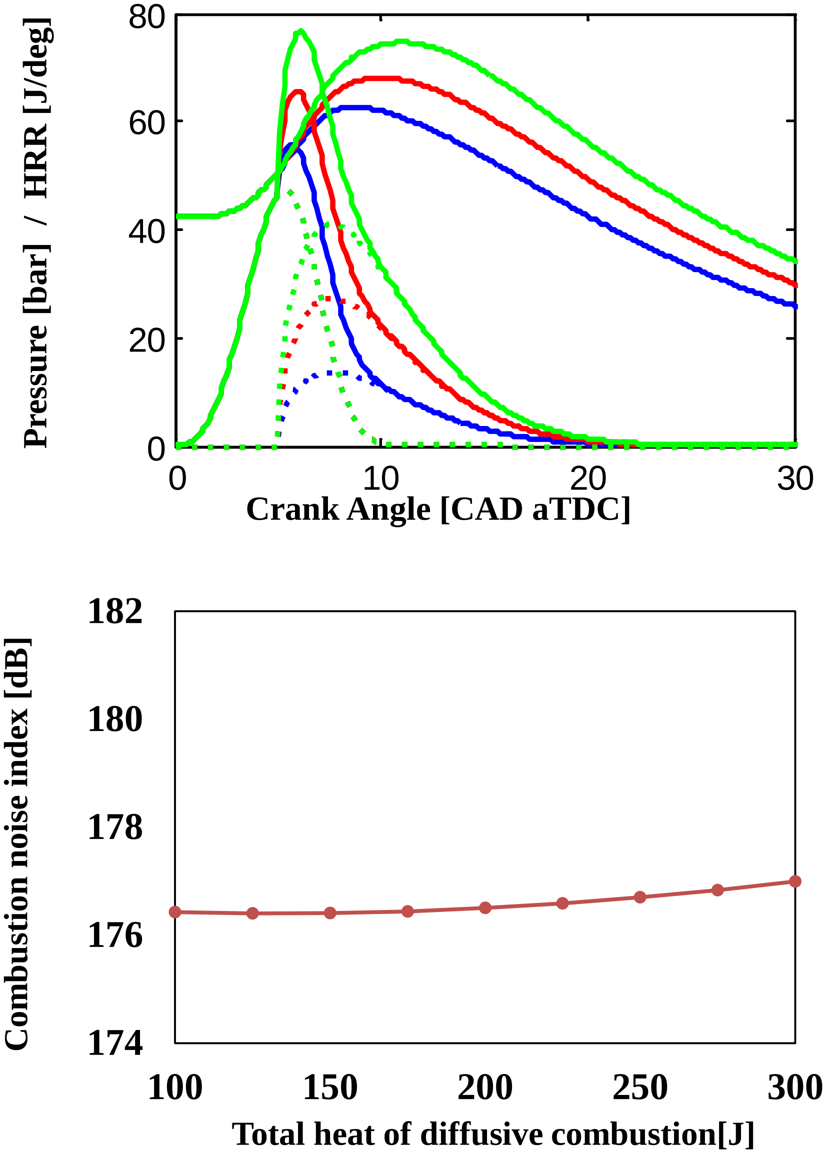

Figure 3.9 Effects of pilot injection quantity

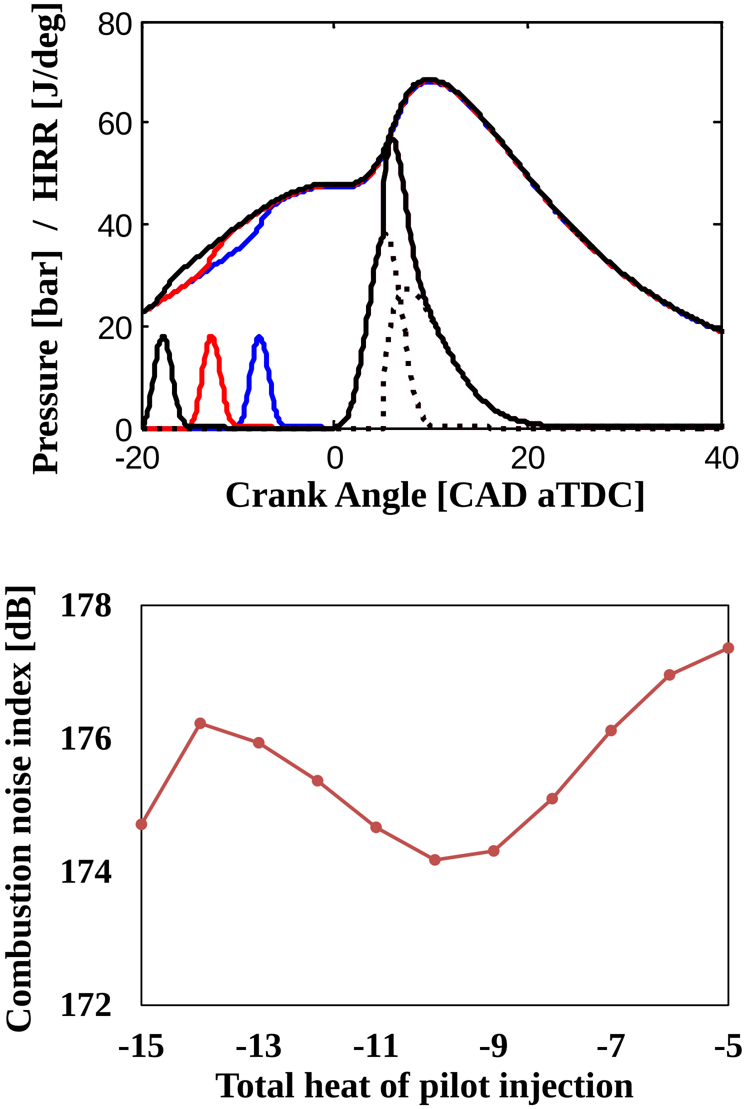

Figure 3.10 Effects of SOC of pilot injection

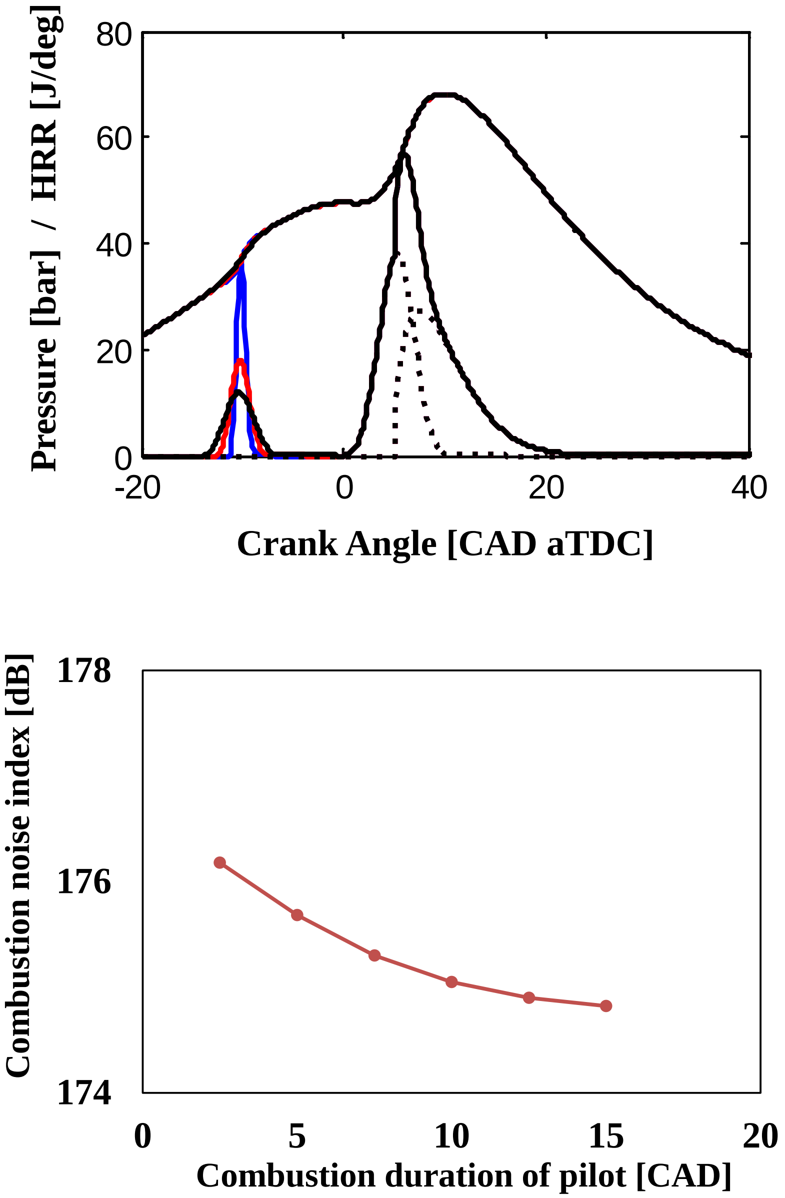

Figure 3.11 Effects of combustion duration of pilot injection

3.3 Optimization of heat release rate shape to reduce combustion noise

3.3.1 Optimization of heat release rate shape to minimize CNI using Wiebe functions

In the previous chapter, the effects of heat release rate shape changing the coefficients of Wiebe functions were described. In this chapter, the optimal shapes to minimize the CNI are investigated. The diesel combustion was simulated using three of Wiebe functions. The one Wiebe function had five coefficients. Thus, fifteen coefficients had to be optimized. The coefficients are constrained by boundary conditions, because unconstrained variables could cause unrealistic shapes. The boundary conditions were determined through experimental results. ʹm_premixed’ was varied from 2.44 to 5, ‘m_mixing’ from 0.4 to 0.8 and m_late’was not significantly varied; however, the variation was just about 1. ‘θ_(premixed,duration)’ was varied from 11.9 to 14.5, ‘θ_(premixed,duration)’ from 25.8 to 29.2 and ‘θ_(late,duration)’ from 62.2 to 70. 91. The boundary is shown in Tables 3.4~3.6. In addition, the system, which have 15 coefficients, has many local optimum points. The starting point can affect the optimum values. Thus, optimum points were determined from the seven of the starting points, then, the final optimum value, which has a minimum CNI level, was determined. The optimization was using ‘fmincon’ which is a optimization function of matlab. The optimization is conducted when engine speed is 1500 rpm and total released heat is 480 J.

3.3.2 Optimized shapes of heat release rate for minimum CNI

The boundary conditions were set as shown in table 3.4. Figure 3.12 shows the heat release rate, pressure curve and results of 1/3 octave band analysis. The determined values of variables were close to the boundary conditions. That means that optimum shape for the reduction of combustion noise was determined when the burning rate was slow and the duration is long and the SOC was retarded. These were already known as ways to reduce combustion noise.

To find new shape, constraint of the SOC was remove. The boundary conditions are shown in table 3.5. The other results are shown in figure 3.13. The start of combustion of figure 3.13 was 20° BTDC CAD. The combustion duration of diffusive combustion was not on the boundary. The duration became short than first optimization, however, the CNI decreased by 8 dB. The premixed phase and diffusive phase were much close and they made a smooth curve. It was observed that one Wiebe function has a long combustion duration.

However, it is impossible that the start of combustion is 20° BTDC CAD in conventional diesel combustion. To find more realistic heat release shape, the SOC was fixed by TDC and the premixed fuel ratio was constrained by 20%. The boundary conditions are shown as table 3.6, and the results are shown in figure 3.14. The CNI was 144 dB which decreased by 19 dB. It was a significant change. It is important for the reduction of combustion noise that the heat release rate being a smooth continuous curve.

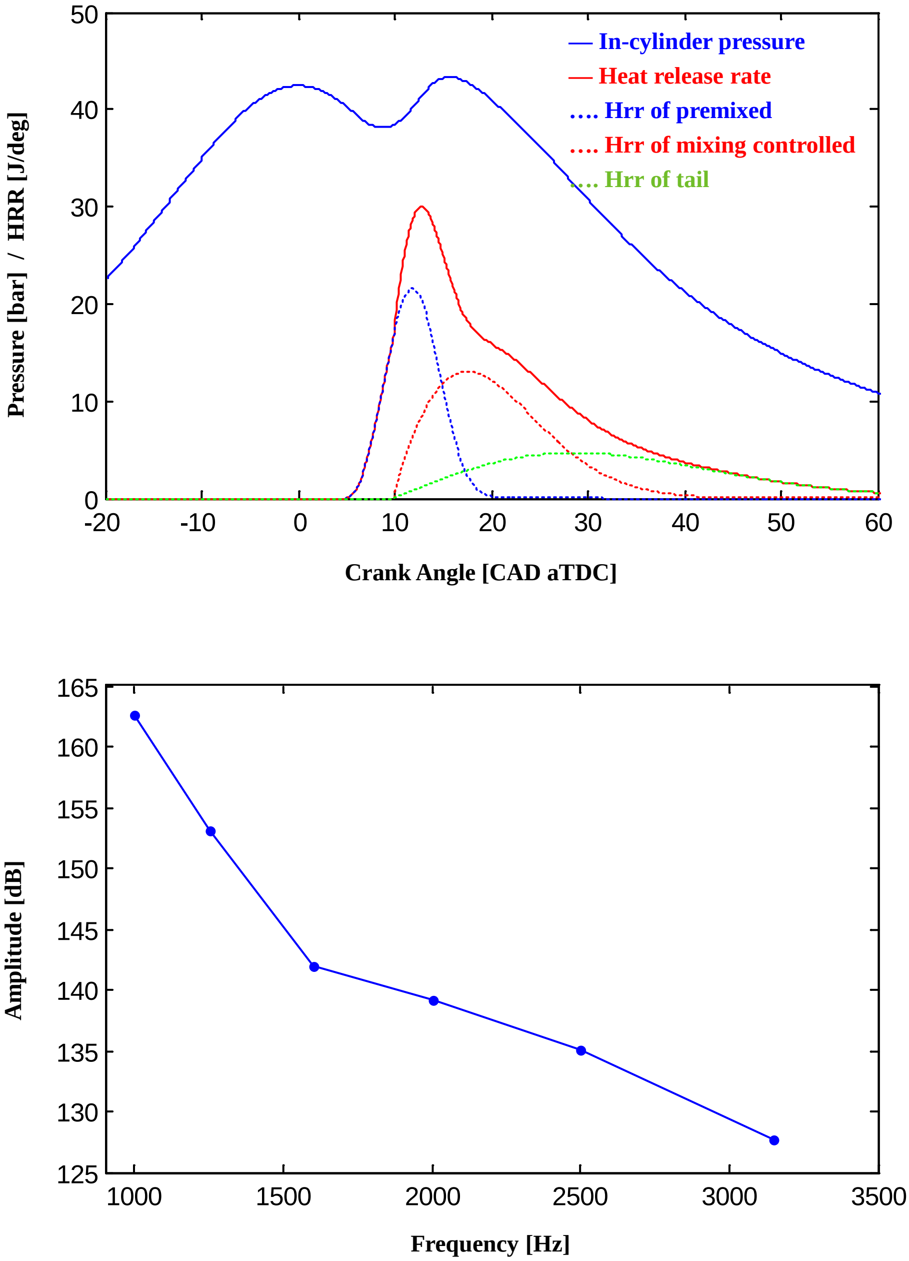

Figure 3.12 Optimal shape of heat release and pressure curve, 1/3 octave band (1)

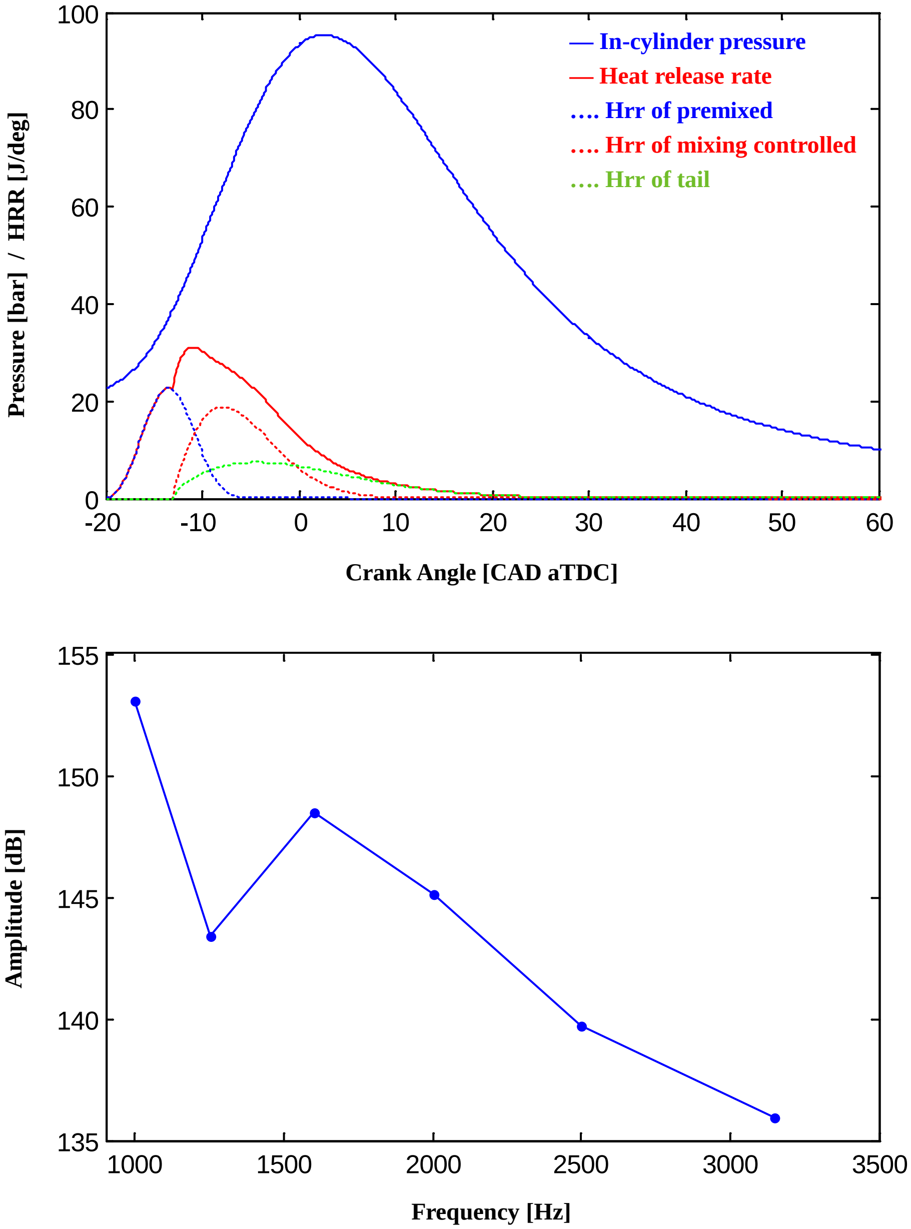

Figure 3.13 Optimal shape of heat release and pressure curve, 1/3 octave band (2)

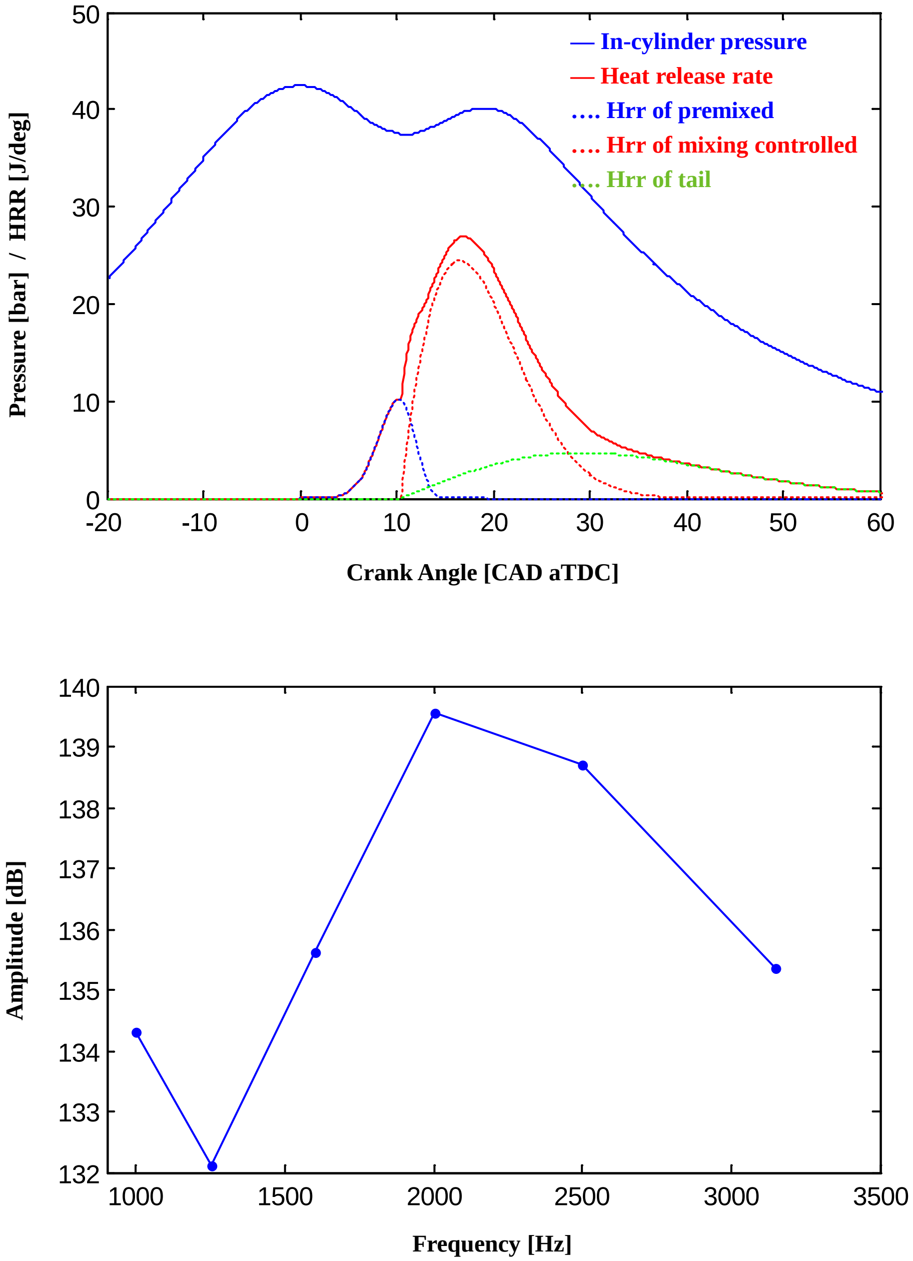

Figure 3.14 Optimal shape of heat release and pressure curve, 1/3 octave band (3)

Table 3.4 Boundary conditions and optimal values of variables (1)

		Coefficients of Wiebe function						CNI
		a	m	SOC	Duration	Q	Q ratio	
Premixed	Low	7	2	-5	5	480	0.1	163.11
	Upper	7	5	5	15	480	0.4	
	Optimum	7	2	5	15	480	0.3	
Diffusion	Low	7	0.4	-5	20	480	0.1	
	Upper	7	0.8	20	60	480	0.4	
	Optimum	7	0.8	10	35	480	0.4	
Tail	Low	7	0.4	-5	40	480	-	
	Upper	7	1	20	70	480	-	
	Optimum	7	1	10	70	480	-	

Table 3.5 Boundary conditions and optimal values of variables (2)

		Coefficients of Wiebe function						CNI
		a	m	SOC	Duration	Q	Q ratio	
Premixed	Low	7	2	-20	5	480	0.1	155.35
	Upper	7	5	5	15	480	0.4	
	Optimum	7	2	-20	14.3	480	0.3	
Diffusion	Low	7	0.4	-20	20	480	0.1	
	Upper	7	0.8	20	60	480	0.4	
	Optimum	7	0.8	-13	24.27	480	0.4	
Tail	Low	7	0.4	-5	40	480	-	
	Upper	7	1	20	70	480	-	
	Optimum	7	0.7	-13	48.5	480	-	

Table 3.6 Boundary conditions and optimal values of variables (3)

		Coefficients of Wiebe function						CNI
		a	m	SOC	Duration	Q	Q ratio	
Premixed	Low	7	3.5	0	5	480	0.1	144.5
	Upper	7	5	0	15	480	0.2	
	Optimum	7	5	0	14.6	480	0.1	
Diffusion	Low	7	0.4	0	20	480	0.1	
	Upper	7	0.8	15	60	480	0.8	
	Optimum	7	0.8	10	27.9	480	0.6	
Tail	Low	7	0.4	-20	40	480	-	
	Upper	7	1	20	70	480	-	
	Optimum	7	1	10.6	70	480	-	

Chapter 4. Injection strategies to reduce combustion noise

4.1 Variation of heat release rate shape according to change of injection strategies via experiment

The CNI variation was investigated when the injection strategies were changed. Injection parameters, which can affect the shape of heat release rate, were SOI, injection pressure, Swirl ratio and EGR rate. Three level of each parameter was compared. The engine speed was 1500 rpm and fuel injection quantity was 13.5mg. In addition, to consider emissions, NO and PM were measured together. The CNI was calculated by using in-cylinder pressure.

4.1.1 Main injection timing

The main injection timings were changed from 3° BTDC CAD to -3° BTDC CAD. When the injection was advanced, the peak of heat release rate decreased. The CNI also decreased. It was because the atmosphere temperature increased when the SOI was advanced. Thus, the ignition delay became short and the fuel quantity of the premixed combustion decreased. At that time, the NO emission increased because the flame temperature increased. The PM emission was also increased because the time to be mixed with air was not sufficient. Figures 4.1 and 4.2 show the in-cylinder pressure, heat release rate and the emissions when the SOI was changed.

4.1.2 Injection pressure

The injection pressures were increased and decreased by 100 bar (figure 4.3). The peak of heat release rate were high when the pressure increased. It was because the mixing of air and fuel was enhanced and more burned fuel in premixed combustion phase. The CNI were also increased. When the injection pressure was low, the PM more produced because the mixing was not enough. The NO decreased because when the pressure decreased, the combustion phase was retarded (figure 4.4).

4.1.3 Swirl rate

The swirl ratio was not measured. The relative intensities of swirl were guessed by the swirl valve openness. The swirl valve were 5%, 20% and 55 %. When the swirl valve is closed, swirl ratio increases. More burned fuel in premixed combustion phase with high swirl ratio because the higher swirl ratio enhances the mixing of air and fuel. The NO increase and PM decrease shown in figures 4.5 and 4.6.

4.1.4 EGR rate

The EGR rate was changed by 5% . When the EGR rate was increased, the peak of heat release rate also became high. It is because the higher EGR rate makes the ignition delay longer. The NO was very sensitive to the EGR rate. When the EGR rate increased 5%, the NOx decreased by 50 %. When the EGR rate increased, the increase in ignition delay allowed time for the fuel and air to mix, thus more fuel was burned in the premixed combustion phase. Therefore, a higher level of EGR rate made the peak of the heat release rate even higher (figure 4.7 and 4.8).

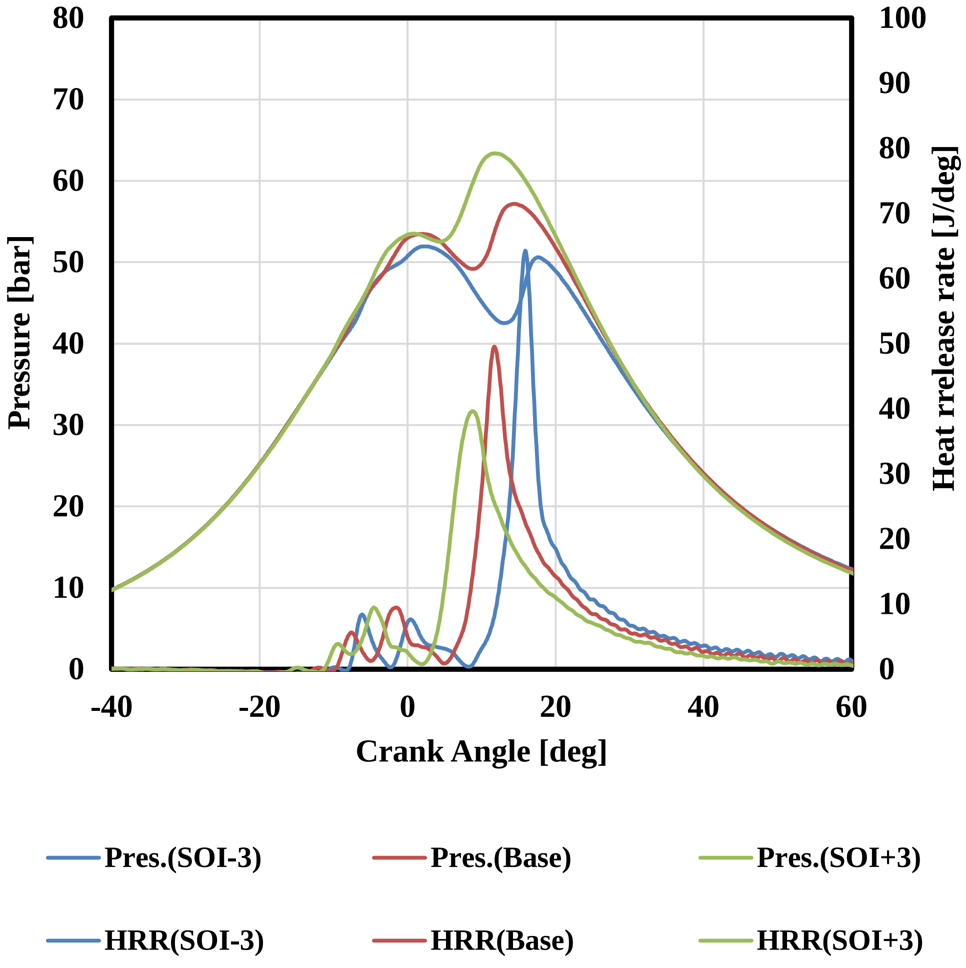

Figure 4.1 Heat release rate & in-cylinder pressure according to SOI change

(Engine speed: 1500 rpm / fuel mass: 15 mg)

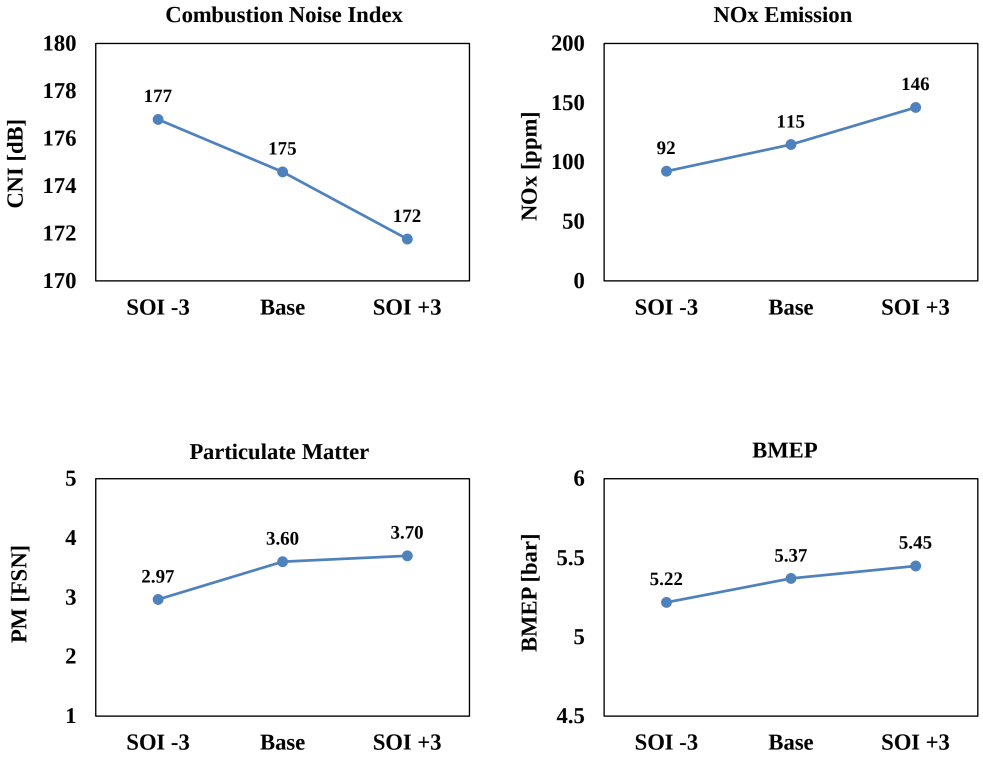

Figure 4.2 CNI, PM, NO and BEMP variation according to SOI change

(Engine speed: 1500 rpm / fuel mass: 15 mg)

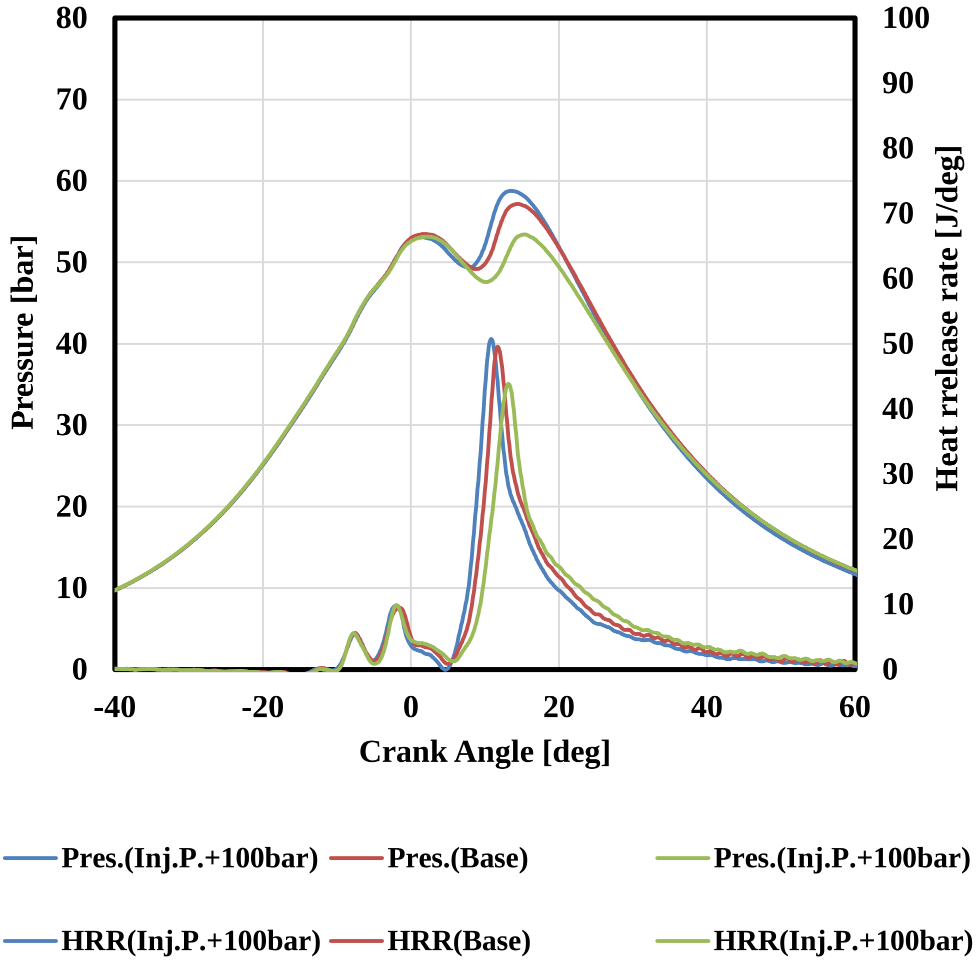

Figure 4.3 Heat release rate & in-cylinder pressure according to injection pressure change (Engine speed: 1500 rpm / fuel mass: 15 mg)

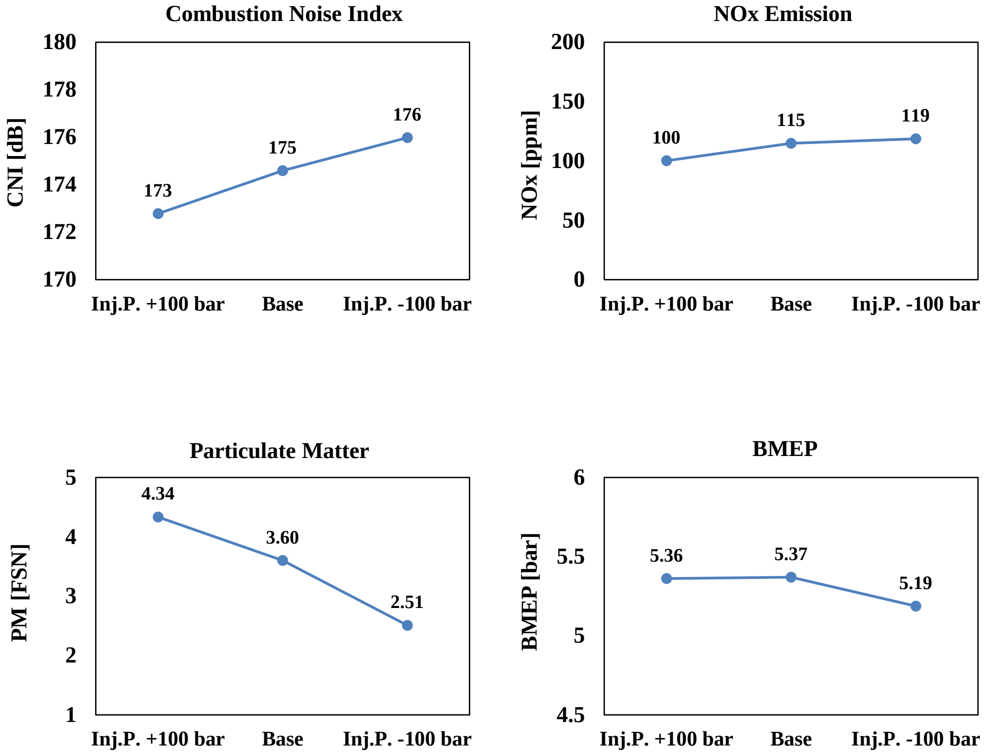

Figure 4.4 CNI, PM, NO and BEMP variation according to injection pressure change (Engine speed: 1500 rpm / fuel mass: 15 mg)

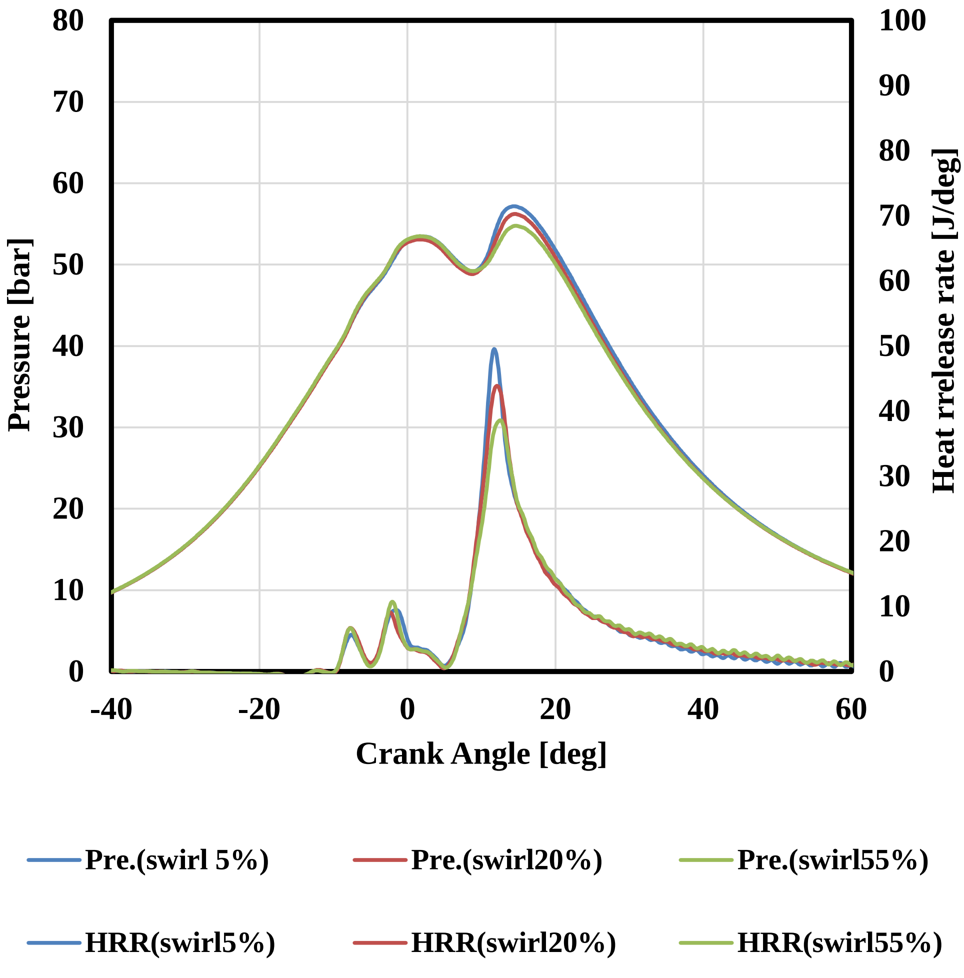

Figure 4.5 Heat release rate & in-cylinder pressure according to swirl valve open rate change (Engine speed: 1500 rpm / fuel mass: 15 mg)

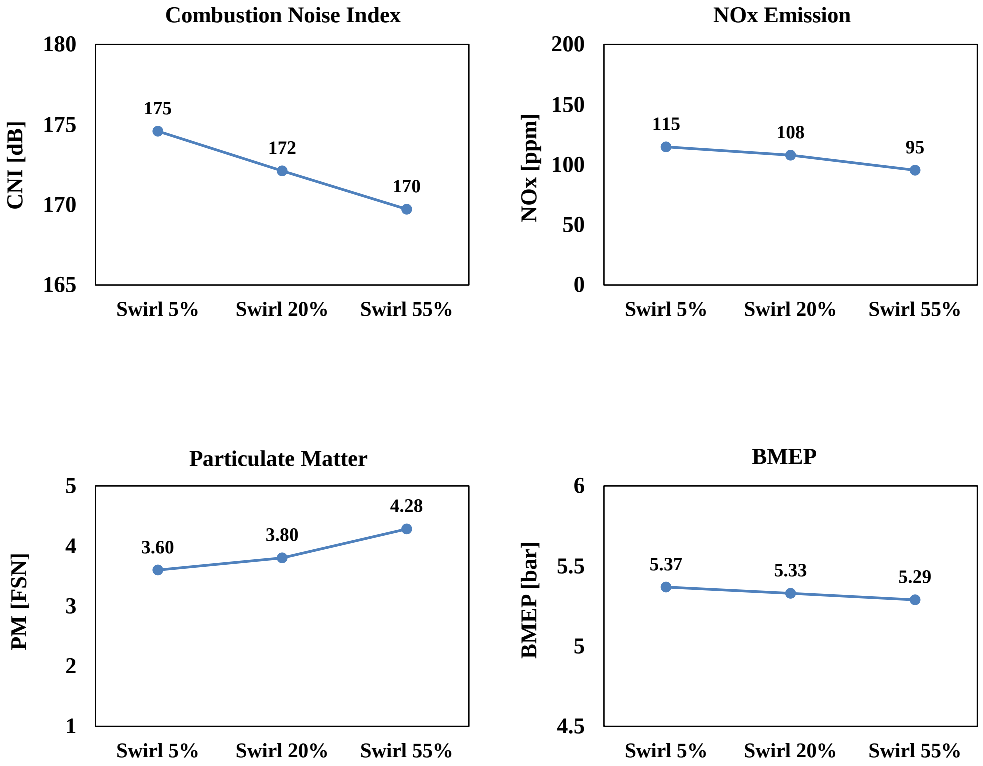

Figure 4.6 CNI, PM, NO and BEMP variation according to swirl open rate change

(Engine speed: 1500 rpm / fuel mass: 15 mg)

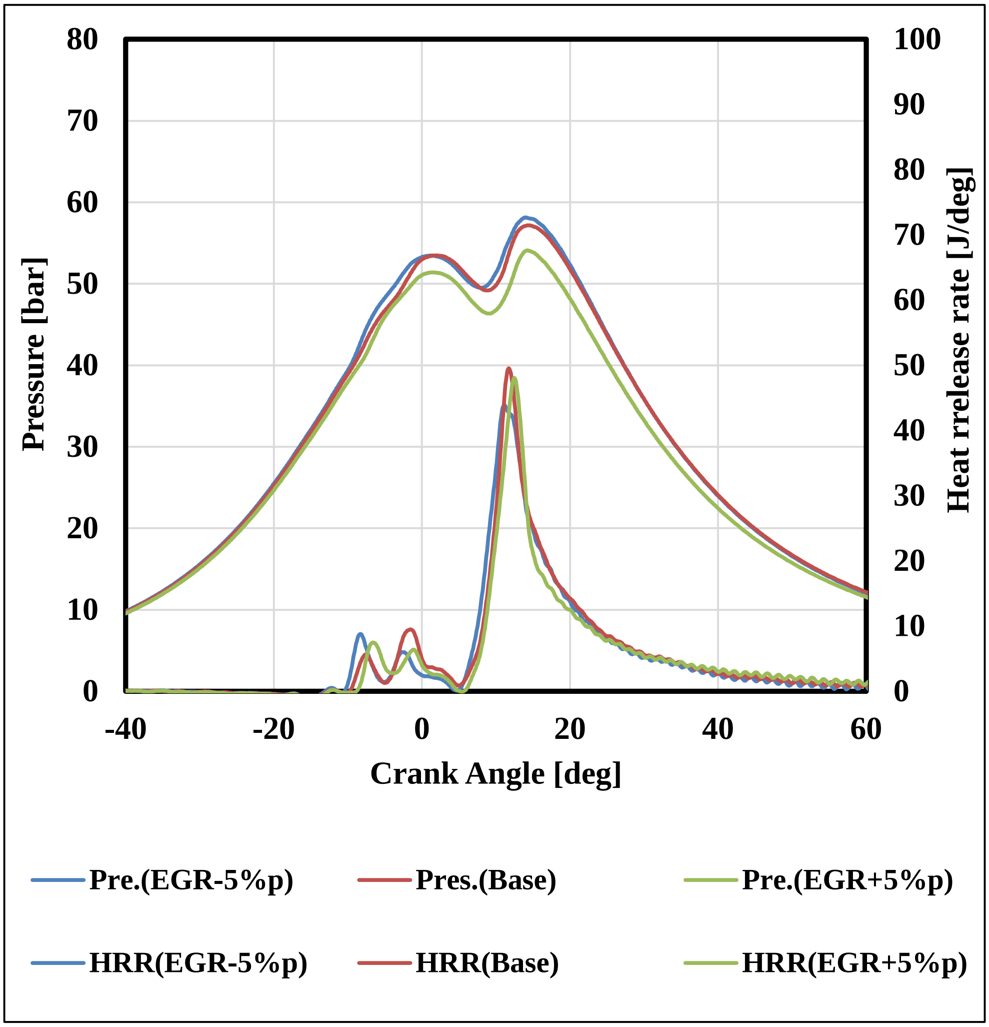

Figure 4.7 Heat release rate & in-cylinder pressure according to EGR rate change

(Engine speed: 1500 rpm / fuel mass: 15 mg)

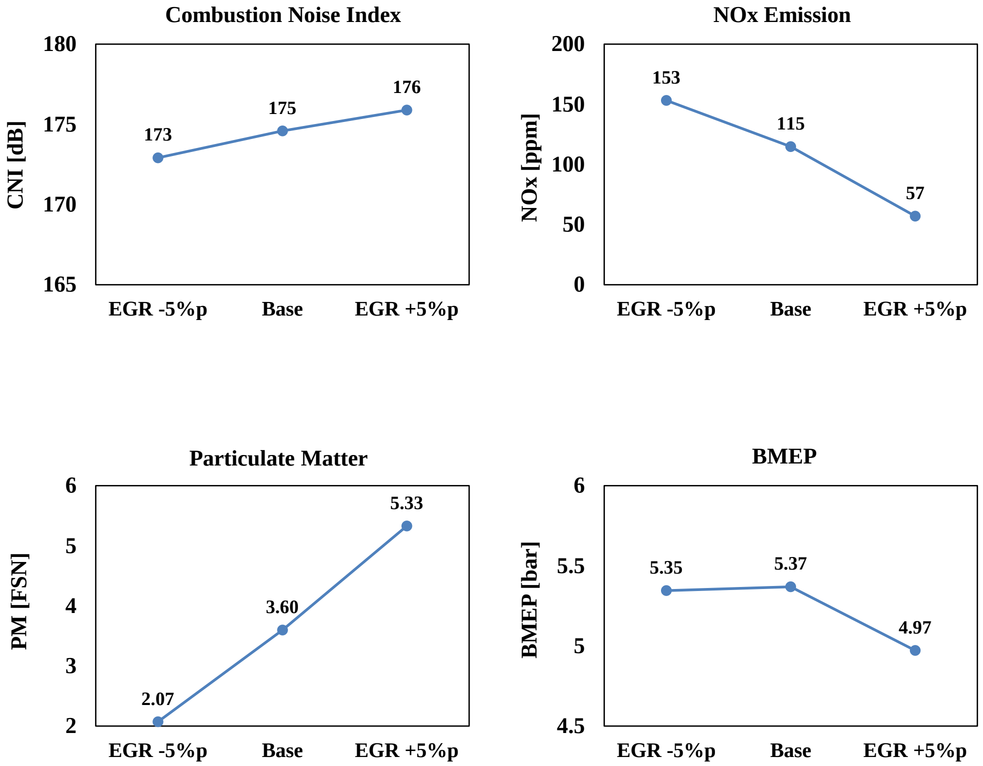

Figure 4.8 CNI, PM, NO and BEMP variation according to EGR rate change

(Engine speed: 1500 rpm / fuel mass: 15 mg)

4.2 Early pilot injection strategy to reduce combustion noise

4.2.1 Limitation of conventional diesel combustion

The conventional fuel injection strategies include pilot injection which is the injection of a little fuel before the main injection. The pilot injection increases the in-cylinder gas temperature and pressure when fuel was mainly injected. Thus, the ignition delay was decreased and the fuel of the main injection was burned smoothly. Moreover, some of the total fuel were already burned, the fuel of the main injection reduced for same IMEP. The pilot injection was very effective to reduce combustion noise. However, more fuel quantity of pilot injection was achievable to increase the soot formation and the combustion noise caused by the pilot burning itself.

4.2.2 PCCI combustion of diesel

The low temperature combustion has been studied as a way to reduce NOx and soot formation simultaneously. The PCCI is an injection strategy for them. In the PCCI, the fuel was injected before TDC (usually before 30° BTDC CAD), then, was mixed with air for much longer time before the ignition. The well-mixed fuel and air make premixed mixture; most of fuel was burned as a premixed combustion after the long ignition delay. Since, the flame temperature are low, less NOx was produced. Moreover, the amount soot was reduced because the fuel and air were mixed well without the fuel rich region, which can enhance the PM formation. However, the PCCI combustion had a short burning duration, and caused the rapid pressure rise which made a louder combustion noise. Moreover, The HC emission increased and the control of ignition timing was difficult. Thus, PCCI was not used in the manufactured vehicles. [47-49]

4.2.3 Early pilot injection combustion

The pilot injection starts at 10~20° BTDC CAD in traditional diesel engine injection. However, in early pilot injection, the fuel is injected before 30° BTDC CAD, thus the injected fuel has enough time to be mixed with air with longer ignition delay. While, the start of main injection is similar to that of the traditional injection. The fuel of pilot injection is combusted by PCCI and fuel of the main injection is burned by the diffusive combustion. In conventional injection strategies, the jet fuel of the main injection is formed around the burned pilot injection, because the pilot and the main injection are close, and local rich region appears. That is the reason why excessive pilot quantity increases the soot formation. The early pilot injection forms a well-mixed air-fuel mixture because it has a long ignition delay. It helps the main injection to be mixed with air, as a result, soot formation is reduced. Therefore, using the early pilot injection and smooth combustion are possible due to the short ignition delay of the main injection and the increased pilot injection quantity. [50-54]

The early pilot injection was tested at 1500 rpm and 13.5 mg of fuel. Figures 4.9 and 4.10 show heat release rates and octave analysis results of a conventional case and a PCCI case. When the early pilot injection was applied, the heat release of both the main injection and the pilot injection was smoother than that of the conventional case and the PCCI case. It leads to reduce the combustion excitation. The CNI deceased from 175 dB to 170 dB. All of frequency was reduced. At that time, the NOx, PM and indicated thermal efficiency (ITE) were equivalent to that of the conventional data.

When the pilot combustion and the main combustion were close, the CNI level was at the lowest as shown in chapter 3.3. However, the strategy was not possible via the traditional injection strategies because the closed split injection caused a lot of smoke. While, it could be possible using the early pilot injection. The heat release rate and frequency analysis results are shown in figure 4.11. Table 4.3 shows the emissions and ITE. The frequency under 1.5 kHz was dramatically reduced and PM was reduced too.

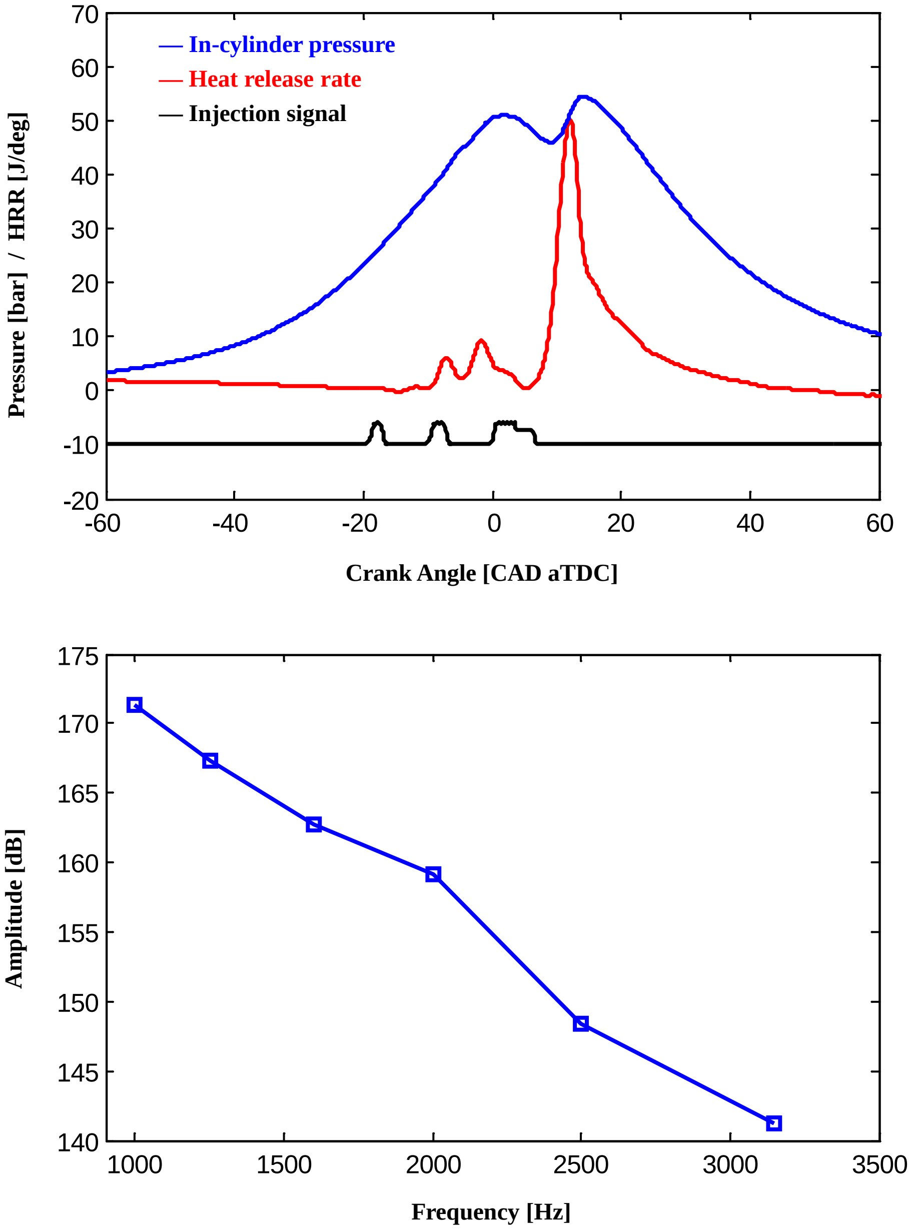

Figure 4.9 Heat release, pressure and 1/3 octave band results of conventional diesel combustion including pilot injections (Engine speed: 1500 rpm / fuel mass: 15 mg)

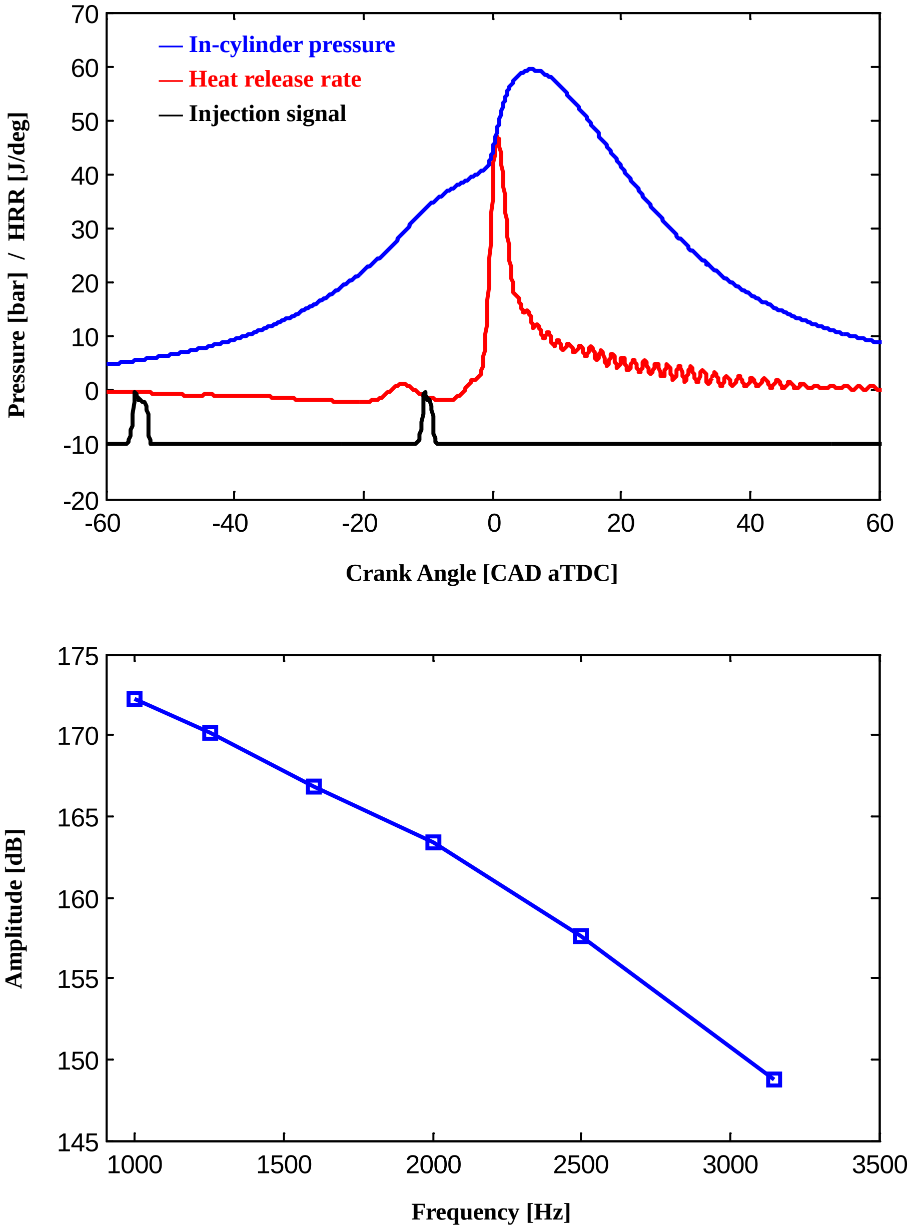

Figure 4.10 Heat release, pressure and 1/3 octave band results of PCCI combustion including pilot injections

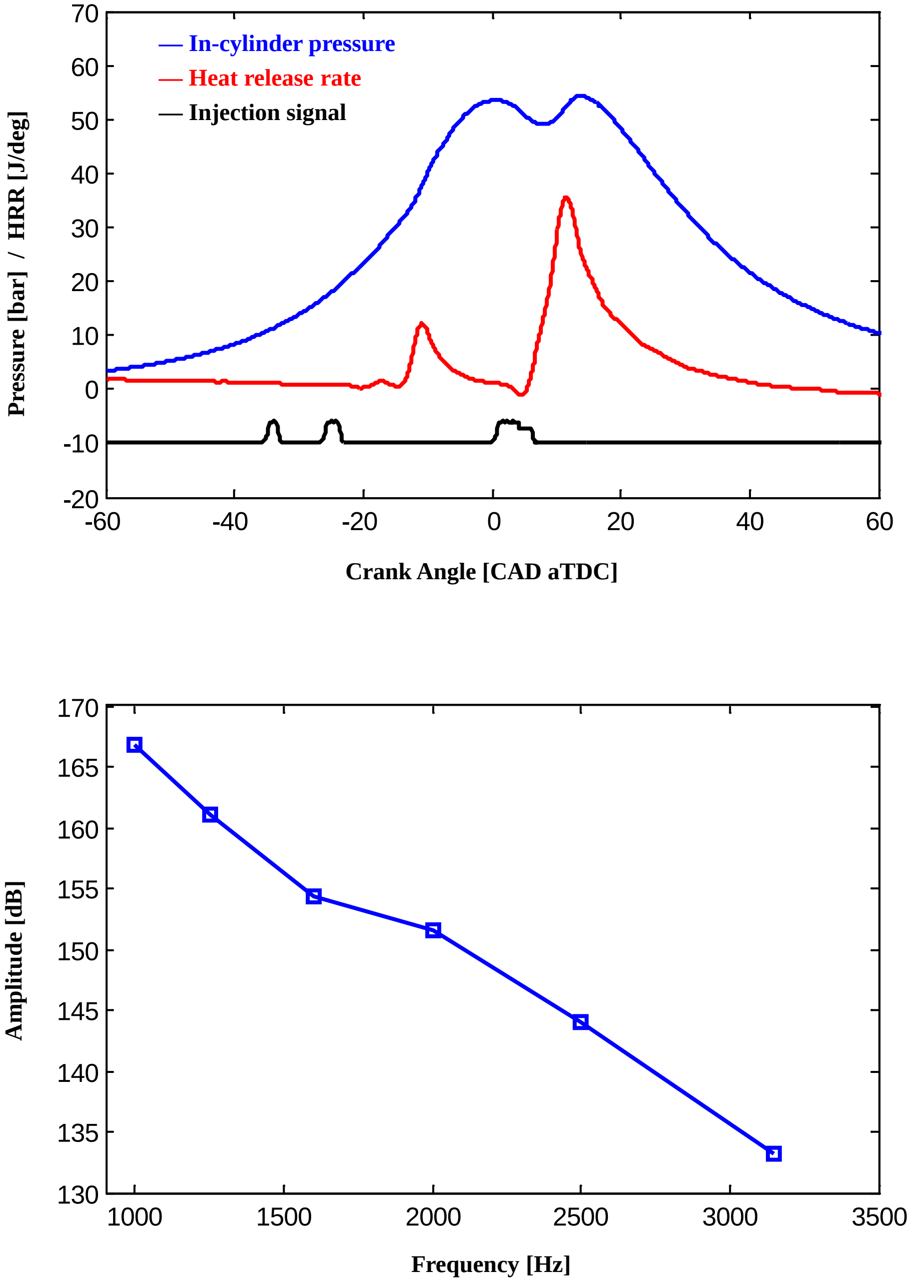

Figure 4.11 Heat release, pressure and 1/3 octave band results of early pilot injection

Table 4.1 Emissions, IMEP and CNI

Case description	NOx [ppm]	PM [FSN]	IMEP [bar]	CNI [dB]
Conventional Diesel	109.4	4.351	6.8	172.6
PCCI including pilot injections	68	0.183	4.9	175.4
Early pilot injection	101.4	4.19	6.78	168.7

Chapter 5. Closed loop control to reduce combustion noise

5.1 Characteristics of diesel engine noise according to EGR rate change during transient operation

In this study, the characteristics of diesel engine noise according to the EGR rate change during transient operation were investigated. A 1.6 liter diesel engine was used. The engine revolution speed and load were changed with a varied ramp time. In addition, this study examined transient operations with a constant engine speed and increased engine load. The EGR rate was measured by using fast response thermocouples during the transient operations. The combustion noise was evaluated via CNI calculation

5.1.1 EGR rate measurement

The EGR rate is usually calculated by measuring the concentration of carbon dioxide in intake and exhaust manifolds. The concentration of carbon dioxide is conventionally determined by the NDIR method, which usually is greater than the 1 second response time; this response time is too slow to measure the EGR rate during a transient engine operation

The methodology of evaluating the EGR rate using the temperature of intake manifold, the cooled air and the EGR gas was explained in the previous research [55]. The EGR rate can be calculated using equation (5.1) with the assumptions that the specific heat capacity of the air and the EGR are assumed to be equal and heat transfer is neglected.

$$EGR\,rate = \frac{m_{EGR}}{m_{EGR} + m_{air}} = \frac{T_{mixture} - T_{air}}{T_{EGR} - T_{air}} \tag{5.1}$$

The cooled EGR gas and air are mixed in the intake manifold; however, the mixture is not uniform because of the considerable temperature differences. Because the gases are temporarily stratified, heat transfer occurs between the EGR gas, the cooled air and the intake manifold. The EGR gas loses heat to the intake manifold while the air gains the heat. The heat transfer model was adopted to consider this phenomenon. [56]

If effects of heat transfer is taken into account,

$$\dot{H}_{mix} = \dot{H}_{air} + \dot{H}_{EGR} + \dot{Q}_{in} + \dot{Q}_{out} \tag{5.2}$$

$$c_p \dot{m}_{mix}(T_{mix,HT} - T_0) = c_p \dot{m}_{air}(T_{air} - T_0) + c_p \dot{m}_{EGR}(T_{EGR} - T_0) + hA_{air}(T_{wall} + T_{air}) - hA_{EGR}(T_{EGR} - T_{wall}) \tag{5.3}$$

$$T_{mix,HT} = (1 - EGRrate) \times T_{air} + EGRrate \times T_{EGR} + hA_{air}(T_{wall} - T_{air}) - hA_{EGR}(T_{EGR} - T_{wall}) \tag{5.4}$$

$$T_{mix,HT} = T_{mix,noHT} + \Delta T \tag{5.5}$$

$$\Delta T = \frac{h}{c_p \dot{m}_{mix}}[A_{air}(T_{wall} - T_{air}) - A_{EGR}(T_{EGR} - T_{wall})] \tag{5.6}$$

$$EGR\,rate = \frac{m_{EGR}}{m_{EGR} + m_{air}} = \frac{(T_{mixture} + \Delta T) - T_{air}}{T_{EGR} - T_{air}} \tag{5.7}$$

where H_{air}, H_{EGR} and H_{mix} are the enthalpies of the air, the EGR gas and the mixed gas, respectively. $c_{p,air}$, $c_{p,EGR}$ and $c_{p,mix}$ are the specific heat capacity at constant pressure of the air, the EGR gas and the mixed gas, respectively. Q_{in} is the heat that the air gains, and Q_{out} is the heat loss by the EGR gas. T_{air}, T_{EGR} and T_{mix} are measured values. The heat transfer coefficient of h is determined from the intake manifold, assumed to be a pipe. Nu and Re are obtained by considering the pressure, rpm and geometry of the intake manifold. ΔT is the temperature variation due to the heat transfer to the inner surface of the intake manifold. The EGR rate considering the heat transfer is represented as equation (5.7). The radiative heat transfer to the surrounding area is ignored.

The temperature of the air, the EGR gas and the intake manifold were measured using fast respond thermocouples which were made by 100 µm diameter R-type wires and exposed type. The response time is less than 0.05 seconds. The gastemperature was measured by NI- with a 100 Hz sampling rate. Figure 5.1 shows the positions of the thermocouples to measure the temperature of cooled air, the cooled EGR gas and the intake manifold. The EGR distribution to each cylinder is different because the mixture of EGR gas and air is not homogenous. To evaluate the EGR rate of the #1 cylinder, the temperature of the mixture was measured close to the cylinder. (figure 5.1). The EGR rate measured using thermocouples was verified with an exhaust gas analyzer (Horiba MEXA 7100 DEGR) at steady states.

5.1.2 Combustion noise according to the EGR rate variation

The combustion noise change according to the EGR rate variation was examined by using the CNI. The operating condition was 1750 rpm and the fuel injection quantities are 17.5 mg. The only EGR valve openness was changed and their EGR rates were 30%, 25% and 18%. Figure 5.2 shows the results and table 1 represents the maximum pressure, pressure rise, RoHR and CNI, respectively. The CNI was at the highest when the EGR rate was at 30%; the value reduced as the EGR rate decreased. The EGR rate affected the ignition delay. The ignition delay became longer when the oxygen concentration was lower. The high level EGR rate limited the concentration due to the dilution effect. The longer ignition delay caused the more fuel to be combusted in the premixed combustion phase, thus the RoHR peak and pressure rise become greater, which have a considerable effect on combustion noise.

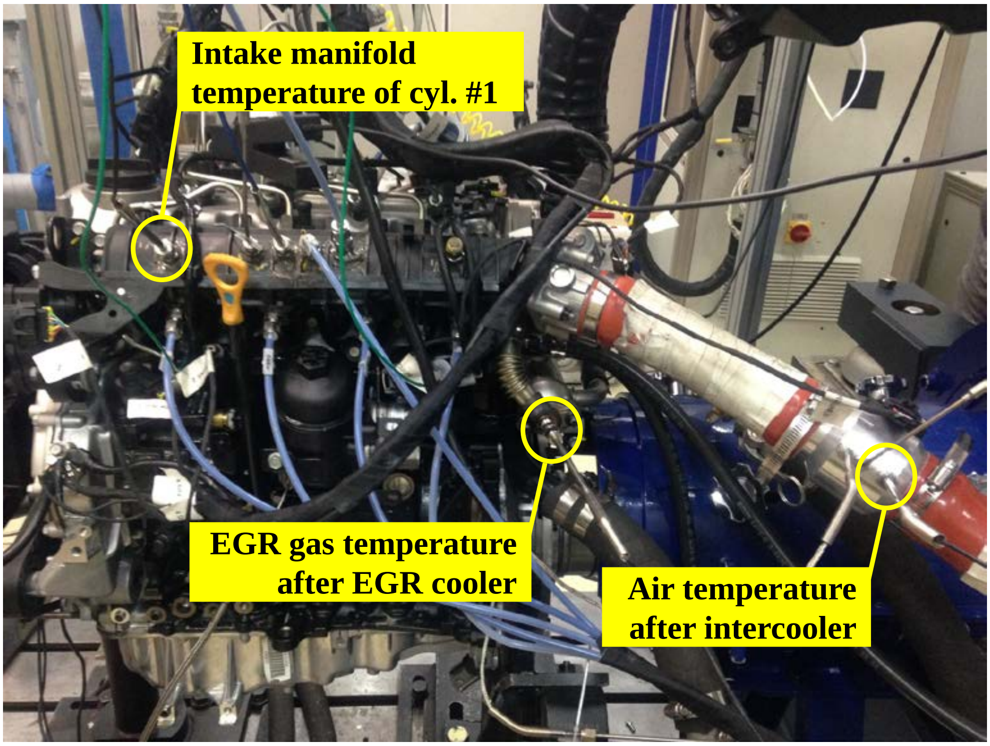
Intake manifold temperature of cyl. #1
EGR gas temperature after EGR cooler
Air temperature after intercooler

Figure 5.1 Thermocouples to measure the temperature of the air, the EGR gas and the intake manifold

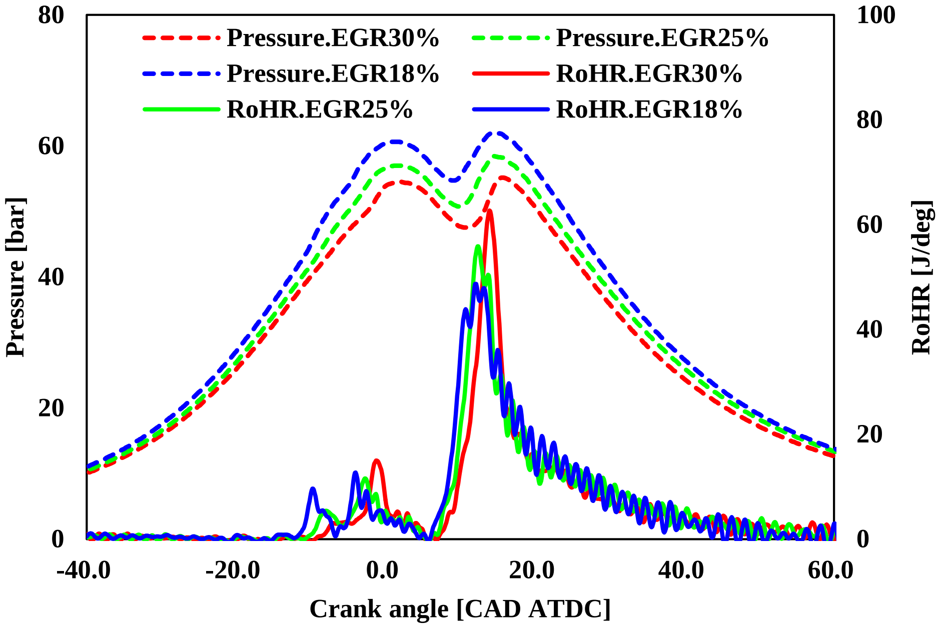

Figure 5.2 In-cylinder pressure and RoHR variation according to EGR rate change

5.1.3 CNI variation during transient operations

5.1.3.1 Transient operation 1. Speed and load change

The CNI was examined when the engine operating condition were changed to 1750 rpm and BMEP 8 bar from 1250 rpm and BMEP 2 bar while varying the ramp time to 2, 5, and 10 seconds. These operating conditions usually occur when a vehicle starts in the first or the second gear. The gear ratio is high and the engine speed rapidly increases. Figures 5.3~ 5.5 show the results. Moreover, to compare to the steady state, the constant engine speed and load states were examined per 100 rpm increase. The blue lines in the figures indicate transient operation results, and the red dots indicate the steady operation results. When the ramp time was shorter, the difference between the transient and the steady results of the CNI were greater; particularly when the engine speed was 1650 RPM and ramp time was 2 seconds, the CNI difference was at the greatest at 4 dB. The EGR rate was measured using the thermocouples. The EGR trends were very similar to that of the CNI. The difference of transient and steady state operations was larger, when the ramp time was shorter.

Figure 5.6 shows the in-cylinder pressure and the RoHR curves of a cycle during the transient operation with 2 seconds ramp time. The blue line shows transient operation and red line shows steady operation. Both were operated at the same engine speed and load, fuel injection quantity, 1650 rpm and 16.13 mg per cycle. The RoHR peak of transient operation was greater than at steady operation. This occured because of the EGR rate difference effect on ignition delay. The steady operation, which has lower EGR rate level, has a shorter ignition delay. As a result, less fuel is combusted in the premixed combustion phase, and the pressure curve is milder. The surplus EGR rate in the transient operation cause the rapid combustion, which lead to the CNI increase.

5.1.3.2 Transient operation 2. Constant speed and load change

The load was increased to 18 mg per cycle from 8 mg with a constant engine speed of1750 rpm. This condition usually occurs when a vehicle is accelerating in a high gear at high speed. Because the effective inertia of the vehicle in a high gear is much greater than a lower gear, the engine speed does not vary rapidly. The ramp times were varied to 1, 2, and 5 seconds. Steady operations were examined when the injected fuel quantities were 10 mg, 12 mg, 14 mg and 16 mg per cycle. Figures 5.7~5.9 show the results.

The CNI was calculated to evaluate the combustion noise. The difference in CNI between transient and steady state operation was the largest at 2 dB when the injection fuel was 16 mg. The EGR rate was measured by the thermocouples; when the fuel quantity changes during transient operation, the EGR rate was higher. When the fuel quantity was 16 mg, the largest EGR rate difference occurs. The higher EGR rate lengthened the ignition delay and raises the peak of the RoHR. Figure 10 shows the in-cylinder pressure and the RoHR curves of a cycle during the transient operation with 1 seconds ramp time. The surplus EGR which caused the sharp combustion lead to higher CNI level. This phenomenon is similar to the ones found in the transient operation.

Table 5.1 Maximum of pressure, pressure rise, RoHR and CNI according to EGR variation

EGR rate	Max. Pressure [bar]	Max. Pressure rise [bar/deg]	Max. RoHR [J/deg]	CNI [dB]
30%	55.2	3.11	62.7	178.2
25%	58.4	2.83	55.9	177.5
18%	61.9	2.50	48.7	176.1

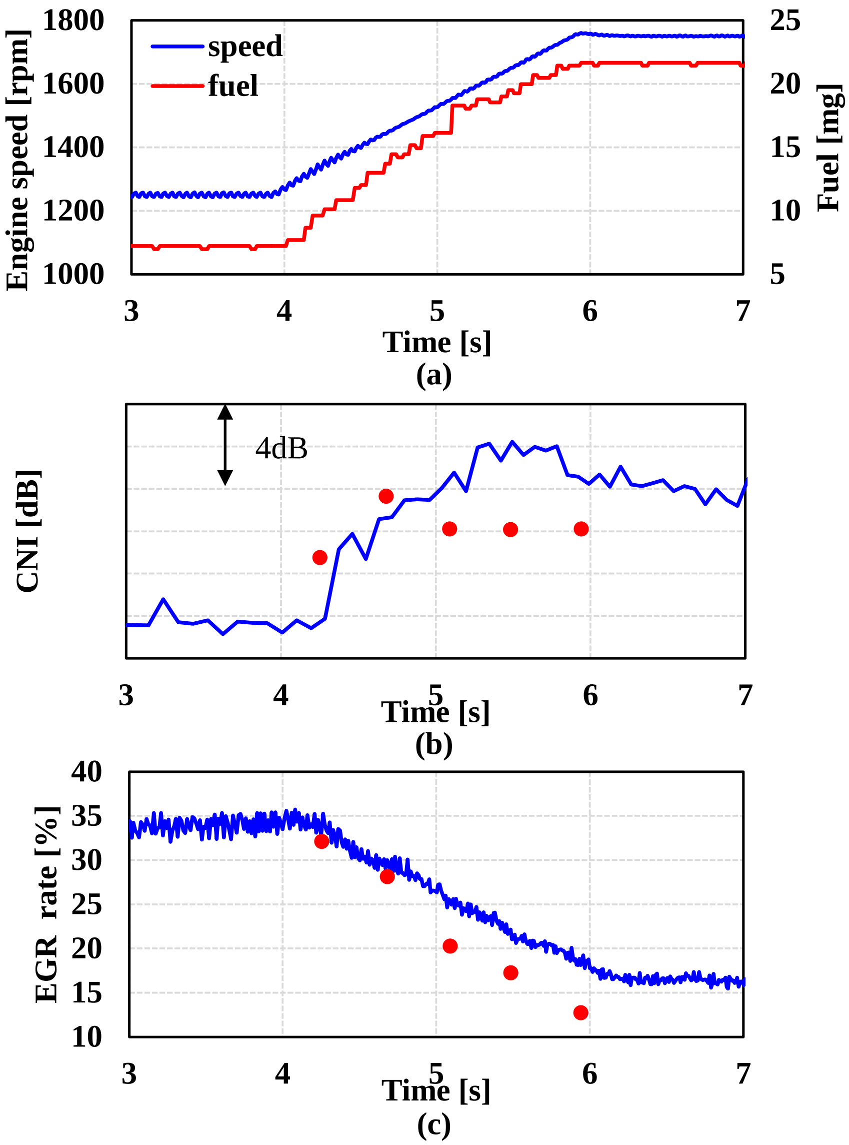

Figure 5.3 Results of speed and load transient operation, ramp time: 2 s (a) Engine speed, (b) CNI, (c) EGR rate

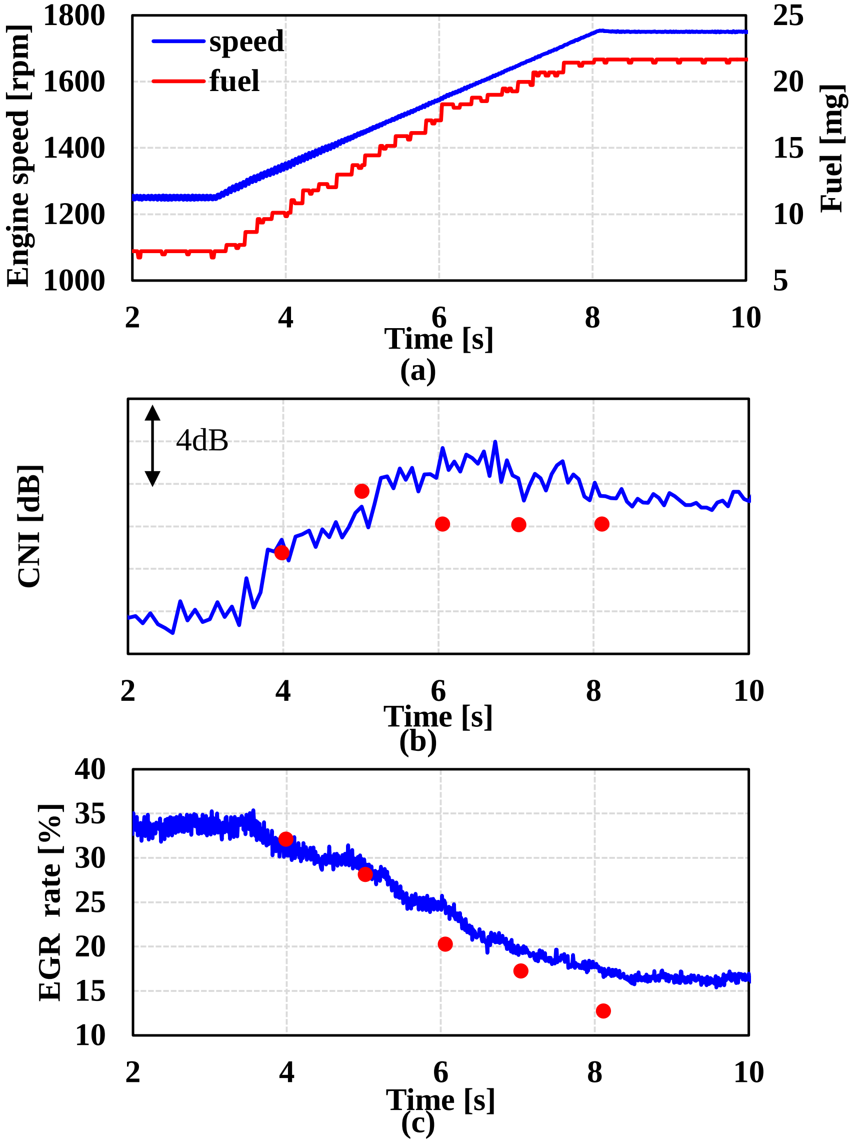

Figure 5.4 Results of speed and load transient operation, ramp time: 5 s

(a) Engine speed, (b) CNI, (c) EGR rate

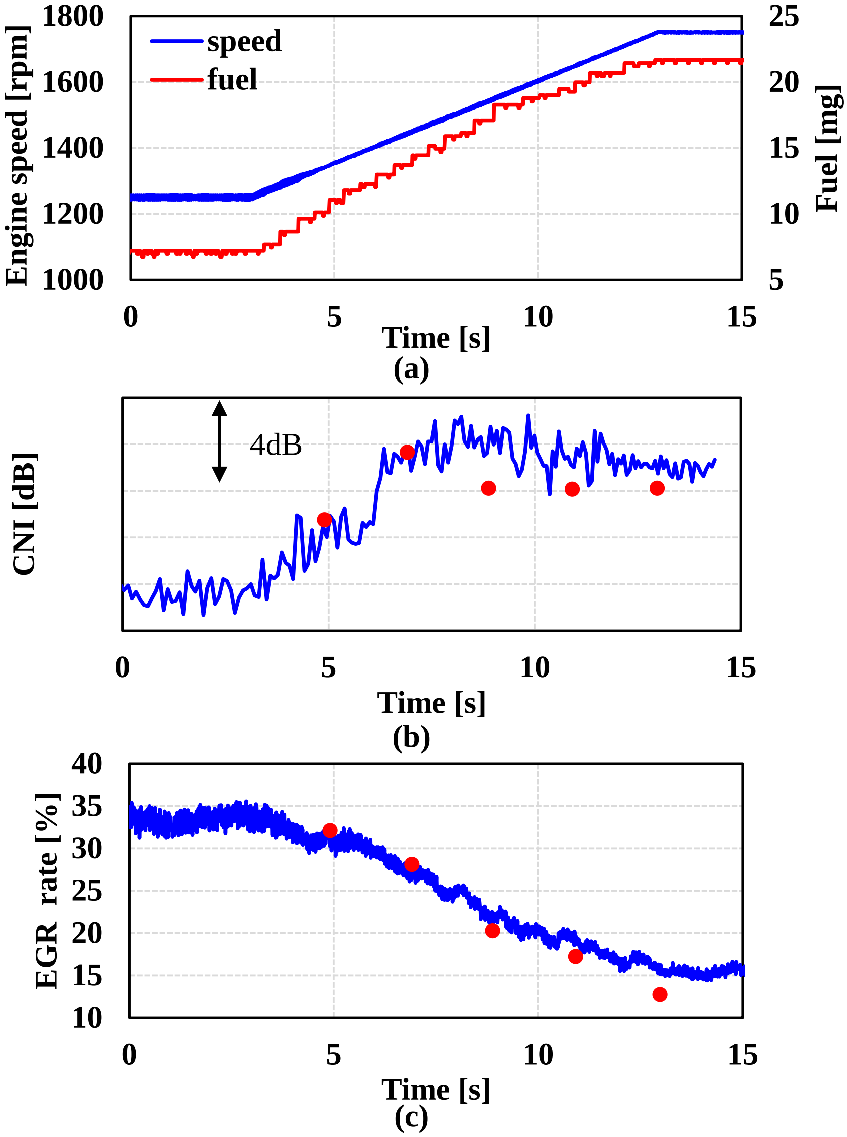

Figure 5.5 Results of speed and load transient operation, ramp time: 10 s

(a) Engine speed, (b) CNI, (c) EGR rate

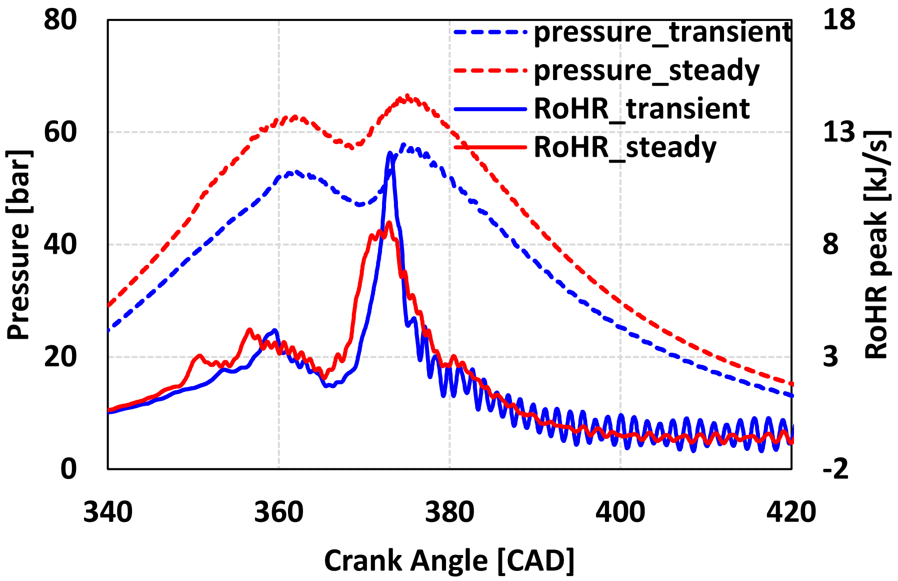

Figure 5.6 Comparison of pressure and RoHR between transient operation and steady state

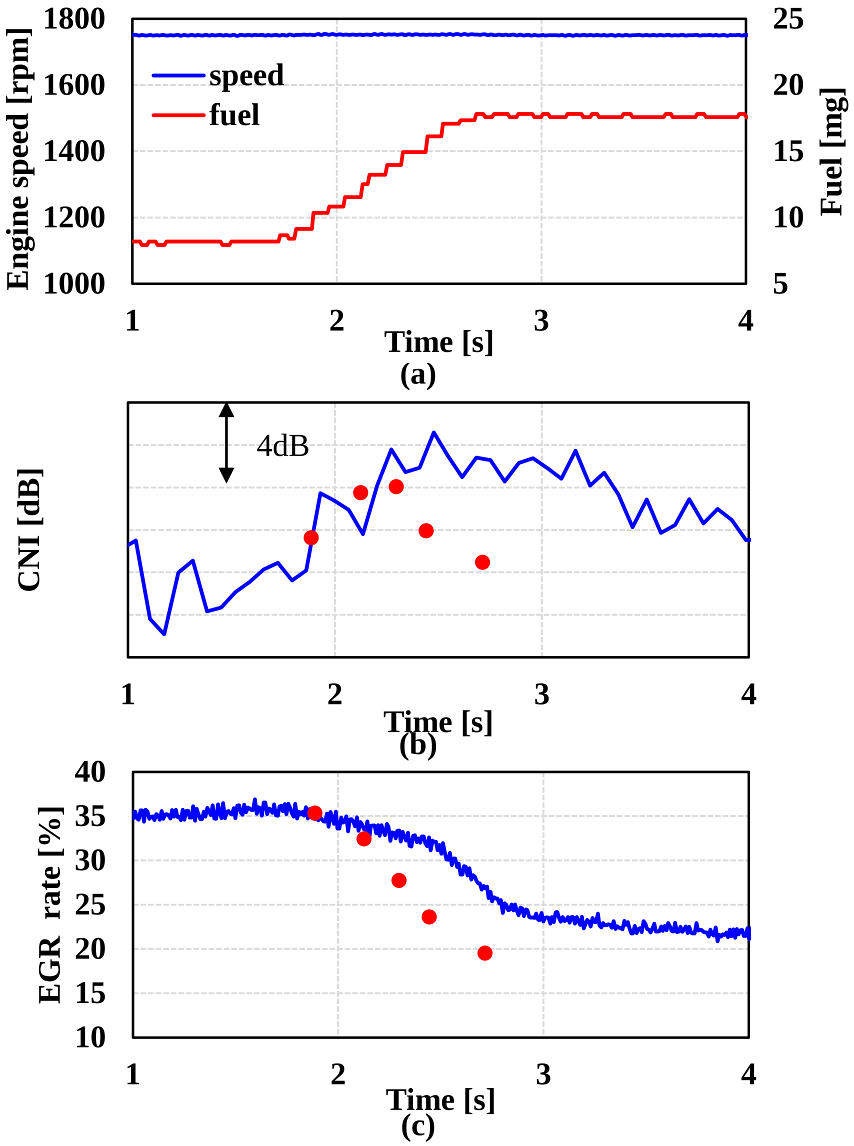

Figure 5.7 Results of load transient operation, ramp time: 1s (a) Engine speed, (b) CNI, (c) EGR rate

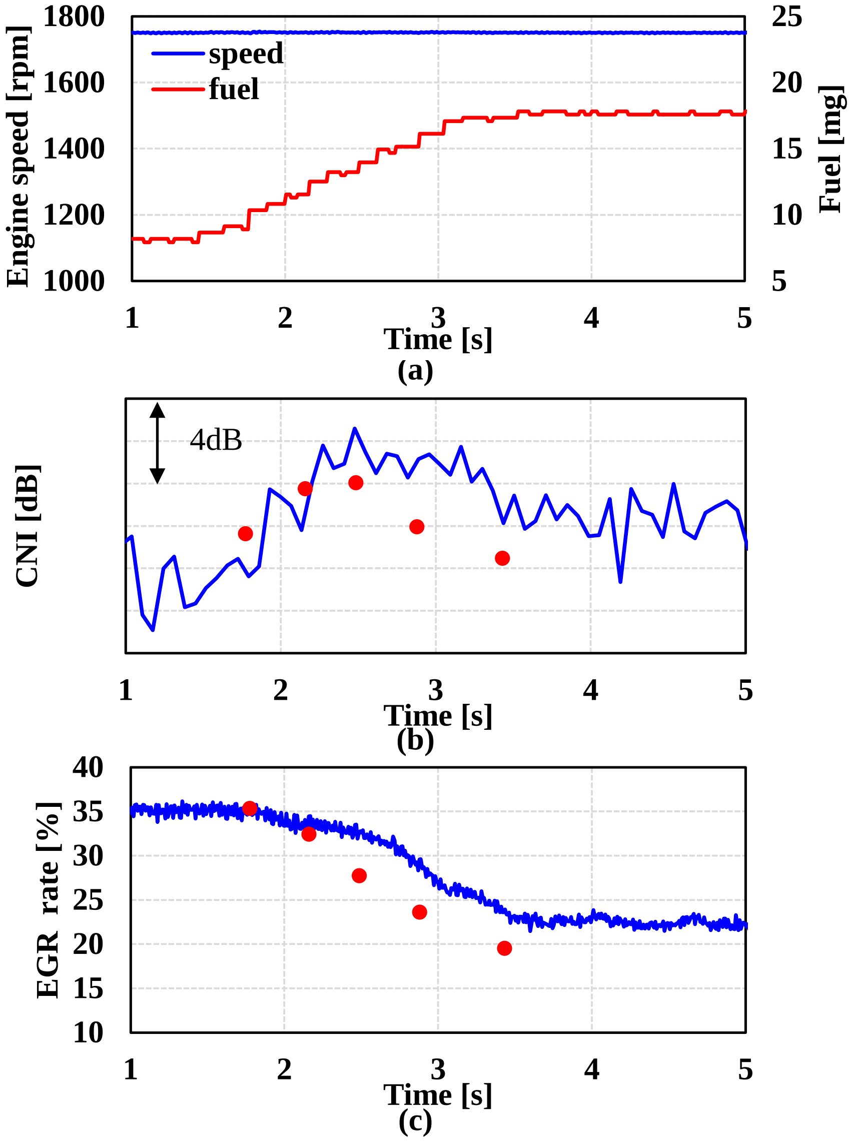

Figure 5.8 Results of load transient operation, ramp time: 2s (a) Engine speed, (b) CNI, (c) EGR rate

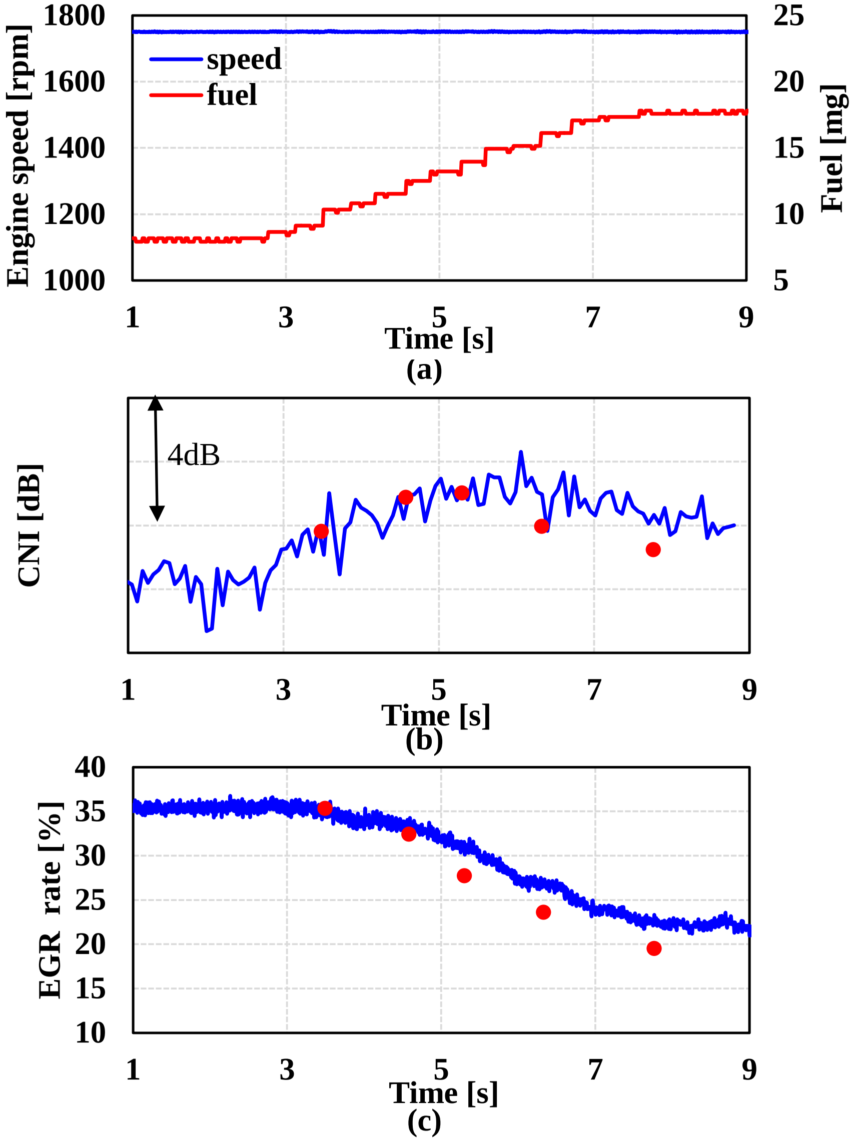

Figure 5.9 Results of load transient operation, ramp time: 5s (a) Engine speed, (b) CNI, (c) EGR rate

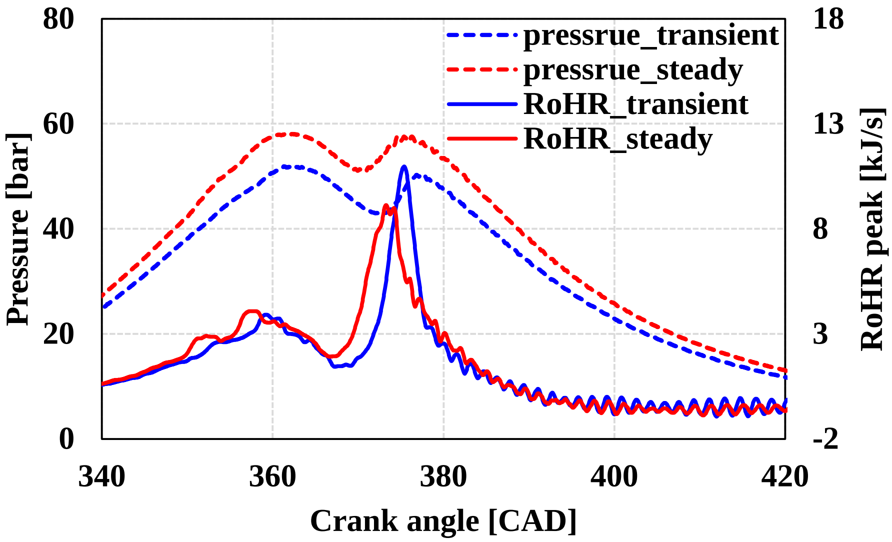

Figure 5.10 Comparison of pressure and RoHR between transient operation and steady state

5.2 Concept of control

Engine noise and emissions are sensitive to environmental condition changes because these changes affect the combustion of diesel. For example, noise can be worsened by reducing the amount of pilot injection due to the injector aging and EGR rate mismatching caused by fouling occurring in the EGR system, turbo charger lag and intake temperature variation. Moreover, the combustion noise could be changed during a transient operation as referred in 5.1. [57-59]

Closed-loop control is one way to solve these problems. The control system uses combustion information, such as the MFB50 and IMEP, which is calculated from the in-cylinder pressure, measured by a pressure sensor integrated with the glow plug. The injection strategy is determined according to the feed-back. Many researchers have developed these technologies aim to reduce emissions. However, if combustion noise is used as feedback in this sense, when applying this closed-loop control principle, the sound quality deterioration could be prevented. Therefore, this study, closed loop combustion control system using CNI for reduction of combustion noise have been developed. [60]

Figure 5.11 shows the concept of combustion control using CNI for combustion noise reduction. The control system consisted of CNI calculation and combustion control. In-cylinder pressure was measured and CNI was calculated in CNI calculator. The results of CNI calculation is passed on combustion controller which can control of EMS variables. The combustion controller was operated to create an algorithm and modify injection strategies to change the combustion characteristics and combustion noise, or combustion noise index. This process was repeated until the target was achieved

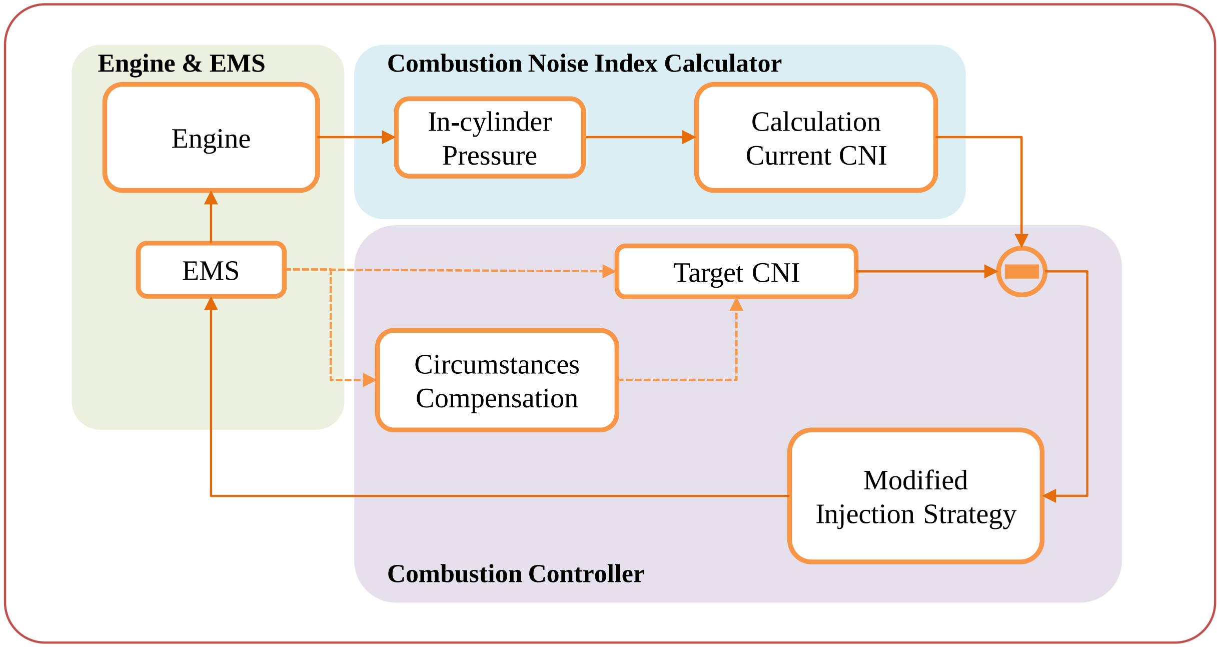
Engine & EMS
Combustion Noise Index Calculator
Engine
In-cylinder Pressure
Calculation Current CNI
EMS
Target CNI
Circumstances Compensation
Modified Injection Strategy
Combustion Controller

Figure 5.11 Concept of combustion control using CNI for combustion noise reduction

5.3 Control parameters

To determine the control parameter for CNI control, the sensitivities of the parameters, which are SOI, pilot quantity, injection pressure and EGR, for CNI were investigated.

5.3.1 Start of injection

The SOI of the main injection were varied from -2° BTDC CAD to 3° BTDC CAD. The engine speed was changed from 1250 rpm to 2500 rpm and fuel quantity was varied from 12.5 mg to 25 mg. Figure 5.12 shows CNI when the SOI were changed. The CNI levels were high where engine speed was 1750 rpm and fuel quantity was about 15 mg, though the SOI were changed.

The sensitivity of SOI for CNI was examined. Figures 5.13 and 5.14 show CNI level and SOI, respectively when the engine speed were 1500 rpm and 2000 rpm. The fuel quantity was varied between 12.5 and 25 mg. The CNI decreased by advancing SOI when the fuel quantity was 12.5~20 mg. However, when the fuel quantity was over 20 mg, the correlation between of CNI and SOI is week. That means the CNI could not be controlled by changing the SOI at the operation points. Figures 5.15 and 5.16 show the heat release rate when the SOI varied. At 15mg of fuel, when the SOI was advanced, the peak of heat release rate lowered. However, at 22.5 mg of fuel, when the SOI was advanced, the peak did not decrease. That was the reason why the CNI could not be controlled by the SOI when the fuel quantity was over 20 mg.

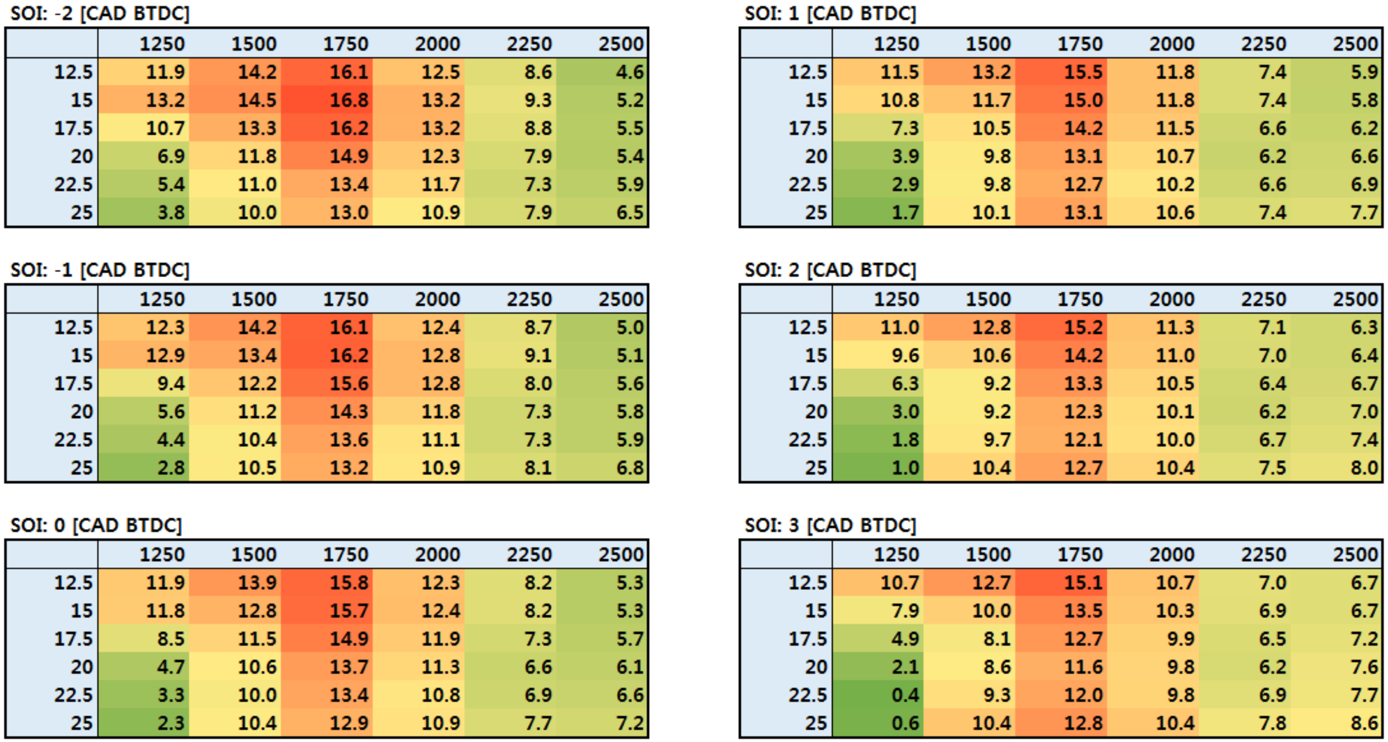

SOI: -2 [CAD BTDC]

	1250	1500	1750	2000	2250	2500
12.5	11.9	14.2	16.1	12.5	8.6	4.6
15	13.2	14.5	16.8	13.2	9.3	5.2
17.5	10.7	13.3	16.2	13.2	8.8	5.5
20	6.9	11.8	14.9	12.3	7.9	5.4
22.5	5.4	11.0	13.4	11.7	7.3	5.9
25	3.8	10.0	13.0	10.9	7.9	6.5

SOI: 1 [CAD BTDC]

	1250	1500	1750	2000	2250	2500
12.5	11.5	13.2	15.5	11.8	7.4	5.9
15	10.8	11.7	15.0	11.8	7.4	5.8
17.5	7.3	10.5	14.2	11.5	6.6	6.2
20	3.9	9.8	13.1	10.7	6.2	6.6
22.5	2.9	9.8	12.7	10.2	6.6	6.9
25	1.7	10.1	13.1	10.6	7.4	7.7

SOI: -1 [CAD BTDC]

	1250	1500	1750	2000	2250	2500
12.5	12.3	14.2	16.1	12.4	8.7	5.0
15	12.9	13.4	16.2	12.8	9.1	5.1
17.5	9.4	12.2	15.6	12.8	8.0	5.6
20	5.6	11.2	14.3	11.8	7.3	5.8
22.5	4.4	10.4	13.6	11.1	7.3	5.9
25	2.8	10.5	13.2	10.9	8.1	6.8

SOI: 2 [CAD BTDC]

	1250	1500	1750	2000	2250	2500
12.5	11.0	12.8	15.2	11.3	7.1	6.3
15	9.6	10.6	14.2	11.0	7.0	6.4
17.5	6.3	9.2	13.3	10.5	6.4	6.7
20	3.0	9.2	12.3	10.1	6.2	7.0
22.5	1.8	9.7	12.1	10.0	6.7	7.4
25	1.0	10.4	12.7	10.4	7.5	8.0

SOI: 0 [CAD BTDC]

	1250	1500	1750	2000	2250	2500
12.5	11.9	13.9	15.8	12.3	8.2	5.3
15	11.8	12.8	15.7	12.4	8.2	5.3
17.5	8.5	11.5	14.9	11.9	7.3	5.7
20	4.7	10.6	13.7	11.3	6.6	6.1
22.5	3.3	10.0	13.4	10.8	6.9	6.6
25	2.3	10.4	12.9	10.9	7.7	7.2

SOI: 3 [CAD BTDC]

	1250	1500	1750	2000	2250	2500
12.5	10.7	12.7	15.1	10.7	7.0	6.7
15	7.9	10.0	13.5	10.3	6.9	6.7
17.5	4.9	8.1	12.7	9.9	6.5	7.2
20	2.1	8.6	11.6	9.8	6.2	7.6
22.5	0.4	9.3	12.0	9.8	6.9	7.7
25	0.6	10.4	12.8	10.4	7.8	8.6

Figure 5.12 CNI variation according to SOI change

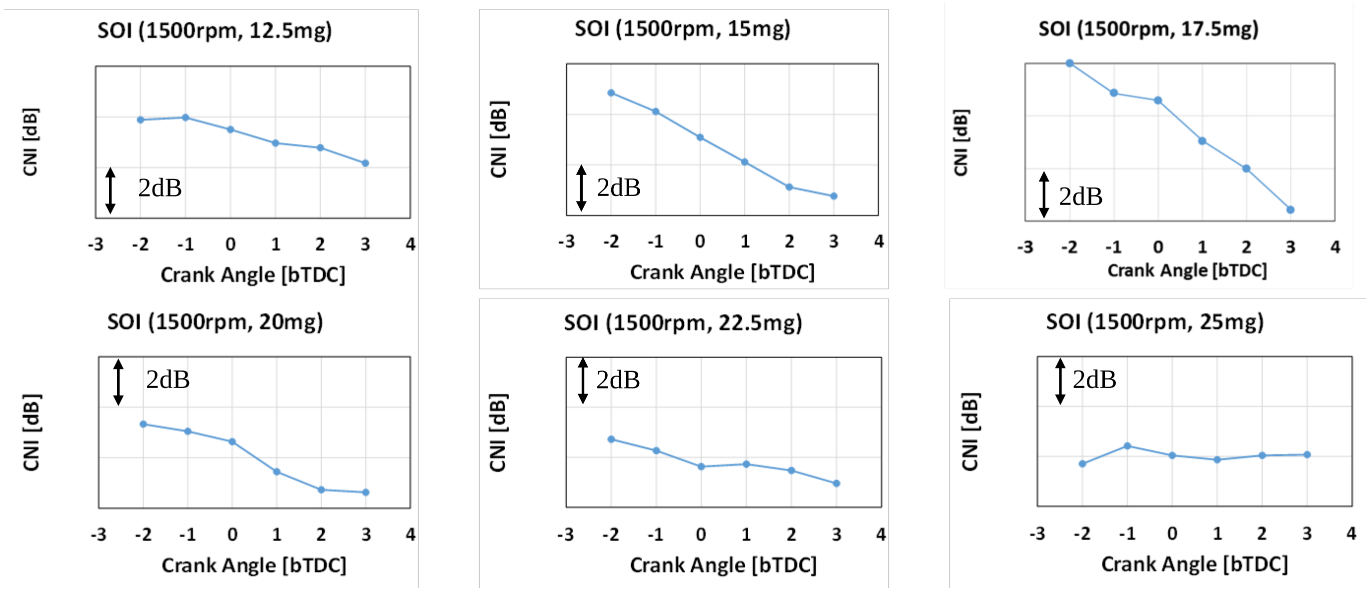

Figure 5.13 Sensitivity analysis of CNI for SOI change @ 1500 rpm

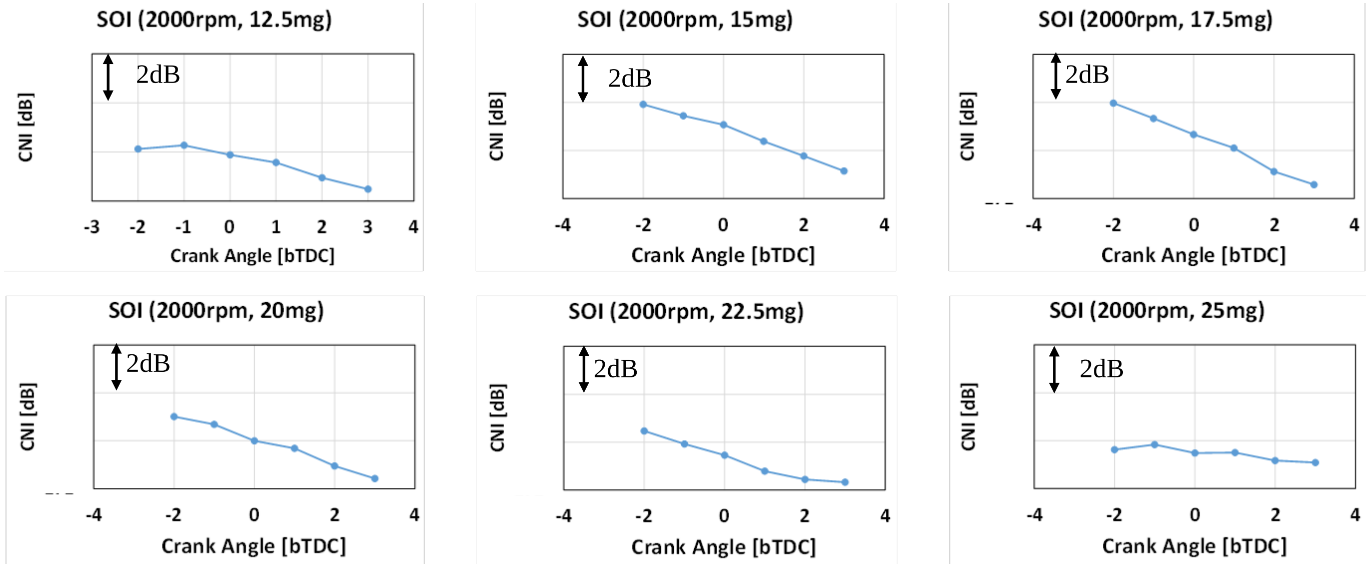

Figure 5.14 Sensitivity analysis of CNI for SOI change @ 2000 rpm

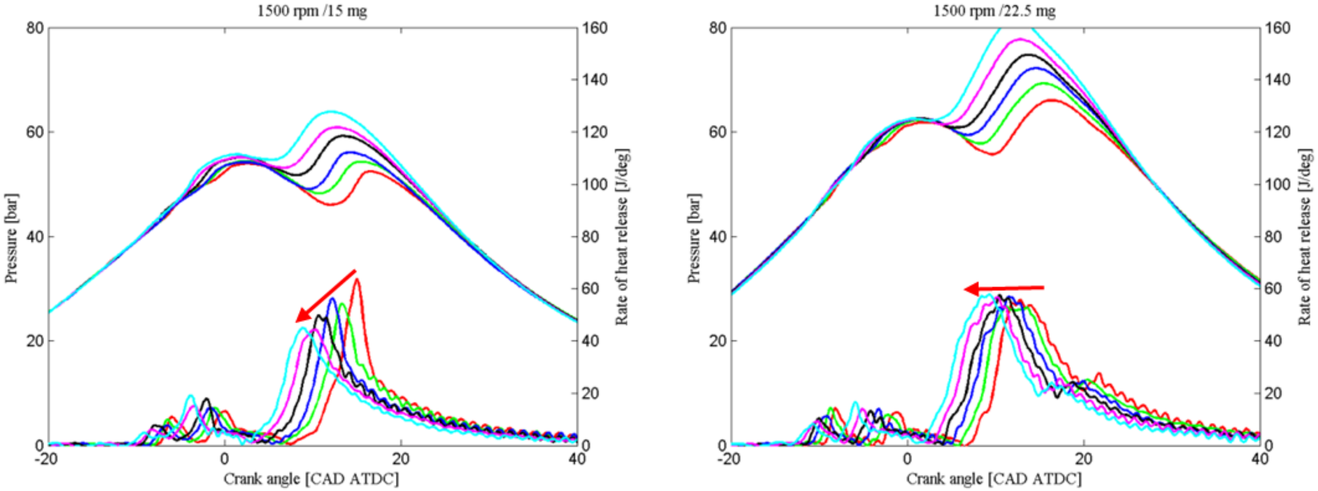

Figure 5.15 Heat release rate and in-cylinder pressure according to SOI change @ 1500 rpm

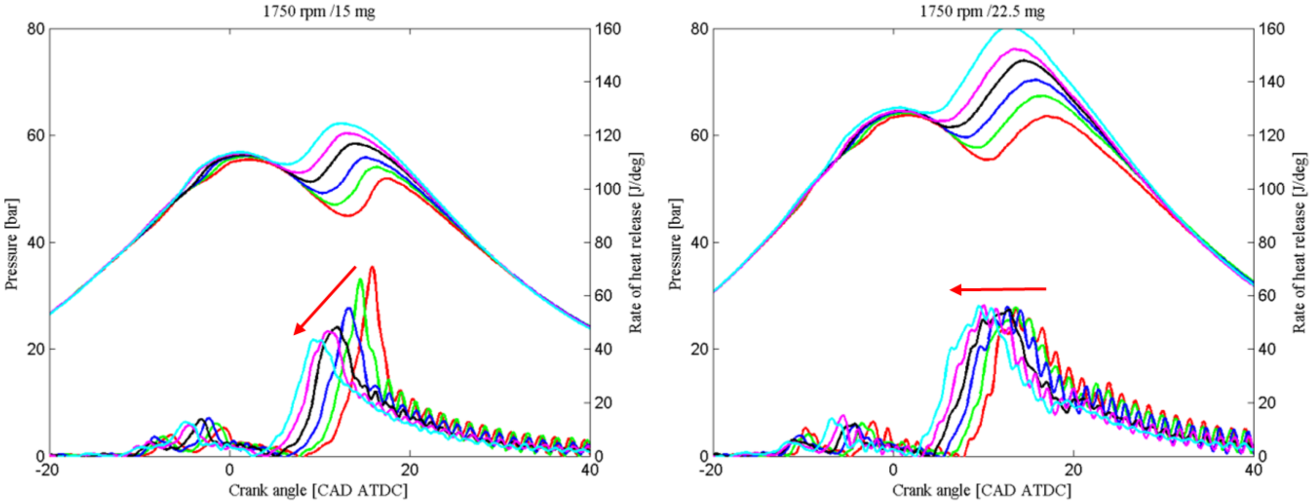

Figure 5.16 Heat release rate and in-cylinder pressure according to SOI change @ 1750 rpm

5.3.2 Other parameters: Pilot injection quantity, pilot injection timing, injection pressure and EGR rate

The sensitivity of other parameters, which are pilot injection quantity, pilot injection timing, injection pressure and EGR rate, are shown in figures 5.17 and 5.18. The pilot injection was increased by 0.3 mg and decreased by 0.3 mg. When the fuel quantity of pilot injection increased, the CNI decreased. However, the sensitivity was very low at 20mg of fuel quantity.

Injection pressure was increased and decreased by 50 bar. When injection pressure was reduced, the CNI decreased. Moreover, when the fuel quantity was even over 20 mg, the linearity was remained. It means that the injection pressure could be a parameter, which can control the CNI level for aboard operating region. Figure 5.19 shows the heat release rate. The peak of heat release rate decreased with a lower injection pressure.

The pilot injection timing was also investigated because it affects the in-cylinder gas temperature and pressure when the main fuel was injected. When the timing was changed, the CNI was varied. According to the operating point, the tendency was changed, thus, the pilot timing was not proper to be used as parameters to control the CNI level.

The EGR rate was also investigated. The EGR rate changed due to oxygen concentration in cylinder and ignition delay. When the EGR rate was high, a rapid combustion occurred because more fuel was burned in the premixed combustion phase. When the EGR rate was low, the CNI also decreased. The tendency and sensitivity were acceptable to be used as parameters to control the CNI. However, air supply system has a delay, thus it is hard to control the CNI by changing the EGR rate. In addition, NOx emission was very sensitive to the EGR rate, thus if the EGR rate was decreased to control CNI, NOx emission could have increased.

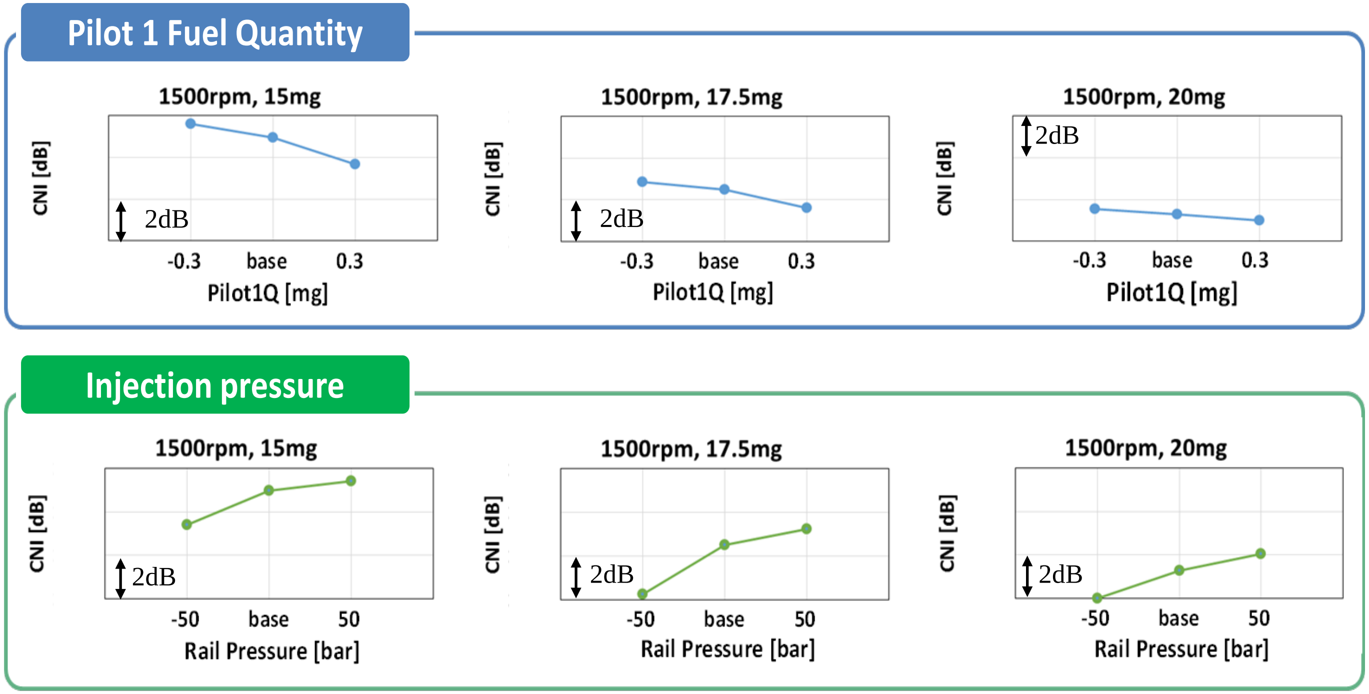

Figure 5.17 Sensitivity analysis of CNI for pilot fuel quantity and injection pressure change

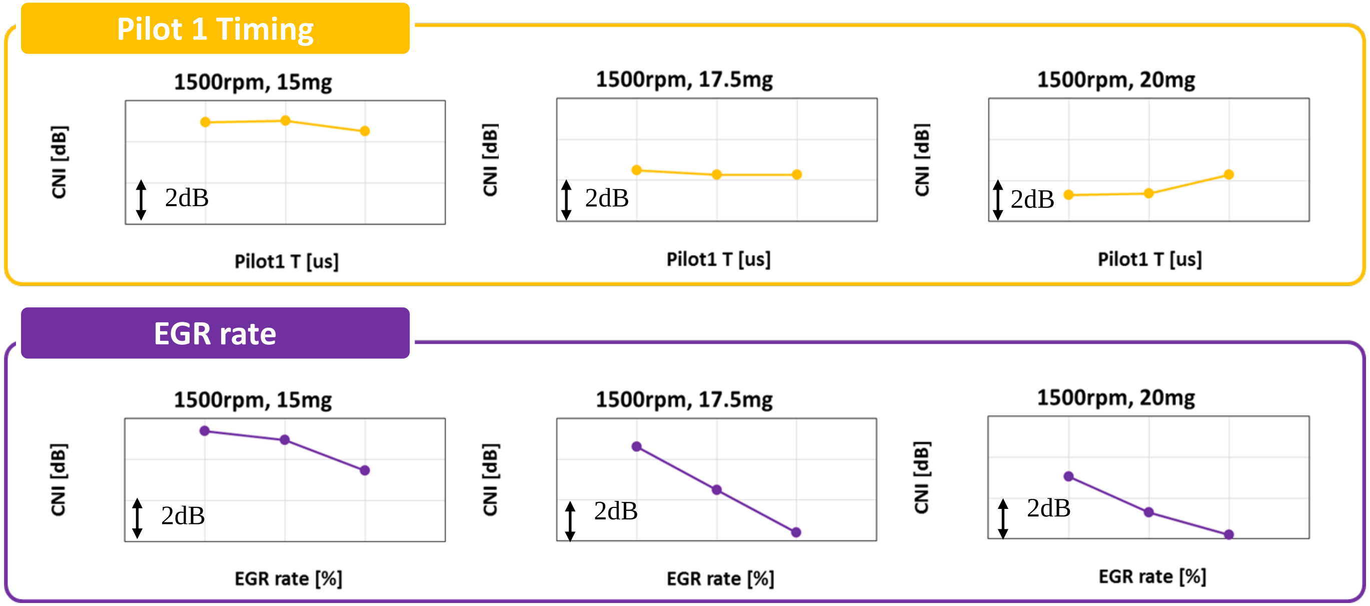

Figure 5.18 Sensitivity analysis of CNI for pilot timing and EGR rate change

5.3.3 Interaction among injection parameters

As previously referred, the main injection timing, pilot quantity and rail pressure were proper to be used as parameters to control CNI level. However, some of them had different tendency according to operating conditions. Thus, if they were simultaneously used to control the CNI level, they would make synergy or potential conflicts with other parameters. To use them together, the interaction among of them were investigated.

At first, the SOI, Pilot quantity and injection pressure were separately changed. The engine speed was changed from 1250 rpm to 2750 rpm and total fuel quantity was changed from 10 mg ~ 40 mg. That was possible to cover the general operating condition. Figure 5.19 shows a different CNI level when the SOI was 3CAD advanced and when the SOI was at the base condition. Blue means decreasing of the CNI and RED means increasing of the CNI. In other words, the blue region means that the SOI can be used as control parameter. The SOI advance was mainly effective in the region of 1250~2000 rpm and 10~20 mg fuel quantity.

The injection pressure was reduced by 60 bar. Figure 5.21 shows the difference of CNI level between reduced injection pressure and the base injection pressure. The control of injection pressure was effective in all operating points. Especially, when the engine speed is under 1500 rpm, changing the rail pressure was effective to reduce the CNI level.

The pilot injection quantity was increased by 0.3 mg. The decreased pilot injection quantity was effective under 25 mg of fuel and all engine speed. However, that was less effective than the SOI and the injection pressure as shown in figure 5.20

To investigate the interaction among the advanced SOI, reduction of injection pressure and increase of pilot injection, they were applied simultaneously. If there were no cross effects among them, effects of each parameters would be linearly summed when they are used together. Figures 5.22 and 5.23 show estimated values when the effects of them were arithmetically summed and results when in-cylinder pressure were measured by experiment, in which the all of parameter were changed. The gap between estimated value and experimental results are not considerable. Thus, they can be simultaneously used to control the CNI level, because they did not have negative cross effects. Moreover, if the operating region, in which each of the parameters is used, is limited, the available operating region is extended. The application operating regions are shown in figures 5.24-26 and the results of CNI are shown in figure 5.27.

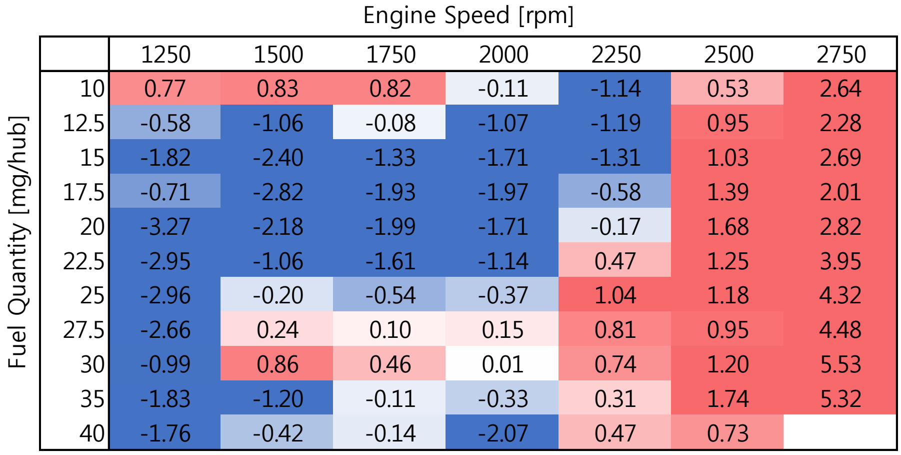
Engine Speed [rpm]
Fuel Quantity [mg/hub]

	1250	1500	1750	2000	2250	2500	2750
10	0.77	0.83	0.82	-0.11	-1.14	0.53	2.64
12.5	-0.58	-1.06	-0.08	-1.07	-1.19	0.95	2.28
15	-1.82	-2.40	-1.33	-1.71	-1.31	1.03	2.69
17.5	-0.71	-2.82	-1.93	-1.97	-0.58	1.39	2.01
20	-3.27	-2.18	-1.99	-1.71	-0.17	1.68	2.82
22.5	-2.95	-1.06	-1.61	-1.14	0.47	1.25	3.95
25	-2.96	-0.20	-0.54	-0.37	1.04	1.18	4.32
27.5	-2.66	0.24	0.10	0.15	0.81	0.95	4.48
30	-0.99	0.86	0.46	0.01	0.74	1.20	5.53
35	-1.83	-1.20	-0.11	-0.33	0.31	1.74	5.32
40	-1.76	-0.42	-0.14	-2.07	0.47	0.73	

Figure 5.19 CNI change when SOI is advanced by 3 CAD

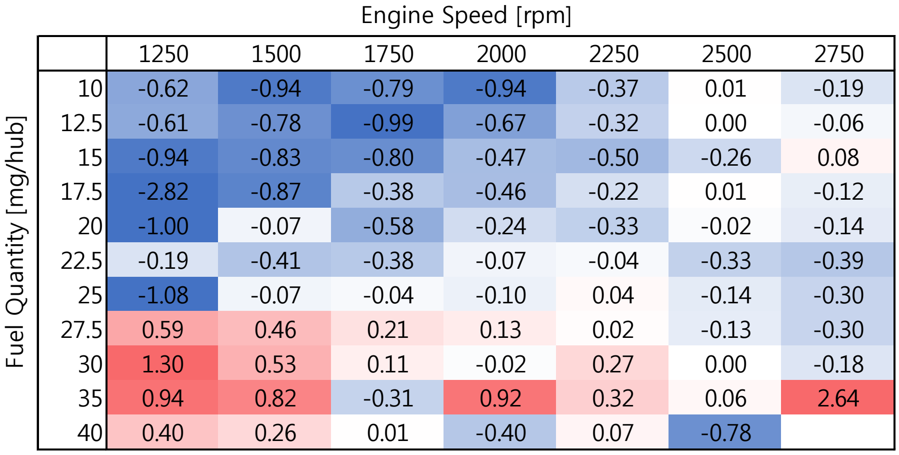
Engine Speed [rpm]
Fuel Quantity [mg/hub]

	1250	1500	1750	2000	2250	2500	2750
10	-0.62	-0.94	-0.79	-0.94	-0.37	0.01	-0.19
12.5	-0.61	-0.78	-0.99	-0.67	-0.32	0.00	-0.06
15	-0.94	-0.83	-0.80	-0.47	-0.50	-0.26	0.08
17.5	-2.82	-0.87	-0.38	-0.46	-0.22	0.01	-0.12
20	-1.00	-0.07	-0.58	-0.24	-0.33	-0.02	-0.14
22.5	-0.19	-0.41	-0.38	-0.07	-0.04	-0.33	-0.39
25	-1.08	-0.07	-0.04	-0.10	0.04	-0.14	-0.30
27.5	0.59	0.46	0.21	0.13	0.02	-0.13	-0.30
30	1.30	0.53	0.11	-0.02	0.27	0.00	-0.18
35	0.94	0.82	-0.31	0.92	0.32	0.06	2.64
40	0.40	0.26	0.01	-0.40	0.07	-0.78	

Figure 5.20 CNI change when Pilot quantity increase by 0.2 mg

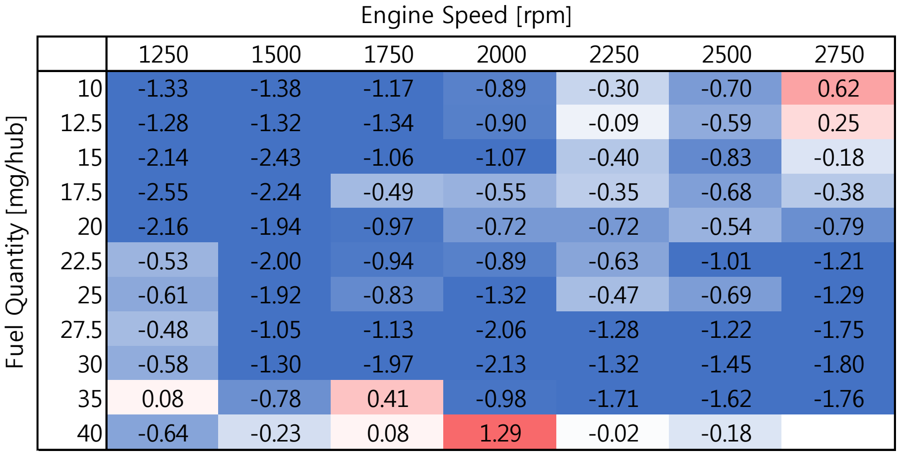

Fuel Quantity [mg/hub]	Engine Speed [rpm]						
	1250	1500	1750	2000	2250	2500	2750
10	-1.33	-1.38	-1.17	-0.89	-0.30	-0.70	0.62
12.5	-1.28	-1.32	-1.34	-0.90	-0.09	-0.59	0.25
15	-2.14	-2.43	-1.06	-1.07	-0.40	-0.83	-0.18
17.5	-2.55	-2.24	-0.49	-0.55	-0.35	-0.68	-0.38
20	-2.16	-1.94	-0.97	-0.72	-0.72	-0.54	-0.79
22.5	-0.53	-2.00	-0.94	-0.89	-0.63	-1.01	-1.21
25	-0.61	-1.92	-0.83	-1.32	-0.47	-0.69	-1.29
27.5	-0.48	-1.05	-1.13	-2.06	-1.28	-1.22	-1.75
30	-0.58	-1.30	-1.97	-2.13	-1.32	-1.45	-1.80
35	0.08	-0.78	0.41	-0.98	-1.71	-1.62	-1.76
40	-0.64	-0.23	0.08	1.29	-0.02	-0.18	

Figure 5.21 CNI change when injection pressure is reduced by 60 bar

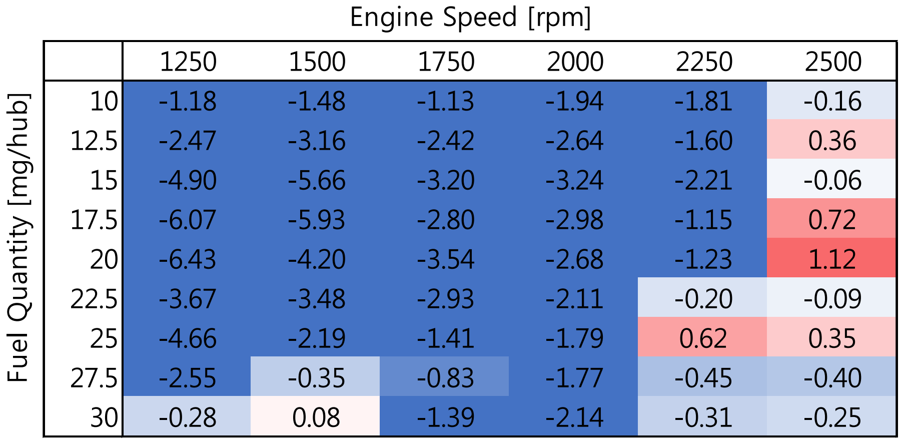

Fuel Quantity [mg/hub]	Engine Speed [rpm]					
	1250	1500	1750	2000	2250	2500
10	-1.18	-1.48	-1.13	-1.94	-1.81	-0.16
12.5	-2.47	-3.16	-2.42	-2.64	-1.60	0.36
15	-4.90	-5.66	-3.20	-3.24	-2.21	-0.06
17.5	-6.07	-5.93	-2.80	-2.98	-1.15	0.72
20	-6.43	-4.20	-3.54	-2.68	-1.23	1.12
22.5	-3.67	-3.48	-2.93	-2.11	-0.20	-0.09
25	-4.66	-2.19	-1.41	-1.79	0.62	0.35
27.5	-2.55	-0.35	-0.83	-1.77	-0.45	-0.40
30	-0.28	0.08	-1.39	-2.14	-0.31	-0.25

Figure 5.22 Arithmetically estimated CNI variation when SOI, pilot quantity and injection pressure are simultaneously changed

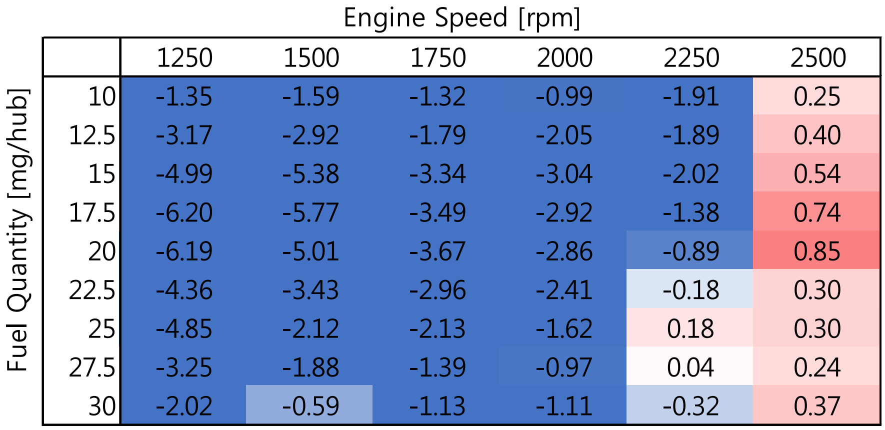

Fuel Quantity [mg/hub]	Engine Speed [rpm]					
	1250	1500	1750	2000	2250	2500
10	-1.35	-1.59	-1.32	-0.99	-1.91	0.25
12.5	-3.17	-2.92	-1.79	-2.05	-1.89	0.40
15	-4.99	-5.38	-3.34	-3.04	-2.02	0.54
17.5	-6.20	-5.77	-3.49	-2.92	-1.38	0.74
20	-6.19	-5.01	-3.67	-2.86	-0.89	0.85
22.5	-4.36	-3.43	-2.96	-2.41	-0.18	0.30
25	-4.85	-2.12	-2.13	-1.62	0.18	0.30
27.5	-3.25	-1.88	-1.39	-0.97	0.04	0.24
30	-2.02	-0.59	-1.13	-1.11	-0.32	0.37

Figure 5.23 Experimental results CNI variation when SOI, pilot quantity and injection pressure are simultaneously changed

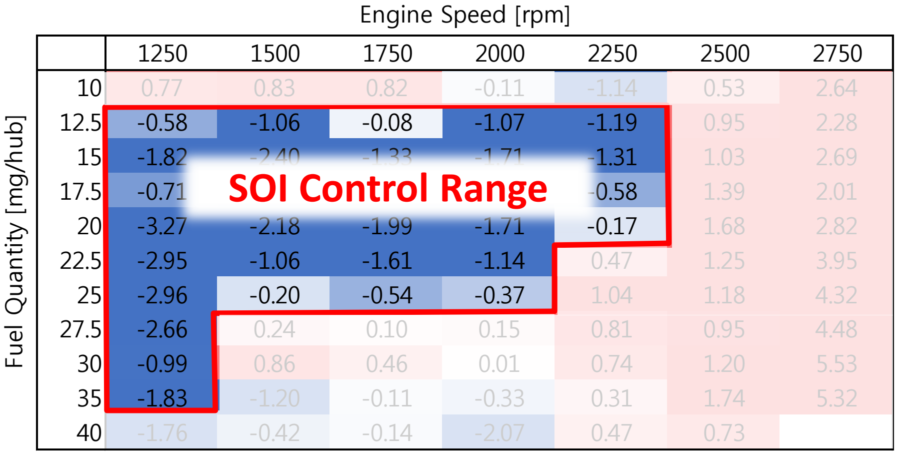
SOI Control Range

Fuel Quantity [mg/hub]	Engine Speed [rpm]						
	1250	1500	1750	2000	2250	2500	2750
10	0.77	0.83	0.82	-0.11	-1.14	0.53	2.64
12.5	-0.58	-1.06	-0.08	-1.07	-1.19	0.95	2.28
15	-1.82	-2.40	-1.33	-1.71	-1.31	1.03	2.69
17.5	-0.71	[illegible]	[illegible]	[illegible]	-0.58	1.39	2.01
20	-3.27	-2.18	-1.99	-1.71	-0.17	1.68	2.82
22.5	-2.95	-1.06	-1.61	-1.14	0.47	1.25	3.95
25	-2.96	-0.20	-0.54	-0.37	1.04	1.18	4.32
27.5	-2.66	0.24	0.10	0.15	0.81	0.95	4.48
30	-0.99	0.86	0.46	0.01	0.74	1.20	5.53
35	-1.83	-1.20	-0.11	-0.33	0.31	1.74	5.32
40	-1.76	-0.42	-0.14	-2.07	0.47	0.73	

Figure 5.24 Control range using SOI

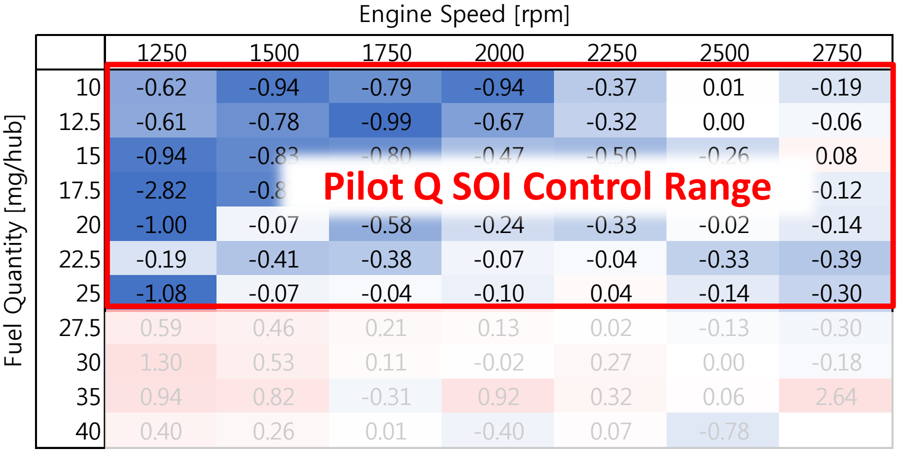
Pilot Q SOI Control Range

Fuel Quantity [mg/hub]	Engine Speed [rpm]						
	1250	1500	1750	2000	2250	2500	2750
10	-0.62	-0.94	-0.79	-0.94	-0.37	0.01	-0.19
12.5	-0.61	-0.78	-0.99	-0.67	-0.32	0.00	-0.06
15	-0.94	-0.83	-0.80	-0.47	-0.50	-0.26	0.08
17.5	-2.82	-0.8	[illegible]	[illegible]	[illegible]	[illegible]	-0.12
20	-1.00	-0.07	-0.58	-0.24	-0.33	-0.02	-0.14
22.5	-0.19	-0.41	-0.38	-0.07	-0.04	-0.33	-0.39
25	-1.08	-0.07	-0.04	-0.10	0.04	-0.14	-0.30
27.5	0.59	0.46	0.21	0.13	0.02	-0.13	-0.30
30	1.30	0.53	0.11	-0.02	0.27	0.00	-0.18
35	0.94	0.82	-0.31	0.92	0.32	0.06	2.64
40	0.40	0.26	0.01	-0.40	0.07	-0.78	

Figure 5.25 Control range using pilot quantity

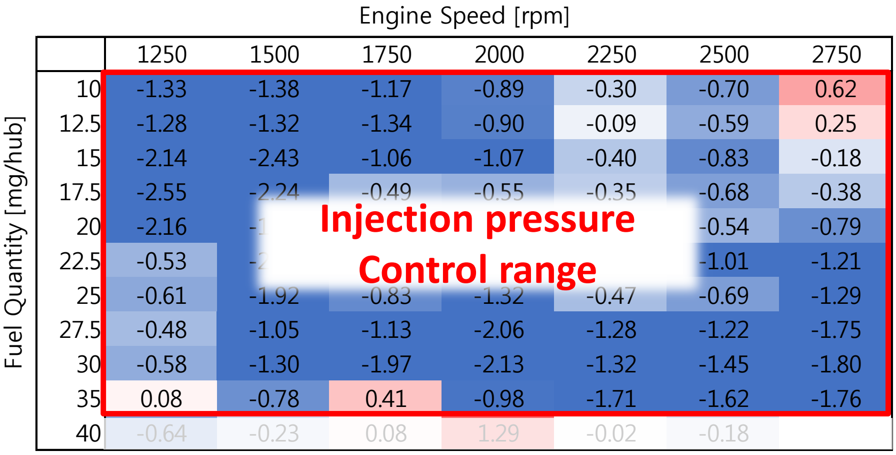
Engine Speed [rpm]
Fuel Quantity [mg/hub]
Injection pressure
Control range

Fuel Quantity [mg/hub]	1250	1500	1750	2000	2250	2500	2750
10	-1.33	-1.38	-1.17	-0.89	-0.30	-0.70	0.62
12.5	-1.28	-1.32	-1.34	-0.90	-0.09	-0.59	0.25
15	-2.14	-2.43	-1.06	-1.07	-0.40	-0.83	-0.18
17.5	-2.55	-2.24	-0.49	-0.55	-0.35	-0.68	-0.38
20	-2.16	[illegible]	[illegible]	[illegible]	[illegible]	-0.54	-0.79
22.5	-0.53	[illegible]	[illegible]	[illegible]	[illegible]	-1.01	-1.21
25	-0.61	-1.92	-0.83	-1.32	-0.47	-0.69	-1.29
27.5	-0.48	-1.05	-1.13	-2.06	-1.28	-1.22	-1.75
30	-0.58	-1.30	-1.97	-2.13	-1.32	-1.45	-1.80
35	0.08	-0.78	0.41	-0.98	-1.71	-1.62	-1.76
40	-0.64	-0.23	0.08	1.29	-0.02	-0.18	

Figure 5.26 Control range using injection pressure

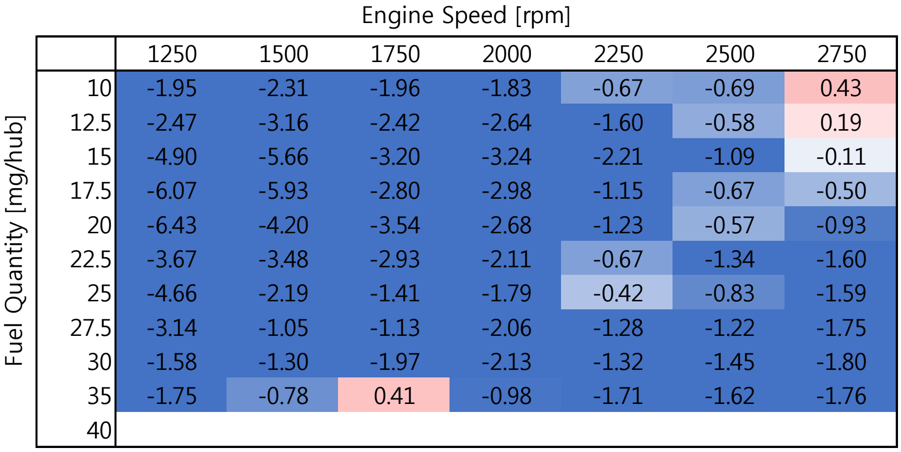
Engine Speed [rpm]
Fuel Quantity [mg/hub]

Fuel Quantity [mg/hub]	1250	1500	1750	2000	2250	2500	2750
10	-1.95	-2.31	-1.96	-1.83	-0.67	-0.69	0.43
12.5	-2.47	-3.16	-2.42	-2.64	-1.60	-0.58	0.19
15	-4.90	-5.66	-3.20	-3.24	-2.21	-1.09	-0.11
17.5	-6.07	-5.93	-2.80	-2.98	-1.15	-0.67	-0.50
20	-6.43	-4.20	-3.54	-2.68	-1.23	-0.57	-0.93
22.5	-3.67	-3.48	-2.93	-2.11	-0.67	-1.34	-1.60
25	-4.66	-2.19	-1.41	-1.79	-0.42	-0.83	-1.59
27.5	-3.14	-1.05	-1.13	-2.06	-1.28	-1.22	-1.75
30	-1.58	-1.30	-1.97	-2.13	-1.32	-1.45	-1.80
35	-1.75	-0.78	0.41	-0.98	-1.71	-1.62	-1.76
40							

Figure 5.27 CNI variation when the control ranges are limited for each parameters

5.4 Real time combustion control system to combustion noise

5.4.1 Overview of real time combustion control system

The system has 3 parts which are measurements of in-cylinder pressure, calculation of CNI and control of injection strategies. Figure 5.32 shows schematic diagram of the control system. The pressure was measured by using a charge type pressure sensor and charge amplifier. The CNI was calculation using the NI-PXI. The software was coded by LabVIEW. The injection strategy were modified in the ES1000. The control software was coded by ASCET. The NI-PXI and ES1000 communicated each other using CAN bus.

5.4.2 Calculation of CNI

The CNI was calculated using NI-PXI as shown in figure 5.33. The process of CNI calculation included FFT, thus the pressure samples had to be measured with same time interval. To obtain the time based samples, a Field-Programmable Gate Array (FPGA) board was used. The FPGA board is an integrated circuit designed to be configured by a customer or a designer after manufacturing. The in-cylinder pressure signal was acquired with Crank Position Sensor (CPS) signal which was also used in EMS (engine management system). Using the CPS signal, the crank angle information of the pressure signal was measured. The CNI calculation has to be finished within one cycle for cycle by cycle control. The whole pressure signal of one cycle was not used, but only pressure signal from -180 CAD to 180 CAD, in which the combustion process occurred, was used for CNI calculation. The acquired pressure data were transferred to real time controller via FIFO in the NI-PXI. In the real time controller, FFT of pressure signal was first calculated. Then, octave analysis of the FFT results were executed, and finally CNI was calculated. The CNI value transfer to ES1000 via CAN bus communication. All of the process were completed within one cycle. The process of calculation was described in figure 5.33.

5.4.3 Control of injection strategies

When the CNI calculation was completed, the results were transferred to combustion controller. The combustion controller compared target CNI level and current CNI level and modifies the injection strategies when the current CNI level higher than target level. Figure5.34 shows the schematic diagram of combustion controller.

The combustion controller consisted of 5 parts. The first part was data input and output. In the part, the EMS data, such as, engine speed, fuel quantity, rail pressure, pilot quantity, SOI, etc. were measured. In addition, the current CNI level, which was calculated in the NI-PXI, was read and current engine operation condition was sent to the NI-PXI via CAN bus communication.

In the control mode part, it was determined whether the control system was activated or deactivated according to the engine operation condition. When the engine speed was too high or when the fuel quantity was too much, the CNI could not be controlled. Thus, the controllable operating condition had to be discriminated. It was able to distinguish the transient of activation and deactivation. That was helpful to reduce the shock of change of operating mode.

Next, the current CNI level, which was obtained via CAN bus, was compared to target CNI level. The target level was determined from lookup table using engine speed and fuel quantity. The table was able to be changed according to operating condition because the original injection strategies of EMS were changed when the operating condition varied. The difference of current value and target was sent to PID controller.

In the PID controller part, the injection parameters, which was SOI, rail pressure and pilot quantity, was controlled to follow the target CNI level for current value. The PID controllers was independent because they have different sensitivity and limitation. The gains of each PID controller were tuned according operating conditions. The limitation of them were set to improve robustness.

The last part was communication with EMS. The ES1000 and EMS communicate via ETK protocol. The original value of variables of EMS were replaced modified values in combustion controller. To apply next cycle, at least the bypass had to be completed before 90° BTDC CAD.

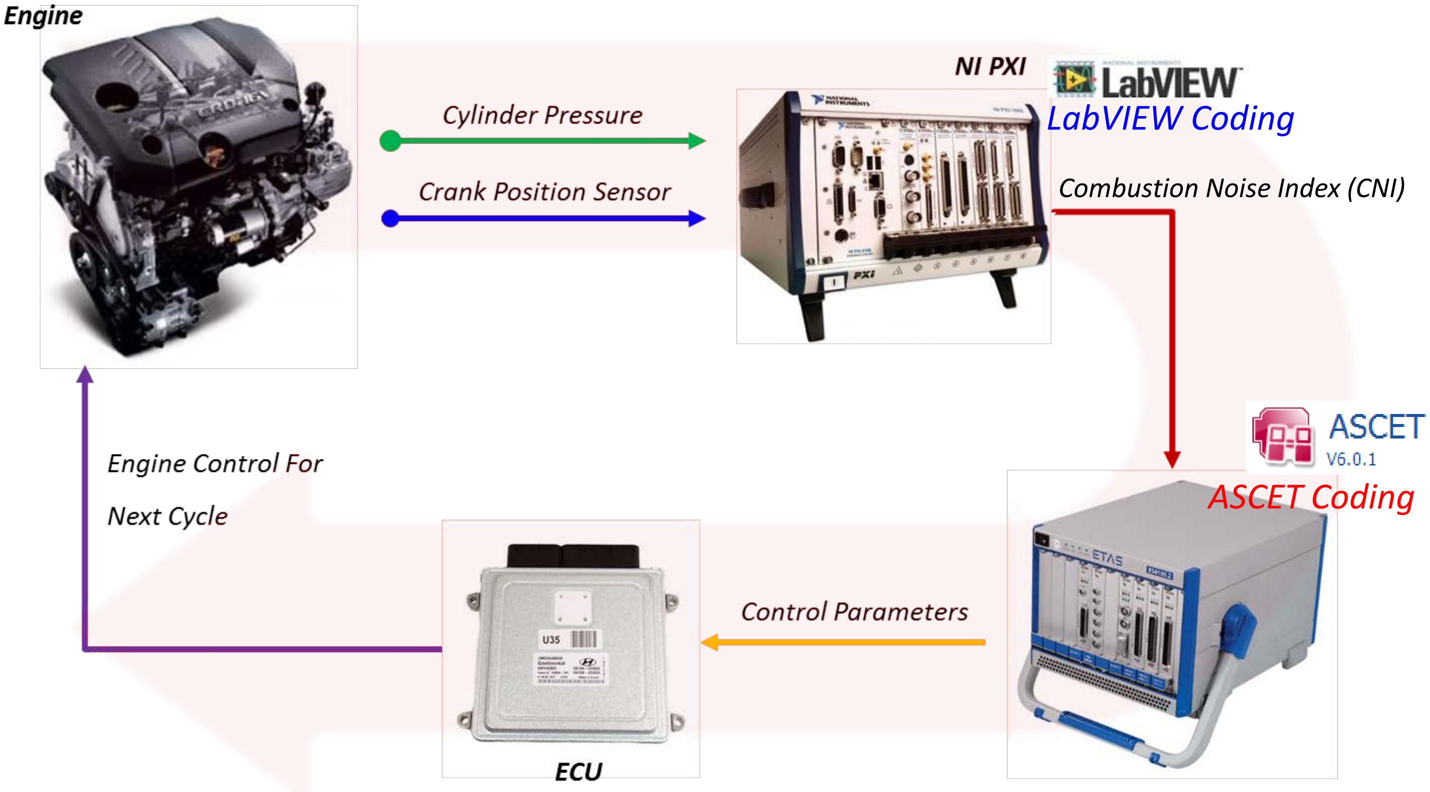
Engine
Cylinder Pressure
Crank Position Sensor
NI PXI
LabVIEW
LabVIEW Coding
Combustion Noise Index (CNI)
ASCET
V6.0.1
ASCET Coding
Control Parameters
ECU
Engine Control For
Next Cycle

Figure 5.28 Schematic diagram of closed loop control system using CNI to reduce combustion noise

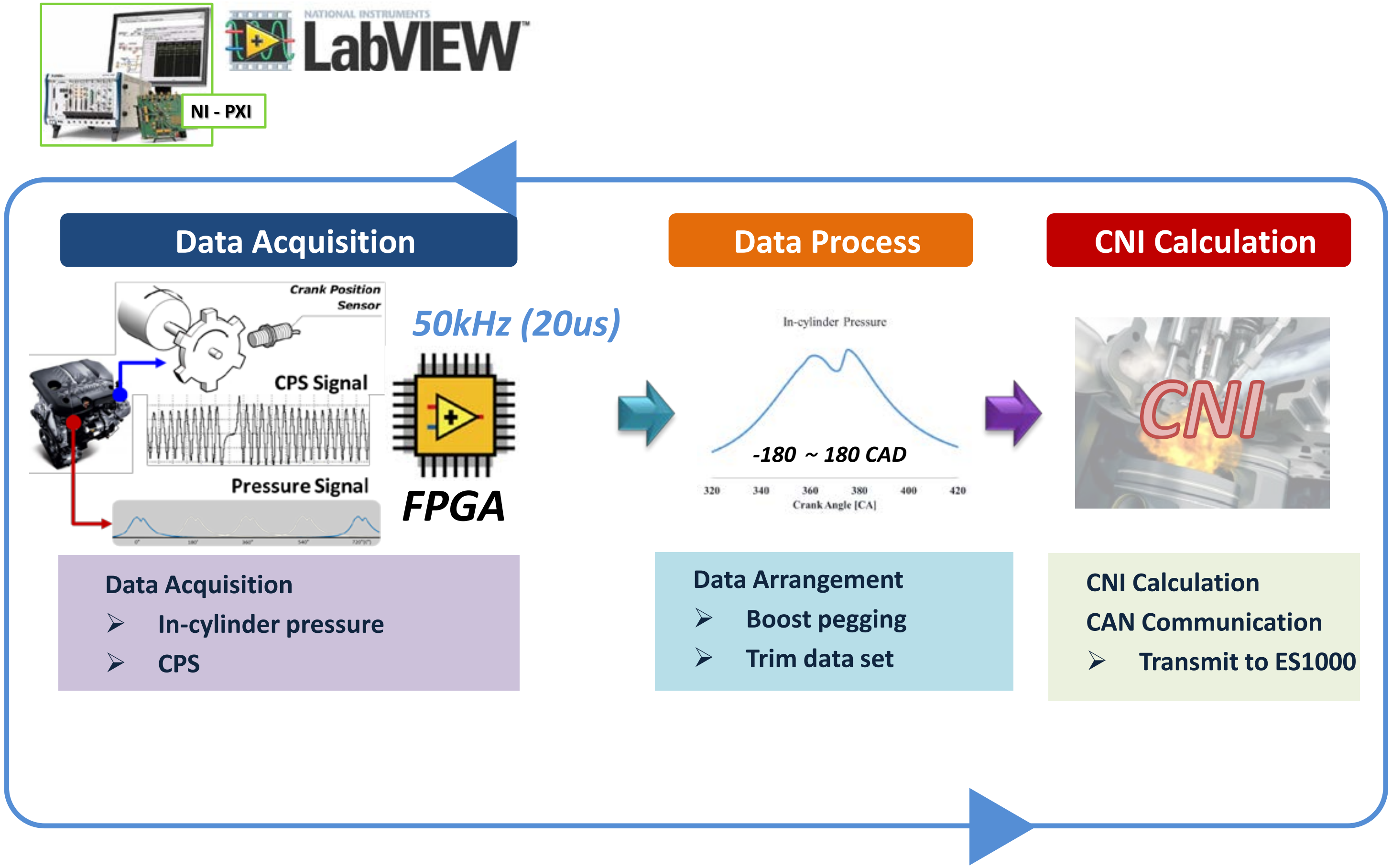
NI - PXI
NATIONAL INSTRUMENTS
LabVIEW
Data Acquisition
Data Process
CNI Calculation
Crank Position Sensor
CPS Signal
Pressure Signal
50kHz (20us)
FPGA
In-cylinder Pressure
-180 ~ 180 CAD
320
340
360
380
400
420
Crank Angle [CA]
CNI
Data Acquisition
➢ In-cylinder pressure
➢ CPS
Data Arrangement
➢ Boost pegging
➢ Trim data set
CNI Calculation
CAN Communication
➢ Transmit to ES1000

Figure 5.29 CNI calculation using NI-PXI & LabVIEW

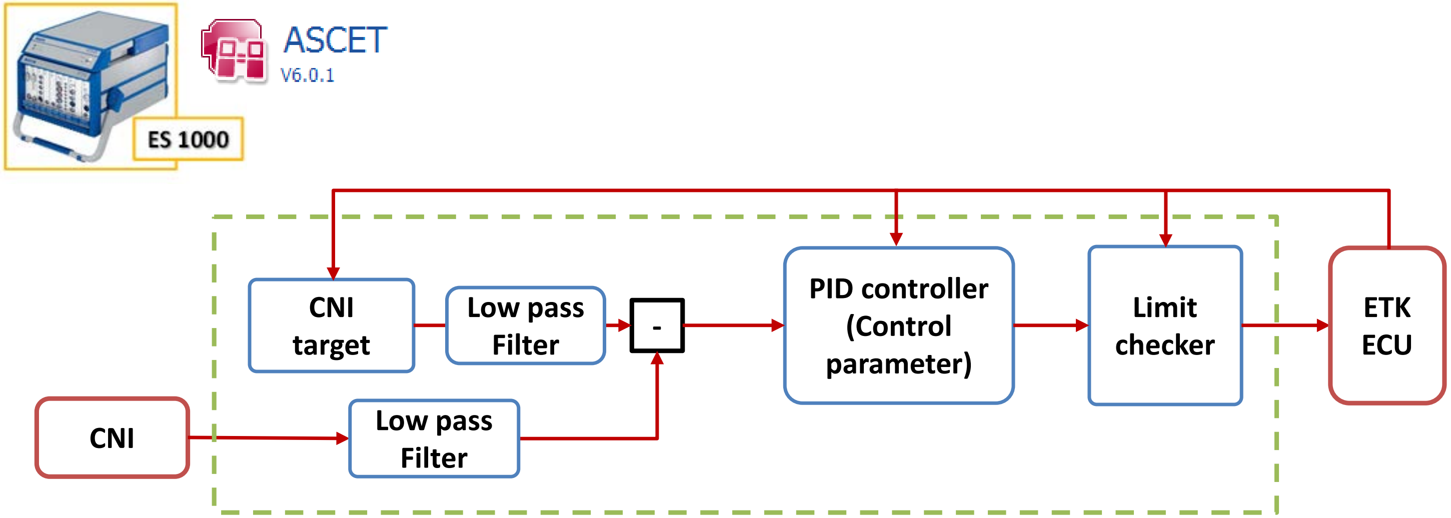
ES 1000
ASCET
V6.0.1
CNI target
Low pass Filter
-
PID controller (Control parameter)
Limit checker
ETK ECU
CNI
Low pass Filter

Figure 5.30 Combustion control algorithm using ES1000 & ASCET

5.5 Results of the closed loop control

5.5.1 Vehicle test

The closed loop control system to reduce combustion noise was applied to a vehicle. Figure 5.36 shows the test vehicle and table 5.2 displays specification of the vehicle. The vehicle is five door small family case and the engine is the same type of one used in test bench. Figure5.36 shows the vehicle in which the control system is equipped. The pressure sensor was installed in the first cylinder. The Kibox, NI-PXI and ES1000 were set up. To power supply, 220V invertor and extra battery were carried too.

The noise was measured in the cabin of the vehicle. A binaurales headset type microphone are used and the noise was measured by SQuadriga II (head acoustics). The driver wore headset type microphone to measure the sound for driver hearing.

5.5.2 Operating conditions and Results

Figure 5.37 shows the operating condition. The vehicle was accelerated to 60 kph with light tip-in. the engine speed was varied from 800 rpm to 2000 rpm and fuel injection quantity was changed from 5 to 23 mg/cycle·cylinder.

Figure5.38 shows the current CNI level and target value when the control system was deactivated. There was a significant gap between the current level and the target, which was up to 6dB. Figure5.39 shows results when the control system was activated. The current CNI level could follow the target value during the transient operation.

Figure 5.40 shows behaviors of injection parameters. SOI, injection pressure and pilot quantity were adjusted to follow the target. At that time, the cabin noise was reduced. Especially, the noise of 1.2 kHz ~2 kHz diminished up to 4 dB(A)

Figure 5.31 test vehicle, 1.6 liter diesel enigne

Table 5.2 Specifications of test vehicle

Criteria	Specification
Vehicle model	K3(YD)
Transmission	6-speed automatic
Driven type	Front-wheel drive
Maximum power	128 hp
Maximum torque	28.5 kg·m
Weight	1,340 kg

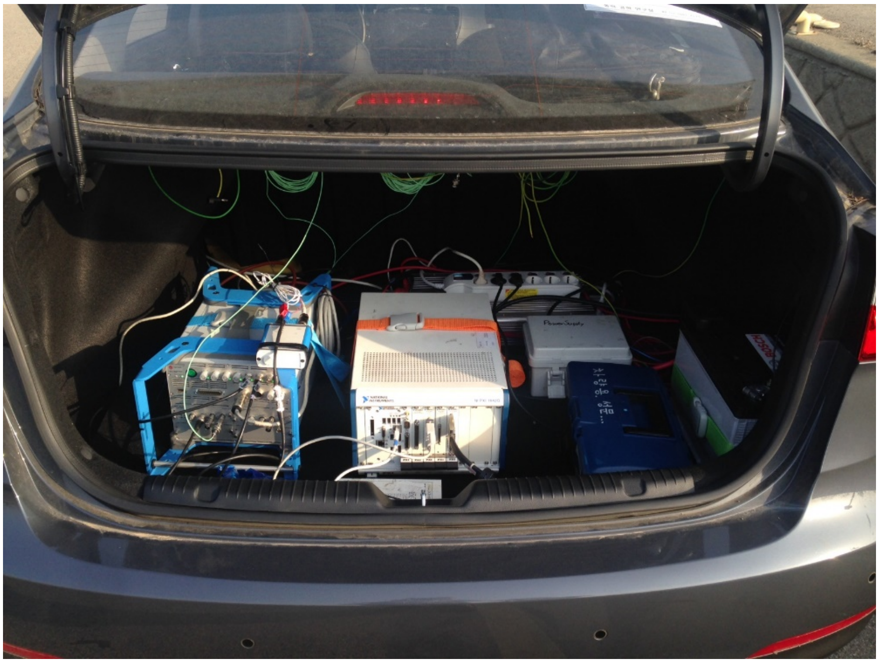

Figure 5.32 closed loop control system set up in test vehicle

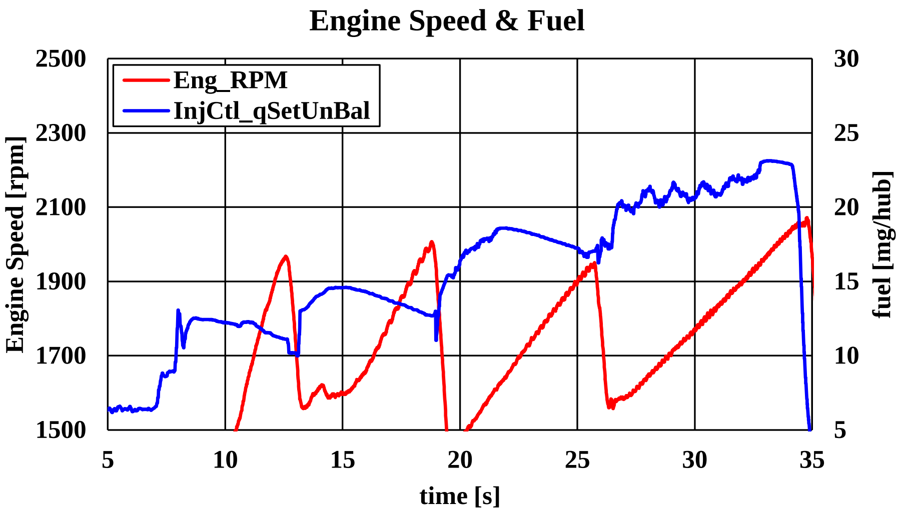

Figure 5.33 Transient operation of test for CNI

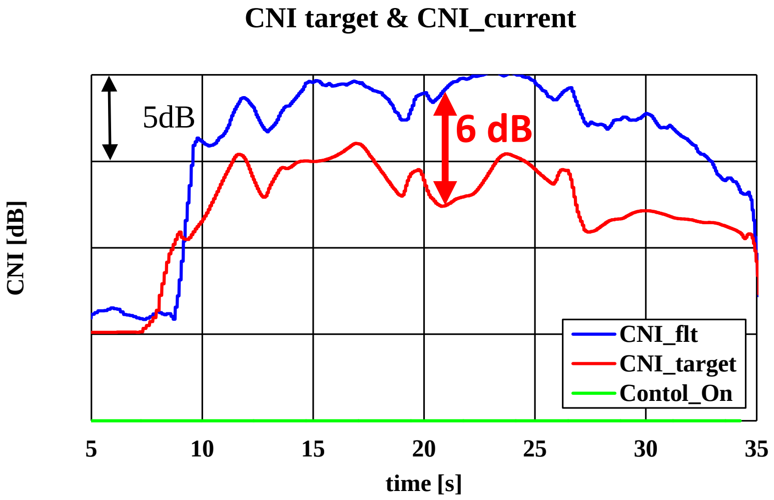

Figure 5.34 Target CNI and current CNI when the control was deactivated

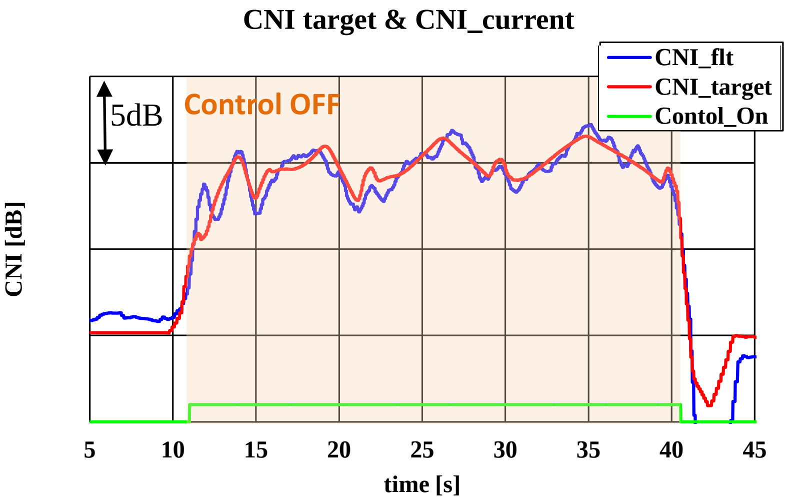

Figure 5.35 Target CNI and current CNI when the control was activated

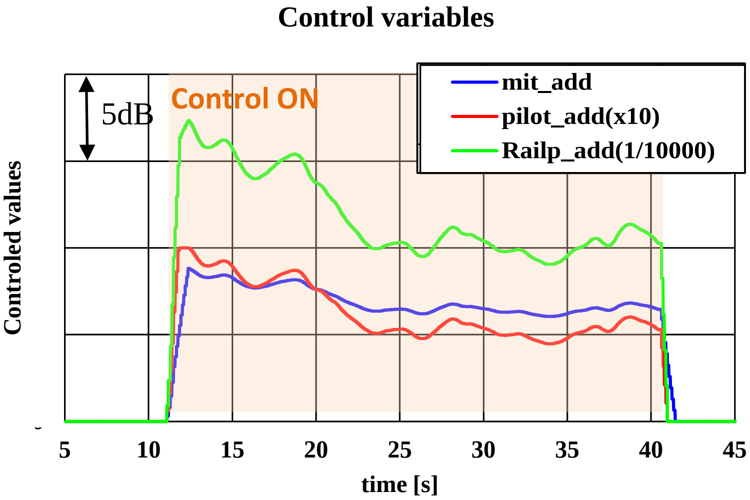

Figure 5.36 Controlled value of parameters during transient operation

Chapter 6. Conclusion

The objective of this study was to look for the methodologies to reduce combustion noise in diesel engines. The relations between diesel engine combustion and combustion noise were examined and the closed loop control system for the noise reduction was developed.

In this study, a 1.6 liter diesel engine was used. The in-cylinder pressure, emissions and PM were measured by using a gas analyzer and a smoke meter. Rapid prototype controllers were used for the real time control system and NI-PXI was used to calculate the current CNI in real time. In addition, a vehicle, which was equipped with the same type engine under the same bench test, was used to evaluate the effects of closed loop control on reduction combustion noise.

First, in this study, the relations between the shape of heat release rate and pressure excitation characteristics were studied. The heat release rate was simulated by Wiebe functions to freely transform the shape. The 3 Wiebe funcions were used to describe the diesel combustion. Each of the function meant the premixed combustion, the mixing controlled combustion and the late combustion. Using the simulated heat release rate, the pressure curve was reproduced and the frequency analysis was conducted. When fuel was rapidly burned, the excitation level increased. When the coefficient ‘m’, which is related with the burning speed, was in between 2 and 3 the combustion excitation was at the lowest. When the combustion duration increased or the fuel quantity decreased, combustion noise decreased. However, the start of combustion did not significantly affect the combustion noise. Pilot injection, which was used to reduce combustion noise, decreased the combustion excitation of combustion from the main injection. However, the combustion of pilot injection considerably affected the total excitation.

The shape of heat release rate for reduction of combustion noise was investigated. When the combustion duration became long and the fuel burned moderately, the combustion noise decreased. In addition, a split injection of the main injection was effective to reduce the excitation. When 30% fuel was burned early, the rest of fuel continuously burned and the combustion noise was dramatically reduced with the same IMEP.

The injection strategies for the reduction of engine noise was examined via the engine bench tests. When injection parameters, SOI, swirl, injection pressure and EGR rate, were changed, the heat release shape and excitation characteristics were studied. The combustion noise could be reduced; however, more smoke was produced except for the EGR control from changing them. The EGR rate significantly affected the NOx emission. To prevent a formation of more emissions and to reduce the combustion noise, early pilot injection strategy was applied. When the pilot injection quantity increased, the main injection quantities decreased for the same IMEP. However, an increase of pilot injection quantity may produce more smoke. To solve the dilemma, the early injection concept was applied to the pilot injection. Since, the early pilot was injected before 30 CAD° BTDC, the fuel of the main injection was deliberately mixed with air; albeit, the pilot injection quantity increased. Through, the early pilot injection, the combustion noise could be reduced without an increase of emission.

Finally, closed loop control system using the CNI was developed to reduce combustion noise. The controller, which can measure the in-cylinder pressure and calculate CNI in real time, were developed using NI-PXI and LabVIEW. The combustion controller, which can modify the injection strategies by communication with EMS, was developed using ES1000 and ASCET. SOI, injection pressure and pilot quantities were used as control parameters. Since, they did not have negative cross effects, the controller changed them simultaneously to follow the target value for the current combustion noise index level. The system was applied to a vehicle. The current CNI level could be controlled to follow the target value in transient operations. During the transient operations, the cabin noise in the vehicle was measured with microphones. AS a result, 1.2~2 kHz frequency of the noise was reduced down to 4 dBA.

Bibliography

[1] T. V. Johnson, "Review of Vehicular Emissions Trends," *SAE International Journal of Engines,* vol. 8, 2015.

[2] G. Sheng, *Vehicle noise, vibration, and sound qualtity*: SAE International, 2012.

[3] Tousignant T., Wellmann T., Govindswamy K., Heuer S., and Workings M., "Application of Combustion Sound Level (CSL) Analysis for Powertrain," *SAE Technical Paper,* 2009.

[4] K. G. Johnson, K. Mollenhauer, and H. Tschöke, *Handbook of diesel engines*: Springer Science & Business Media, 2010.

[5] M. E. Badaoui, J. Danière, F. Guillet, and C. Servière, "Separation of combustion noise and piston-slap in diesel engine—Part I: Separation of combustion noise and piston-slap in diesel engine by cyclic Wiener filtering," *Mechanical Systems and Signal Processing,* vol. 19, pp. 1209-1217, 2005.

[6] C. Servière, J. L. Lacoume, and M. El Badaoui, "Separation of combustion noise and piston-slap in diesel engine—Part II: Separation of combustion noise and piston-slap using blind source separation methods," *Mechanical Systems and Signal Processing,* vol. 19, pp. 1218-1229, 2005.

[7] K. Torii, "Method Using Multiple Regression Analysis to Separate Engine Radiation Noise into the Contributions of Combustion Noise and Mechanical Noise in the Time Domain," *SAE International Journal of Engines,* vol. 7, pp. 1502-1513, 2014.

[8] S. Raveendra, S. Sureshkumar, M.-T. Cheng, L. Na, and T. Abe, "Noise Source Identification in an Automotive Powerplant," *SAE Technical Paper,* 2003.

[9] X. Liu and R. B. Randall, "Blind source separation of internal combustion engine piston slap from other measured vibration signals," *Mechanical Systems and Signal Processing,* vol. 19, pp. 1196-1208, 2005.

[10] J. B. Heywood, *Internal combustion engine fundamentals* vol. 930: Mcgraw-hill New York, 1988.

[11] D. N. Assanis, Z. S. Filipi, S. B. Fiveland, and M. Syrimis, "A Predictive Ignition Delay Correlation Under Steady-State and Transient Operation of a Direct Injection Diesel Engine," *Journal of Engineering for Gas Turbines and Power,* vol. 125, p. 450, 2003.

[12] N. Ladommatos, S. M. Abdelhalim, H. Zhao, and Z. Hu, "Effects of EGR on heat release in diesel combustion," *SAE Technical Paper*1998.

[13] M. Badami, F. Millo, and D. D'amato, "Experimental investigation on soot and NOx formation in a DI common rail diesel engine with pilot injection," *SAE Technical Paper*2001.

[14] A. Maiboom, X. Tauzia, and J.-F. Hétet, "Experimental study of various effects of exhaust gas recirculation (EGR) on combustion and emissions of an automotive direct injection diesel engine," *Energy,* vol. 33, pp. 22-34, 2008.

[15] A. Maiboom, X. Tauzia, J.-F. Hétet, M. Cormerais, M. Tounsi, T. Jaine*, et al.*, "Various effects of EGR on combustion and emissions on an automotive DI Diesel engine: numerical and experimental study," *SAE Technical Paper*2007.

[16] W. Ping, S. Xi-geng, X. Dong-xin, Z. Hai-tao, M. Xiao-wen, and G. Yu-lin, "Effect of Combustion Process on DI Diesel Engine Combustion Noise," *SAE Technical Paper*, 2007.

[17] M. Pontoppidan, A. Demaio, G. Bella, and R. Rotondi, "Parametric Study of Physical Requirements for Optimization of the EGR-rate and the Spray Formation for Minimum Emissions Production over a Broad Range of Load/Speed Conditions," *SAE Technical Paper*2006.

[18] L. Zhang, "A study of pilot injection in a DI diesel engine," *SAE Technical Paper*, 1999.

[19] A. Trueba, B. Barbeau, O. Pajot, and K. Mokaddem, "Pilot injection timing effect on the main injection development and combustion in a DI diesel engine," *SAE Technical Paper*2002.

[20] P. Carlucci, A. Ficarella, and D. Laforgia, "Effects of pilot injection parameters on combustion for common rail diesel engines," *SAE Technical Paper*, 2003.

[21] R. Mobasheri and Z. Peng, "Investigation of pilot and multiple injection parameters on mixture formation and combustion characteristics in a heavy duty DI-Diesel engine," *SAE Technical Paper*, 2012.

[22] T. Fuyuto, M. Taki, R. Ueda, Y. Hattori, H. Kuzuyama, and T. Umehara, "Noise and Emissions Reduction by Second Injection in Diesel PCCI Combustion with Split Injection," *SAE International Journal of Engines,* vol. 7, pp. 1900-1910, 2014.

[23] P. Dimitriou, W. Wang, J. Peng, L. Cheng, M. Wellers, and B. Gao, "Analysis of Diesel Engine In-Cylinder Air-Fuel Mixing with Homogeneity Factor: Combined Effects of Pilot Injection Strategies and Air Motion," *SAE International Journal of Engines,* vol. 7, pp. 2045-2060, 2014.

[24] S. Kohketsu, K. Tanabe, and K. Mori, "Flexibly controlled injection rate shape with next generation common rail system for heavy duty DI diesel engines," *SAE Technical Paper*, 2000.

[25] F. Atzler, O. Kastner, R. Rotondi, and A. Weigand, "Multiple injection and rate shaping Part 1: Emissions reduction in passenger car Diesel engines Computational investigation ", S. T. Paper, Ed., ed, 2009.

[26] F. Atzler, O. Kastner, R. Rotondi, and A. Weigand, "Multiple injection and rate shaping Part 2: Emissions reduction in passenger car Diesel engines Computational investigation," *SAE Technical Paper*2009.

[27] J. Hinkelbein, C. Sandikcioglu, S. Pischinger, M. Lamping, and T. Körfer, "Control of the diesel combustion process via advanced closed loop combustion control and a flexible injection rate shaping tool," *SAE International Journal of Fuels and Lubricants,* vol. 2, pp. 362-375, 2009.

[28] C. Jörg, T. Schnorbus, S. Jarvis, B. Neaves, K. Bandila, and D. Neumann, "Feedforward Control Approach for Digital Combustion Rate Shaping Realizing Predefined Combustion Processes," *SAE International Journal of Engines,* vol. 8, 2015.

[29] A. A. Saad and N. El-Sebai, "Combustion noise prediction inside diesel engine," *SAE Technical Paper*, 1999.

[30] T. Papenfus, D. Genuit, K. Kang, I. Jung, and J. Jin, "Method of NVH quality rating of diesel combustion noise using typical driving modes," *SAE paper,* pp. 01-2078, 2009.

[31] R. P. Bhagate, V. Nadanasabapathy, and K. Mohan, "Powertrain Noise & Sound Quality Refinement for New Generation Common Rail Engines," *SAE Technical Paper*, 2010.

[32] M. V. Rao, J. Frank, and P. Raghavendran, "Measurement Technique for Quantifying Structure Borne and Air Borne Noise Levels in Utility Vehicle," *SAE Technical Paper,* vol. 1, 2014.

[33] T. Tousignant and K. Govindswamy, "Virtual Powertrain Installation for Diesel Engine Sound Quality Development in a Light Duty Vehicle Application," *SAE Technical Paper,* vol. 1, 2014.

[34] M. D. Redel-Macías, C. Hervás-Martínez, S. Pinzi, P. A. Gutiérrez, A. J. Cubero-Atienza, and M. P. Dorado, "Noise prediction of a diesel engine fueled with olive pomace oil methyl ester blended with diesel fuel," *Fuel,* vol. 98, pp. 280-287, 2012.

[35] A. J. Torregrosa, A. Broatch, J. Martín, and L. Monelletta, "Combustion noise level assessment in direct injection Diesel engines by means of in-cylinder pressure components," *Measurement Science and Technology,* vol. 18, pp. 2131-2142, 2007.

[36] F. Payri, A. Broatch, B. Tormos, and V. Marant, "New methodology for in-cylinder pressure analysis in direct injection diesel engines—application to combustion noise," *Measurement Science and Technology,* vol. 16, pp. 540-547, 2005.

[37] F. Payri, A. Broatch, X. Margot, and L. Monelletta, "Sound quality assessment of Diesel combustion noise using in-cylinder pressure components," *Measurement Science and Technology,* vol. 20, p. 015107, 2009.

[38] Engine Sound Level Measurement Procedure (J1074), SAE International, 2000

[39] I. Jung, J. Jin, H. So, C. Nam, and K. Won, "An Advanced Method for Developing Combustion Noise through the Analysis of Diesel Combustion," *SAE International Journal of Engines,* vol. 6, pp. 1379-1385, 2013.

[40] T. Schnorbus, S. Pischinger, T. Körfer, M. Lamping, D. Tomazic, and M. Tatur, "Diesel combustion control with closed-loop control of the injection strategy," *SAE Technical Paper*, 2008.

[41] R. Finesso and E. Spessa, "A Feed-Forward Approach for the Real-Time Estimation and Control of MFB50 and SOI In Diesel Engines," *SAE International Journal of Engines,* vol. 7, pp. 528-549, 2014.

[42] Q. Zhu, S. Wang, R. Prucka, M. Prucka, and H. Dourra, "Model-Based Control-Oriented Combustion Phasing Feedback for Fast CA50 Estimation," *SAE International Journal of Engines,* vol. 8, 2015.

[43] J. Ghojel, D. Honnery, and K. Al-Khaleefi, “Performance, emissions and heat release characteristics of direct injection diesel engine operating on diesel oil emulsion”, *J.Appl. Thermal Enging,* 2006, Vol. 26, 2132-2141.

[44] S. Loganathan, R. Murali Manohar, R. Thamaraikannan, R. Dhanasekaran, A. Rameshbabu, and V. Krishnamoorthy, "Direct Injection Diesel Engine Rate of Heat Release Prediction using Universal Load Correction Factor in Double Wiebe Function for Performance Simulation," *SAE Technical Paper,* vol. 1, 2012.

[45] C. Saad, F. maroteaux, J.-B. Millet, and F. Aubertin, "Combustion Modeling of a Direct Injection Diesel Engine Using Double Wiebe Functions: Application to HiL Real-Time Simulations," *SAE Technical Paper,* vol. 1, 2011.

[46] S. Kulah, T. Donkers, and F. Willems, "Virtual Cylinder Pressure Sensor for Transient Operation in Heavy-Duty Engines," *SAE International Journal of Engines,* vol. 8, 2015.

[47] J. s. Benajes, S. Molina, R. Novella, and R. r. Amorim, "Study on Low Temperature Combustion for Light-Duty Diesel Engines," *Energy & Fuels,* vol. 24, pp. 355-364, 2010.

[48] E. Doosje, F. Willems, R. Baert, and M. Van Dijk, "Experimental Study into a Hybrid PCCI/CI Concept for Next-Generation Heavy-Duty Diesel Engines," *SAE Technical Paper,* vol. 1, 2012.

[49] A. Wagemakers and C. Leermakers, "Review on the effects of dual-fuel operation, using diesel and gaseous fuels, on emissions and performance," *SAE Technical Paper*, 2012.

[50] D. Sahoo, P. C. Miles, J. Trost, and A. Leipertz, "The Impact of Fuel Mass, Injection Pressure, Ambient Temperature, and Swirl Ratio on the Mixture Preparation of a Pilot Injection," *SAE International Journal of Engines,* vol. 6, pp. 1716-1730, 2013.

[51] D. Laforgia, A. Ficarella, and P. Carlucci, "Effects on combustion and emissions of early and pilot fuel injections in diesel engines," *International Journal of Engine Research,* vol. 6, pp. 43-60, 2005.

[52] A. J. Torregrosa, A. Broatch, A. García, and L. F. Mónico, "Sensitivity of combustion noise and NOx and soot emissions to pilot injection in PCCI Diesel engines," *Applied Energy,* vol. 104, pp. 149-157, 2013.

[53] H. Ogawa, K. Tashiro, M. Numata, T. Obe, and G. Shibata, "Influence of Fuel Volatility on Evaporation Characteristics of Diesel Sprays in Various Low Temperature and Low Density Surrounding Conditions Like at Early Pilot or Late Post Injections," *SAE Technical Paper*, 2015.

[54] M. Huo, M. Wang, and C.-F. Lee, "Computational Study of the Equivalence Ratio Distribution from a Diesel Pilot Injection with Different Piston Geometry, Injection Timing and Velocity Initialization in a HSDI Engine," *SAE Technical Paper,* vol. 1, 2014.

[55] Y. Han, Z. Liu, J. Zhao, Y. Xu, J. Li and K. Li, “EGR Response in a Turbo-charged and After-cooled DI Diesel Engine and its Effects on Smoke Opacity”, *SAE Technical Paper*, 2008.

[56] S. Lee, J. Lee, S. Lee, D. Kim and Y. Lee, "Study on Reduction of Diesel Engine Out Emission through Closed Loop Control based on the In-Cylinder Pressure with EGR Model," *SAE Technical Paper*, 2013.

[57] S. Lee, S. Lee, K. Min, and I. Jung, "Characteristics of Diesel Engine Noise According to EGR Rate Change during Transient Operation," *SAE Technical Paper* 0148-7191, 2015.

[58] C. D. Rakopoulos, A. M. Dimaratos, E. G. Giakoumis, and D. C. Rakopoulos, "Study of turbocharged diesel engine operation, pollutant emissions and combustion noise radiation during starting with bio-diesel or n-butanol diesel fuel blends," *Applied Energy,* vol. 88, pp. 3905-3916, 2011.

[59] M. Dhaenens, G. Van Der Linden, J. Nehl, and R. Thiele, "Analysis of Transient Noise Behavior of a Truck Diesel Engine," *SAE Technical Paper*, 2001.

[60] S. Yu, H. Choi, S. Cho, K. Han, and K. Min, "Development of engine control using the in-cylinder pressure signal in a high speed direct injection diesel engine," *International Journal of Automotive Technology*, vol. 14, pp. 175-182, 2013.

국문초록

디젤 엔진은 효율이 좋은 반면 소음이 많이 발생한다는 단점이 있다. 특히, 연소에 의하여 발생하는 소음인 연소음은 디젤 엔진의 주요 소음원이다. 실린더 내의 압력은 점화 지연 후 연료의 동시다발적인 연소로 인하여 급격히 상승하게 되는데 이것이 연소음의 주요 가진원으로 알려져 있다.

따라서 본 연구에서는 연소 특성과 연소음 간의 관계에 대한 연구를 열 발생률의 형상과 연소음 지수를 이용하여 수행하였다. 뿐만 아니라 연소로 인한 가진을 최소화 할 수 있는 방법에 대한 연구를 수행하였다. 끝으로, 연소음 지수를 피드백 컨트롤에 적용하여 연소 소음 수준을 제어할 수 있는 실시간 제어 시스템을 개발하였다.

본 연구에서는 1.6 리터 디젤 엔진을 사용하였다. 연소 압력센서 (Kistler)와 charge amplifier 를 이용하여 연소 압력을 측정하고, 이를 통하여 열발생률 및 연소음 지수를 구하였다. NOx(NO) 등 배기 가스는 Horiba Mexa-7100 을 이용하여 측정하였으며, smoke 의 경우 smoke meter (AVL)를 이용하여 측정하였다. 실시간 제어 시스템은 ES1000 과 NI-PXI 를 이용하여 개발하였다. 실험 차량은 대상시험에서 사용한 것과 같은 1.6 리터 디젤 엔진과 자동 변속기가 장착되어 있는 승용차량을 이용하였다.

디젤 엔진의 연소 특성은 실린더 압력 측정 후 열 발생률을 계산하여 분석할 수 있으나 실험적으로 열 발생률의 모양을 임의로 변경하는 것은 제약이 매우 크다고 할 수 있다. 그러한 이유로 Wiebe 함수를 이용하여 모사하였다. 디젤 연소를 정확하게 모사하기 위하여 3 개의 Wiebe 함수를 사용하였으며, 각각 premixed combustion, mixing controlled combustion 그리고 late combustion 을 대표한다. 열 발생률의

형상은 Wiebe 함수의 계수 변경을 통하여 여러 형태로 변형되었고, 만들어진 열 발생률을 이용하여 압력 곡선을 생성한 후 이를 FFT 및 1/3 옥타브 밴드 분석, 연소음 지수를 이용하여 가진 정도를 평가하였다. 연소 속도가 초반에 급격히 상승하거나 또는 후반부에 급격히 상승할 경우 모두 연소 가진이 크게 발생하였으며, Wiebe 함수의 계수 m 이 2 ~ 3 인 경우의 열 발생률 형상이 가장 적은 연소 가진을 보였다. 또한 연소 구간이 길게 일어날 수록 가진이 적게 나타났고, 연소되는 연료의 양이 많을수록 연소 가진이 크게 일어났다. 그러나 열 발생률 형태가 같을 경우에는 연소 시작 시점은 연소 가진에 큰 영향을 미치지 않았다. 한편 Mixing controlled 연소의 경우, 연소음 지수의 수준에는 큰 영향을 미치지 않았으나 주파수 분석 결과 1.6 kHz 이상의 영역에서 영향을 미치는 것으로 나타났다. 또한 premixed combustion phase 와 mixing controlled phase 간의 시간 간격 및 pilot 연소와 main 연소 간의 시간 간격 또한 연소 가진에 상당한 영향을 미치면서 최적점이 생겨났다. Pilot 연소는 main 연소 가진을 획기적으로 줄일 수 있기 때문에 소음 저감에 매우 큰 효과가 있다. 그러나 pilot 연소에 의해 발생하는 소음 또한 전체 수준을 증가 시키는 원인이 될 수 있기 때문에 pilot 의 연소 특성 개선 또한 연소음을 줄이기 위한 중요한 요인이라고 할 수 있다. 뿐만 아니라 Wiebe 함수를 이용하여 IMEP 수준을 유지하면서 연소 가진을 최소화 할 수 있는 열 발생률 모양을 최적화를 통하여 도출하였다.

다음으로 엔진 시험에서 연소 가진을 최소화 할 수 있는 분사 전략에 대한 연구를 수행하였다. 주분사 시기, 분사 압력, swirl 및 EGR 율에 대한 열 발생률 모양의 변화를 살펴 보았다. 열 발생률의 기울기가 완만할수록, 그리고 연소 시간이 길수록 소음이 적게 발생하는 것을 발견하였다. 그러나 ERG rate 를 제외한 모든 경우에 대해서는 연소 가진이 적게 발생할 경우, PM 이 증가하는 것을 확인할 수 있었다. EGR rate 의 경우 연소음 감소를 위하여 수준을 낮출 경우 NO 발생이 급격히

증가하였다. 따라서 기존의 방법으로는 배출가스 악화 없이 소음을 줄이는 것은 어렵기 때문에 이를 보안하고자 early pilot 분사 전략을 적용하였다. Pilot 의 연료량이 증가하게 될 경우, 열 발생률의 상승을 억제 할 수 있기 때문에 소음을 저감할 수 있지만 과도한 PM 이 발생할 수 있다. 이는 연속된 연료 jet 의 분사로 인하여 공기와의 혼합이 어렵기 때문이다. 이러한 단점을 해결하고자 PCCI 연소를 pilot 연소에 적용하였다. Pilot 을 20~40° BTDC 부근에서 분사하여 점화 지연을 증가시켜 PCCI 연소가 이루어 질 수 있도록 한 후 나머지 연료를 분사를 하였다. 이를 통하여 주분사의 연료와 공기와의 혼합이 개선되어 smoke 의 증가 없이 연소음을 감소 시킬 수 있었다.

마지막으로, 연소음 지수를 활용하는 연소 제어를 통하여 발생하는 연소음 수준을 제어하는 연구를 수행하였다. 이를 위하여 실시간으로 연소 압력을 측정하고, 연소음 지수를 산출할 수 있는 장치를 NI-PXI 를 이용하여 개발하였으며 이를 이용한 연소음 제어 알고리즘은 ES1000 을 이용하여 구성하였다. 주분사 시기, 분사 압력 및 pilot 분사량 조절은 모두 소음에 효과가 있었으며, 상호작용이 크지 않았다. 이 세 가지의 연소 제어 인자를 이용하여 엔진에서 실시간으로 발생하는 연소음 수준이 목표 값을 추종할 수 있도록 제어기를 구성하였다. 이를 위하여 차량 실험을 설계하여 그 효과를 확인하였다. 그 결과, 완가속 조건에서 차량의 실내 소음은 1.2 kHz~ 2 kHz 의 구간에서 최대 4dB 감소 하였다.

주요어 : 디젤 엔진 소음, 연소음, 연소제어, 연소 가진, 열발생률

학번 : 2013-30207